



UNIVERSITÀ
DEGLI STUDI
DI PADOVA

Sede Amministrativa: Università degli Studi di Padova
Dipartimento di Scienze dell'Antichità

SCUOLA DI DOTTORATO DI RICERCA IN STUDIO E
CONSERVAZIONE DEI BENI ARCHEOLOGICI E ARCHITETTONICI
INDIRIZZO: Scienze e Tecnologie Per i Beni Archeologici e Architettonici
CICLO XXIV

**GLASS IN NORTHERN ADRIATIC AREA FROM
ROMAN TO MEDIEVAL PERIOD: A
GEOCHEMICAL APPROACH FOR PROVENANCE
AND PRODUCTION TECHNOLOGIES**

Direttore della Scuola: Ch.mo Prof. Giovanni Leonardi
Supervisore: Ch.mo Prof. Gianmario Molin

Dottoranda: Filomena Gallo

ABSTRACT

English

Glass is one of the oldest materials produced and extensively used by man, thanks to its unique mechanical and chemical-physical properties. For these reasons it has a great importance in both archaeological and artistic fields. So far, notwithstanding the essential lines of development of glass production are known, there are still some particular 'critical moments' in the history of glass production. In this context the present work investigated the evolution of glass technology in a particular geographical area, the northern Adriatic Italy, which, for its peculiar position, had a central role in trades and acted as a commercial hub between the Mediterranean and the Padan and Transalpine area. The sample set, including a total of 178 glasses, covers a large chronological period (6th century BC-15th century AD) and comes from some of the most important sites in the period and in the area considered, such as Aquileia, Adria and Rocca di Asolo. Few samples coming from Tuscan sites (San Genesio, Pieve di Pava and Pieve di Coneo), similar in age and types to Aquileia glasses, were also analyzed, in order to have a comparison among eastern and western Italy. The analytical approach involved textural, mineralogical, chemical and isotopic (Sr, Nd, O) analyses and the results proved the complementarity of these techniques, suggesting that the preferred approach in investigation of ancient glasses should be the combined use of these methods. A substantial continuity in the use of the type of raw materials (siliceous-calcareous sand in addition to natron) from Pre-Roman period until early Middle Ages was testified, whereas a complete change in the use of flux is evident in High/Late Medieval glasses. The extraordinary consistency of natron glass here analyzed and the principal compositional groups widespread in Mediterranean sites tends to support the model of the localized production, organized in a small number of primary workshops which supplied raw glass to a great number of secondary workshops, where the glass was re-melted and shaped into objects. For what concerns the provenance of raw materials, the combination of isotopic and chemical data,

together with archaeological evidence and literature data on both raw materials and glass from primary furnaces, suggests that the vast majority of Roman and Late Roman/early Medieval glasses analyzed in this study were likely produced in workshops located on the Syro-Palestinian and Egyptian coasts, although the use of primary sources located in western Mediterranean cannot be definitely excluded.

Italiano

Grazie alle sue peculiari caratteristiche meccaniche e chimico-fisiche, il vetro è uno dei materiali più antichi utilizzati dall'uomo e, per questa ragione, riveste una grande importanza sia in campo artistico che archeologico. Ad oggi, nonostante le principali linee di sviluppo della produzione vetraria siano state tracciate, permangono dei particolari 'momenti problematici' nella storia del vetro, connessi all'introduzione di nuove materie prime e/o nuove tecnologie di produzione. In questo contesto si inserisce il presente lavoro di ricerca, che ha indagato l'evoluzione della produzione vetraria in una specifica area, quella dell'Italia nord-adriatica la quale, grazie alla sua peculiare posizione geografica, ha svolto in passato un ruolo cruciale nei commerci, fungendo da connettore tra il Mediterraneo orientale e l'area padana e transalpina. La campionatura, oggetto di studio, proviene pertanto da alcuni dei più interessanti siti nord-adriatici (Aquileia, Adria, Rocca di Asolo); inoltre anche un piccolo gruppo di campioni provenienti da siti toscani (San Genesio, Pieve di Pava e Pieve di Coneo), cronologicamente e tipologicamente confrontabili con i reperti aquileiesi, è stato analizzato, al fine di rilevare eventuali analogie/differenze tra il versante adriatico e quello tirrenico. La cronologia dei campioni è molto ampia (VI a.C. -XV secolo d.C.), ma una particolare attenzione è stata rivolta ai reperti di periodo Romano e Tardo Antico. L'approccio analitico ha previsto analisi di tipo tessiturale, mineralogico, chimico e isotopico (Sr, Nd, O). I risultati hanno dimostrato la complementarietà di queste tecniche, indicando che il loro uso combinato costituisce l'approccio ideale per lo studio del vetro antico. Per quanto concerne la tipologia di materie prime impiegate nella produzione vetraria, è emersa una sostanziale continuità dal periodo Pre-Romano fino all'Altomedioevo, caratterizzata dall'uso di sabbie siliceo-calcaree in aggiunta a natron, mentre per i vetri Bassomedievali si assiste ad un radicale cambiamento di fondente (ceneri sodiche). La sorprendente omogeneità chimica tra il vetro al natron

analizzato nel presente studio e i principali gruppi composizionali riportati in letteratura supporta l'ipotesi che, almeno in epoca Romana e Tardo Antica, il vetro venisse prodotto in poche officine primarie, successivamente commercializzato in forma di pani di vetro grezzo e lavorato in officine secondarie sparse in tutto il Mediterraneo. A tale proposito,

l'uso combinato dei dati chimici ed isotopici, supportati da dati di letteratura e da evidenze archeologiche, suggerisce che l'origine della maggior parte di tale vetro sia da collocarsi nel Mediterraneo orientale, in particolare sulle coste Siro-Palestinesi ed Egiziane, sebbene non possa totalmente escludersi anche l'uso di sorgenti di materie prime collocate nel Mediterraneo occidentale.

INDEX

CHAPTER 1. INTRODUCTION	1
1.1 Research topic and aims	1
1.2 Raw materials of the northeastern Italian glasses from Pre-Roman period until the Late Middle Ages	4
CHAPTER 2. ARCHAEOLOGICAL CONTEXTS AND MATERIALS	13
2.1 Adria	14
2.2 Aquileia	16
2.3 Rocca di Asolo	20
2.4 Tuscan sites	22
CHAPTER 3. EXPERIMENTAL METHODS	25
3.1 Optical Microscopy (OM)	26
3.2 Scanning Electron Microscopy with Energy Dispersive System (SED-EDS)	26
3.3 X Ray Powder Diffraction (XRPD)	26
3.4 X Ray Fluorescence (XRF)	27
3.5 Electron Probe Mycroanalysis (EPMA)	27
3.6 Laser Ablation Inductively Coupled Plasma Mass Spectrometry (LA-ICP-MS)	29
3.7 Multi Collector Inductively Coupled Plasma Mass Spectrometry (MC-ICP-MS)	30
3.8 High Temperature Laser Fluorination	32
CHAPTER 4. RAW MATERIALS IN GLASS PRODUCTION: THE TEXTURAL, CHEMICAL AND MINERALOGICAL STUDY	35
4.1 Pre-Roman and Roman glass from Adria	35
4.1.1 Textural characterization	35
4.1.1.1 <i>Residual and newly formed phases</i>	35
4.1.1.2 <i>Opacifying agents</i>	42
4.1.2 Chemical characterization	47
4.1.2.1 <i>Transparent glass</i>	47
4.1.2.2 <i>Opaque glass</i>	68
4.2 Late Roman glass from Aquileia	71
4.2.1 Bulk chemistry	71
4.3 Late Roman/early Medieval glasses from Tuscany: a comparison with Aquileia glasses	83
4.3.1 Bulk chemistry	83
4.4 Early and High/Late Medieval glass from Rocca di Asolo	87
4.4.1 Bulk chemistry	88
4.4.2 Colouring and decolouring agents	94
4.5 Conclusions	98

CHAPTER 5. THE PROVENANCE OF RAW MATERIALS IN GLASS: THE ISOTOPIC APPROACH	101
5.1 Features and principles of the technique	101
5.1.1 Strontium and neodymium	102
5.1.2 Oxygen isotopes	106
5.2 Materials	107
5.3 Results and discussion	107
5.3.1 Strontium and neodymium isotopes	107
5.3.2 Oxygen isotopes	116
5.4 Conclusions	120
CONCLUDING REMARKS	123
REFERENCES	127
APPENDIX A	147
APPENDIX B	165
APPENDIX C	173
APPENDIX D	179
APPENDIX E	199

CHAPTER 1

INTRODUCTION

1.1 Research topic and aims

Glass, defined as the product of the fusion of inorganic materials which have cooled to a solid condition without crystallising, is one of the oldest materials produced and extensively used by man, thanks to its unique mechanical and chemical-physical properties. For these reasons it has a great importance in both archaeological and artistic fields. Chrono-typological studies on glass have a long tradition (Isings, 1957), whereas archaeometric studies have been developed since the 1970s, giving important contributions to the knowledge in this sector. So far, notwithstanding the essential lines of development of glass production are known, there are still some particular ‘critical moments’ in the history of glass production. For some reasons, generally associated to political and economic instabilities, during these moments new raw materials and/or new production technologies became predominant in glass production, determining changes in glass types.

In this context the present work investigated the evolution of glass technology in a particular geographical area, the northern Adriatic Italy, which, for its peculiar position, had a central role in trades and acted as a commercial hub between the Mediterranean and the Padan and Transalpine area. A total of 178 glass objects were analyzed, already characterized from the archaeological point of view: 68 from the Archaeological Museum of Adria (RO, Italy), 62 from the excavation of *Casa delle bestie Ferite* in Aquileia (UD, Italy) and 33 from Rocca di Asolo (TV, Italy). Furthermore 15 glasses from three archaeological sites in Tuscany (San Genesio, Pieve di Pava and Pieve di Coneo), chronologically and typologically comparable with Aquileia samples, were selected in order to have a comparison between the eastern and the western part of the Italian peninsula. The sample set covers a large chronological period, from the 6th century BC until the 15th century AD, with particular attention to the Roman and Late Roman/early Medieval productions. This large sample set allowed to investigate some

1. Introduction

of the ‘critical moments’ in glass history, which are listed and briefly described in the following:

- Technological transition between the Iron Age glass and the Hellenistic-Roman production: during Iron Age radical changes occurred in glass production, in particular in the use of fluxing agents. It is well known that in the Late Bronze Age glass was produced using plant ashes as the batch fluxing component (Angelini et al., 2002), while the Final Bronze Age was characterized by the appearance in Europe of the so-called ‘mixed alkali glasses’ (Angelini et al., 2004). From the 7th century BC onwards, glass composition changed radically and the so-called ‘natron based’ glass became widespread in eastern and western regions. Actually, the data are numerically scarce with respect to the complexity of glass production, and therefore the production technologies and types of raw materials used during the Iron Age are not at present clearly identified.
- Provenance of raw materials and production models in large-scale Roman production: the current literature on Roman glass production is dominated by two competing models, centralized and dispersed production. The former establishes that glass was produced in a small number of primary glass-making installations, the location of which is still up for intense debate. Raw glass was broken up and traded throughout the Mediterranean as chunks and then re-melted and shaped into vessels and other objects in secondary workshops (Foy et al., 2000). In opposition, the dispersed production model hypothesizes that glass was made on a small scale in a large number of regional workshops (Wedepohl et al., 2003) (for further details on Roman production models see section 1.1). In the North Adriatic area Roman kilns have not yet been found, so there are no evidences of local production. However, on the basis of the large number of glass samples found in urban excavations of both Adria and Aquileia, some authors have inferred the presence of glass industries (Zecchin, 1956; Calvi, 1968; Fogolari and Scarfi, 1970; De Min, 1987, Toniolo, 2007. See chapter 2).
- Technological transition between Late Antiquity and early Middle Ages: during Late Roman period a change in glass colour and a general decline in the range of vessel types and quality is apparent (Foster and Jackson, 2009), suggesting

changes in the raw materials used for glass-making. At least two new glass compositions, introduced in the 4th century AD, have been identified and continued to be produced until the late 8th century, probably in a limited number of primary production centers, mainly located in Egypt and Levant. In any case, the identification of raw materials, primary workshops and trades during Late Roman and early Medieval glass is still debated.

- Technological transition between early Middle Ages and high/late Middle Ages: in the early Medieval period (6th-10th century AD) a series of events caused a radical change in the glass manufacture and natron was substituted by plant ash. In the West, wood ash had become the main flux agent, whereas in the Middle East and southern Europe the alkali source is generally believed to be ash from marsh plants. In northern Adriatic area the soda ash glass is generally attributed to Venetian production (Verità et al., 2002). Indeed this city played a fundamental role in glass production during Middle Ages, but a systematic and exhaustive study on trades between the Venetian area and inland is still lacking.

Generally speaking, the main aim of this project was to expand the current knowledge on the evolution of glass production and to identify possible commercial and technological exchanges between different cultures. In particular, in order to shed more light on the questions related to the previously described ‘critical moments’, the following aspects have been extensively developed:

- Characterisation of raw materials and production technologies employed in Pre-Roman, Roman, Late Roman/early Medieval and Late Medieval glasses from northern Adriatic area;
- Study of the provenance of raw materials;
- Comparison between analyzed samples and known glass types founded in the Mediterranean basin;
- Identification of possible relationships among chemical composition, type, chronology and production technique of an object.

The glass samples were carefully characterized by means of a combined approach, chemical and isotopic. Indeed, as demonstrated by previous studies, the determination

1. Introduction

of the chemical composition and especially analyses of trace elements (Freestone et al., 2002), are useful tools to identify compositional groups, while stable and radiogenic isotopes, specifically those of oxygen, strontium and neodymium, are promising indicators for provenance determination of primary glass, even after its transformation or recycling in secondary workshops (Degryse and Schneider, 2008).

For a clearer comprehension of the results reported and discussed in chapters 4 and 5, a detailed overview on glass production from Pre-Roman period to Medieval time (raw materials, production technologies and production models) is given in the following section.

1.2 Raw materials of the northeastern Italian glasses from Pre-Roman period until the Late Middle Ages

Roman period saw a prodigious use of glass in domestic, industrial and funerary contexts. Glass was used primarily for the production of vessels, although mosaic tiles and window panes were also produced. Roman glass production developed from Hellenistic technical traditions, initially concentrating on the production of intensely coloured cast glass vessels (Fleming, 1999). The production technique was time-consuming –the products were vessels with thick walls which required to be finished– and for this reason glass was an expensive and high status material. However, during the 1st century AD the introduction of glassblowing revolutionized glass production, allowing glass workers to produce vessels with considerably thinner walls and so decreasing the amount of glass needed for each vessel. Glassblowing was also considerably quicker than other techniques, and vessels required considerably less finishing, representing a further saving in time, raw material and equipment. As consequence of these factors, the cost of production was reduced and glass moved from a luxury material to a material commonly available (Fleming, 1999). A large variety of production techniques were employed in Roman glassworking, some of these, strictly related to the analyzed materials, are briefly described below.

- **Core-forming**: this technique dates from about the middle of the 2nd millennium BC and is one of the oldest techniques to form hollow-ware glass before the invention of blowing. The core was modeled with the desired shape in clay or vegetable material, covered by a layer of calcite and placed on the end of

a metal rod. The glass was heated and, when molten, poured onto the core. During this, the metal rod was slowly rotated in order to distribute the glass evenly. The core, covered with glass, was rolled on a stone or metal slab and finally decorated with glass trails of different colour (Sternini, 1995; Ferrari et al., 1998).

- **Casting:** the modeling was achieved by pouring the crushed glass into a mold. The mold had hollowed interior walls in order to create the negative form. By heating the mold, the glass melted into the form. This was probably the first technique used for glassforming; from the earliest times, molds were used for making clay and metal objects, and the procedure was later adopted for shaping glass (Sternini, 1995; Ferrari et al., 1998). In fact, forms produced show clear inspiration from the Roman bronze and silver industries, and in the case of carinated bowls and dishes, from the ceramic industry (Allen, 1998). Cast vessel forms became more limited during the late 1st century AD, but continued in production into the second or third decade of the 2nd century AD (Grose, 1991).
- **Sagging glass on former molds:** this technique was used for making monochrome and coloured striped bowls. Monochrome bowls were made by placing a flat circular blank in a upside-down form, suspended by two supports. In the furnace the two supports were taken away and the blank sagged on the concave form. The coloured bowls were formed by fusing coloured strips into a flat circular blank. Afterwards a glass stripe was put all around the blank to form the edge (Sternini, 1995; Ferrari et al., 1998).
- **Ribbing:** there are three hypothesis about this technique. The first is the lost-wax process, already used for making metal objects; the process consists of filling the open space inside the mold with powdered glass after melting wax. In the second hypothesis a still soft glass disk was punched with a tool in the form of a star; afterwards the bowl was formed by sagging the glass former molds. The third hypothesis explains the forming of this vase with the use of the pottery wheel: on a upside-down bowl a hot glass disk was sagged; then it was ribbed by using a suitable tool while turning the wheel. At the end the vase was polished, especially on the rim (Sternini, 1995; Ferrari et al., 1998).

1. Introduction

- **Reticella glass:** this glass is a particular kind of sagging glass on former molds. The *reticella* items are made of colourless or blue strips of glass that are decorated with thin filaments, usually white or yellow, which form a spiral pattern. To achieve the strips a hot glass body was rolled over two narrow glass rods, which had been laid out on a marble slab, until the rods penetrated the glass. A pontil was then applied and the body was stretched to make a thread, while quickly twisting the other end to form the spiral pattern. The strips were then placed on a flat surface, parallel to one another, in order to obtain a blank which was heated and sagged over a form, or they were placed in a mold in parallel fashion and fused (Sternini, 1995; Ferrari et al., 1998).
- **Blowing:** this technique revolutionized glass production around the middle of the 1st century AD, rendering the production of glass containers a fast and economical process, and as a consequence promoting their spread amongst the less well-off. During the blowing process, molten glass, gathered on the end of an iron tube (the blow pipe), was inflated to form a bubble which, after being rolled on a flat surface and shaped with appropriate tools, was then inflated further and manipulated to create the final form. The vessel was then detached from the blow pipe to finish the neck and rim by tooling. In order to do this, a pontil (an iron rod about one meter long) was attached to the base with a blob of glass (Sternini, 1995; Ferrari et al., 1998).
- **Mold-blowing:** this method came after the invention of free-blowing during the first part of the second quarter of the 1st century AD (Lightfoot, 1987; Price, 1991). A glob of molten glass was placed on the end of the blowpipe which was then inflated into a wooden or metal carved mold. In this way, the shape and the texture of the bubble of glass was determined by the design on the interior of the mold rather than the skill of the glassworker (Cummings, 2002).

The raw materials for making glass in ancient times were naturally occurring rocks and minerals: a mixture of silica, alkali and lime with, in some cases, transition metal oxides. Transition metal ions, such as those of manganese (Mn^{2+}), iron (Fe^{2+}/Fe^{3+}), cobalt (Co^{2+}), and copper (Cu^{2+}/Cu^{+}), acted as colouring agents in ancient glass. However, the final colour of a glass is the result of a complex interplay of parameters

such as how the glass batch is prepared, the heating cycle of the furnace, the fuels used, the gaseous atmosphere of the furnace, and the chemical environment of the colouring agents (Pollard and Heron, 1995).

It has been established that the earliest glass production known dates back to the second half of the 3rd millennium BC in Mesopotamia (present day Iraq and Syria). In the following centuries, glass production spread and reached the Eastern Mediterranean region and the European coastline, as attested by the intense trade between Aegean communities and Western provinces in the first centuries of the Bronze Age (Grose, 1989; Oppenheim et al., 1989; Stern and Schlick Nolte, 1994). In their studies, Sayre and Smith (1961) and Turner (1956) discussed the chemical composition of early glass from Eastern regions (Egypt, Mycenaean Greece, Mesopotamia), mainly dated between 1500 and 800 BC. The glass of this period is characterized by high levels of Na₂O and high, often correlated, MgO and K₂O levels, resulting from the use of plant ashes as the batch fluxing component. Glass of this composition was widespread in the Bronze Age, and also present in western Mediterranean regions, in Italy (Santopadre and Verita', 2000; Angelini et al., 2002), central Germany (Hartmann et al., 1997) and France (Gratuze and Billaud, 2003). The Final Bronze Age (12th to 10th centuries BC) was characterized by the appearance in Europe of the so-called "mixed alkali glasses" (Henderson, 1988, 1993; Guilaine et al., 1990; Hartmann et al., 1997; Angelini et al., 2004, 2006;), but, from the 7th century BC onwards, glass composition changed radically, and the so-called "natron-based" glass became widespread in eastern and western regions. Therefore, the typical Roman glass is natron glass, the predominant type of ancient glass in the Mediterranean and Europe until the 9th century AD (Sayre and Smith, 1961). Natron glass is a silica-soda-lime glass, essentially made with natron as flux and siliceous–calcareous sand as network former. The major source of lime, an essential component of the glass since it reduces its solubility in water, would have been calcium carbonate, which either was added deliberately to the glass batch as a separate component or accidentally as particles of shell or limestone in the sand used as the source of silica (Freestone, 2006). The term natron is used to define an evaporitic deposit, often polyphase, rich in sodium carbonates; natron deposits usually contain also significant amounts of chlorides and/or sulphates. This kind of deposits is available from Egypt and possibly from other locations, such as at-Tarabiya in the Eastern Delta,

1. Introduction

al-Kab in Upper Egypt and Bi'r Natrun on the route to Darfur in Sudan. Potential alternative sources outside of Egypt include the salt lakes near al-Jabbul in northern Syria, Lake Van in Armenia and Lake Pikrolimni near ancient Chalastra in Macedonia (Shortland, 2004; Shortland et al., 2006). The Egyptian deposits, known mainly today from the Wadi Natrun, about 100km NW of Cairo, but also from al-Barnuj in the Western Delta, comprise predominantly one or more of the minerals trona ($\text{Na}_3(\text{CO}_3)(\text{HCO}_3)\cdot 2\text{H}_2\text{O}$), thenardite (Na_2SO_4), burkeite ($\text{Na}_6(\text{CO}_3)(\text{SO}_4)_2$) and halite (NaCl) (Freestone, 2006). Although the source of natron was the same throughout the Roman period, the source of sand, which mostly provides the SiO_2 content of glass, is more debatable. The only bibliographic indications about the sand sources employed during Roman time are from Pliny the Elder (I AD). In Book XXXVI of his *Naturalis Historia*, the only surviving written account about Roman glassmaking, he writes that besides Levantine sands, from the mouth of Belus river (Israel), sands from the coast of Italy, particularly from deposits near the mouth of the Volturno river between *Cumae* and *Liternum*, and from the Gallic and Spanish provinces were used.

“In this district, it is supposed, rises the river Belus, which, after a course of five miles, empties itself into the sea near the colony of Ptolemis...The shore upon which this sand is gathered is not more than half a mile in extent; and yet, for many ages, this was the only spot that afforded the material for making glass...Sidon was formerly famous for its glass-houses, for it was this place that first invented mirrors. Such was the ancient method for making glass: but, at the present day, there is found a very white sand for the purpose, at the mouth of the river Volturnus, in Italy. It spreads over an extent of six miles, upon the sea-shore that lies between Cuma and Liternum...Indeed, at the present day, throughout the Gallic and Spanish provinces even, we find sand subjected to a similar process” (Nat. Hist. XXXVI Chap. 65-66; Eichholz, 1962)

Previous studies carried out on Belus sand (Turner 1956; Brill 1999; Vallotto and Verità 2000) have proved that it may be considered suitable for glass production. The sand from the Bay of Haifa is the palest on the Israeli coast (Emery and Neev, 1960), indicating a relatively iron oxide content, which is desirable in the production of weakly coloured glass. In addition, the Belus sand contains about 15% of calcium carbonate,

mainly as fragments of beach shells (Vallotto and Verità 2000), which, when mixed with alkali, would produce a soda-lime-silica glass with 8-9% CaO, which is around the level required to produce a stable glass (Freestone, 2006, 2008). It is unlikely that the beach in the vicinity of the Belus was the only source of glassmaking sand. The presence of primary glassmaking installations further down the Levantine coast, at Apollonia-Arsuf (Tal et al., 2004) and Bet Eli'ezer, Hadera (Gorin Rosen, 2000) suggest that other sands in the eastern Mediterranean region were suitable for this purpose (Freestone, 2006). Studies performed on the Volturno river sand established that it is not suitable for glassmaking, due to its mineral contents, which can introduce high percentages of Al_2O_3 , CaO and Fe_2O_3 in the final glass (Turner 1956; Vallotto and Verità 2000). Otherwise, more recent studies (Silvestri et al., 2006) have demonstrated that the Volturno river sand can become suitable for glassmaking after a specific treatment. In particular, the combination of crushing, grinding in wooden mortar and washing resulted in an overall 'improvement' in the chemical composition of the sand by progressive Al_2O_3 , Fe_2O_3 and CaO decrease, mainly due to carbonate, augite and feldspar loss, and a relative SiO_2 increase, mainly contained in quartz. An experimentally melted glass prepared from sand treated in this way, was chemically very similar to typical Roman glass (Silvestri et al., 2006). As concern France and Spain, no direct archaeological evidences have been found to support the hypothesis of a primary glass production in these regions. In a recent work, Brems et al. (submitted *a*) have evaluated the suitability for making glass of 178 sands, coming from Spain, France and Italy. The results indicate that good glassmaking sands are rather rare and occur in the Basilicata and Puglia regions (Southern Italy) and Tuscany (Western Italy). After the addition of an extra source of lime also sands from the Huelva province (SW Spain), the Murcia region (SE Spain) and from the Provence (SE France) would produce glasses with a typical Roman composition (Brems et al., submitted *a*). Notwithstanding the various potential sand sources, a limited number of compositional groups were identified in Mediterranean and European area during the first millennium AD. An extraordinary homogeneous type of Roman glass, defined as 'typical Roman glass' (Sayre and Smith, 1961) is diffused until the end of the 3rd century AD, but afterwards some important changes occurred from the 4th century onwards (Fiori and Vandini, 2004). Freestone et al. (2000, 2002) and Foy et al. (2003) have identified at least two

1. Introduction

glass compositions, dubbed Levantine I and HIMT, which were introduced in the 4th century AD and continued in production until the late 1st millennium AD. The reasons of this transition are not yet clear, but they were probably connected to political and economic changes that took place in this period (Fiori and Vandini, 2004). The main differences of the HIMT glasses with respect to the earlier Roman glass are represented by higher levels of iron, manganese, titanium, magnesium and by lower contents of lime. On the other hand, Levantine glass shows lower soda, higher lime and often has low levels of iron and relatively high alumina.

In the early Medieval period a series of events, comprising lack of sufficient supplies, climatic change and/or political instability (Shortland et al., 2006) caused a radical change in glass manufacture both in the Islamic world and in the West (Newton and Davison 1996; Henderson 2002). In both areas, natron, the source of alkali used from the middle of the first millennium BC, was replaced by plant ash. In the West, following a period of transition of about 200 years between *ca.* 800 and 1000 AD, tree ash had become the main source of alkali for the manufacture of the massive quantities of glass needed for the windows of cathedrals in Northern Europe. The ash of inland plants contains potash, which began to replace soda as the regular source of alkali. The monk Theophilus in his *Schedula de diversis artibus*, written in about 1100 AD, strongly recommended the use of beechwood ash and quartz sand to produce glass. So the glass-makers probably moved into areas where beech forests grew, thus ensuring both a plentiful supply of fuel for their furnaces and alkali for their glass. Newton (1985) has related the glass-making centres in Europe to the distribution of beechwood pollen in 1000 AD and such centres are found in Northern Europe (Germany, France, England), since beech is scarce south of the Alps. On the other hand, in the Middle East and Southern Europe, the alkali source is generally believed to be ash from marsh plants such *Salicornia* spp. of the family of *Chenopodiaceae* plants, which grows on Mediterranean and Atlantic coasts (Henderson 2002; Tite et al. 2006).

As concern the organization of the glassmaking industry in ancient time, the small range of compositional variations of Roman glass, led to hypothesize that raw glass was already traded as ‘ingots’ or chunks from late Bronze age to early Medieval times (Foy et al., 2000). ‘Primary’ workshops produced raw glass and were distinct from ‘secondary’ workshops that shaped glass into specific objects. A single primary

workshop could then supply many secondary workshops over a large geographical area (Nenna et al., 1997, 2000). Archaeological excavations revealed that large quantities of 4th-8th century AD natron glass were made in a limited number of ‘primary’ glass production centers mainly in Egypt and the Levant (Freestone et al., 2000; Gorin-Rosen, 2000; Picon and Vichy, 2003; Tal et al., 2004; Nenna et al., 2005). Blocks of raw glass were produced in a single firing, as testified by the 8 tonnes glass slab at Beth She'arim in Israel, probably dated to the early 9th century AD (Freestone and Gorin-Rosen 1999) and the excavations of 17 tank furnaces of similar capacity at Bet Eli'ezer, Hadera, Israel, probably dated to the 7th to 8th centuries AD (Gorin-Rosen, 2000). Three similar furnaces of 6th to 7th century AD have been excavated at Apollonia-Arsuf, Israel (Tal et al. 2004) and four 10th to 11th century AD furnaces at Tyre, Lebanon, one of which has an estimated capacity in excess of 30 tonnes (Aldsworth *et al.* 2002). Further evidence to support the ‘centralized’ production model is the discovery of wrecked merchant ships, (2nd-3rd centuries AD), containing raw glass, as slabs and glass chunks (Foy and Jézégou 1998; Gratuze and Moretti 2001), clearly indicating that the trade of raw glass was a widespread practice during Roman time. In opposition to this model is the idea that glass was made on a small scale at a large number of local or regional workshops (‘dispersed’ model), where raw materials were locally available (Wedepohl et al., 2003). Both models have been projected to earlier periods, although the archaeological and scientific evidence for either is difficult to interpret (Baxter et al. 2005). Some authors have suggested that early Roman primary production may have taken place elsewhere in the Hellenistic and early Roman world (Leslie et al., 2006; Degryse and Schneider, 2008), as small-scale glassmaking has been reported from Roman York (Jackson et al., 2003) and fourth century AD Hambach, Germany (Wedepohl et al., 2003).

Models on the organization of glass production in Medieval period still lack. In particular, in Italy, the transition of the glass industry from Roman to Medieval periods has not been completely understood (Silvestri et al., 2005; Silvestri and Marcante, 2011). Studies performed on glass findings coming from Venice, one of the most centres of glass manufacture in Western Europe in this period, identified a gradual change of glass composition from natron-based Roman production towards the ash-based glass (Verità et al., 2002). During early Middle Ages, only secondary workshops

1. Introduction

were active and objects were made by resoftening raw glass and cullet. Therefore, the transition from natron to soda ash glass would have occurred in Venice initially by simple resoftening of raw glass produced elsewhere, but already in the 12th-13th century AD soda ash glass was certainly produced in Venice using raw materials (flux) imported from the Levant (Verità et al., 2002; Verità and Zecchin, 2009).

CHAPTER 2

ARCHAEOLOGICAL CONTEXTS AND MATERIALS

Glass, object of the present work, covers a wide chronological range (from the 6th century BC until the 12-15th centuries AD) but come from the same geographical location, i.e. the Northern Adriatic area in Italy (Fig. 2.1). In particular, the Pre-Roman, Roman and Late Roman/early Medieval glasses come from Adria and Aquileia, two of the most important ports in Mediterranean during Roman time, and the High/Late Medieval glasses come from Rocca di Asolo, an inland site which was under the influence of Venice, that was the most important centre of glass production during Middle Ages and Renaissance.



Figure 2.1: Geographical location of the sites from which glass, here considered, comes.

2. Archaeological contexts and materials

Some Late Roman glasses, coming from the Tuscan sites of Pieve di Pava, Pieve di Coneo and San Genesio (Fig. 2.1), were also analyzed, in order to have a comparison between the Eastern and the Western part of the Italian peninsula.

The following sections briefly describe the archaeological and historical context of the sites from which the glass fragments come, as far as the period of interest and the analyzed samples.

2.1 Adria

Adria is located in Northern-Eastern Italy, actually 25 Km far from the Adriatic sea. The first settlements are of Venetic origin and were built during the 12th-9th century BC; in 6th century BC the city of Adria was founded (Fogolari and Scarfi, 1970). In the past, the city was only 12 Km far from the sea and it was in a position of connection of the three main rivers of Southern Veneto: Adige, Tartaro-Po and Po. According to a Venetic and Etruscan-Italic model, Adria was founded in the hinterland, as fluvial port, but it is probable that the city was also furnished of a maritime port located on the coast. For its peculiar geographical position, Adria was the main commercial port in North Adriatic area: between the 6th and the 2nd century BC goods coming from Aegean and South Adriatic area were distributed in the Padan and Etruscan area, as many findings of Attic pottery in the necropolis of Bologna and Marzabotto testify. From the 5th century BC Adria was under the influence of the Padanian Etruria and extended its trade also in the transalpine area (mainly France, Germany and Switzerland) (Fogolari and Scarfi, 1970). At the half of the 5th century the Greek importations completely stopped, due to the end of the power of Athens, as consequence of the Peloponnesian War. This event, in association with the Gallic incursions in Padanian Etruria, determined a temporary crisis of Adria, which regained its importance in Mediterranean trades between the end of 4th and the 3rd century BC. Since the 2nd century BC the process of Romanization interested the Cisalpine region; in 131 BC *Via Popilia* connected Adria to Rimini and consequently to Rome, between *Via Flaminia*. In 128 BC *Via Annia* connected Adria to Padova and, crossing Altino and Concordia, to the important port of Aquileia (Fig. 2.1.1). In the 1st century BC Adria became definitely a Roman *municipium*, but already in the 2nd century AD it lost its economic predominance, due to the ascent of the port of Ravenna.



Figure 2.1.1: some of the most important Roman roads (Via Postumia and Via Popilia-Annia) in Northern Italy.

The wealth and the importance of the city during the Imperial age are testified by numerous findings of glasses of precious workmanship, mainly dating the 1st century AD. For this reason, some authors have supposed the presence of a glass industry in Adria (Fogolari and Scarfi, 1970; Zecchin, 1956; De Min, 1987), at least for objects of common use (Fogolari and Scarfi, 1970), notwithstanding this hypothesis lacks objective evidences (Bonomi, 1996).

In this context, 68 glass objects coming from the Archaeological Museum of Adria (RO, Italy) were analyzed; a detailed description of all glass fragments is listed in Table A.1, reported in Appendix A. The sample set includes principally glasses of Roman age, predominantly dating from the 1st to 2nd century AD, but spanning the 1st to 3rd-4th centuries AD; seven objects dating Pre-Roman period, from the 6th to the 2nd century BC, are also present (Table A.1). The Pre-Roman objects include essentially three types, produced with the technique of the core-forming: *oinokai*, *aryballoi* and *amphoriskoi* (Table A.1). They belong to the so-called ‘Mediterranean Groups’ (Grose, 1989; Stern and Schlick-Nolte, 1994) and were used to store oils, ointments and cosmetics. Roman glasses include cups, jars, bottles, toilet bottles, ewers, dishes and one glass chunk. A great variety of forms and production techniques (ribbing, sagging

2. Archaeological contexts and materials

glass on former molds, *reticella glass* technique) is also testified (Table A.1). All Pre-Roman artefacts and the vast majority of Roman objects (53 samples) are intentionally coloured (or decoloured): 26 of them are completely transparent (blue, colourless, green, purple, black), 4 completely opaque (3 white or *lattimo* glass and 1 blue) and 23 have a transparent body (blue, purple, colourless, green, light blue or amber) with opaque decorations (white, light blue, yellow and/or wisteria). The remaining is naturally coloured glass (15 samples), typically light blue or light green in colour.

2.2 Aquileia

Aquileia was founded as a colony by the Romans in 180/181 BC, in an alluvial plain in Northern Eastern Italy, along the Natisone river, once navigable, as testified by the presence of the port. The colony was in a strategic position: it served as a frontier fortress at the North-East corner of transpadane Italy and act as a buttress to check the advance of warlike people, such as Carni and Histri tribes. The colony was established with Latin rights by the triumvirate of Publius Cornelius Scipio Nasica, Caius Flaminius, and Lucius Manlius Acidinus. They led 3000 *pedites* (infantry), probably from central Italy, who, with their families, formed the bulk of the settlers and were soon supplemented by native Veneti. It is likely that Aquileia had been a center of Venetia even before the coming of the Romans (Chiabà, 2009). In 148 BC Aquileia was connected with Genoa by means of the *Via Postumia*, which passed through Cremona, Bedriacum and Altino; in 132 BC the construction of the *Via Popilia*, from Rimini to Aquileia, through Ravenna, Adria and Altino, improved the communications still further and in 131 BC the *Via Annia* connected Aquileia to Padova (Fig. 2.1.1) (Bertacchi, 2003). Aquileia was also connected with the central Italy by the *Via Emilia* (from Piacenza to Rimini, Fig. 2.1.1). The original Latin colony became a *municipium* in 90 BC and colony of Roman rights in the Augustan period. Notwithstanding the crisis of the 3rd century, Aquileia maintained its importance and, after the Diocletian's reform, it assumed political and administrative functions complementary to those of Mediolanum. The city became the residence of the provincial governors and an imperial palace was constructed, in which the emperors frequently resided after the time of Diocletian. During the 4th century Aquileia reinforced its role of connection between the Mediterranean and the Balkan area, as testify the *Edictum de Pretiis* (301 AD),

which reports the maritime exchanges between Aquileia, Alexandria of Egypt and the Levant (Marano, 2009; Sotinel, 2001). At the end of the 4th century, Ausonius enumerated Aquileia as the ninth among the great cities of the world, placing Rome, Mediolanum, Constantinople, Carthage, Antioch, Alexandria, Trier, and Capua before it. However, in 452 AD the city was besieged and destroyed by Attila and Huns; the fall of Aquileia was the first of Attila's incursions into Roman territory, followed by cities like Mediolanum and Ticinum. The Roman inhabitants, together with those of smaller towns in the neighborhood, fled to the lagoons, and so founded the cities of Venice and nearby Grado. The process of decadence, triggered by the fall of Attila, continued during the 5th century, under the domination of the Ostrogoths. In this period, the cities of the inner *Venetia*, such as Verona, assumed more importance while Aquileia was gradually marginalized. The short Byzantine domination (555-568 AD) tried to reorganize the ancient province of *Venetia et Histria*, but it was interrupted by the invasion of the Lombards in 568 AD. Aquileia was once more destroyed (590 AD) and the patriarch Paolo fled to the island town of Grado, which was under the protection of the Byzantines. The flight of the patriarch represents the final act of the ancient history of Aquileia; the city continues its existence during the Lombard period, but deprived of the political and economical importance that it had had in Roman and Late Roman Period (Marano, 2009).

As previously said, the peculiar geographical position, the fluvial port connected with the sea and the road network attributed to Aquileia a central role in trades during Roman and Late Roman period. This city acted as a commercial hub between the Mediterranean area and the Padan and Transalpine area. A huge quantity of goods circulated in the port and in the market: mainly wine and oil, but also livestock, wood, iron, fruit, leather, clothing, wheat, pottery, glass (Zaccaria et al., 2009). For this reason, in the 1st century BC the Greek geographer Strabo underlined the role of emporium assumed from Aquileia (Strabo 5,1,8) and in the 3rd century the historian Herodian defined the city *emporium of Italy* (Herodian 8, 2).

As concern the glass, a large collection of objects of different age, type and colour is preserved in the Archaeological Museum (Mandruzzato and Marcante, 2005, 2007). In the past years, C. Calvi (1968) has supposed the presence of a glass production in Aquileia, based on the finding of glass debris with the typical Roman composition and

2. Archaeological contexts and materials

on the presence of silica source (*saldame*) in the close Histria. To support the above hypothesis, C. Calvi also mentioned the inscription *Sentia Secundia facit Aquileia vitra* on two bottles founded at Linz in the early 19th century.

At the present, other authors tend to hypothesize the presence of secondary workshops in Aquileia rather than of a centre of primary production (Buora et al., 2009). Notwithstanding the findings of furnaces are actually missing, the presence of glass slags, chunks and debris (drops, filaments) is testified both in the urban area and suburbs (Buora et al., 2009), but never studied from the archaeological point of view.

The sample set of Aquileia glasses analyzed in this work comes from the roman *domus*, called *Casa delle Bestie Ferite*. The University of Padova started the archaeological excavation of this building in 2007. The house is situated in the North of the city, in a residential area, and occupied a surface area of about 800 m² (Fig. 2.2.1).

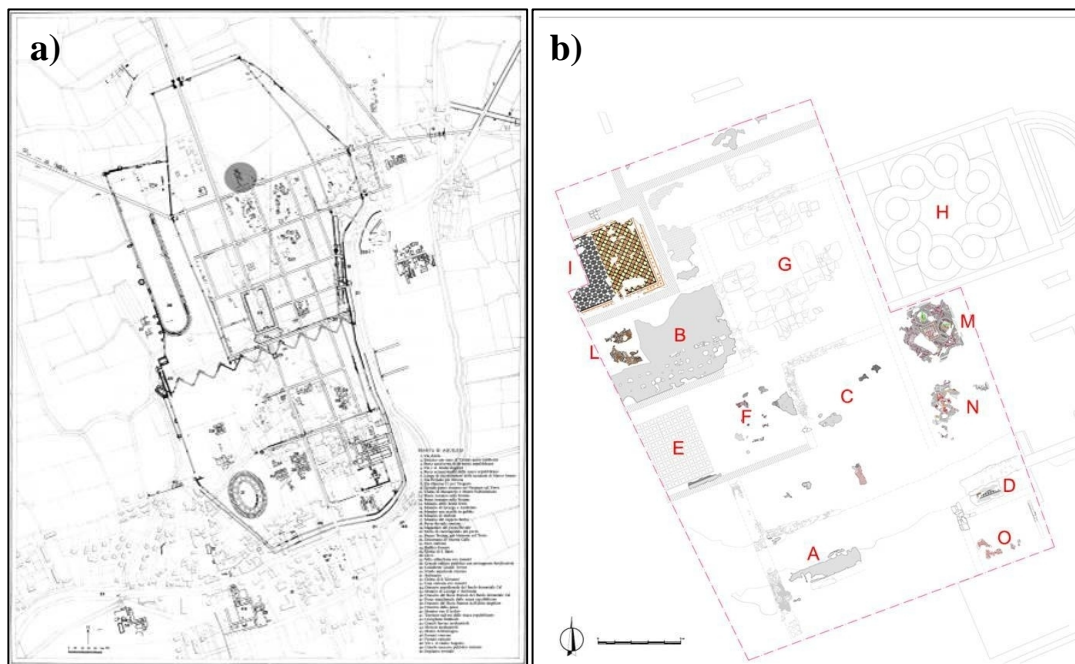


Figure 2.2.1: (a) location of Casa delle Bestie Ferite (grey circle) in the north side of the archaeological site of Aquileia; (b) Plan of Casa delle Bestie Ferite.

The reconstruction of the site history is difficult, due to the divestments in Late Antiquity, which determined, in the 7th century AD, the removal of building materials and the partial destruction of the floors. A first phase of the *domus* is well documented in the 1st century AD by remains of mosaic floors with geometric decorations;

subsequently the life of the building continued for four centuries. During the middle Imperial age the *domus* was subjected to a first restoration and in Late Antiquity (4th century AD) it was completely restructured (Bonetto and Salvadori, in press).

So far, the excavation has involved mainly the Late Antiquity phases, yielding 688 glass fragments. The findings dating between the 3rd and the 5th century AD, well corresponds to the material preserved in the Archaeological Museum of Aquileia for types, colour and production techniques (mainly mold blowing). The principal types are beakers/cups (Isings 106, 109, 96, 116, 117), bottles (Isings 104, 132, 126) and plates (Isings 118) (Isings, 1957). Otherwise, the findings dating post 5th century do not have a correspondence with the material of the Museum. They were produced by free blowing and the most represented type is the footless beaker (Isings 111) (Gallo et al., 2011).

In the present study a total of 62 glass objects, coming from this excavation, were selected and analyzed; the features of each sample (type, age, colour and production technique) are listed in Table A.2, Appendix A. The artefacts date all Late Roman/early Medieval period, from the late 3rd to the 8th century AD; in particular, two chronological groups can be distinguished: the first includes objects spanning from the late 3rd to the 5th century AD, the second from the 5th to the 8th (Table A.2).

The different chronological pattern with respect to the early Roman glasses from Adria determines differences in the aesthetic characteristics of the glass. While Adria glasses were generally intensely coloured, the typical colour of Aquileia samples is yellowish-green, sometimes colourless or light blue (Table A.2).

The analyzed objects are essentially cups (21 samples), bottles (8 samples) and beakers (32 samples); only one lamp was analyzed. The archaeological types are attributable to Isings 106c, 116, 117, 104, 87 or 120, 111 and 132 forms (Isings, 1957, Fig. 2.2.2) and the production techniques were blowing and mold-blowing (Table A.2).

2. Archaeological contexts and materials

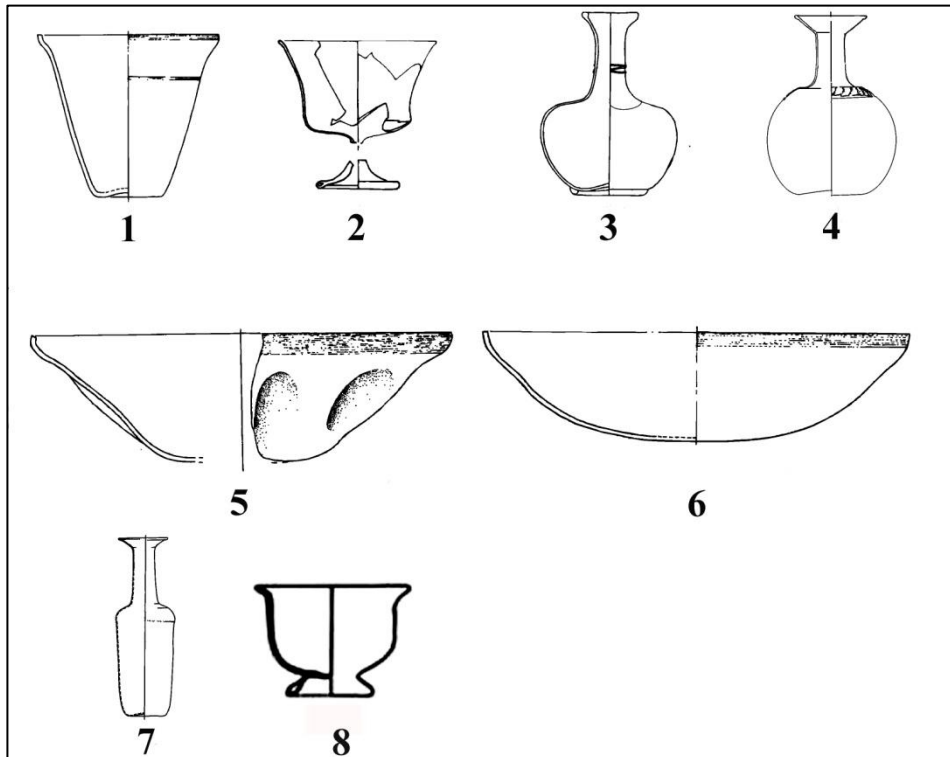


Figure 2.2.2: the archaeological types of Aquileia sample. 1) *Isings 106c*; 2) *Isings 111*; 3) *Isings 104 var a*; 4) *Isings 104var b*; 5) *Isings 117*; 6) *Isings 116*; 7) *Isings 132*; 8) *Isings 87 or 120* (courtesy of A. Marcante).

2.3 Rocca di Asolo

The Rocca di Asolo is a fort on the summit of Montericco, in Northeastern Italy, dominating the town of Asolo, an ancient settlement of the Veneti (*ca.* 9th century BC) and later a Roman *municipium*. Archaeological excavations have revealed several phases in the Montericco site. The first evidence of occupation dates to about the 6th century AD and was connected with the presence of a small church. Later (7th-10th centuries AD) the church was transformed into a monument, but already at the end of the 10th century it had decayed and was replaced by a burial area. Subsequently (10th-12th centuries) a settlement arose in the area, destroyed at the end of the 12th century when the military fortification (*Rocca*) was built. The *Rocca di Asolo* passed through various hands - including the Bishopric of Treviso, the Carraresi family from near Padova, and the Republic of Venice - until its decay, at the end of the 16th century (Bonetto, 1993; Rosada, 1989).

About 7000 glass fragments have been found in this site. There are few finds - only about 100, including window panes - dating to the early Middle Ages; otherwise, high/late Middle Ages finds are more abundant and comprise various kinds of objects (beakers, bottles, lamps) (Rigoni, 1986).

In the present study thirty-three samples were analyzed: 12 fragments of window panes, eight dating to the Early Middle Ages (7th-10th centuries AD) and four to the Late Middle Ages (15th century AD), and 21 fragments of objects dating to the High/Late Middle Ages (12th-15th centuries). For five samples decorated with blue rims, both the colourless body and the blue decoration were analysed separately, for a total of 38 samples. The age and features of the samples are listed in Table A.4, in Appendix A.

The glass window panes are pale blue, greenish, yellowish and pale brown in colour; four are fragments of pieces with regular shape: one circular (*ruo*) and three triangular (*crosetta*) (Table A.4). Two production techniques were identified: crown process (2 samples) and cylinder process (10 samples) (Table A.4). In these processes, a molten glass bubble was blown and then rolled on a smooth surface to obtain a disc-shaped crown or cylinder. In the former case, the crown was removed and cut; in the latter, the cylinder was cut lengthwise to obtain a flat sheet. The glass produced with these techniques is thinner than that produced by casting and has two smooth sides (Arletti et al., 2010; Wolf et al., 2005). The analysed objects are all for common use and include beakers and bottles. The first are of two types: beakers decorated with drops (*nuppenbecher*) (Stiaffini 1991, 1999) and flat-based beakers with blue rims (Fig. 2.3.1). The second are also of two types: the so-called *anghostere* (or *inghostere*) (Moretti, 2002), bottles with a long neck and small body, and the *kropfflaschen* (Stiaffini, 1991), characterized by a swelling at the base of the neck (Fig. 2.3.1).

2. Archaeological contexts and materials

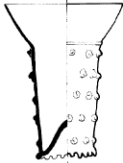

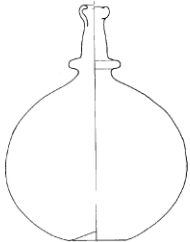
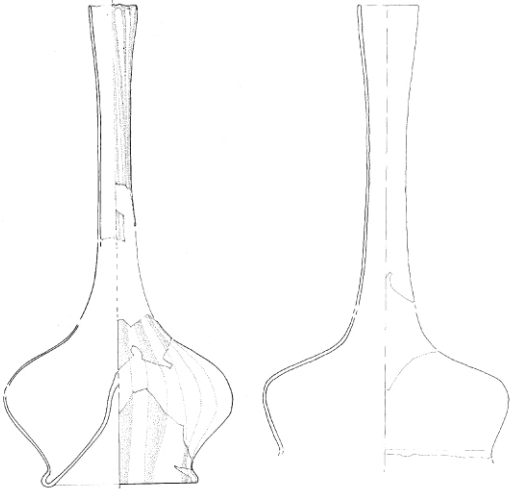
	<p>NUPPENBECHER or PRUNTED BEAKER</p>	<p><i>Stiaffini 1991, Type H2c</i></p>	
	<p>FLAT-BASED BEAKER WITH BLUE RIM</p>	<p><i>Stiaffini 1991, Type H3c</i></p>	
	<p>KROPFFLASCHE</p>	<p><i>Stiaffini 1991, Type O2b</i></p>	
		<p>INGHISTERA or ANGHISTERA</p>	<p><i>Moretti 2001</i></p>

Figure 2.3.1: Sketches of analyzed archaeological types (*nuppenbecher*, *flat-based beaker with blue rim*, *kropfflasche* and *anghistera*). References are also given (courtesy of A. Marcante).

2.4 Tuscan sites

San Genesio

The archaeological site of San Genesio, excavated from 2001 onwards, is located in the municipality of San Miniato (PI). The first finds attesting human occupation of the site are dated to the middle of the 6th century BC; the first remains of housing structures, instead, are dated to the 3rd century BC (Ciampoltrini. 2008). At the start of the 1st

century BC, the settlement was made of simple houses in wood and unfired clay. The economical crisis of the 2nd-3rd century affected also San Genesio and the surrounding area, of which the population decreased. The increase of coins, glass and ceramic finds, instead, is an indication of expansion during the 4th and the first half of the 5th century (Cagno et al., 2011). From the end of the 5th century, part of the area was used as a large necropolis; it is also possible that the area was fortified in the first half of the 6th century (Cantini 2010). In the second half of the 6th century the settlement is a well-structured village and between the end of the 6th and the beginning of the 7th century, a first small church was constructed. During the mid-11th and the second half of the 12th century the village increased in size, but, in the same period, the inhabitants of the adjacent town of San Miniato started a long series of hostilities against the village. San Genesio survived many attacks but eventually lost the war: in 1248 the San Miniatese plundered and destroyed the village (Cagno et al., 2011).

Pieve di Coneo

The church of Ss. Ippolito and Cassiano, located in the municipality of Coneo, Valdelsa (SI), was excavated during two campaigns, in 2007 and 2009. So far, the majority of excavation data are unpublished.

The first phase of the site dates to Roman Republic and is characterized from the presence of *dolia defossa*, big containers for foodstuff. For this reason it was supposed that the site was a farm. The second phase is characterized by the presence of burials, dating to Late Antiquity (6th-7th century AD). Finally the third phase show the presence of the first structure of the church, which arose in the area likely during early Middle Ages.

Pieve di Pava

The church of S. Pietro in Pava, located close San Giovanni d'Asso (SI), was excavated from 2004 onwards, but at the present the majority of the data are unpublished. The site is a long frequented context, the chronology lays between the Etruscan Period and the Middle Ages. During the excavations conducted in 2004 and 2005 were discovered a church (dated from 6th to 12th centuries AD), a necropolis (dated from 10th to 13th

2. Archaeological contexts and materials

centuries AD) and a brick-kiln (probably previous the 8th century). These chronological articulations results from carbon-14 dating (Campana et al., 2006).

A total of fifteen glass findings coming from San Genesio, Pieve di Pava and Pieve di Coneo were analyzed in the present work. The samples are typologically and chronologically similar to those of Aquileia. In particular, the majority of them (14 samples) are beakers type Isings 111 (5th-8th century AD), but one beaker type Isings 106c (late 3rd-5th century AD) is also included in the sample set. The features of each sample (type, age, colour and production technique) are listed in Table A.3, Appendix A.

CHAPTER 3

EXPERIMENTAL METHODS

In the present work a broad range of analytical techniques was employed, in order to investigate the type and the provenance of raw materials employed in the production of the 178 glass objects. For clarity, Table B.1 (Appendix B) reports all the analytical techniques used to characterize each sample. After the sample selection, the first step of the study was to evaluate the homogeneity and the texture of the glass by means of optical and electron microscopes (OM and SEM). In case of residual, newly formed and opacifying phases, a chemical semi-quantitative analysis was performed to determine their composition. Furthermore, X Ray Powder Diffraction (XRPD) was employed to identify the crystalline phase of four white glasses. The second step of the work consisted of the bulk chemistry analysis. In the case of decorated objects, both the transparent and the opaque glass were analyzed and considered as separated samples (Table B.1, Appendix B). Major, minor and trace elements of transparent samples with a sufficient weight (≥ 700 mg) were determined by X-Ray Fluorescence; S, Cl, Sb and Sn were checked by Electron Microprobe (EPMA) (Table B.1, Appendix B). On the other hand, the chemical composition of transparent glasses with a weight not sufficient to carry out XRF analysis and of glassy matrix in opaque glasses was determined by EPMA (Table B.1, Appendix B). Laser Ablation Inductively Couple Plasma Mass Spectrometry (LA-ICP-MS) was used to analyze trace elements of almost all Adria transparent glasses. Since samples AD-BB-11b, AD-I-2, AD-I-3, AD-AM-1 have been completely crushed, it was not possible to perform LA-ICP-MS analysis: their traces are therefore obtained by means XRF or EPMA (Table B.1, Appendix B). Finally, Sr, Nd and O isotopic analysis were performed on a selection of Roman and Late Roman samples from Adria and Aquileia (Table B.1, Appendix B). They were opportunely chosen in order to represent the different colour and compositional groups recognized in glass assemblages.

3. Experimental methods

A more detailed description of the experimental methods and analytical conditions employed for the textural, mineralogical, chemical and isotopic characterization of the samples is reported in the following.

3.1 Optical Microscopy (OM)

Optical microscopy, both stereoscopic and in reflected light, was carried out on whole fragments and polished sections, for a preliminary evaluation of the homogeneity, texture and state of conservation of the findings. In order to obtain polished sections, the glass artefacts were cut perpendicularly to their surfaces with a diamond saw, embedded in epoxy resin blocks, and then polished with a series of diamond pastes from 6 to 1 μm . The microscopes used are a Nikon Eclipse ME600 and a Zeiss Stemi 2000 C, of the Geoscience Department at the University of Padova.

3.2 Scanning Electron Microscopy with Energy Dispersive System (SEM-EDS)

SEM analysis, carried out at the CNR-ICIS of Padova, was performed for high-resolution morphologic inspection of glass and semi-quantitative chemical analysis of the residual, newly formed and opacifying phases present into the glass. The instrument used is a FEI Quanta 200 FEG ESEM, equipped with a field emission gun for optimal spatial resolution; it was used in high vacuum mode (HV). For chemical semi-quantitative analysis an EDAX Genesys energy-dispersive X-ray spectrometer was used, with accelerating voltage of 25 keV.

3.3 X Ray Powder Diffraction (XRPD)

X-ray diffraction analyses, carried out at the Department of Geosciences (University of Padova), were performed on a selection of four white opaque samples to identify crystalline phases dispersed in the glass matrix. Due to the small quantity of material available, the whole fragments were mounted on a goniometric head and the experiments were carried out with a Philips X'Pert PRO diffractometer, with parafocusing geometry Bragg-Brentano. The instrument is provided with a ceramic tube LFF, with copper anode and graphite crystal monochromator. The analyses were performed in the range 10° - 80° 2θ , with a step-time of 60s. To identify the phases, the

database provided by X-Pert Panalytical software was employed. The obtained spectra are reported in Appendix C.

3.4 X Ray Fluorescence (XRF)

The bulk chemistry of 105 transparent samples (Table B.1, Appendix B) was determined by X Ray Fluorescence at Geoscience Department of the University of Padova. The instrument is a Philips PW 2400, equipped with a Rh tube having a rated capacity of 3 kW (60 kV/ 125 mA max.). Three primary collimators (150, 300 and 700 μm spacing) and four analytical crystals (TlAp100, LiF200, Ge111 and PE002) were selected. The spectrometers was interfaced to a personal computer with SuperQ software from Philips which allowed determination of Si, Ti, Al, Fe, Mn, Mg, Ca, Na, K e P (major and minor elements, expressed as percentage concentrations of element oxides) and Sc, V, Cr, Co, Ni, Cu, Zn, Ga, Rb, Sr, Y, Zr, Nb, Ba, La, Ce, Nd, Pb, Th e U (trace elements, expressed as parts per million, ppm).

About 70 geological standards were used for calibration. The samples were first cleaned from possible alteration patina and then crushed into an agate mortar. The resulting powders were put in an oven at 110°C for 12 h and the loss on ignition (LOI) was determined. The powders were then mixed with $\text{Li}_2\text{B}_4\text{O}_7$ in a 1:10 ratio and beads were prepared. Precision is better than 0.6% for major and minor elements, and about 3% for trace elements. The XRF accuracy was checked by reference standards (Govindaraju, 1994) and was within 0.5 wt% for Si, lower than 3% for other major and minor elements, and lower than 5% for traces. The lowest detection limits of XRF were within 0.01 wt% for Al_2O_3 , MgO and Na_2O , within 0.2 wt% for SiO_2 , within 0.005 wt% for TiO_2 , Fe_2O_3 , MnO, CaO, K_2O and P_2O_5 and within a range between 1 and 10 ppm for trace elements. The XRF analyses allowed determination of all the chemical components that characterize archaeological glass, excluding Cl, S, Sn and Sb, which were checked by EPMA.

3.5 Electron Probe Microanalysis (EPMA)

A total of 99 bulk glass compositions were determined by EPMA: 76 are relative to transparent samples and 23 to glassy matrices of opaque glasses (Table B.1, Appendix B). EPMA measures were checked against a homogeneous soda–lime glass, analyzed

3. Experimental methods

previously by XRF and the results fitted perfectly: the differences fall into the experimental error of EPMA. The electron microprobe used for quantitative analysis of major and minor elements was a CAMECA SX50 of the IGG-CNR of Padova, equipped with four wavelength-dispersive spectrometers (WDS). Analyzed elements were: Na, Mg, Al, Si, P, S, Cl, K, Ca, Ti, Mn, Fe, Sb, Co, Ni, Cu, Zn, Sn and Pb. The followed standards were employed: synthetic pure oxides for Mg, Al, Fe, Sn, a synthetic MnTi oxide for Mn and Ti, albite for Na, diopside for Si and Ca, apatite for P, sphalerite for Zn and S, vanadinite for Cl, orthoclase for K, Sb₂S₃ for Sb, PbS for Pb, and pure elements for Co, Ni, Cu.

For the transparent glasses, ten analytical points were made along a line crossing the thickness of the polished sections of each sample, and means and standard deviations were calculated. The standard deviations range between 0.02 and 0.80 for major elements and from 0.01 to 0.45 for minor and trace elements, thus proving the homogeneity of the glass fragments. For Na, K, Si and Al the operating conditions were 20 kV and 2 nA sample current, with beam defocused at not less than 10 μ m and an acquisition time of 10 s for peak and background, in order to minimize the loss of alkali elements and better evaluate Si contents. For the other elements the operating conditions were 20 kV and 30 nA sample current; the acquisition time was 10 s peak and 10 s background for Ca, 10 s peak and 5 s background for Mg, P, Ti, Mn and Fe, 40 s peak and 20 s background for S, Cl, Co, Cu, Zn, Sn and Pb. X-ray counts were converted to oxide weight percentages with the PAP (CAMECA) correction program. The detailed analytical conditions used and the precision, accuracy and detection limits of EPMA are given in Silvestri and Marcante (2011), as the present samples were subjected to the same analytical protocol. It is stressed here that the precision and accuracy of data were calculated by comparisons with measures on the international reference standard, Corning glass B, in the same analytical conditions as the Adria glass. The precision of EPMA data was generally between 0.5% and 10% for major and minor elements, respectively. Accuracy was better than 1% for SiO₂, Na₂O and FeO, better than 5% for CaO, K₂O, P₂O₅ and Sb₂O₃, and not worse than 12% for other major and minor elements, except TiO₂ (Silvestri and Marcante, 2011).

The glassy matrix of opaque glass was analyzed using a different analytical protocol, in order to minimize the chemical contribution of the inclusions and obtain a bulk

composition as clean as possible. In a first step, Na, Mg, Al, Si, P, K, Ca, Mn and Fe were measured on about eight analytical points, randomly made. Since the inclusions are essentially constituted of lead and calcium antimonate (See section 4.1.1), Sb was also measured, as check of the analysis. For Na, K, Si and Al, operating conditions were 20 kV and 2 nA sample current and acquisition time of 10 s for peak and background, in order to minimize the loss of alkali. For Fe, Mn, P, Ca, Sb, Mg operating conditions were 20 kV and 30 nA sample current and acquisition time of 10 s for peak and 5 s for the background. The beam was focused at around 1 μm and standard deviations range between 0.01 and 1.50. X-ray counts were converted to oxide weight percentages with the PAP (CAMECA) correction program. In the second step, back-scattered electrons images were acquired for each sample and Sb, Pb, S, Cl, Ti, Cu, Co, Ni, Zn were measured on about eight analytical points, avoiding the inclusions. The operating conditions were 20 nA and 20 kV; the beam was focused at around 1 μm and the acquisition time was 10 s for peak and background for S, Cl, Sb and Pb, 20 s peak and 10 s background for the other elements. Standard deviations range between 0.01 and 0.99. Finally, to match the analyses acquired during the two steps, Sb data were used as ‘control element’: only first step analyses with Sb contents comparable with those of the second step were chosen, since considered representative of the only glass matrix, without the contribution of the opacifiers.

3.6 Laser Ablation Inductively Coupled Plasma Mass Spectrometry (LA-ICP-MS)

LA-ICP-MS, carried out at the IGG-CNR of Pavia, was employed as complementary technique to XRF and EPMA for measuring trace elements concentrations of 62 transparent samples from Adria (Table B.1, Appendix B). The probe was composed of an Elan DRC-e mass spectrometer coupled with a Qswitched Nd:YAG laser source (Quantel Brilliant), the fundamental emission of which (1064 nm) was converted to 266 nm by two harmonic generators. Helium was used as carrier gas, mixed with Ar downstream of the ablation cell. Each sample was analyzed in spot mode; routine analyses consisted in acquiring 1 min background and 1 min ablated sample: spot diameter was typically in the range of 50 μm and penetration rate was about 1 $\mu\text{m/s}$. NIST SRM 610 glass was used as external standard and Ca44 as internal standard, the

3. Experimental methods

concentration of which was also compared with that already measured by EPMA. Precision and accuracy, both better than 10% for concentrations at ppm level, were assessed by repeated analyses of the BCR-2g standard. Detection limits varied as a function of background counts and the sensitivity of the various masses: they were typically in the range 1-3 ppm for Ti, Cr and Fe, 100-500 ppb for Sc, V, Zn and Mn, 10-100 ppb for Rb, Sr, Zr, Cs, Gd, Sn, Sb, Ba, Hf and Pb, and 1-10 ppb for Y, Nb, Sm, Eu, Tb, Dy, Er, Yb, Th, U, La, Ce, and Nd. The precision and accuracy of data were calculated by comparisons with measures on the international reference standard, Corning glass B, in the same analytical conditions of the Adria glass (Silvestri and Marcante, 2011); for most trace elements, precision was about 2% and accuracy highly variable, but usually within 5-20%. In any case, the same accuracy range was also reported for LA-ICP-MS measurements, carried out on the same standard by Vicenzi et al. (2002). Some minor or trace elements were determined by both EMPA (Ti, Mn, Fe, Sb, Co, Cu, Zn, Sn, Pb) or XRF (Ti, Mn, Fe, Co, Cu, Zn, Ni, Rb, Sr, Ba, Zr, Nd, La, Ce, Th, U, V, Ga, Y, Nb, Cr, Pb) and LA-ICP-MS. When the considered elements are present in concentrations above the EPMA detection limits, EPMA and LA-ICP-MS data show good accuracy. However measures on some elements (e.g. Mn, Ti, Sb, Cu, Pb), are affected by low accuracy, likely due to a systematic error. On the other hand, a generally good precision and accuracy appear when comparing XRF and LA-ICP-MS data, except for Rare Earth Elements (REE). Taking into account the lower detection limits and the high precision of LA-ICP-MS for trace elements, its data were therefore chosen and reported in the present study (see Table D.2, Appendix D)..

3.7 Multi Collector Inductively Coupled Plasma Mass Spectrometry (MC-ICP-MS)

Thirty-eight samples, 20 Roman glasses from Adria and 18 Late Roman glasses from Aquileia, were selected to perform Sr and Nd isotope analysis (Table B.1, Appendix B). The analyses were performed in collaboration with the Prof. Patrick Degryse (Earth Science Department of the University of Leuven, Belgium); the lab work was conducted at Ghent University (Belgium).

Dissolution of glass was accomplished by hotplate digestion in Savillex screw-top beakers. Prior to analysis, glass samples were carefully cleaned of any alteration

products, in order to avoid contamination of results, and then finely crushed in an agata mortar. About 100 mg of the resulting powder were put into the Savillex screw-top beakers and a 3:1 mixture of 22 M HF and 14 M HNO₃ was added, followed by heating at 110°C for 24 h. The sample digests were subsequently evaporated and dissolved in a mixture 3:1 of 12 M HCl and 14 M HNO₃ (aqua regia). Again, the samples were heated for 24 h at 110 °C and subsequently evaporated to dryness; 2 ml of 7 M HNO₃ was added to the residue and heated on the hotplate for about 30 minutes. The concentrations of Sr and Nd were doubled-checked using a quadrupole-based Perking-Elmer SCIEX Elan 5000 ICP-MS instrument. An internal standard (In) was used to correct for the signal fluctuation, and the calibration was performed with an external standard containing known amounts of the element analyzed. For the isolation of Sr and Nd sequential extraction methods (Pin et al., 1994; Pin and Zalduegui, 1997; De Muynck et al., 2009) were followed and slightly modified.

The Sr fraction of the sample digests was isolated from the sample matrix via an extraction chromatographic separation using a Sr-selective resin (Sr specTM); 0.1 ml of sample, dissolved in 7M HNO₃, were loaded onto the resin. Then, the resin was rinsed first with 5 ml of 7 M HNO₃ and then with 500 µl of 0.05 M HNO₃ solution to remove matrix elements, while Sr is retained by the resin. The purified Sr fraction was subsequently stripped off the resin by rinsing with 5 ml of 0.05 M HNO₃.

The isolation of Nd involved a 2-step chromatographic separation. The sample, taken up in 1 ml of 2M HNO₃, was loaded into Micro-BioSpin columns (BioRad) filled with TRUSpec resin (Eichrom), and was washed with 4 ml of 2M HNO₃. The Micro-BioSpin column was then coupled with an Eichrom column filled with LnSpec resin (Eichrom), and was rinsed with 7 ml of 0.05M HNO₃ in order to elute the LREE fraction from the TRUSpec resin into the LnSpec resin. The LnSpec resin was then washed with 5 ml of 0.25M HCl, and the Nd fraction was stripped off using 9 ml of 0.25M HCl.

All measurements were carried out using a Thermo Scientific Neptune multi collector inductively coupled plasma mass spectroscopy (MC-ICP-MS), equipped with a micro-flow PFA-50 Teflon nebuliser, and running in static multicollection mode. The operating parameters are given in Table 3.7.1. NIST SRM 987 standard was used as

3. Experimental methods

reference material for Sr isotope ratio measurements ($^{86}\text{Sr}/^{88}\text{Sr} = 0.1194$) to correct for instrumental mass discrimination based on external standardization.

Conditions	Sr	Nd
Power	1.2 kW	1.3 kW
Plasma gas flow	15 L/min	15 L/min
Auxiliary gas flow	0.6 L/min	0.6 L/min
Nebulizer flow	1.05 L/min	1.05 L/min
Data acquisition	30 cycles	50 cycles
Integration time	5 s	5 s
Mass resolution	400	400
Sample delivery	Auto aspiration	Auto aspiration

Table 3.7.1: MC-ICP-MS operating parameters

Repeated analyses of NIST SRM 987 SrCO₃ yielded average $^{87}\text{Sr}/^{86}\text{Sr}$ ratios with corresponding 2σ uncertainty interval of 0.710263 ± 0.00001 , in perfect agreement with the accepted $^{87}\text{Sr}/^{86}\text{Sr}$ ratio of 0.710248 for this material (Thirlwall, 1991). For the measurements of $^{143}\text{Nd}/^{144}\text{Nd}$, JNdi-1 standard (Geological Survey of Japan) was used as reference material ($^{143}\text{Nd}/^{144}\text{Nd} = 0.51515$, $^{146}\text{Nd}/^{144}\text{Nd} = 0.7219$).

3.8 High temperature fluorination

Oxygen isotope measurements were carried out in collaboration with Prof. A. Longinelli (Department of Earth Science, University of Parma). The sample set is composed of the same 38 samples analyzed by MC-ICP-MS; in addition two other Roman glasses from Adria were analyzed, for a total of 40 samples (Table B.1, Appendix B). The analyses were performed according to the well-established technique of high-temperature fluorination. About 6–7 mg of the glass powder were put into the nichel vessels of a fluorination line. After degassing the vessels to better than 10^{-3} mmHg for at least 2 h and freezing them to the temperature of liquid nitrogen, a five-fold stoichiometric amount of BrF₅ was introduced into each vessel and the samples were reacted at 600 ± 5 °C for periods of 20 h. The O₂ liberated by the reaction was

converted to CO₂ by cycling over hot graphite in the presence of a platinum catalyst and the CO₂ was measured in a Finnigan Delta S mass spectrometer versus a laboratory standard CO₂ prepared from very pure Carrara marble, the isotopic compositions of which, calibrated periodically versus NBS- 19 and NBS-20¹, are +2.45‰ (δ¹³C versus VPDB) and -2.45‰ (δ¹⁸O versus VPDB). For these calibrations, NBS-19 isotopic values were taken as +1.95‰ (δ¹³C) and -2.20‰ (δ¹⁸O) and NBS-20 values as -1.06‰ (δ¹³C) and -4.14‰ (δ¹⁸O). The reported δ¹⁸O values of glass samples are the mean of two consistent measurements of each sample; the standard deviation ranges between 0 and 0.2. Isotopic results are reported in the usual delta terminology versus the VSMOW isotopic standard, delta being defined as follows:

$$\delta = [(R_{\text{sample}} - R_{\text{standard}})/R_{\text{standard}}] \times 1000$$

where R is the ratio between the heavy and the light isotope.

¹ NBS 20 standard material is no more available from a very long time. In the laboratory where the analyses were performed there are reasonable amounts of NBS 19 and NBS 20 inherited from various research centers where the Prof. A. Longinelli has worked through time. However, NBS 20 is now consumed, raising the serious problem of finding a reliable reference material to calibrate the laboratory standard. The existing LSVEC is isotopically too far from the Carrara laboratory standard, both oxygen and carbon, and is consequently unreliable for calibration purposes

CHAPTER 4

RAW MATERIALS IN GLASS PRODUCTION: THE TEXTURAL, CHEMICAL AND MINERALOGICAL STUDY

4.1 Pre-Roman and Roman Glass from Adria

The textural, chemical and mineralogical and characterization of the 68 glass findings coming from Adria are reported in the following. As detailed in section 2.1, the sample set is mostly composed of Roman glass (1st-3rd century AD), although Pre-Roman objects (*oinokai*, *aryballoi* and *amphoriskoi*) are also present. All Pre-Roman artefacts and the majority of Roman objects are intentionally coloured; some of them are completely transparent, some completely opaque and some have a transparent body with opaque decorations. As concerns the last type, the transparent body and the glassy matrix of the decorations were analyzed separately, for a total of 89 bulk chemical analyses (Table B, Appendix B).

4.1.1 Textural characterization

OM and SEM analyses on polished sections revealed that all Roman transparent glasses are homogeneous, nor newly formed neither residual phases were recognized. On the other hand the seven Pre-Roman samples, all core-formed, show numerous inclusions in the transparent blue body, discussed in the following sections.

4.1.1.1 Residual and newly formed phases

On the basis of the microtextural examinations, the inclusions observed in core-formed glasses can be distinct into residual and newly formed phases. The formers have not a regular geometrical shape, usually appear like drops dispersed into the glassy matrix or crystal partially dissolved, with rounded edges (Fig. 4.1.1); the latter have instead euhedral habit, with well-formed faces (Fig. 4.1.2). Residual phases have been recognized in all the seven core-formed glasses, while newly formed crystals have been observed in four of them (AD-NF-1; AD-NF-2; AD-NF-6; AD-NF-7). Semiquantitative

4. Raw materials in glass production: the textural, chemical and mineralogical study

EDS analyses of each of these phases are reported in Tables 4.1.1 and 4.1.2 and the correspondent analysis points are indicated in Figs. 4.1.1 and 4.1.2.

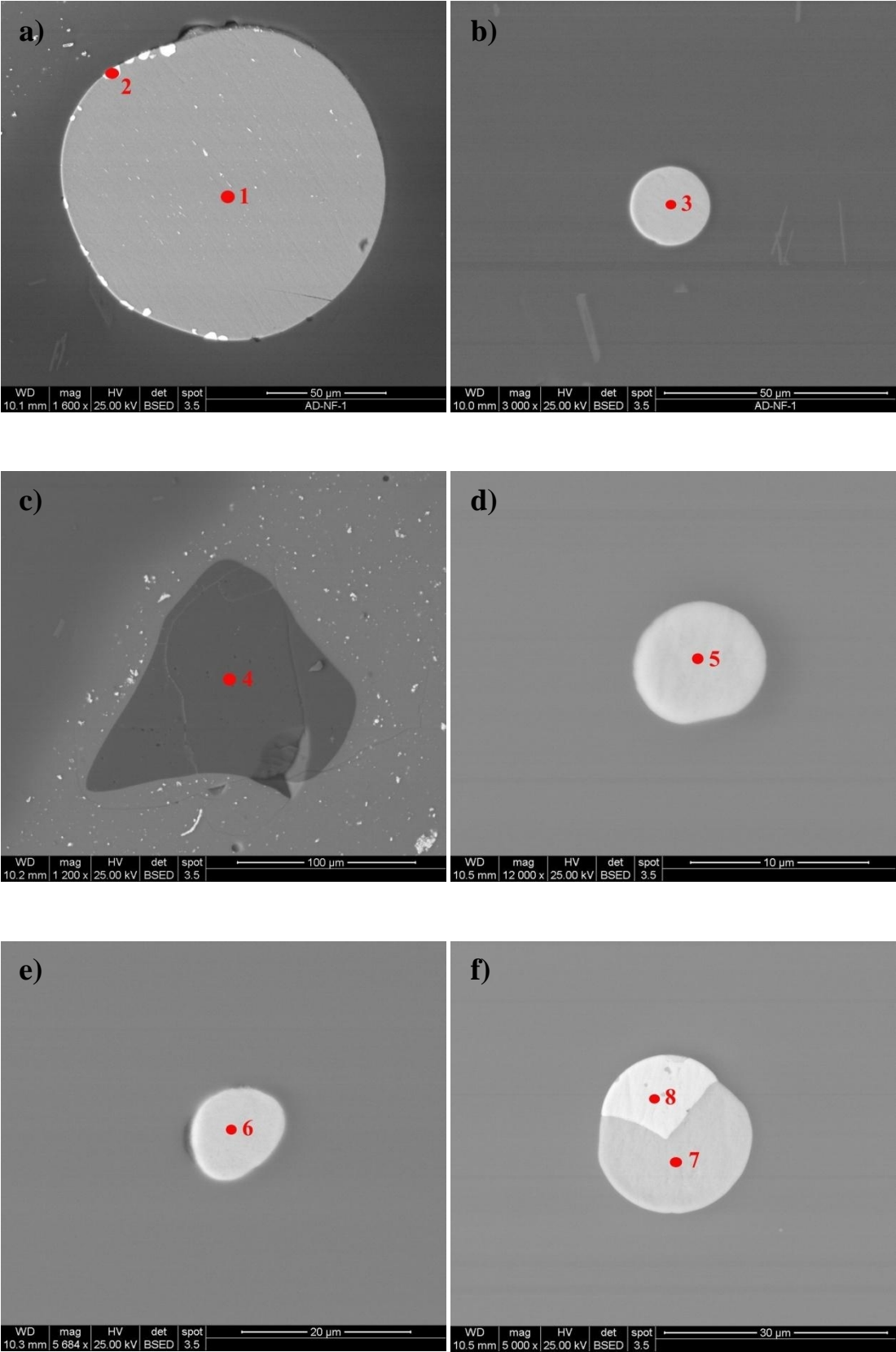
RESIDUAL PHASES																	
SAMPLE ANALYSIS	1	2	3	4	5	6	7	8	9	10	11	12	13	14	15	16	17
MgO	-	-	-	-	-	-	-	-	-	0.7	-	-	-	1.7	0.6	-	-
Al ₂ O ₃	-	-	-	-	-	-	-	-	-	-	-	-	-	1.2	3.6	-	-
CaO	-	-	-	-	-	-	-	-	-	-	-	-	-	-	0.6	-	-
SiO ₂	-	-	-	100	0.6	-	-	-	-	1.2	-	-	-	0.9	1	-	100
Sb ₂ O ₃	-	-	-	-	-	-	-	45.9	-	30.6	-	-	-	-	-	-	-
SO ₃	35.7	-	36.1	-	36.8	37	36.3	-	35.6	4	34.8	-	35.8	-	-	1.7	-
Fe ₂ O ₃	-	-	-	-	0.5	-	-	-	-	-	-	0.5	-	33.4	58.7	2.3	-
CoO	-	-	-	-	-	-	-	-	-	-	-	2.7	-	50.4	27.3	1.8	-
NiO	-	-	-	-	-	-	-	-	-	-	-	1.5	-	13.4	7.3	6.7	-
CuO	64.3	7.9	63.9	-	62.1	63	63.7	50.9	64.4	63.5	65.2	98.3	64.2	-	-	80	-
As ₂ O ₃	-	-	-	-	-	-	-	3.1	-	-	-	-	-	-	-	5.6	-
PbO	-	92.1	-	-	-	-	-	-	-	-	-	-	-	-	-	-	-

Table 4.1.1: chemical composition, expressed as wt%, of the residual phases observed in core-formed vessels. Data are semiquantitative (EDS data).

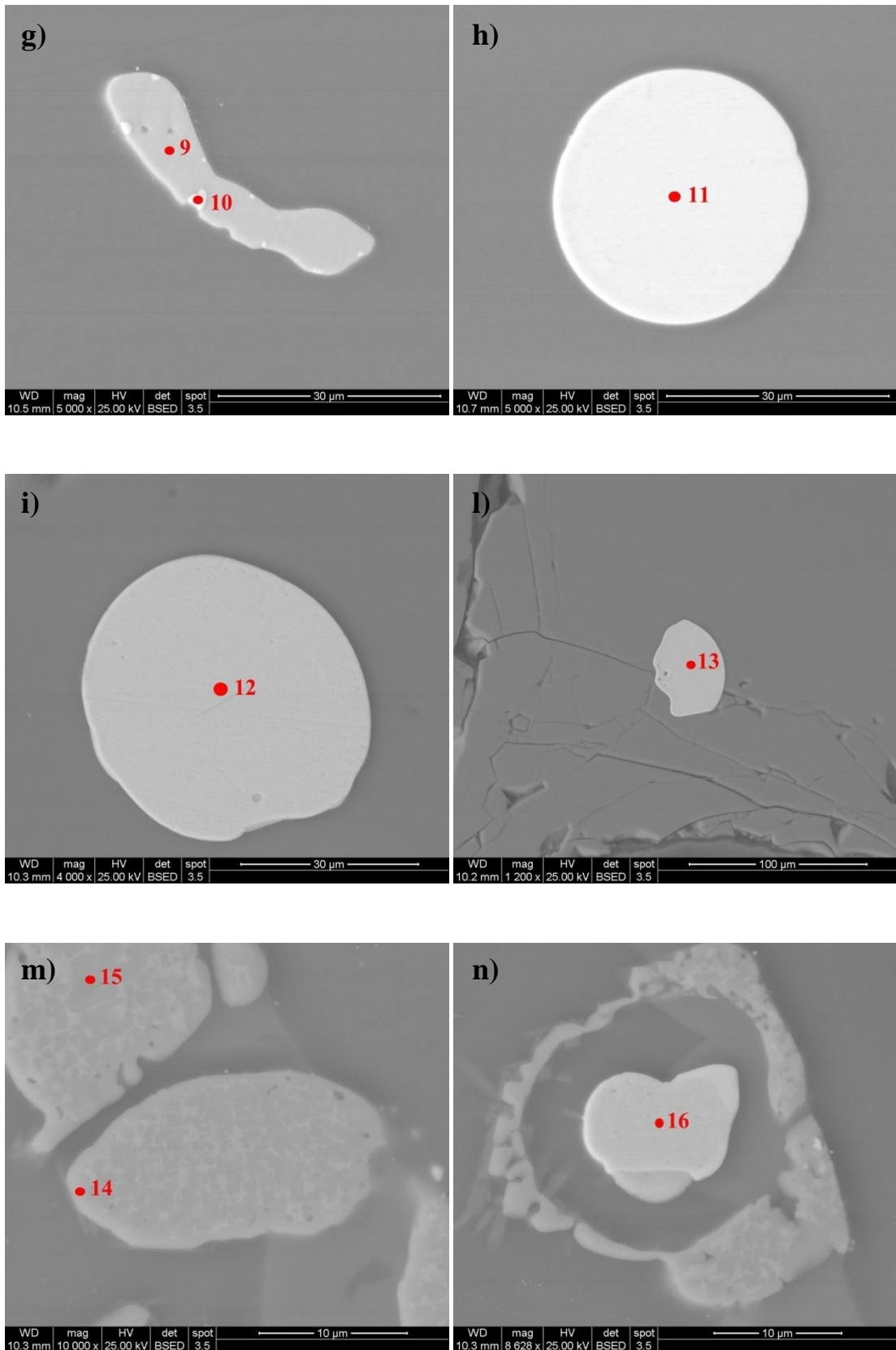
NEO-FORMATION PHASES						
SAMPLE ANALYSIS	AD-NF-1	AD-NF-2	AD-NF-6	AD-NF-7	AD-NF-7	AD-NF-7
ANALYSIS	19	20	21	22	22	22
Na ₂ O	-	1.39	-	1.75	-	-
MgO	-	-	-	0.41	-	-
Al ₂ O ₃	-	1.5	-	0.88	-	-
CaO	46.74	43.31	46.3	42.49	-	-
SiO ₂	53.26	53.8	53.7	54.47	-	-

Table 4.1.2: chemical composition, expressed as wt%, of the newly formed phases recognized in some core-formed glasses. Data are semiquantitative (EDS data).

4. Raw materials in glass production: the textural, chemical and mineralogical study



4. Raw materials in glass production: the textural, chemical and mineralogical study



4. Raw materials in glass production: the textural, chemical and mineralogical study

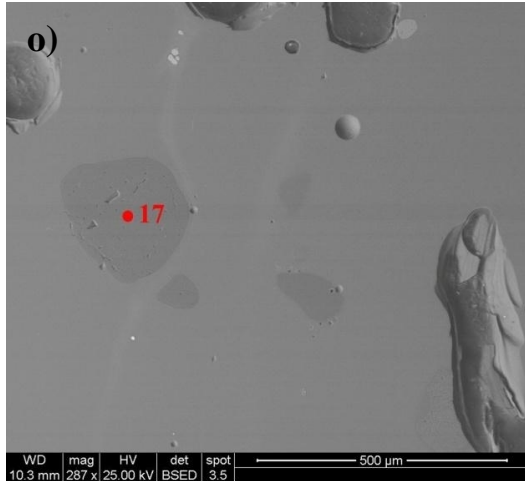


Figure 4.1.1: SEM-BSE images of the residual phases in blue glass bodies (a-b; d-o) or in the decorations (c). Numbers indicate the EDS analyses reported in Table 4.1.1. (a)-(c) AD-NF-1; (d) AD-NF-2; (e) AD-NF-3; (f)-(g) AD-NF-5; (h) AD-NF-6; (i)-(o) AD-NF-7.

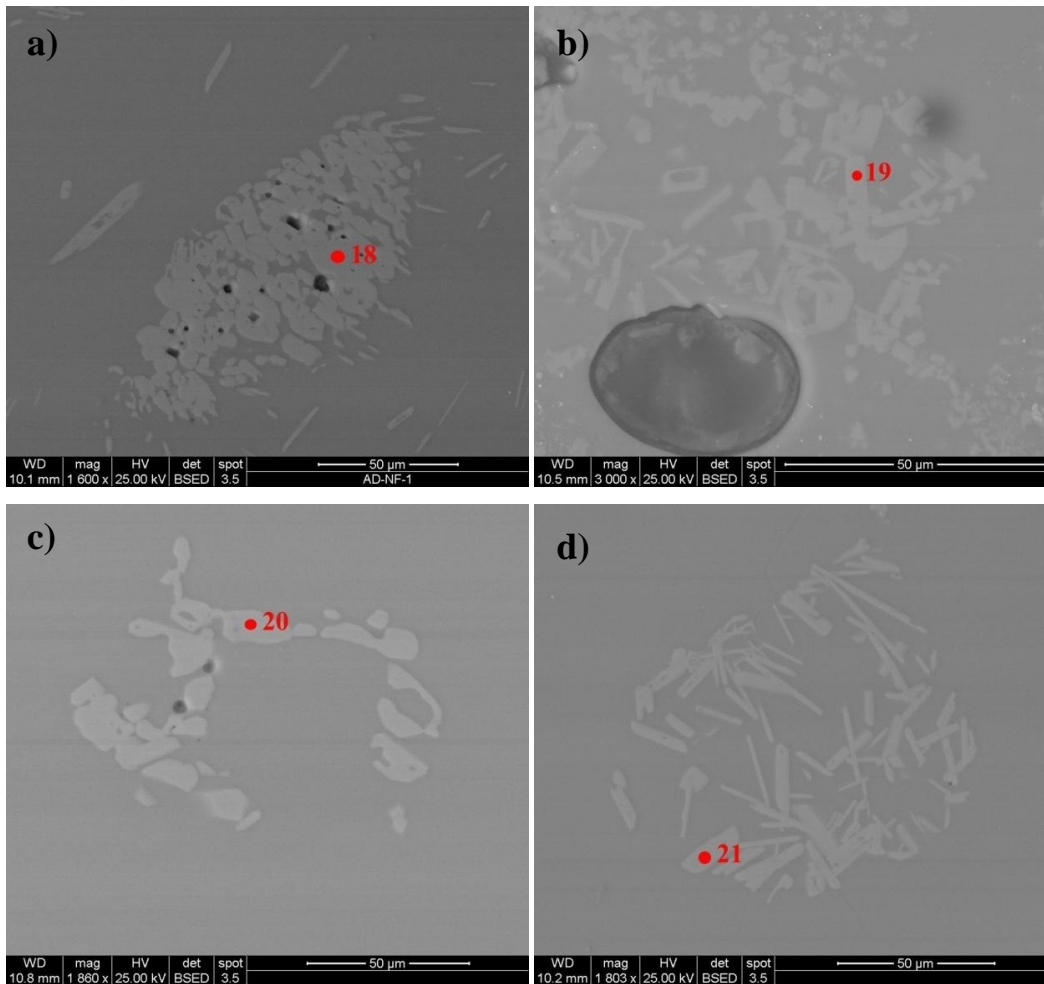


Figure 4.1.2: SEM-BSE images of the newly formed phases in blue glass bodies (a; c-d) or in the decorations (b). Numbers indicate the EDS analyses reported in Table 4.1.2. (a) AD-NF-1, (b) AD-NF-2; (c) AD-NF-6; (d) AD-NF-7.

4. Raw materials in glass production: the textural, chemical and mineralogical study

Some residual phases are composed of relics of quartz (analyses 4, 17, Tab. 4.2.1, Fig. 4.1.1, c, o) and have been observed both in the blue transparent glass and in the opaque decorations (Fig. 4.1.1, c). They are probably residues of the siliceous raw material (sand) partially dissolved in the glass during its making. The other residual phases are all drop-shaped, with a diameter from about 10 to 70 μm , and are dispersed only in the blue body. The vast majority of them are constituted of copper sulfides (analyses 1, 3, 5, 6, 7, 9, 11, Tab. 4.1.1., Fig. 4.1.1) with a rather homogeneous chemical composition ($\text{CuO} = 60.8\text{-}65.2 \text{ wt}\%$, $\text{SO}_3 = 31.4\text{-}36.3 \text{ wt}\%$, Tab. 4.1.1) and a stoichiometric ratio close to that of chalcocite (Cu_2S). In two glasses the copper sulfides show metallic segregations: Pb with small quantity of copper in AD-NF-1 (analysis 2, Tab. 4.1.1, Fig. 4.1.1, a) and Sb-Cu, sometimes with As, in AD-NF-5 (analyses 8, 10, Tab. 4.1.1, Fig. 4.1.1, f, g). Metallic drops of copper alloyed with Fe-Co-Ni (analysis 12, 16, Tab. 4.1.1, Fig. 4.1.1, i, n) and inclusions containing Fe-Co-Ni in different amounts (analyses 14, 15, Tab. 4.1.1, Fig. 4.1.1, m) have been recognized in sample AD-NF-7. Small quantity of SiO_2 , Al_2O_3 , MgO and CaO in some analyses (4, 10, 14, 15, Table 4.1.1) are probably attributable to the contribution of the glass embedding the inclusions, since their small sizes.

As it will be discussed in the section 4.1.2, cobalt is the main colouring agent in all these blue glasses. This element may occur in copper minerals, in iron and manganese ores (absolites), and in combination with arsenic and sulphur (as cobaltite CoAsS), or nickel and arsenic (as skutterudite $(\text{Co}, \text{Ni}, \text{Fe})\text{As}_3$). Trace elements often associated with cobalt minerals are Pb, Sb, Ni, Mn, Zn, Bi, Fe (Henderson, 1985). In the light of these considerations, the inclusions found in the Pre-Roman blue samples could likely interpreted as melted residues of a cobalt-bearing raw material added to colour the glass and not completely homogenized in the melt (for more details see section 4.1.2.1).

The only newly formed phase recognized in four core formed samples, both in the transparent and opaque glass, is constituted of wollastonite (CaSiO_3 , analyses 18, 19, 20, 21, Table 4.1.2, Fig. 4.1.2, a-d). It is a typical devitrification product, representing the onset of crystallization within a slowly cooled melt (Messiga and Riccardi, 2001); furthermore the presence of wollastonite indicates that the minimum temperature reached during the glass production was between 900° and 1000°C .

4. Raw materials in glass production: the textural, chemical and mineralogical study

4.1.1.2 Opacifying agents

Glass is usually opacified by small crystalline particles, called opacifiers, dispersed in the vitreous matrix and having a size higher or equal to the visible light wavelength. The difference of refractive index between the two phases prevents light from being completely transmitted and leads to the opacification of the glass (Lahlil et al., 2008). Opacifiers can be distinguished in primary and secondary on the basis of their production technology. Primary opacifiers are directly added to the glass melt and have a melting temperature higher than the kiln temperature; generally they are characterized by anhedral habitus and are distributed in inhomogeneous aggregates in the glassy matrix (Verità, 2000). On the other hand secondary opacifiers crystallize *in situ* during the glass production process and usually present a euhedral habitus (Verità, 2000).

Calcium Antimonate

Calcium antimonate, either $\text{Ca}_2\text{Sb}_2\text{O}_7$ or CaSb_2O_6 , was the first opacifying agent used in glass production (Mirti et al., 2002; Newton and Davison, 1996; Henderson, 1985). It was employed since the 2nd millennium BC (Mass et al., 1998), but the end of its production is still debated. Notwithstanding the presence of calcium antimonate in opaque glasses is documented until the end of the first millennium AD (Henderson, 1985; Freestone, 1993) and in some glasses dating 16th century AD (Costagliola et al., 2000), many authors assert that its use stopped at the end of 4th century AD, since antimony-based opacifiers were gradually replaced by tin-based opacifiers (Mass et al., 1998; Henderson, 2000; Greiff and Schuster, 2008).

The use of calcium antimonate opacifiers in all white (17 samples), light blue (2 samples), opaque blue (1 sample) and wisteria (2 samples) glasses from Adria, both Pre-Roman and Roman in date, is suggested by SEM/BSE observations coupled with EDS analysis, which revealed the presence of Ca and Sb in the crystals dispersed in the glassy matrix. Unfortunately the calculation of the ratio Ca/Sb was not possible, due to the overlap between CaK and SbL peaks in the EDS spectra. However XRD measurements performed on four white glasses (AD-BB-3, AD-BO-1, AD-BO-2, AD-BO-3) clearly revealed the presence of calcium antimonate in the orthorhombic form $\text{Ca}_2\text{Sb}_2\text{O}_7$ (Appendix C), suggesting they were produced below 927°C , since orthorhombic calcium antimonate is the stable phase under this temperature (Butler et al., 1950; Lahlil et al., 2008).

4. Raw materials in glass production: the textural, chemical and mineralogical study

As shown in Figg. 4.1.3, a, b, the microstructure of white and wisteria glasses (AD-BO-2, AD-P-1) is characterized by a homogeneous distribution of small geometrical crystals (size 1-5 μm), randomly dispersed in a vitreous matrix, with several aggregates of various size (from 5 to 50 μm). On the contrary, opacifiers in light blue and opaque blue glass show different microtextures: they are partially dissolved into the glassy matrix and lower in number than in white and wisteria glasses (Fig. 4.1.3, c), suggesting a different production technology.

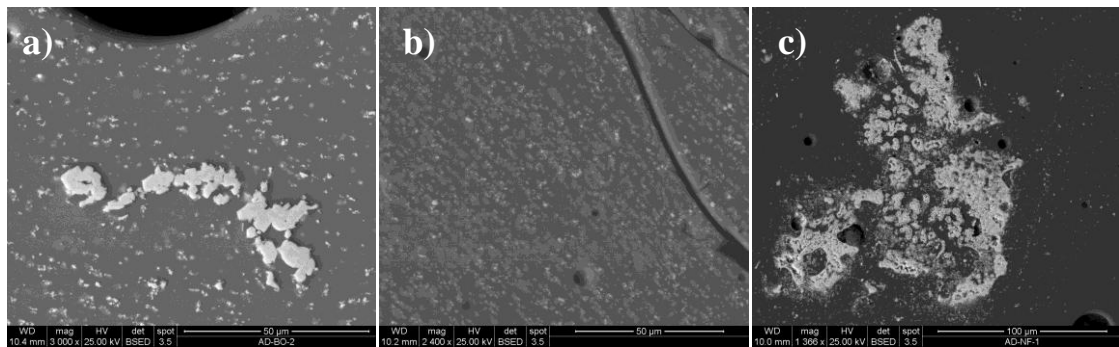


Figure 4.1.3: SEM-BSE images of calcium antimonate opacifiers (lighter grey) embedded in a glassy matrix (darker grey). (a)-(b) white and wisteria glass (AD-BO-2, AD-P-1); (c) light blue glass (AD-NF-1).

As reported in many studies (Bimson, 1983; Lahlil et al., 2006; Lahlil et al., 2008; Lahlil et al., 2010 a, b), the euhedral shape of calcium antimonate in white/wisteria glass suggests that it is a secondary opacifier, precipitated *in situ* from antimony and calcium raw materials separately introduced into the batch. The light blue/blue glass was likely obtained by adding an opaque white glass, previously produced, to a transparent light blue/blue glass, as already observed by Tonietto, (2010) for paleo-Christian glass mosaics.

Lead and Lead-Tin Antimonate

Lead antimonate ($\text{Pb}_2\text{Sb}_2\text{O}_7$) was the main yellow opacifying colourant in ancient glasses and glazes from the 15th BC to the 4th century AD (Brill, 1988; Mass *et al.*, 1998). The natural $\text{Pb}_2\text{Sb}_2\text{O}_7$ is the mineral bindheimite, also known as Naples yellow (Mass *et al.*, 1998). For synthetic lead antimonate different raw materials have been hypothesized; Mass *et al.* (2002) suggested that both lead and antimony originate from the same raw material, such as antimonial litharge from the cupellation of antimonial

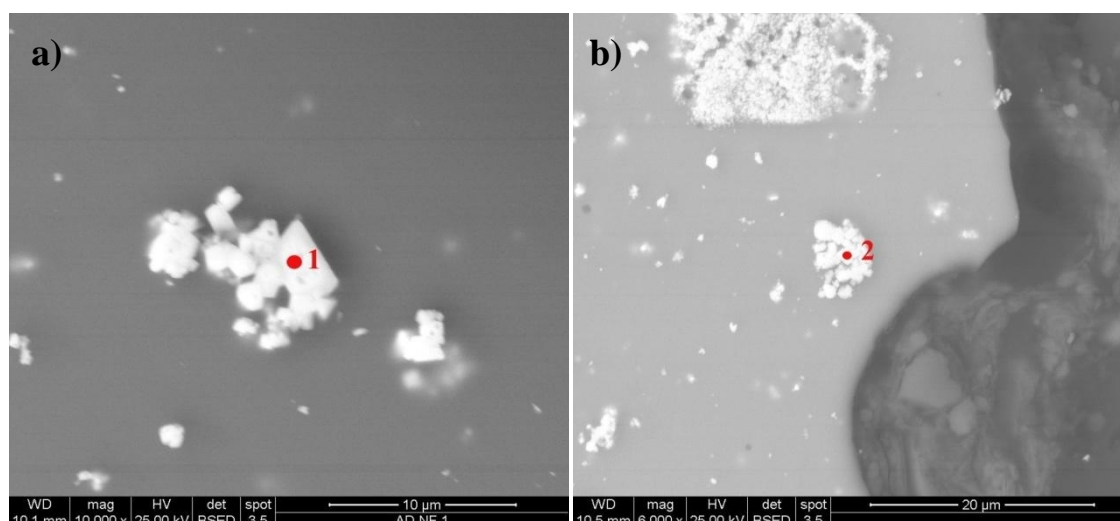
4. Raw materials in glass production: the textural, chemical and mineralogical study

silver ores. In contrast, other authors (Shortland, 2002, 2003; Arletti et al., 2006) stated that lead and antimony come from different sources and that lead antimonate opacifiers were produced by roasting galena and stibnite in an excess of lead.

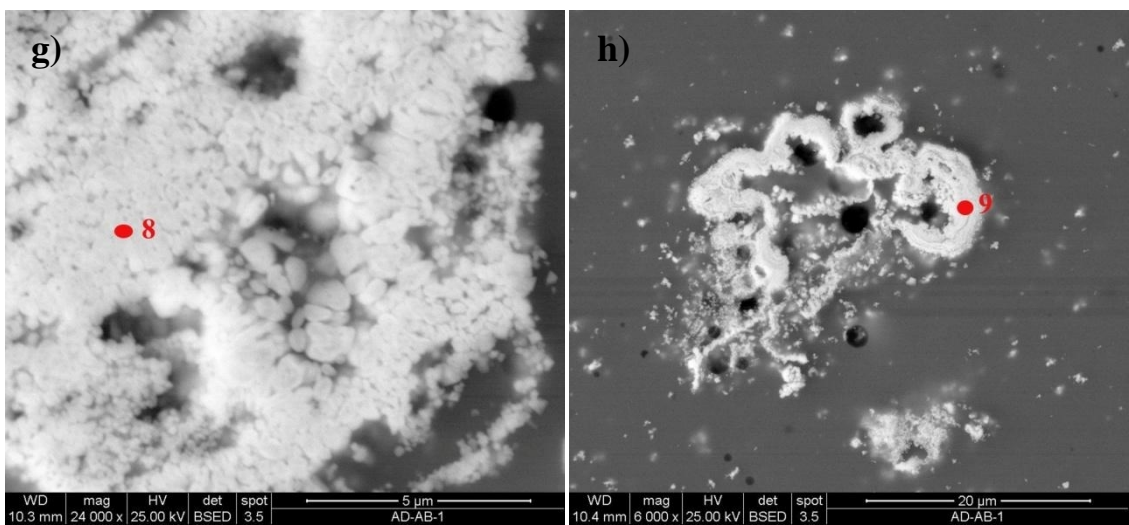
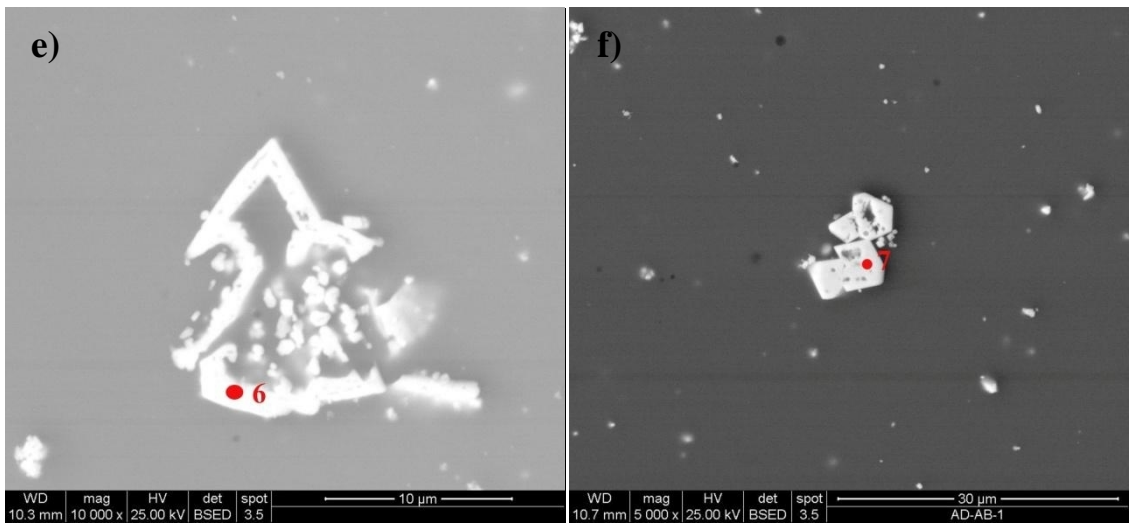
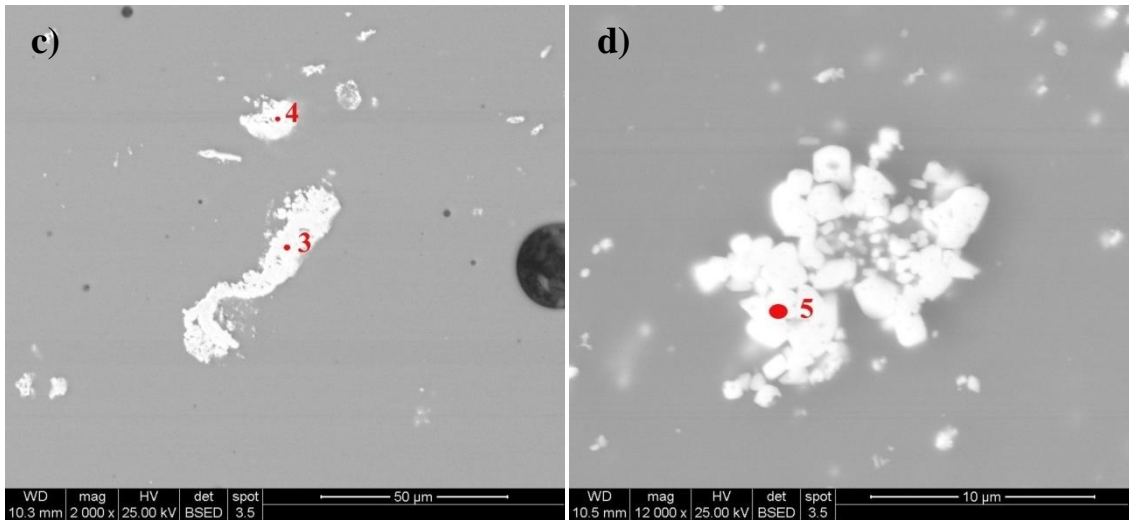
EDS analysis of all yellow glasses from Adria, dating both Pre-Roman and Roman period, show the presence mainly of lead and antimony (analyses 1-7, Table 4.1.3, Fig. 4.1.4, $PbO_2 = 43.6\text{-}58.6$ wt%, $Sb_2O_3 = 28.5\text{-}38.3$ wt%, PbO_2/Sb_2O_3 ranges between 2.2-1.4), suggesting the use of opacifiers composed of lead antimonate.

PRE-ROMAN GLASS					ROMAN GLASS					
SAMPLE	AD-NF-1	AD-NF-2	AD-NF-6		AD-NF-7	AD-AG-1	AD-BG-1			
ANALYSIS	1	2	3	4	5	6	7	8	9	10
Na_2O	5.1	1.4	3.6	4.3	2.5	–	2.2	3	2.1	2.8
CaO	2.6	–	–	–	8.3	–	–	–	–	–
Al_2O_3	–	–	–	–	–	–	–	–	–	–
SiO_2	–	5.8	12.5	17.2	–	–	4.1	8.9	5.9	9.2
Sb_2O_3	30	29	32.4	30.2	34.6	28.5	38.3	23.9	23.5	24.4
Fe_2O_3	5.3	4.8	5.1	4.6	4.3	10.2	3.6	2.1	2.1	2.1
PbO_2	57.1	58.6	46.4	43.6	50.4	61.4	51.8	45.5	45.2	49
SnO_2	–	–	–	–	–	–	–	16.6	21.2	12.5

Table 4.1.3: chemical composition, expressed as wt%, of the yellow opacifier (EDS data)s. Numbers represent the analysis points, reported in Figure 4.1.4.



4. Raw materials in glass production: the textural, chemical and mineralogical study



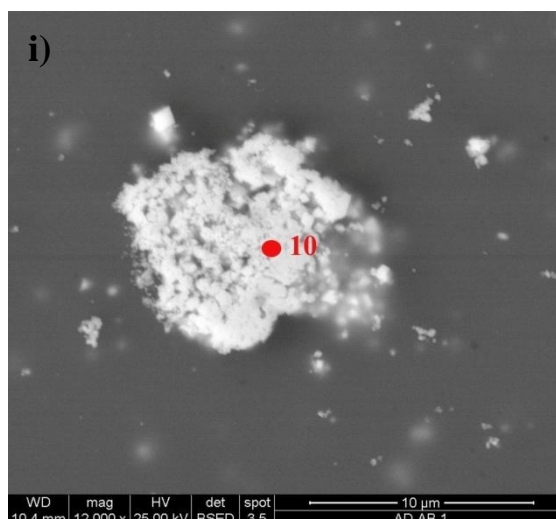


Figure 4.1.4: SEM-BSE images of yellow opacifiers (lighter grey) embedded in a glassy matrix (darker grey). (a) AD-NF-1; (b) AD-NF-2; (c)-(d) AD-NF-6; (e) AD-NF-7; (f) AD-AG-1; (g)-(i) AD-BG-1.

The opacifier crystals, both with anhedral and euhedral habitus, are typically 1-5 µm in size and are homogeneously dispersed in the glassy matrix; several aggregates constituted from very fine crystals were also observed. Considering the small size of the crystals, EDS analysis shows the contribution of the elements proper to the glassy matrix (Na_2O , MgO , CaO , SiO_2). In all lead antimonate crystals which have been analyzed, also the presence of iron was detected ($\text{Fe}_2\text{O}_3 = 3.6\text{-}10.2$ wt%, Table 4.1.3), suggesting that this element, too high in concentration to be ascribed to the glassy matrix, comes from Sb and/or Pb sources or alternatively that it was added during crystals synthesis in order to modify the colour: it is known that iron in lead antimonate produces a yellow-orange colour (Dik, 2005). In one sample, AD-BG-1, EDS analysis revealed the presence of some aggregates containing also tin in addition to lead, antimony and iron ($\text{PbO}_2 = 45.2\text{-}50.00$ wt%, $\text{Sb}_2\text{O}_3 = 23.5\text{-}24.4$ wt%, $\text{Fe}_2\text{O}_3 = 2.1\text{-}2.1$ wt%, $\text{SnO}_2 = 12.5\text{-}21.2$ wt%) (analysis 8, 9, 10, Table 4.1.3, Fig. 4.1.4, g-i), suggesting the use of different raw materials with respect to the other yellow glasses. The use of lead antimonate containing tin was already observed in green and yellow Roman and Byzantine mosaic tesserae (Lahlil et al., 2008, Tonietto, 2010, Van Der Werf, 2009) and in Late Roman *sectilia panels* (Santagostino Barbone et al., 2008). While the occurrence of tin in green coloured opaque glass might be related to the addition of bronze scale for the introduction of copper (Lahlil et al., 2008), in the case of yellow opaque glass, its presence has yet to be clarified.

4.1.2 Chemical characterization

4.1.2.1 Transparent glass

The chemical data of transparent glasses from Adria are listed in Tables D.1 and D.2, reported in Appendix D. The composition of major and minor elements is given by XRF or EPMA and is expressed as weight per cent of oxides. Traces are expressed as part per million (ppm) and have been analyzed by LA-ICP-MS; trace elements of samples AD-BB-11b, AD-I-2, AD-I-3 and AD-AM-1 are given by EPMA or XRF, for the reasons explained in the chapter 3.

All samples are soda-lime-silica glass with SiO₂, Na₂O and CaO in the ranges of 60.66-71.02wt%, 14.17-20.27 wt% and 4.15-10.32 wt%, respectively (Table D.1). On the basis of magnesium, potassium and phosphorous contents, indicative of the flux employed, it was possible to subdivide the glasses in two main groups. The first group, called Group AD/N (natron), includes the majority of the analyzed glasses, both Roman and Pre-Roman, and it is characterized by levels of potassium and magnesium lower than 1.5 wt% as K₂O and MgO (Fig. 4.1.5, a), suggesting the use of natron as flux (Freestone et al., 2003). The high amounts of Cl (0.78-1.89 wt%) and SO₃ (0.10-0.53 wt%) (Table D.1) are also due to natron, which contains NaCl and Na₂SO₄ in various proportions as a contaminant (Shortland, 2004). The second group, named Group AD/A (ash), includes only six samples: four emerald green, one blue and one black (AD-VE-2, AD-VE-3, AD-VE-4, AD-BG-1, AD-B-2, AD-N-1). They are soda glasses but present higher values of MgO (1.44-2.51 wt%), K₂O (1.01-1.97 wt%) and P₂O₅ (0.36-1.29 wt%) with respect to the Group AD/N (MgO= 0.21-1.03 wt%, K₂O= 0.32-0.95 wt%, P₂O₅= <0.05-0.29wt%) (Table D.1, Fig.4.1.5, a, b), indicating the use of a soda-rich plant ash as flux.

4. Raw materials in glass production: the textural, chemical and mineralogical study

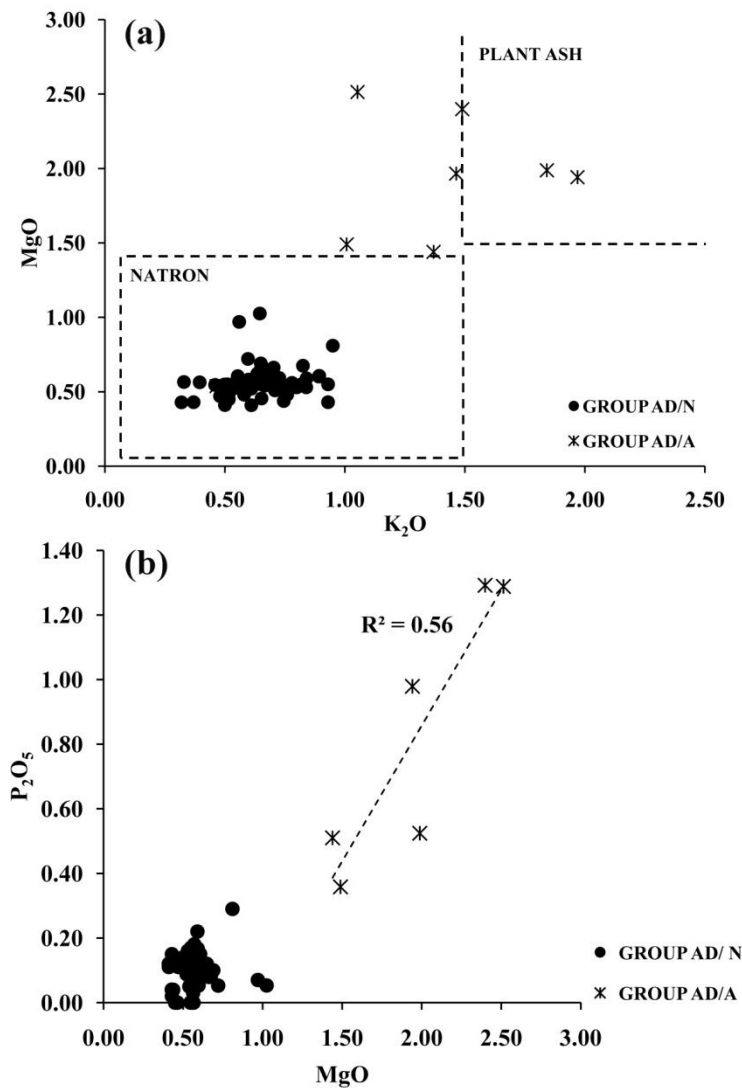


Figure 4.1.5: Plots of natron and soda ash samples: (a) MgO vs K₂O, compositional fields of natron and plant ash glasses (dotted lines) refer to Freestone *et al.*, 2003; (b) P₂O₅ vs MgO.

Some major and minor chemical elements, such as lime, alumina, iron and titanium, are particularly diagnostic of the sand source employed for silica–soda–lime glass, as they reflect the impurities (calcite, feldspar, clay minerals and heavy minerals fraction) present in the sand (Freestone *et al.*, 2000). On the basis of these elements, Adria natron and soda ash glass was subdivided in subgroups, related to the use of different raw materials. In particular, two subgroups, called Group AD/A1 and AD/A2, have been identified for soda ash glass, and three, called Group AD/N1, AD/N2a and AD/N2b for natron glass. The chemical differences among them become clearer when, within each group, the average composition together with the corresponding standard deviation are

4. Raw materials in glass production: the textural, chemical and mineralogical study

calculated (Tab. 4.1.4). The compositional group for each sample is also reported in Table D.1. Notwithstanding the samples included in Groups AD/N2a are only two, they were considered as a compositional group, since their evident chemical homogeneity. On the other hand, sample AD-B-4, with a peculiar bulk composition, was considered as an outlier (Tab. 4.1.4).

wt%	NATRON GLASS				SODA ASH GLASS	
	AD/N1 (N= 53)	AD/N2a (N= 2)	AD/N2b (N=4)	OUTLIER (N=1)	AD/A1 (N= 3)	AD/A2 (N= 3)
SiO₂	68.26±1.51	68.32±2.39	69.46±1.03	68.21	65.53±1.90	61.35±1.13
Na₂O	17.66±1.37	17.75±0.15	18.41±0.88	16.32	16.26±0.51	19.61±1.55
CaO	7.91±0.76	4.41±0.36	5.14±0.61	4.63	6.57±1.31	6.88±0.21
Al₂O₃	2.46±0.18	2.01±0.31	1.77±0.27	4.29	1.83±0.05	2.69±0.11
K₂O	0.64±0.13	0.67±0.39	0.53±0.16	0.93	1.46±0.47	1.45±0.42
MgO	0.57±0.11	0.69±0.17	0.49±0.06	0.43	1.96±0.54	1.96±0.46
Fe₂O₃	0.63±0.42	1.50±0.33	0.43±0.11	1.77	1.08±0.17	1.44±0.42
TiO₂	0.06±0.03	0.20±0.05	0.08±0.02	0.08	0.13±0.03	0.22±0.05
MnO	0.51±0.53	1.15±0.37	0.11±0.07	1.31	0.90±0.50	0.55±0.24
Sb₂O₃	0.03±0.08	0.01±0.01	0.68±0.31	0.02	0.03±0.03	0.02±0.02
P₂O₅	0.11±0.04	0.16±0.18	0.04±0.02	0.15	1.03±0.45	0.62±0.32
SO₃	0.23±0.09	0.22±0.04	0.31±0.03	0.1	0.22±0.08	0.32±0.18
Cl	1.36±0.25	1.29±0.14	1.57±0.05	1.3	1.25±0.35	1.43±0.31

Table 4.1.4: Mean chemical compositions in weight per cent (element oxides) and standard deviations for identified natron and soda ash groups (N= number of samples).

As shown in Figure 4.1.6, all the natron glass of Groups AD/N1, AD/N2a and AD/N2b has similar contents of silicon (SiO₂= 68.26±1.51 wt%, 68.32±2.39 wt% and 69.46±1.03 wt%, respectively) and sodium (Na₂O= 17.66±1.37 wt%, 17.75±0.15 wt% and 18.41±0.88 wt%, respectively) (Table 4.1.4), also consistent with the SiO₂/Na₂O compositional field of the well known Roman and Pre-Roman glass. Since the levels of SiO₂ and Na₂O are related to the sand:soda ratio employed by glassmakers (Freestone et al., 2000), their substantial homogeneity suggests the use of a similar recipe. On the other hand, soda ash glass, particularly that of Group AD/A2, has lower SiO₂ contents (Table 4.1.4, Fig. 4.1.6), indicating a different production technologies.

4. Raw materials in glass production: the textural, chemical and mineralogical study

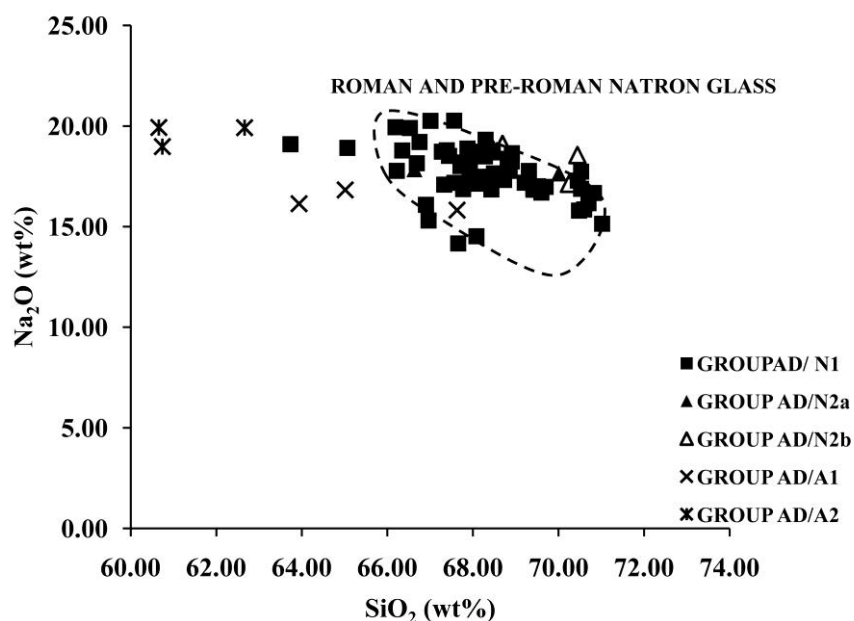


Figure 4.1.6: Na_2O vs SiO_2 plot for all Adria groups. The compositional fields of Roman and Pre-Roman glasses are overlapped and refer to Silvestri, 2008; Foy et al., 2003; Silvestri et al., 2005; Arletti et al., 2010 b and Arletti et al., 2011.

Both natron and soda ash groups differ essentially for their CaO , Al_2O_3 , Fe_2O_3 , TiO_2 and Sb_2O_3 contents. For what concerns natron glass, Group AD/N1 is the most numerous (53 samples) and includes the majority of the Roman and all the Pre-Roman glasses, independently from their colour, type and production technology.

In Figure 4.1.7 the CaO versus Al_2O_3 content for the three subgroups of natron glass (Group AD/N1, AD/N2a and AD/N2b) is plotted, along with the main 1st-3rd century AD compositional groups found in the Western provinces ('typical' Roman glass and Sb-colourless glass, Group CL1) (Silvestri, 2008; Silvestri et al., 2008; Silvestri et al., 2005; Foy et al., 2003) and with the compositional groups of some Pre-Roman blue glass vessels (Groups Mediterranean 1 and 2), coming from the necropolis of Bologna and Spina, chronologically and typologically consistent with Pre-Roman Adria samples (Arletti et al., 2010 b, 2011).

4. Raw materials in glass production: the textural, chemical and mineralogical study

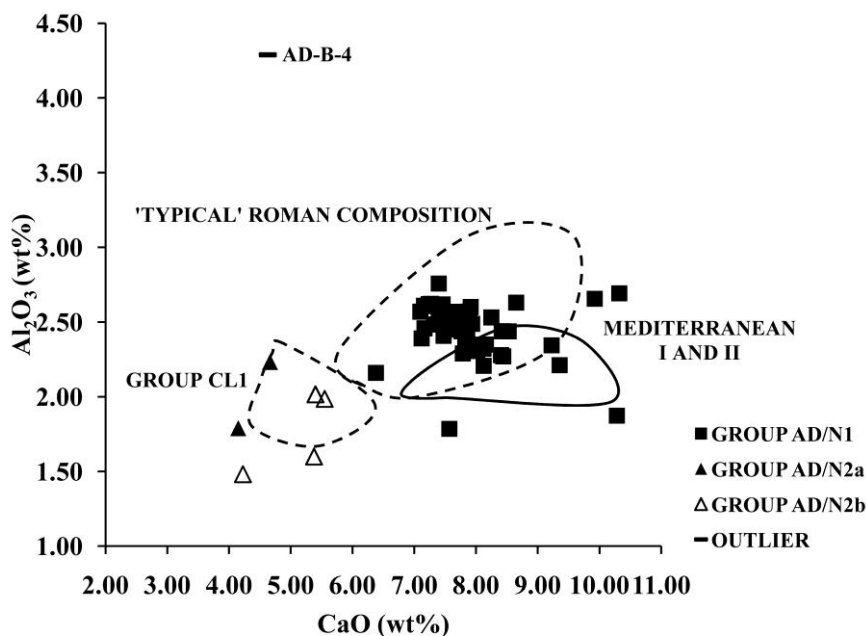


Figure 4.1.7: Al_2O_3 vs CaO plot for all natron groups. The compositional fields of Roman glasses (dotted lines) refer to Silvestri, 2008; Silvestri et al., 2008; Silvestri et al., 2005; Foy et al., 2003. The compositional field of Pre-Roman Mediterranean I and II glasses (continuous line) refer to Arletti et al., 2010 a and Arletti et al., 2011.

Group AD/N1 is characterized by higher CaO and Al_2O_3 contents than Group AD/N2a and AD/N2b ($CaO = 7.91 \pm 0.76$ wt%; $Al_2O_3 = 2.46 \pm 0.18$ wt% vs $CaO = 4.41 \pm 0.36$ wt% and 5.14 ± 0.61 wt%; $Al_2O_3 = 2.01 \pm 0.31$ wt% and 1.77 ± 0.27 wt%, Table 4.1.4) and it is consistent with the field of the ‘typical’ soda-silica-lime Roman glass, which includes also the compositional groups of the older glass, suggesting that the same sand source was likely employed to produce these glasses. The extraordinarily consistent composition of Roman glass from different sites located in Western Europe has already been noted by many authors and led to the supposition of a common origin for all the glass of the entire Empire (Silvestri, 2008; Silvestri et al., 2005; Foy et al., 2003; Arletti et al., 2008; Picon and Vichy 2003; Nenna 1997).

As already discussed, the Roman glass is thought to have been made from coastal sands of the Syro-Palestinian region, probably near the mouth of the river Belus (now Nahr Na’aman), a small waterway flowing between Haifa and Acre (Israel) (Foy et al., 2003). On the other hand, the production centres of Pre-Roman glass vessels are not yet known. The core-formed items of the so-called ‘Mediterranean Groups’ were very common on the island of Rhodes and in the Greek area in general; the large number of

4. Raw materials in glass production: the textural, chemical and mineralogical study

Mediterranean vessels found here and in the neighbouring area is taken to be an indication of proximity to a production centre (Triantafyllidis, 2003). Moreover, the presence of a primary production glass site on the island has been recently attested (Rehren et al., 2005). However, it is not possible to exclude the Syrian-Palestinian regions as potential production sites for these artefacts, since in these areas the presence of an important glass tradition is attested for long time (Whitehouse, 1988; Grose, 1989).

The other two groups of natron glass, Group AD/N2a and Group AD/N2b, include only two blue (AD-B-6, AD-B-7) and four colourless samples (AD-I-2, AD-I-4, AD-I-5, AD-I-6), respectively (Table D.1). The former is characterized by lower CaO values ($\text{CaO} = 4.41 \pm 0.36$ wt%) and the second by lower CaO and Al_2O_3 values ($\text{CaO} = 5.14 \pm 0.61$ wt%; $\text{Al}_2\text{O}_3 = 1.77 \pm 0.27$ wt%) than Group AD/N1. In addition, Group AD/N2b shows the highest Sb_2O_3 content ($\text{Sb}_2\text{O}_3 = 0.68 \pm 0.31$) of all natron groups (Table 4.1.4). These data suggest that the samples of Groups AD/N2a and AD/N2b were produced with sand purer than that employed for Group AD/N1, poorer in calcite (Group AD/N2a) or in calcite and feldspars (Group AD/N2b), and that antimony was deliberately added in the batch of Group AD/N2b as decolourant, since antimony contents >0.2 % are considered to be intentional additions (Jackson, 2005) (this aspect is extensively discussed in next section, about colouring and decolouring agents).

A further distinction can be observed between Groups AD/N2a and AD/N2b when considering their iron and titanium contents. The TiO_2 versus Fe_2O_3 plot (Fig. 4.1.8) does show that the contents of these two elements are closely related in most of the samples, independently from their compositional group, indicating that iron was added unintentionally, together with titanium, as mineral impurities in the sand. The group of samples with higher iron in the dotted area (Fig. 4.1.8) includes only blue samples: in this case, the iron was probably introduced in the glass not only with the sand but also with the colouring raw materials. For this reason the Group AD/N2a, including blue glasses, is characterized by higher contents of iron ($\text{Fe}_2\text{O}_3 = 1.50 \pm 0.33$ wt%) with respect Group AD/N2b, composed only of colourless glasses ($\text{Fe}_2\text{O}_3 = 0.43 \pm 0.11$ wt%) (Table 4.1.4). However, Group AD/N2a shows also major titanium levels ($\text{TiO}_2 = 0.20 \pm 0.05$ wt%) when compared to Groups AD/N2b and AD/N1 ($\text{TiO}_2 = 0.08 \pm 0.02$ wt% and 0.06 ± 0.03 wt%, respectively, Table 4.1.4). Since titanium can be related to the

4. Raw materials in glass production: the textural, chemical and mineralogical study

heavy and mafic mineral fraction present in the sand batch (e.g. rutile, ilmenite, biotite, pyroxene, amphibole), these chemical evidences suggest that glass of Group AD/N2a was, in any case, produced with a sand richer of heavy and/or mafic minerals than that used in the manufacture of AD/N1 and AD/N2b samples.

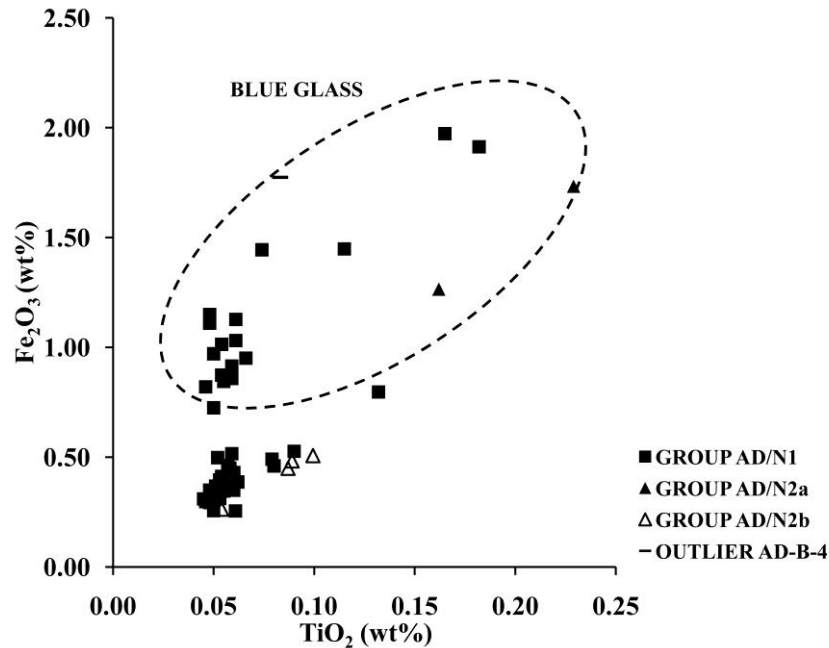


Figure 4.1.8: Fe_2O_3 vs TiO_2 plot for the natron groups. In the dotted area all the blue samples are included. Note the higher TiO_2 contents of Group AD/N2a (black triangles) than that of Group AD/N2b (empty triangles).

No comparisons have been found in literature for the ‘low calcium’ blue glasses of Group AD/N2a, while the Sb-colourless ‘low calcium-aluminium’ glasses of Group AD/N2b well corresponds to a group of glasses which appeared in the West during the 2nd to the 3rd centuries AD, characterized by the use of antimony as decolourant. Examples are ‘group 4’ of Picon and Vichy (2003), a group which appeared in the West during the 2nd to 3rd century AD; ‘group 1a’ of Jackson (2005), which comprises Romano-British colourless glasses spanning from the 1st to the 4th century AD; the ‘antimony-only BCL’ samples of Paynter (2006), composed of most colourless Roman glass of the 1st-3rd century AD from Binchester, Lincoln and Colchester and ‘group CL1’ of Silvestri et al. (2008), including 3rd century colourless glass from the *Iulia Felix* shipwreck. The production centres for this type of glass have not yet been localized, but some authors hypothesized that centres of colourless glass manufacture

4. Raw materials in glass production: the textural, chemical and mineralogical study

may have been present in both the eastern and northwestern provinces (Baxter et al., 2005; Huisman et al., 2009).

Only one natron glass, AD-B-4 (blue), has a peculiar bulk composition, different from that of all other samples. It is characterized by the highest content of Al_2O_3 (4.29 wt%), and lower CaO (4.63 wt%) (Table 4.1.4, Fig. 4.1.7), suggesting the use of a different sand source, richer in feldspars and poorer in calcite. Since no similar compositions have been recognized in literature for Roman glasses, the sample AD-B-4 can be considered an outlier.

The soda ash glass groups contain only three samples for each, all intensely coloured. Group AD/A1 includes two emerald green and one blue glass, Group AD/A2 two emerald green and one black (Table D.1). They differ substantially for the SiO_2 , Na_2O and Al_2O_3 contents (Table 4.1.4), as highlighted in the plots SiO_2 vs Na_2O and CaO vs Al_2O_3 (Fig. 4.1.9, a, b). Group AD/A1 is characterized by lower aluminum (Al_2O_3 = 1.78-1.89 wt%), lower sodium (Na_2O = 15.83-16.17 wt%) and higher silicon (SiO_2 = 63.93-67.63wt%) with respect to the Group AD/A2 (Al_2O_3 = 2.59-2.80 wt%, Na_2O = 18.98-19.93 wt% and SiO_2 = 60.66-62.66 wt%) (Table 4.1.4). The low level of Al_2O_3 characteristic of Group AD/A1 indicates the use of a purer sand, i.e. richer in silica, such as quartz or chert pebbles, rather than a siliceous calcareous sand. The high level of CaO in both soda ash groups (5.10-7.62 wt%, Table 4.1.4) is due to plant ash and not to the carbonatic fraction of sand, as confirmed by analyses of Levantine plant ash, which typically have high CaO (Brill, 1970; Ashtor and Cevidalli, 1983; Verità, 1985). The presence of soda ash glass in Early Roman assemblages is unusual, since it is generally well accepted that natron is the flux used in the Mediterranean and Europe from the middle of the first millennium BC through to the 9th century AD (Sayre and Smith, 1961). For this reason it is quite difficult to find in literature data about Western Roman soda ash glass. In Figure 4.1.9 Group AD/A1 and AD/A2 are compared with a small group of green/black 1st century soda ash glass found in the Northern provinces of the Empire (Van Der Linden et al., 2009).

4. Raw materials in glass production: the textural, chemical and mineralogical study

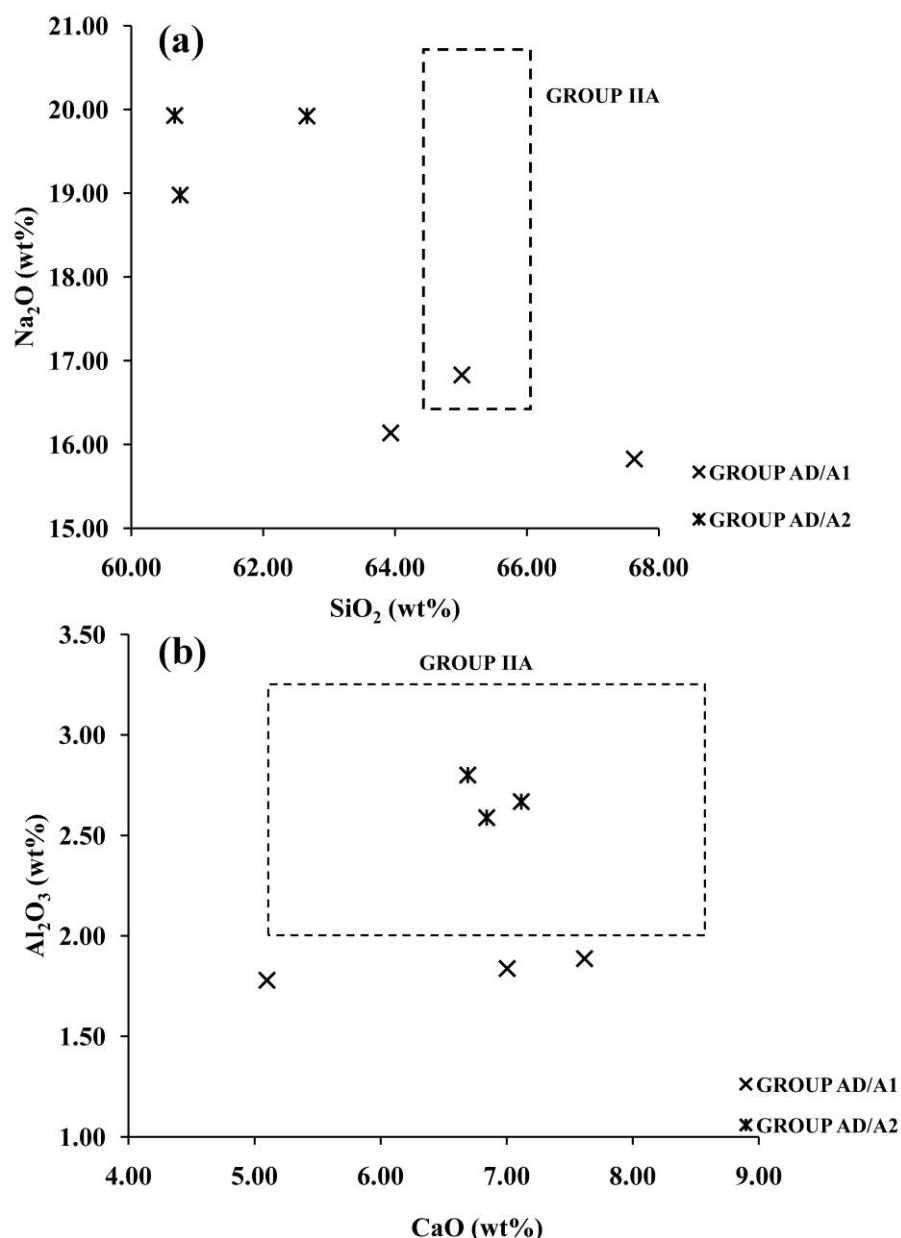


Figure 4.1.9: plots of the soda ash groups. (a) Na₂O vs SiO₂; (b) Al₂O₃ vs CaO. The dotted area refers to the compositional field of 1st century AD green/black soda ash glass (from Van Der Linden et al., 2009).

For what concerns CaO and Al₂O₃ contents, the samples of Group AD/A2 show a good agreement with this group, suggesting the use of similar sand, but of a different recipe, since they present a different SiO₂/ Na₂O ratio. On the other hand, glass of Group AD/A1 likely represents a distinction production (Fig. 4.1.9). High potassium/magnesium Early Roman glasses, generally emerald green or black in colour, have been noted also by other authors (Lemke, 1998, Henderson, 1996, Jackson et al.,

4. Raw materials in glass production: the textural, chemical and mineralogical study

2006), which have hypothesized their importation from other geographical areas, such as Mesopotamia, where glass was also produced by means of sodic ashes (Brill, 1999). However, since Adria soda ash glasses present forms well attested in Roman glass production (Isings form 46/a, form 2, see Table A.1), it can be hypothesized that this type of glass was likely imported as raw chunks and then shaped into finished objects. Mirti et al. (2008, 2009) have recently analyzed some soda ash glass from the archaeological sites of Seleucia and Veh Ardašîr, in modern Iraq, dating to the Parthian (2nd-3rd century AD) to Sasanian (3rd-7th century AD) epochs, mainly blue–green and green to yellow–green in colour. The soda ash glasses from Adria is chemically different from this glass, mainly for lower MgO and K₂O contents (MgO= 1.96±0.54 wt% and 1.96±0.46 wt% vs 4-5 wt% in Mesopotamian glass; K₂O= 1.46±0.47 wt% and 1.45±0.42 wt% vs 3-4 wt%), suggesting a different provenance, probably from workshops not yet localized.

As proved in recent studies, further information on the type and origin of raw materials employed in glass manufacture can be provided by the analysis of the trace elements. Rare Earth Element (REE) patterns (Degryse and Shortland, 2009; Freestone et al., 2002), Zr-Ti (Aerts et al., 2003), Zr-Ti-Cr-La (Shortland et al., 2007) and Zr-Ba (Silvestri et al., 2008) have proved promising in distinguishing between various sand silica raw materials, as these elements may be typical for a geological environment. Since the Adria samples includes a great variety of coloured glasses (blue, light blue, green, purple, amber, black) and also colourless glass, a consistent number of trace elements may be accidentally included in the glass alongside colouring and decolouring raw materials. Of the elements analyzed in this study a large number of the trace elements (Li, B, Ti, Cr, Rb, Sr, Y, Zr, Nb, Cs, Th, U, Hf, Ta, W, Tl and REE) show similar level in both colourless and coloured glasses, proving that they are not colorant-derived, but are due to other components of the glass. Their means and standard deviations, within each group, are listed in Table 4.1.5.

4. Raw materials in glass production: the textural, chemical and mineralogical study

ppm	NATRON GLASS			SODA ASH GLASS	
	AD/N1 (N= 53)	AD/N2a (N= 2)	AD/N2b (N=4)	AD/A1 (N= 3)	AD/A2 (N= 3)
Li	4.3±1.8	5.2±0.5	4.3±1.5	3.8±1.1	5.7±1.0
B	174±60	120±1	202±59	147±47	205±51
Cr	11±3	28±8	9.6±2	16±2	32±4
Rb	9.1±1.8	6±2	5.1±2.0	5.6±1.6	7.6±2.1
Sr	460±101	361±55	363±15	534±198	445±20
Y	6±0.6	5.7±0.2	4.7±0.5	4.8±0.14	6.4±0.5
Zr	34±9	124±40	48±12	62±11	91±14
Nb	1.2±0.3	2.4±0.2	1.4±0.3	2.1±0.5	3.1±0.4
Cs	0.10±0.07	0.10±0.0	0.07±0.03	0.08±0.02	0.20±0.2
La	6.1±0.5	6.6±0.5	5.1±0.5	5.8±0.4	7.3±0.6
Ce	11±0.8	12±1	9.5±1.1	10±0.3	14±0.9
Nd	5.9±0.5	6.1±1.3	4.8±0.4	5.4±0.2	6.8±0.6
Sm	1.2±0.2	1.1±0.3	1.1±0.3	1.0±0.1	1.4±0.1
Eu	0.36±0.05	0.26±0.04	0.24±0.01	0.30±0.02	0.36±0.07
Gd	1.1±0.2	0.89±0.26	0.85±0.15	0.98±0.13	1.3±0.2
Tb	0.16±0.03	0.15±0.02	0.13±0.02	0.16±0.01	0.17±0.02
Dy	1.0±0.1	0.98±0.09	0.82±0.07	0.96±0.15	1.1±0.1
Er	0.55±0.06	0.54±0.06	0.48±0.10	0.47±0.04	0.66±0.07
Yb	0.53±0.09	0.61±0.16	0.47±0.18	0.51±0.09	0.63±0.07
Lu	0.08±0.02	0.10±0.02	0.05±0.01	0.09±0.01	0.10±0.02
Hf	0.83±0.21	3.1±1.1	1.1±0.2	1.5±0.4	2.2±0.5
Ta	0.07±0.03	0.17±0.02	0.09±0.02	0.13±0.02	0.19±0.02
Th	0.75±0.17	1.4±0.4	0.82±0.08	1.1±0.1	1.5±0.2
U	1.1±0.4	1.3±0.1	1.1±0.2	0.92±0.08	1.1±0.1
W	0.09±0.06	0.15±0.01	0.07±0.01	0.15±0.08	0.10±0.05
Tl	0.06±0.06	0.14±0.10	0.08±0.09	0.09±0.09	0.04±0.03

Table 4.1.5: Mean trace compositions, expressed as ppm, and standard deviations for identified natron and soda ash groups. LA-ICP-MS data (N= number of samples).

In Figure 4.1.10, a, b the average patterns of trace elements for the natron and soda ash glass groups, normalized to the average continental crust (Wedephol, 1995), are reported; in Figure 4.1.11 the covariation of Zr with Hf, closely associated to the heavy minerals concentration in the sand, is also shown. The trace element pattern of the outlier AD-B4 is not reported, since it is substantially similar to that of Group AD/N1.

4. Raw materials in glass production: the textural, chemical and mineralogical study

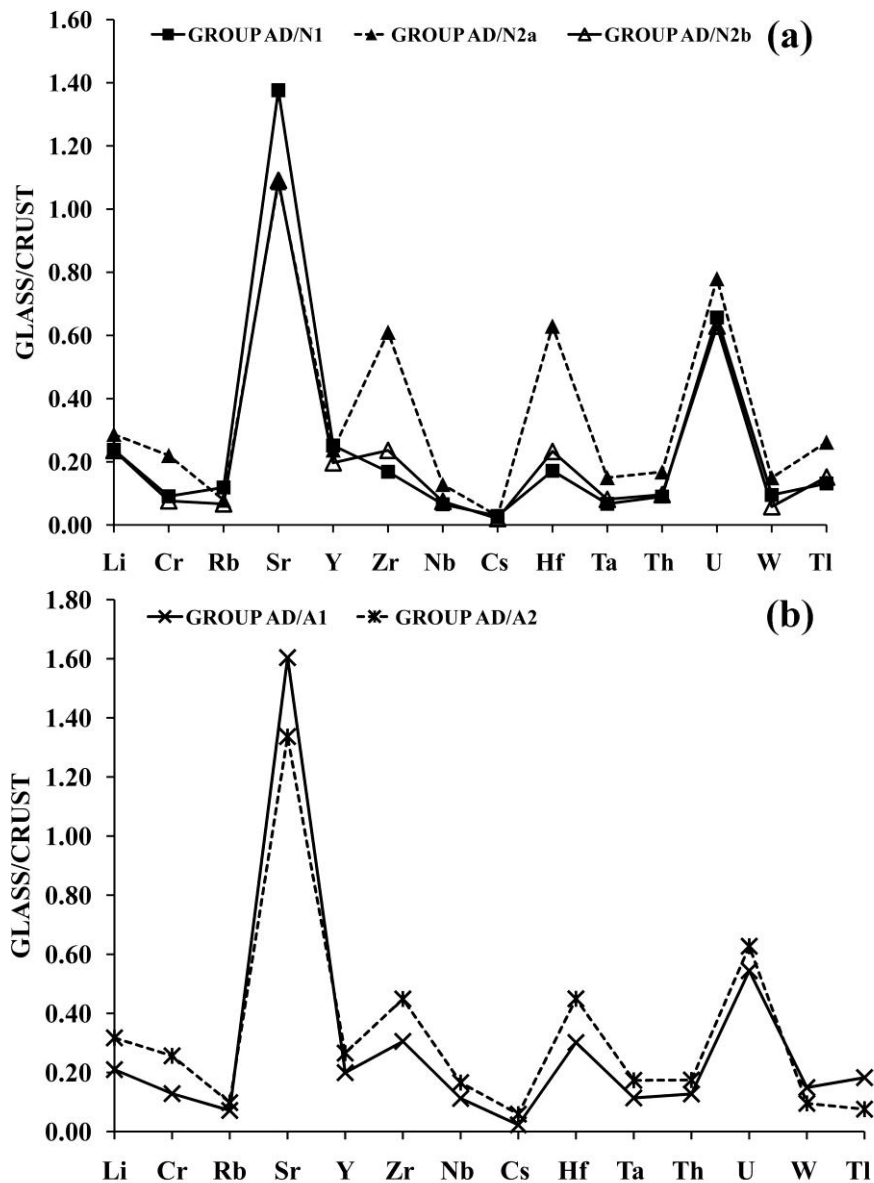


Figure 4.1.10: average patterns of trace elements, normalized to the average continental crust (Wedephol, 1995) for: (a) natron groups; (b) soda ash groups.

In both natron and soda ash group the average composition is depleted in most trace elements, an exception in this respect is strontium, which is about 50% higher than the mean crustal concentration (Fig. 4.1.10, a, b). The general pattern of Adria glasses is similar to that of many ancient glasses (Freestone et al., 2000; Freestone et al., 2002). The generally low levels of trace elements are a reflection of the use of a mineralogically mature sand to manufacture the glass, which was rich in quartz and poor in heavy minerals and clay minerals, which are likely to host elements such as zirconium, thorium and the Rare Earth Elements (REE).

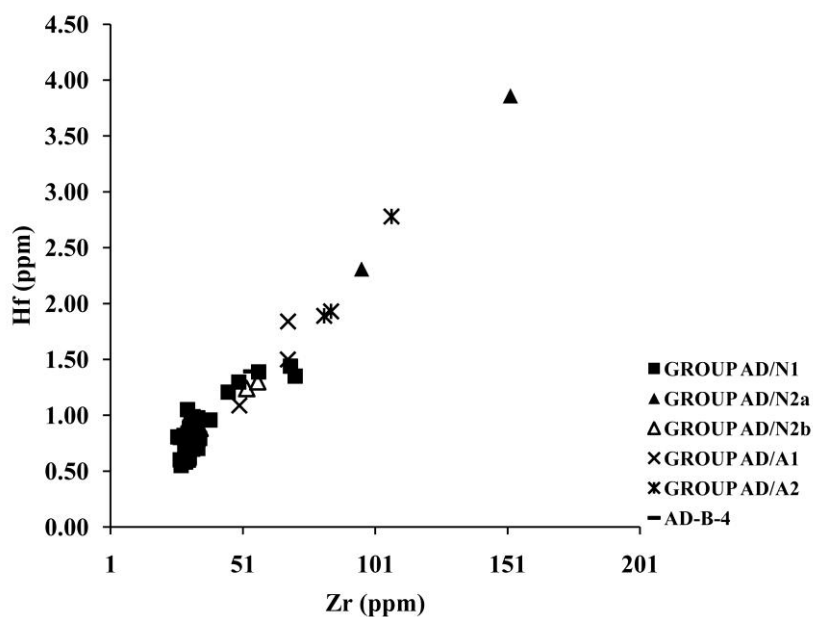


Figure 4.1.11: *Hf vs Zr plot for natron and soda ash groups.*

Strontium shows similar geochemical behavior to its fellow alkaline earth element calcium, which was present as calcium carbonate particles in the sand. The trace element patterns and the Zr-Hf covariation of Adria glasses confirm the subdivision in five compositional groups made on the basis of major and minor element composition. As concerns natron groups (AD/N1, AD/N2a and AD/N2b), Figure 4.1.10, a and 4.1.11 show that Cr, Zr and Hf, mostly related to heavy minerals such as chromite and zircon, are significantly higher in Group AD/N2a (Cr= 28±8 ppm, Zr= 124±40 ppm; Hf= 3.1±1.1 ppm) than in Groups AD/N1 (Cr= 11±3 ppm, Zr= 34±9 ppm; Hf= 0.83±0.21 ppm) and AD/N2b (Cr= 9.6±2, Zr= 48±12 ppm; Hf= 1.1±0.2 ppm) (Table 4.1.5), indicating a major amount of heavy minerals in the sand employed in its manufacture.

A similar behavior is shown by the soda ash groups, where Group AD/A2 presents slightly higher values of Cr, Zr and Hf (Cr= 32±4, Zr= 91±14, Hf= 2.2±0.5 ppm) with respect to the Group AD/A1 (Cr= 17±2, Zr= 62±11, Hf= 1.5±0.4 ppm) (Fig. 4.1.10 a, 4.1.11, Table 4.1.5).

In synthesis, the five compositional groups recognized on the basis of major, minor and trace elements composition are likely related to the use of different raw materials and can be resumed as follows:

- Group AD/N1 (53 samples)= natron + siliceous-calcareous sand, similar to that utilized to manufacture the ‘typical’ Roman glass.

4. Raw materials in glass production: the textural, chemical and mineralogical study

- Group AD/N2a (2 samples)= natron + siliceous-calcareous sand with a lower content of calcite than Group AD/N1, but with a higher content of heavy and/or mafic minerals.
- Group AD/N2b (4 samples)= natron + siliceous-calcareous sand with a lower content of calcite and feldspars with respect to Group AD/N1.
- Group AD/A1 (3 samples)= soda ash + pure silica source, maybe constituted by quartz pebbles
- Group AD/A2 (3 samples)= soda ash + a less pure silica source, with a major contents of feldspars and heavy minerals than Group AD/A1

In Figure 4.1.12 are reported the REE patterns of the five compositional groups.

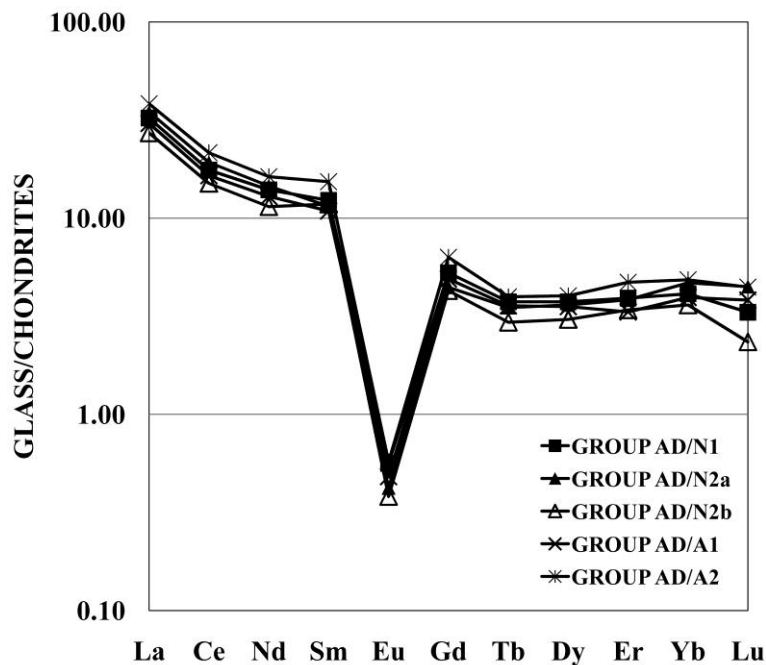


Figure 4.1.12: REE patterns, normalized to average chondritic meteorites (Mason, 1979), for all identified groups.

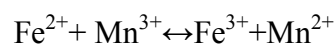
The REE contents were normalized to average chondritic meteorites (Mason, 1979), likely parallel to the primordial abundances in the solar nebula and parallel to bulk earth abundances. REE patterns are homogeneous for all groups and show LREE (Light Rare Earth Elements) enrichment, flat HREE (Heavy Rare Earth Elements) distributions and a significant negative Eu anomaly (Fig. 4.1.12). This pattern was already observed in other Roman glasses (Wedepohl et al., 2011) and is characteristic of sedimentary REE

4. Raw materials in glass production: the textural, chemical and mineralogical study

(Degryse and Shortland, 2009). In a sediment, the bulk of the REE resides in the silt and clay fraction (Cullers et al., 1979); heavy minerals, which may be concentrated during sedimentary sorting due to their high density and resistance to weathering, can contain significant abundances of REE (e.g. monazite and zircon) and when their patterns differ significantly from the average source rock composition, an effect on the sedimentary REE pattern may occur (McLennan, 1989). However, it has been shown by McLennan (1989) that, though sand may be prone to effects of heavy minerals, substantial enrichments in these minerals do not result in significant changes in the sedimentary REE patterns of silt, clay or shales. The homogeneity in REE abundances and patterns of the analyzed glass can be explained in this way: no anomalous values due to heavy minerals influencing the REE patterns are discernable, so the REE patterns likely reflect the pattern of the clay fraction of the sand raw material.

Colouring agents and recycling indicators in natron glasses (Group AD/N1, AD/N2a, AD/N2b)

Adria natron glasses show a great variety of colours, which can be resumed in six: green/light blue, blue, purple, amber, and colourless. The vast majority of these coloured glasses belong to Group AD/N1, with a 'typical' Roman composition, while only two blue and all the Sb-colourless glasses are included in Groups AD/N2a and AD/N2b, respectively. The light blue/green is the most common colour in Roman glass. Iron was probably the main colouring element and was introduced into the glass as an impurity. Adria light blue/green glasses are in total 17 and their iron content varies from 0.31 to 0.80 wt% (Table D.1). Iron can produce many different colours, from green or blue, when Fe(II) ions are present, to brownish-yellow with Fe(III) ions. The common blue–green glass is produced by a mixture of ferrous [Fe(II)] and ferric [Fe(III)] ions in the melt (Pollard and Heron 1995); the different oxidation state of iron must be ascribed either to the furnace atmosphere or to different amounts of manganese deliberately used by glass-makers as a decolouring agent. In fact, manganese added to the batch causes oxidation of iron from Fe²⁺ to Fe³⁺: the greenish colour of the glass changes to a yellow tinge, which is compensated by the purple colour due to Mn³⁺ ions, according to the following equation:



4. Raw materials in glass production: the textural, chemical and mineralogical study

Since MnO contents higher than 0.5 wt% are considered to be intentional additions (Jackson, 2005), it can be asserted that this decolouring agent was deliberately added in nine light blue-green glasses, with MnO varying from 0.59 to 0.90 wt% (Table D.1).

The trace elements that usually give information about the extent of recycling, such as Co, Zn, Sn, Cu, Pb (Freestone et al., 2002) are generally low in light blue/green glasses: only in four sample (AD-A-5, AD-A-6, AD-A-7, AD-A-8, AD-A-10) Cu and Pb are in the range 100-1000 ppm (Table D.2), suggesting the recycling of earlier glass and blue glass frit or cullet added during melting.

Amber glasses are 9 and form a very homogeneous group, which shows the lowest contents of iron and manganese of all analyzed samples ($\text{Fe}_2\text{O}_3 = 0.26\text{-}0.37$ wt%; $\text{MnO} = 0.02\text{-}0.04$ wt%, Table D.1); also trace elements levels are very low. For this reason, these glasses can be considered representative of the base glass composition with no additives. In absence of discernable colouring agents, the main chromophores are likely Fe^{2+} and a $(\text{Fe}^{3+}, \text{S}^-)$ complex, which formed when the glass was melted under strongly reducing conditions, produced by altering the furnace atmosphere and/or by the presence of carbon in the batch (Jackson et al., 2006; Green and Hart, 1987; Schreurs and Brill, 1984). In the absence of the ferri-sulfide complex the glass is bluish aqua, but with increasing concentrations of the complex the colour changes from blue to green and finally to amber (Schreurs and Brill, 1984).

As concerns the eight colourless samples, their decolouring agents are manganese and/or antimony (Table D.1), the principal decolourisers used in ancient time. Antimony and manganese decolourise the glass by oxidizing iron, although the relationship between iron, manganese and antimony in glass is complex. In general, the amount of decolouriser used is related to the amount of iron and, as antimony is a stronger decolouriser than manganese, smaller quantity renders the glass colourless (Silvestri et al., 2008). For this reason, as already said, it is generally accepted that manganese contents >0.5 % are indicative of intentional additions (Jackson, 2005) while the limit for the antimony is 0.2 % (Jackson, 2005; Sayre, 1963). Adria colourless glasses fall in two compositional groups: four of them (AD-I-1, AD-I-3, AD-R-1t, AD-R-2), dating mostly 1st century AD, belong to Group AD/N1, with a typical Roman composition, and the other four (AD-I-2, AD-I-4, AD-I-5, AD-I-6), dating 2nd -3rd century AD, belong to Group AD/N2b, with lower contents of calcium and aluminium.

4. Raw materials in glass production: the textural, chemical and mineralogical study

The colourless glasses of Group AD/N2b were decolourised by the addition of antimony ($\text{Sb}_2\text{O}_3 = 0.47\text{-}1.14$ wt %, Table D.1) and well correspond to most prevalent groups of Roman antimony colourless glass, as ‘group 1a’ of Jackson (2005) (Fig. 4.1.13). On the other hand, the Adria colourless glasses of Group AD/N1 were decolourised by the addition of MnO (AD-I-1, AD-R-1t, AD-R-2, $\text{MnO} = 0.84\text{-}1.26$ wt%), or equal quantity of antimony and manganese (AD-I-3, $\text{Sb}_2\text{O}_3 = 0.41$ wt%; $\text{MnO} = 0.54$ wt% (Table D.1). They are also consistent with ‘group 2a’ and ‘group 2b’, respectively, of Jackson (2005) (Fig. 4.1.13). Therefore it appears that the different bulk composition well corresponds to the use of different decolouring agents, indicating standardized technology and a careful selection of raw materials.

As already observed for other chromatic groups, also in the colourless glass trace elements are generally low, suggesting a limited or a selective recycling. Only the sample AD-I-2 shows higher Pb contents ($\text{Pb} = 1192$ ppm, Table D.2), indicating a possible recycle of coloured cullets.

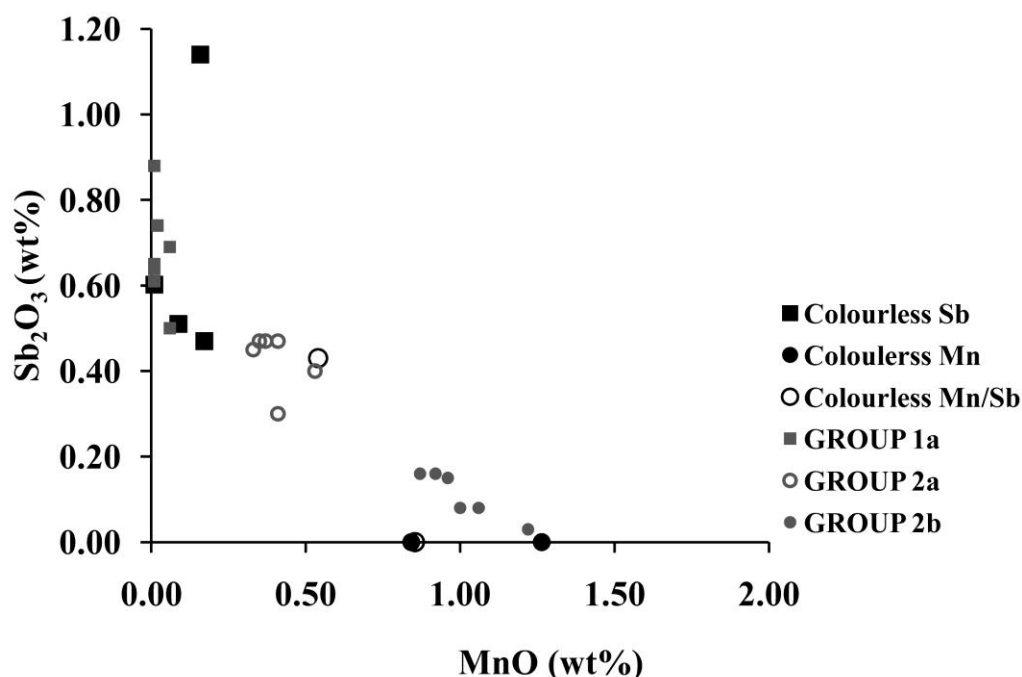


Figure 4.1.13: Sb_2O_3 vs MnO plot for the colourless glasses. The compositional groups refer to Jackson (2005).

In the five purple glasses manganese was employed as chromophore, having these samples the highest MnO contents (1.55-2.01 wt%, Table D.1) of all coloured samples.

4. Raw materials in glass production: the textural, chemical and mineralogical study

The use of MnO as colouring agent in purple and pink glass is well documented since the Iron age (Tite et al., 2008) and its presence in Roman glass is frequent (Arletti et al., 2006; Jackson et al. 2006). Silvestri (2008) indicates wad as possible source of manganese, an ore composed of manganese oxides/hydroxides, often of poor crystallinity, with small quantities of psilomelane $[(Ba, H_2O)_2Mn_5O_{10}]$. This hypothesis could be supported by the positive correlation between Ba and Mn, observed in all coloured glasses of Group AD/N1 (Fig. 4.1.14, a). As shown in Figure 4.1.14, b, c, manganese is also correlated with Sr and V, indicating that they were retrieved from the same source.

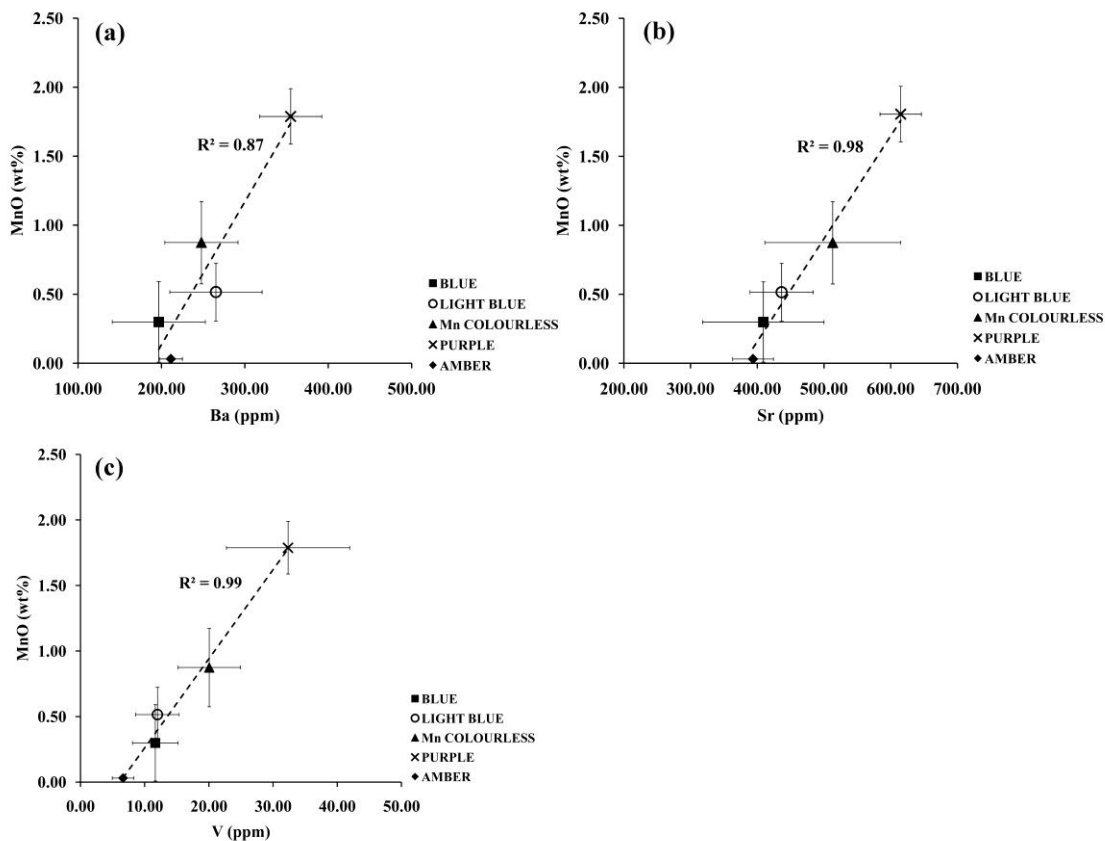


Figure 4.1.14: (a) MnO vs Ba; (b) MnO vs Sr; (c) MnO vs V of all the chromatic groups identified for natron glasses (sample AD-V-2 was not considered in the averages of purple glass group).

Only one sample, AD-V-2, clearly differs from other purple glasses for higher barium and also iron (Ba= 1277 ppm vs 300-383 ppm; Fe_2O_3 = 1.13 wt% vs 0.31-0.45 wt%; Table D.1), suggesting the use of different raw materials as source of manganese.

4. Raw materials in glass production: the textural, chemical and mineralogical study

Trace elements are generally low in purple glasses, only one sample (AD-V-1) has copper contents higher than 100 ppm (Table D.2), suggesting a possible recycling of coloured cullets and/or scraps.

Blue glasses are numerous in Adria sample set (22 samples). The vast majority of them belongs to Group AD/N1, including a glass chunk (AD-B-5), two samples constitute Group AD/N2a and also the ‘outlier’ AD-B-4 is a blue glass (Table D.1).

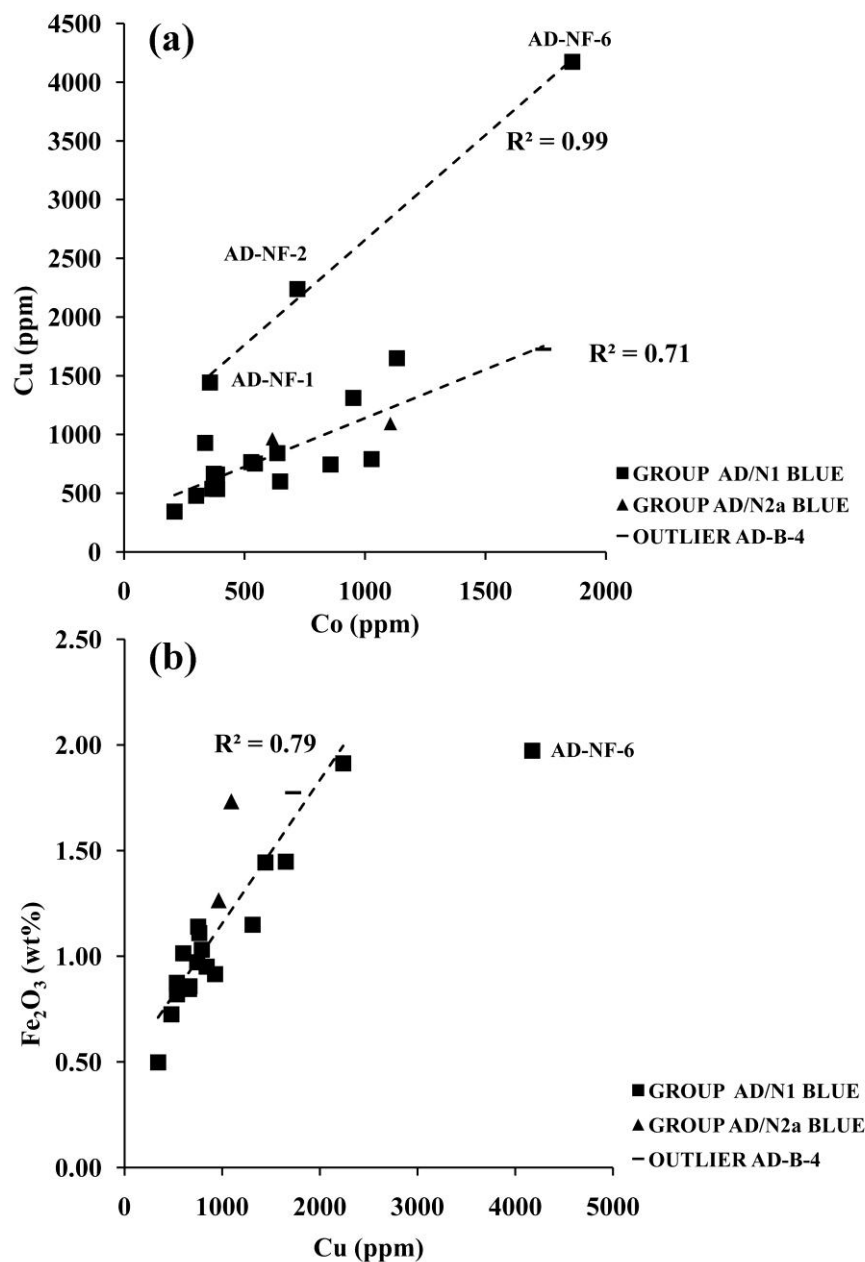


Figure 4.1.15: Plots of all natron blue glasses: (a) Cu vs Co; (b) Fe_2O_3 vs Cu.

4. Raw materials in glass production: the textural, chemical and mineralogical study

Independently from their bulk composition, all Adria blue glasses have high iron (0.50-1.97 wt%), copper (343-4173 ppm) and cobalt (209-1861 ppm). Cobalt is likely the main chromophore since its absorption coefficient is higher than that of the copper and iron (Mirti et al., 2002; Gliozzo et al., 2010). Plots in Figure 4.1.15, a, b reveal that cobalt, copper and iron are positively correlated in the majority of blue glasses, indicating they were intentionally added to the glass from the same source. In fact, cobalt is often found in rock mineralization associated with copper and/or iron, such as trianite ($2\text{CoO}_2 \cdot \text{CuO} \cdot 6\text{H}_2\text{O}$) and skutterudite ($(\text{Co}, \text{Fe}, \text{Ni})\text{As}_3$) (Henderson, 1985). Three Pre-Roman samples (AD-NF-1, AD-NF-2, AD-NF-6, Tables D.1 and D.2) clearly show a different correlation line (Fig. 4.1.15, a); in addition the sample AD-NF-6 has an iron content particularly high and not correlated with copper (Fig. 4.1.15, b). These evidences, although low in number, could suggest that these samples come from an ore with some different geochemical characteristics. As observed by (Gratuze et al., 1992), some trace elements can be associated to the cobalt-bearing raw material, such as Ni, As, Pb, Zn, In and Sb. These elements are generally low in Roman blue glasses: on 15 samples only 5 present higher lead contents (AD-B-1, AD-B-2, AD-B-7, AD-B-10, AD-R-1b, Pb= 155-638 ppm, Table D.2). Conversely, all Pre-Roman vessels show high lead contents (125-2506 ppm,) and, in some cases, high Sb (0.18-0.26 wt%), Ni (126-274 ppm) and/or Zn (113-214 ppm) (Tables D.1 and D.2). This evidence, in association with the presence of residual phases observed only in Pre-Roman blue glasses, could suggest that Co-bearing raw materials were less treated in glass manufacture before the Roman period. In particular two samples, AD-NF-6 and AD-NF-7, have in common higher Ni (126-274 ppm), As (14-26 ppm) and In (8-4.6 ppm) with respect to the other core-formed glasses (Table D.2). Moreover, in sample AD-NF-7 residual phases containing Fe-Co-Ni were observed (see section 4.1.1), suggesting that the mineral skutterudite ($(\text{Co}, \text{Ni}, \text{Fe})\text{As}_3$) was likely the source of cobalt.

MnO contents are highly variables in blue samples. Ten glasses show MnO <0.5 wt% (MnO= 0.01-0.42 wt%), the others present higher values (0.50-1.41 wt%,) (Table D.1). This could suggest that manganese was intentionally added in some glasses in order to modify their colour or, alternatively, it could be related to a recycling of Mn-containing glass.

4. Raw materials in glass production: the textural, chemical and mineralogical study

Colouring agents in soda ash glass (Group AD/A)

As already said, this little group of soda ash glass includes four emerald green, one blue and one black glasses; the black glass shows an intense green colour when observed in thin section.

In the emerald green samples copper and tin are both present (Cu= 16702-24029 ppm; Sn= 999-1981 ppm, Table D.2) and correlated (Fig. 4.1.16); lead in range 151-762 ppm was also revealed (Table D.2). Furthermore, the Cu:Sn ratio is approximately 9:1, the same that in ancient bronzes. These evidences suggest that emerald green colour is derived from the addition of bronze, as already observed by Jackson et al. (2006) for some 1st century AD emerald green glasses, coming from France and United Kingdom, and produced with a soda plant ash as flux.

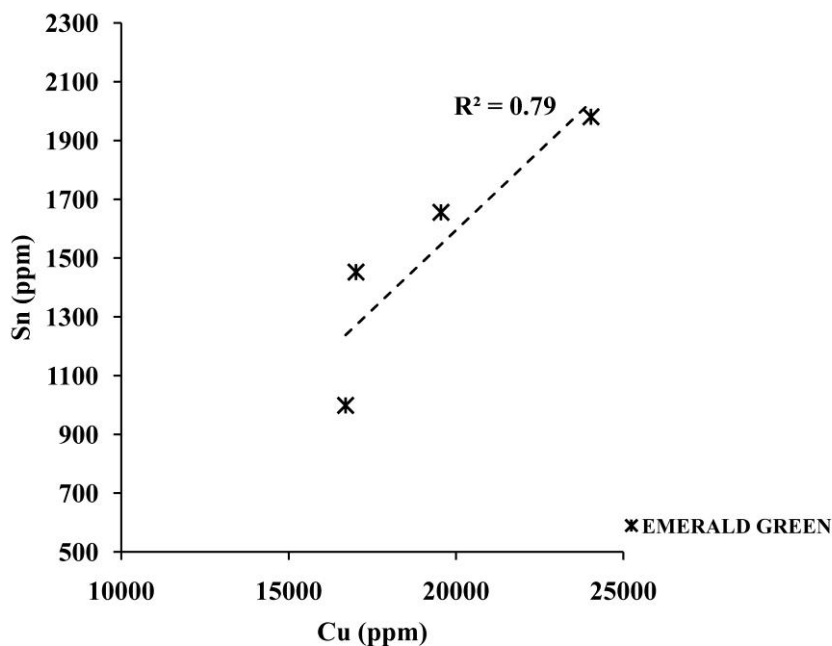


Figure 4.1.16: Sn vs Cu plot for the emerald green glasses. Note the good correlation between the two elements ($R^2 = 0.79$).

In the black glass, no particular colouring agents have been revealed. As observed also by Van der Linden et al. (2009) for some black glasses coming from the Northern Europe, the black colour is attributable to the high iron content ($\text{Fe}_2\text{O}_3 = 1.88 \text{ wt}\%$), not contrasted by addition of manganese ($\text{MnO} = 0.32 \text{ wt}\%$) (Table D.1). Notwithstanding the blue glass AD-B-2 was produced with a different flux with respect to other Adria

4. Raw materials in glass production: the textural, chemical and mineralogical study

blue glasses, its colouring agents are the same and are characterized by high cobalt (742 ppm), iron (1.28 wt%) and copper (1178 ppm) (Tables D.1 and D.2).

4.1.2.2 Opaque glass

The chemical results of the glass matrices of 23 opaque glasses, given by EPMA, are listed in Table D.3. The majority of opaque glasses are decorations of the transparent glasses discussed in the above section. For this reason, their label is followed by a letter specifying the color ('w' white; 'lb' light blue; 'y' yellow, 'wt' wisteria). The composition of major and minor elements is expressed as weight per cent of oxides, traces are expressed as part per million (ppm). According to the classification of Fiori et al. (2003), proposed for byzantine mosaics, the majority of white samples can be classified as soda-lime-silica glass with SiO₂, Na₂O and CaO in the ranges 61.19-71.56 wt%, 8.67-15.07 wt%, 4.84-9.54 wt%, respectively. Two white glasses differ from the others, since they are a soda-lead-silica glass (AD-R-1w, SiO₂= 63.88 wt%, Na₂O= 12.96 wt%, CaO= 5.66 wt% and PbO= 5.34 wt%) and a lead glass (AD-BO-1, SiO₂= 59.83 wt%, Na₂O= 8.67 wt%, CaO= 4.84 wt% and PbO= 13.06 wt%) (Table D.3). All the yellow samples are lead glasses with SiO₂, Na₂O, CaO and PbO in the ranges 57.35-65.96 wt%, 10.94-13.65 wt%, 3.38-7.04 wt% and 8.76-20.36 wt%, respectively (Table D.3). Independently from their bulk composition, the opaque samples have in common low contents of MgO (0.42-1.37 wt%) and K₂O (0.22-1.23 wt%), indicating the use of natron as flux, as observed for the majority of the transparent glass. The sample AD-BG-1 is quite singular, since it has a transparent body produced with a plant ash glass (Table D.1), but opaque yellow decoration of natron glass (Table D.3).

As shown in Figure 4.1.17, the majority of the white, blue and light blue soda-lime-silica glasses have a chemical composition similar to that determined for the transparent glasses (Group AD/N1, see the above section), suggesting the use of same raw materials and of similar production technologies. On the other hand, the soda-lead-silica glass and the lead glasses are generally characterized by lower CaO and Al₂O₃ contents, indicating that different production technologies were employed in their manufacture. It is quite difficult to find in literature comparisons for the compositions of glassy matrices of opaque glasses, since they are usually bulk analyses (Arletti et al., 2010 b, 2011). However Figure 4.1.17 shows that the soda-lead-silica glass and the lead glasses

4. Raw materials in glass production: the textural, chemical and mineralogical study

from Adria have a good agreement with some 6th century yellow mosaic tesserae, made of lead glass and opacified by lead antimonate crystals (Tonietto, 2010). This evidence suggests a probable continuity, at least as concerns the yellow glass, in the use of raw materials and in production technologies in a broad chronological period, from the 6th century BC until 6th century AD. Conversely, white, blue and light blue glasses from Adria generally show higher values of CaO and Al_2O_3 than the Byzantine tesserae (Fig. 4.1.17), notwithstanding the opacifiers are the same (calcium antimonate). Furthermore is worth noting that in Adria glasses only calcium antimonate crystals of low temperature ($\text{Ca}_2\text{Sb}_2\text{O}_7$) were revealed (see section 4.1.1.2), whereas in S. Giustina tesserae both the phases are present. Therefore, these data may indicate that different production technologies were employed for the manufacture of white, blue and light blue opaque glasses in Pre-Roman/Roman and Byzantine periods.

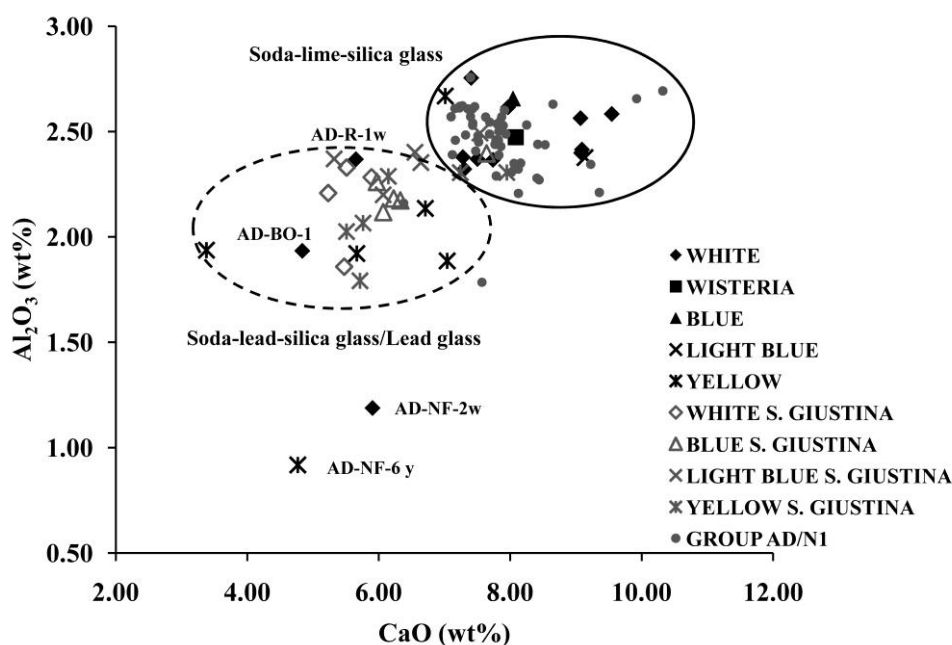


Figure 4.1.17: Al_2O_3 vs CaO plot for all opaque glasses. Data of transparent glass from Adria (Group AD/N1, present work) and of yellow lead glasses of mosaic tesserae (Tonietto, 2010) are also reported for comparison.

Plot in Figure 4.1.18 shows that, as already observed by other authors for Roman white glasses (Lahlil at al., 2006, 2008), the concentrations of Sb_2O_3 and CaO are not correlated in glasses opacified by means of calcium antimonate crystals. This data suggests that antimony and calcium raw materials would have been introduced

4. Raw materials in glass production: the textural, chemical and mineralogical study

separately, and consequently that calcium antimonate would have precipitated *in situ*, as also hypothesized on the basis of the euhedral morphology of the crystals observed in white and wisteria glasses (see paragraph 4.1.1.2). The *in situ* crystallization of calcium antimonate opacifiers in Roman glass have been suggested by many authors, who sometimes propose the addition of antimony as stibnite (Sb_2S_3) or roasted stibnite to the glass raw materials or in the melt (Mass et al., 1998; Ubaldi and Verità, 2003, Verità et al., 2002; Bimson and Freestone, 1983). However the light and opaque blue samples (AD-NF-1b, AD-NF-51b, AD-BLO-1) clearly differ from the white glass for lower Sb_2O_3 contents ($\text{Sb}_2\text{O}_3 = 1.27\text{-}1.90$ wt% vs $2.93\text{-}7.48$ wt%, Fig. 4.1.18, Table D.3). This evidence in addition to the different morphology of the calcium antimonate crystals, partially dissolved into the glassy matrix (see section 4.1.1.2), supports the hypothesis that these colours were obtained by means of a different production technology.

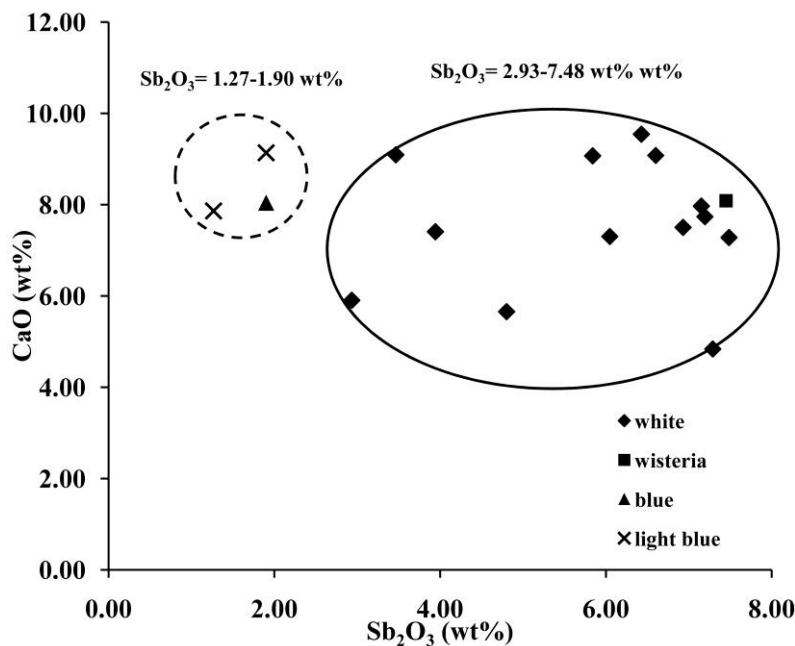


Figure 4.1.18: CaO vs Sb_2O_3 plot for the glasses opacified with calcium antimonate. 'High Sb' group (white glasses, continuous ellipse) and 'low Sb' group (light blue and blue samples, dotted ellipse) are highlighted.

White, wisteria, blue/light blue samples, all opacified by addition of calcium antimonate, are differentiated by traces present in the glass matrices. No significant amounts of colourants, such as Co and/or Cu, were revealed in white glasses. On the other hand it is evident that colouring agents were opportunely added in wisteria, blue

4. Raw materials in glass production: the textural, chemical and mineralogical study

and light blue glass matrices, in order to obtain the desired hue; wisteria and blue glasses show intentional additions of both cobalt (518-896 ppm) and copper (789-2192 ppm) and light blue glasses only of copper (1292-2233 ppm). Intentional additions of MnO have been revealed in six white glasses (AD-BB-1w, AD-R-1w, AD-R-2w, AD-VB-1w, AD-AB-4w, AD-BO-1, Table D.3).

Yellow glasses were coloured and opacified by the addition of lead antimonate and, only in one sample (AD-BG-1), by both lead antimonate and lead-tin antimonate crystals (see section 4.1.1.2). No differences were observed between Pre-Roman and Roman yellow opaque glasses. All yellow glass matrices contain variable amount of lead ($\text{PbO} = 8.76\text{-}20.36 \text{ wt}\%$) and generally lower amounts of antimony ($\text{Sb}_2\text{O}_3 = 0.65\text{-}1.51 \text{ wt}\%$) than white glass matrices (Table D.3); the sample AD-BG-1, with lead-tin antimonate opacifiers, show also Sn in the glass matrix ($\text{Sn} = 1784 \text{ ppm}$). No other trace elements were observed in yellow glasses. Lahlil et al. (2008) had suggested that yellow Roman glass, conversely to white glass, were opacified by the addition to the melt of natural or previously synthesized crystals, but this model has yet to be confirmed.

4.2 Late Roman Glass from Aquileia

As previously said (chapter 2), the sample set of Aquileia glasses includes various types of objects (Table A.2, Appendix A), largely attested in the site. In order to verify possible relationship between the type of object and the production technique and/or the chronology, a group of object (Isings 106c, 116, 117) with similar chronology (late 3rd-5th century AD) and production technique (mold-blowing) has been compared on one hand with a group of objects (Isings 104, Isings 87 or 120, Isings 132) of similar dating but different production technique (blowing) and on the other with objects (Isings 111) dissimilar for both chronology (5th-8th century AD) and production technique (blowing) (Table A.2, Appendix A). Chemical data and their discussion are reported in the following section.

4.2.1 Bulk chemistry

The bulk chemistry of Aquileia glass was obtained by means of XRF and chemical data are listed in Tables D.4 and D.5; Cl, S, Sb and Sn were checked by EPMA. The composition of major and minor elements is expressed as weight per cent of oxides;

4. Raw materials in glass production: the textural, chemical and mineralogical study

traces are expressed as part per million (ppm). All samples are soda-lime-silica glass with SiO₂, Na₂O and CaO in the ranges of 62.57-71.48 wt%, 14.93-21.42 wt% and 4.97-11.43 wt%, respectively. The levels of magnesium and potassium are lower than 1.5 wt% (MgO= 0.44-1.44 wt%, K₂O= 0.32-1.50 wt%), suggesting the use of natron as flux. By analyzing the compositional data with the help of bi-plots and comparing the compositions with known glass types, three main groups, called Group AQ/1, Group AQ/2 and Group AQ/3, can be recognized, not strictly related to chronology, types and production technique. As shown in the plot CaO-Al₂O₃ in Figure 4.2.1, these three groups are well separated and are also different with respect to the ‘typical’ Roman glass (e. g. Group AD/N1 of Adria glasses), dating 1st-3rd century, suggesting changes within the glass making raw material (Foster and Jackson, 2009).

Group AQ/1 and AQ/2 may be further divided into subgroups, with a slightly different bulk composition: Group AQ/1a, Group AQ/1b, Group AQ/2a and Group AQ/2b. The average composition, together with the corresponding standard deviation, was calculated within each group and reported in Table 4.2.1.

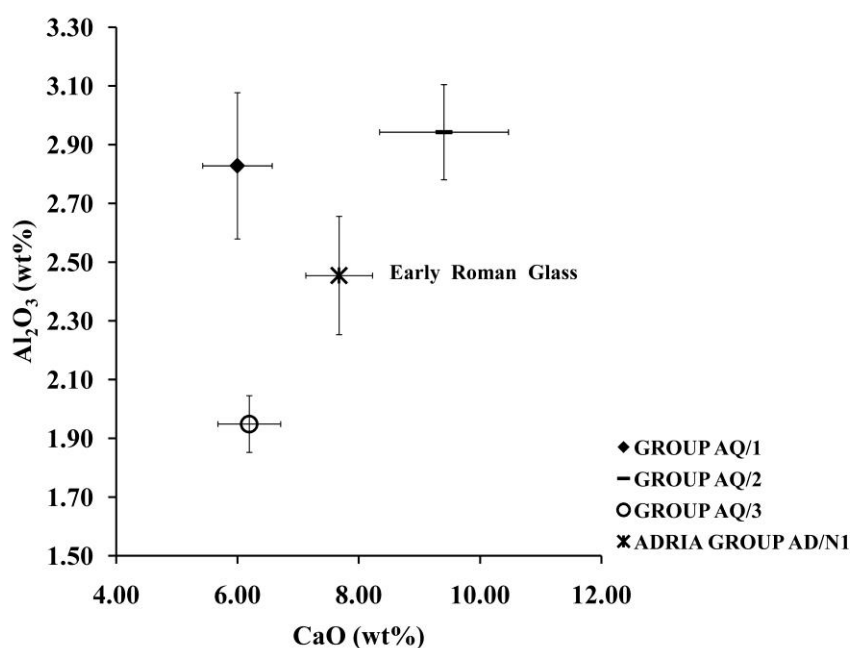


Figure 4.2.1: Al₂O₃ vs CaO plot of the average compositions for the three glass groups recognized at Aquileia, compared with the earlier glass from Adria (Group AD/N1).

4. Raw materials in glass production: the textural, chemical and mineralogical study

	AQ/1a	AQ/1b	AQ/2a	AQ/2b	AQ/3
wt%	(N= 7)	(N= 31)	(N= 10)	(N= 5)	(N= 9)
SiO₂	64.97±1.09	65.59±1.64	66.85±1.62	66.35±1.84	68.40±1.97
Na₂O	17.89±0.81	18.66±1.44	16.58±0.60	17.44±0.95	19.24±1.30
CaO	5.70±0.57	6.04±0.49	9.09±0.94	10.03±1.11	6.19±0.52
Al₂O₃	3.00±0.11	2.79±0.26	2.92±0.18	2.98±0.14	1.95±0.10
K₂O	0.54±0.10	0.46±0.08	1.29±0.28	0.82±0.09	0.41±0.04
MgO	1.15±0.15	1.04±0.14	0.51±0.05	0.59±0.06	0.64±0.10
Fe₂O₃	3.23±0.57	1.76±0.38	0.47±0.09	0.47±0.15	0.79±0.21
TiO₂	0.55±0.07	0.51±0.11	0.08±0.01	0.08±0.03	0.12±0.02
MnO	1.78±0.27	1.90±0.45	1.18±0.22	0.14±0.11	0.98±0.25
P₂O₅	0.12±0.02	0.06±0.02	0.16±0.04	0.07±0.01	0.05±0.01
Sb₂O₃	<0.04	<0.04	<0.04	<0.04	<0.04
SO₃	0.23±0.05	0.26±0.06	0.20±0.03	0.19±0.07	0.28±0.08
Cl	1.22±0.07	1.34±0.16	0.75±0.19	1.38±0.13	1.56±0.18
<i>ppm</i>					
Co	12±4	12±4	5±3	<3	5±3
Ni	36±7	18±6	10±3	14±10	13±5
Cu	146±42	147±110	57±40	33±27	51±24
Zn	46±8	34±15	18±3	13±5	20±4
Sn	<400	<400	<400	<300	<400
Pb	53±52	87±106	56±54	87±98	31±14
Rb	14±1	13±1	23±3	20±2	12±1
Sr	435±38	450±49	481±56	557±89	445±39
Ba	480±245	656±286	388±77	417±310	242±37
Zr	249±29	243±51	45±7	45±11	63±11
Nd	13±2	<10	<10	<10	11±2
La	12±3	16±4	13±2	14±4	8±3
Ce	21±7	19±6	18±7	16±5	10±7
Th	<3	<3	<3	<3	<3
U	4±1	3±1	4±1	<3	5±2
V	84±12	52±11	22±8	11±5	27±6
Ga	6±1	8±2	9±2	<5	3±2
Y	15±2	11±2	8±1	8±1	7±2
Nb	6±1	6±2	2±1	4±0	3±0
Cr	68±9	62±17	14±6	35±25	14±5

Table 4.2.1: Mean chemical compositions and standard deviations for the identified groups. Major and minor elements are expressed as weight per cent, traces as ppm. (N= number of samples).

4. Raw materials in glass production: the textural, chemical and mineralogical study

Groups AQ/1a and AQ/1b, composed of seven and thirty-one samples respectively, include bottles, beakers, cups and also a lamp, dating mostly late 3rd-5th century AD (Table A.2). The typical colour of the glass belonging to these groups is yellow/green. Groups AQ/1a and AQ/1b differ from the other Aquileia groups for higher content of MgO (1.15 ± 0.15 wt%, 1.04 ± 0.14 wt%, respectively, vs 0.51 ± 0.05 wt%, 0.59 ± 0.06 wt%, 0.64 ± 0.10 wt%), Fe₂O₃ (3.23 ± 0.57 wt%, 1.76 ± 0.38 wt% vs 0.47 ± 0.09 wt%, 0.47 ± 0.15 wt%, 0.79 ± 0.21 wt%), TiO₂ (0.55 ± 0.07 wt%, 0.51 ± 0.11 wt% vs 0.08 ± 0.01 wt%, 0.08 ± 0.03 wt%, 0.12 ± 0.02 wt%) and MnO (1.78 ± 0.27 wt%, 1.90 ± 0.45 wt% vs 1.18 ± 0.22 wt%, 0.14 ± 0.11 wt%, 0.98 ± 0.25 wt%) (Table 4.2.1). They present also higher contents of high atomic number elements, such as Zr (249 ± 29 ppm, 243 ± 51 ppm vs 45 ± 7 ppm, 45 ± 11 ppm, 65 ± 11 ppm), V (84 ± 12 ppm and 52 ± 11 ppm vs 22 ± 8 ppm, 11 ± 5 ppm, 27 ± 6 ppm) and Cr (68 ± 9 ppm and 62 ± 17 ppm vs 14 ± 6 ppm, 35 ± 25 ppm, 14 ± 5 ppm) (Table 4.2.1). Since iron, titanium, zirconium, vanadium and chromium are related to the heavy minerals and or mafic fraction present in the sand (e.g. zircon, rutile, ilmenite, chromite, garnet, biotite), the chemical characteristics of Groups AQ/1a and AQ/1b suggest the use of an impure sand source for their production. Indeed, these two groups present all the key characteristics of HIMT glass (High Iron, Manganese and Titanium), which appeared in the Mediterranean in the 4th century AD and is defined by high levels of iron (≥ 0.7 wt%), manganese (usually ~ 1 -2 wt%), magnesium (usually ≥ 0.8 wt%) and titanium (≥ 0.1 wt%), with a positive correlation between Fe and Al. Its typical yellow-green colour is due to levels of iron, suggestive of a relatively impure sand source (Foster and Jackson 2009). The acronym HIMT was first used by Freestone (1994) for raw glass from Carthage and glass vessels from Cyprus (Freestone et al. 2002), although a glass with high contents of iron, manganese and titanium was first identified by Sanderson et al. (1984). This kind of glass is also common in Britain, the western Mediterranean and Egypt (Foster and Jackson 2009), France (Foy et al. 2003) and Italy (Mirti et al. 1993; Silvestri et al. 2005; Arletti et al. 2010 a). As shown in Figure 4.2.2, Group AQ/1a and Group AQ/1b are very similar to one another in terms of lime (CaO= 5.70 ± 0.57 wt% and 6.04 ± 0.49 wt%) and alumina (Al₂O₃= 3.00 ± 0.11 wt% and 2.79 ± 0.26 wt%) (Table 4.2.1), and present a good agreement with the compositional field including HIMT glasses founded in Mediterranean and Northern provinces (Foster and Jackson, 2009; Foy et al. 2003).

4. Raw materials in glass production: the textural, chemical and mineralogical study

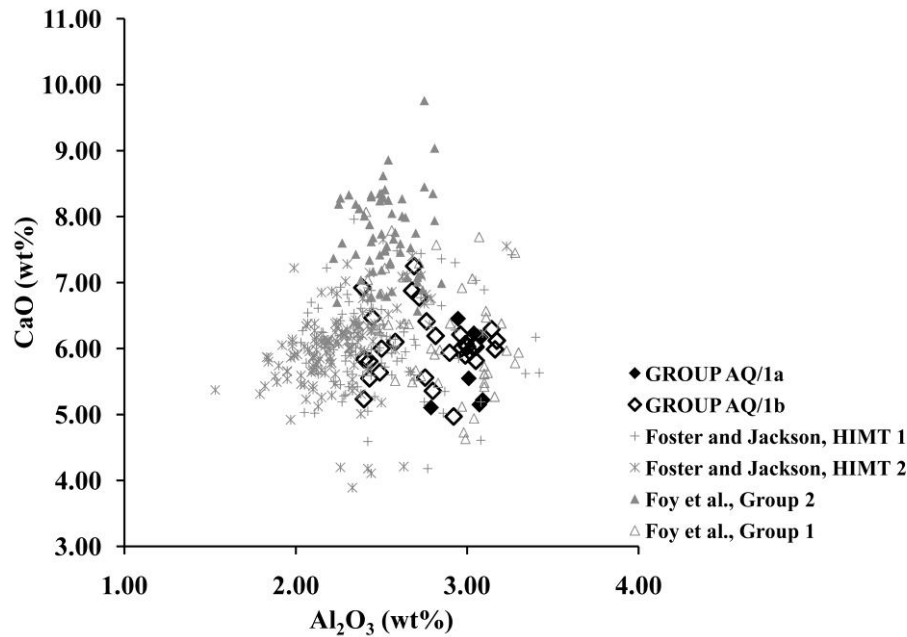


Figure 4.2.2: CaO vs Al₂O₃ plot. Aquileia HIMT glasses (GroupAQ/1a and AQ/1b, represented by rombs) are compared with reference data for other HIMT glasses (in grey; data from Foster and Jackson, 2009; Foy et al. 2003).

On the other hand, Figure 4.2.3, a shows that Group AQ/1a differs from Group AQ/1b for higher iron ($\text{Fe}_2\text{O}_3 = 3.23 \pm 0.57$ wt%, vs 1.76 ± 0.38 wt%), with a most positive correlation between iron and titanium, higher vanadium ($\text{V} = 84 \pm 12$ ppm vs 52 ± 11 ppm) and slightly higher nickel ($\text{Ni} = 36 \pm 7$ ppm vs 18 ± 6 ppm) (Table 4.2.1, Fig. 4.2.3, b, c). These evidences, in particular the different Fe/Ti ratio between Groups AQ/1a and AQ/2a glasses (Fig. 4.2.3, a), are independently from the types and indicate that the glass of the two groups was produced with sands coming from ores with different geochemical characteristics, suggestive of a different provenance. The division of the HIMT glasses into two groups, was also demonstrated by Foy et al. (2003), termed ‘Group 1’ and ‘Group 2’, and by Foster and Jackson (2009), called ‘HIMT 1’ and ‘HIMT 2’. However, there is a difference among the reference groups and the Aquileia ones. The Fe_2O_3 - TiO_2 plot (Fig. 4.2.3, a) indicates that the ‘weaker’ (Group 2 and HIMT 2) and the ‘stronger’ HIMT groups (Group 1 and HIMT 1) identified by Foy et al. (2003) and Foster and Jackson (2009) well corresponds each other. Group AQ/1b from Aquileia is similar to the ‘stronger’ literature groups (Group 1 and HIMT 1), but, as already said, it represents the ‘weaker’ term of the Aquileia assemblage (Fig. 4.2.3, a, b, c, Table 4.2.1).

4. Raw materials in glass production: the textural, chemical and mineralogical study

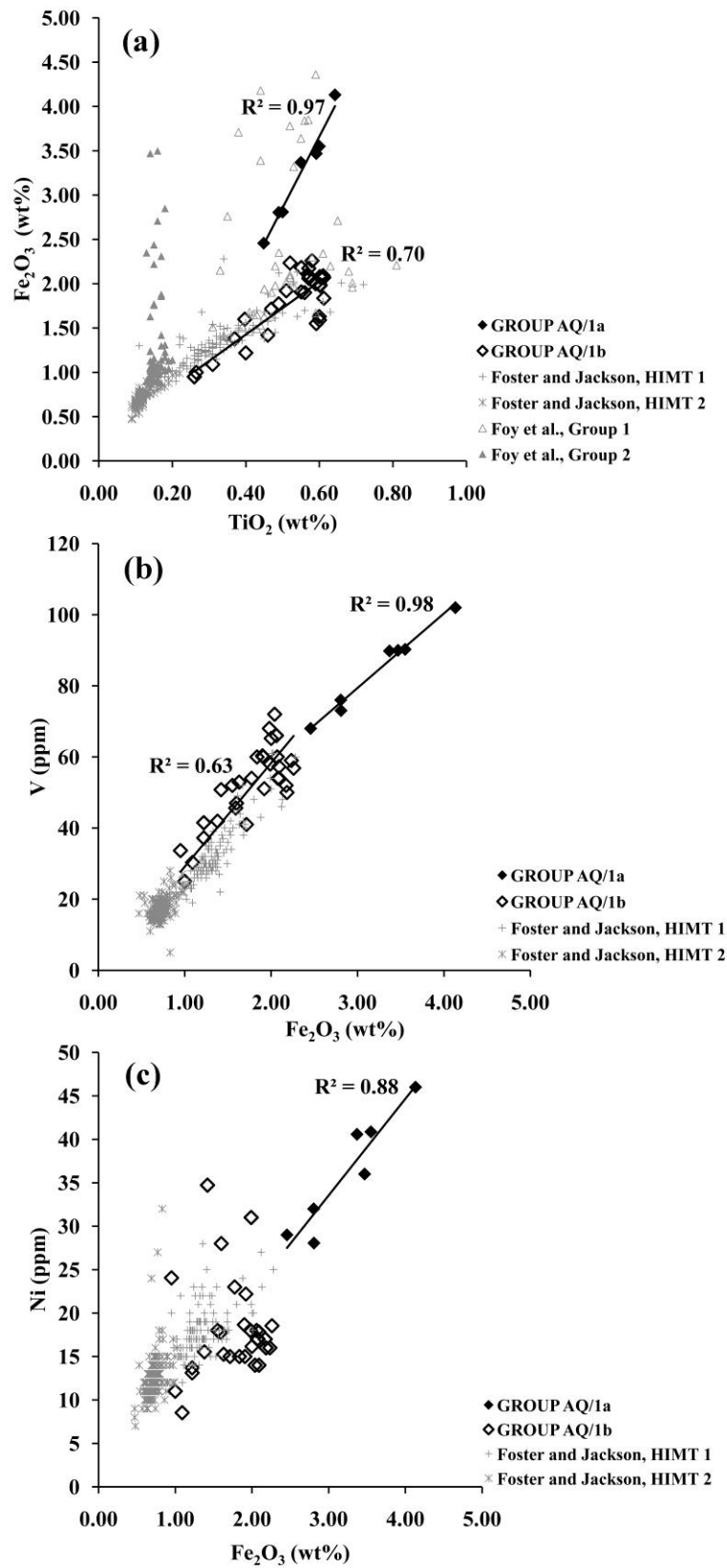


Figure 4.2.3: Plots for Aquileia Group AQ/1a and AQ/1b; reference data are also reported (from Foster and Jackson, 2009; Foy et al. 2003). (a) Fe_2O_3 vs TiO_2 ; (b) V vs Fe_2O_3 ; (c) Ni vs Fe_2O_3 .

4. Raw materials in glass production: the textural, chemical and mineralogical study

The same similarity between Group AQ/1b and HIMT 1 of Foster and Jackson (2009) is observed also for nickel and vanadium contents (Fig. 4.2.3, b, c), suggesting that they were manufactured with a similar sand source. No considerations can be made about vanadium and nickel contents with respect to Groups 1 and 2 of Foy et al. (2003), since these elements were not measured.

Notwithstanding the ‘stronger’ Group AQ/1a is chronologically similar to the ‘weaker’ Group AQ/1b, it seems to be less popular in the Mediterranean: no comparisons have been found with literature data, except for few (and scattered) samples of Group 1 of Foy et al. (2003) (Fig. 4.2.3, a); this suggests that the Group AQ/1a from Aquileia could be considered a new compositional group within the HIMT assemblage. As concerns the provenance of HIMT glass, Freestone et al. (2005) and Foy et al. (2003) suggest an Egyptian source. This is based on the high titanium content which is common to Egyptian glasses, the lead, neodymium, oxygen and strontium isotope signatures and the high soda content which may indicate a location close to a natron source (for a detailed discussion on the provenance of the raw materials see the chapter 5).

Groups AQ/2a (10 samples), AQ/2b (5 samples) and AQ/3 (9 samples) are composed of cups and beakers; bottles are the only types not present in these groups. Groups AQ/2a and AQ/3 include glasses dating both late 3rd-5th and 5th-8th century AD, while Group AQ/2b includes only samples dating late 3rd-5th century AD; glasses of these groups are typically light blue/pale green in colour (Table A.2).

The Fe_2O_3 - Al_2O_3 and CaO - Al_2O_3 plots in Figure 4.2.4, a, b indicates that Groups AQ/2a, AQ/2b and AQ/3 have similar iron contents ($\text{Fe}_2\text{O}_3 = 0.47 \pm 0.09$, 0.47 ± 0.15 and 0.79 ± 0.21 wt%, respectively), but lower than those observed in Groups AQ/1a and AQ/1b (Table 4.2.1). Groups AQ/2a and AQ/2b differ from Group AQ/3 substantially for higher calcium ($\text{CaO} = 9.09 \pm 0.94$ wt% and 10.03 ± 1.11 wt% vs 6.19 ± 0.52 wt%) and alumina ($\text{Al}_2\text{O}_3 = 2.92 \pm 0.18$ wt% and 2.98 ± 0.14 wt% vs 1.95 ± 0.10 wt%, Table 4.2.1, Fig. 4.2.4), indicative of a different sand source, likely richer in calcite and feldspars for Groups AQ/2a and AQ/2b. As shown in Table 4.2.1, Groups AQ/2a and AQ/2b have a very similar chemical composition, which perfectly fits with that of the so called Levantine I glass (Figure 4.2.4, a, b).

4. Raw materials in glass production: the textural, chemical and mineralogical study

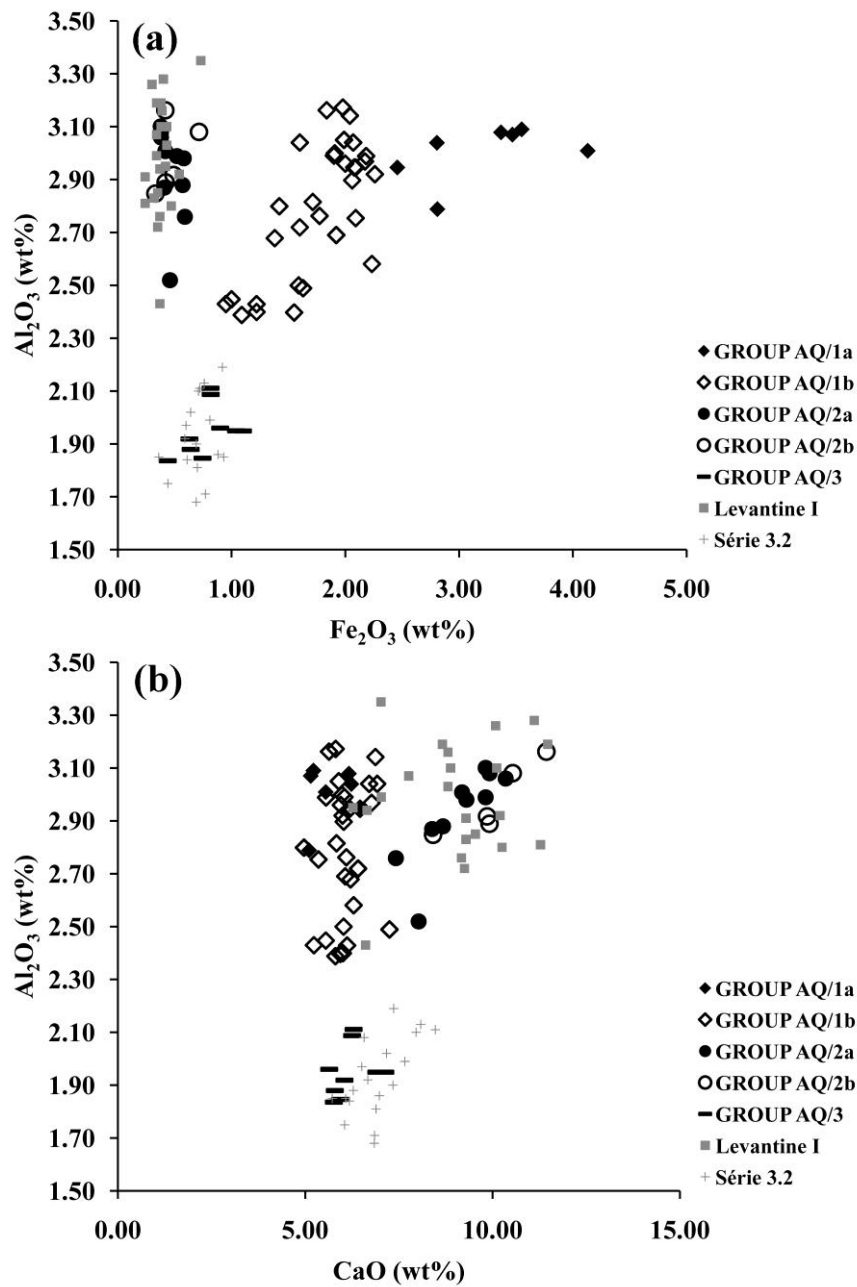


Figure 4.2.4: plot for all Aquileia groups: a) Al_2O_3 vs Fe_2O_3 ; b) Al_2O_3 vs CaO. Reference data for Levantine I and Série 3.2 glass are also reported (grey symbols, from Freestone et al., 2000; Foy et al., 2003).

The term ‘Levantine I production’ has been used in literature by Freestone et al. (2000, 2002, 2003) to refer to glasses from 4th century from Jalame, Apollonia, Dor and later Byzantine sites in Israel. Levantine I glass appears to have been the typical glass of the Levant between the 4th and the 7th centuries (Freestone et al., 2002), but it has been found also in France, Tunisia, Egypt, Cyprus, Britain and Italy (Foy et al., 2003;

4. Raw materials in glass production: the textural, chemical and mineralogical study

Freestone et al., 2002; Silvestri et al., 2005). This glass is characterized by lower levels of iron oxide (~0.4 %) and soda (~15 %) and higher levels of lime (~ 8.5 %) (Foster and Jackson, 2009). The production location of Levantine I glasses, from the 4th century and beyond, is thought to be somewhere in Palestine, using the sands of the Levantine coasts (Freestone, 2003).

The two Aquileia groups with a Levantine I composition, Group AQ/2a and AQ/2b, are distinguished essentially on the basis of the MnO content: Group AQ/2a contains appreciable levels of MnO (1.18 ± 0.22 wt%), whereas Group AQ/2b contains only trace amounts (0.14 ± 0.11 wt%) (Table 4.2.1, Fig. 4.2.5).

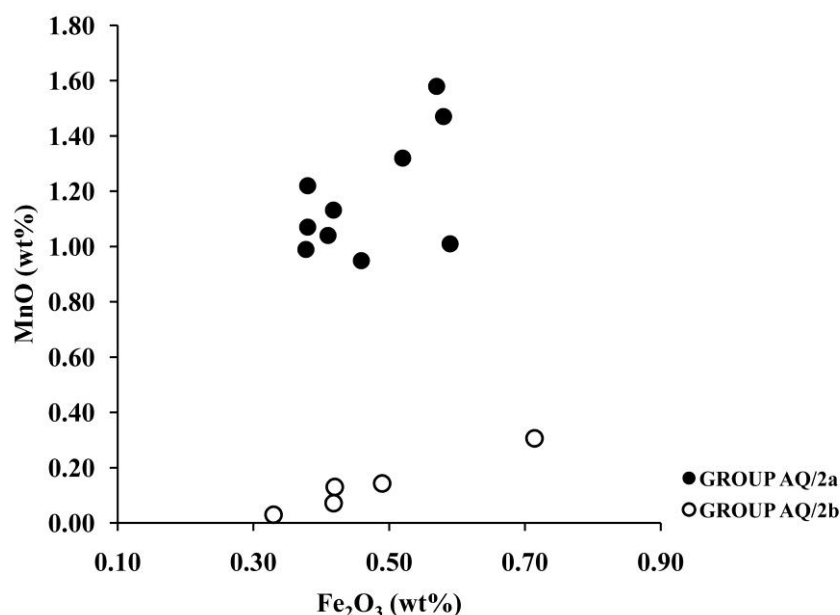


Figure 4.2.5: MnO vs Fe₂O₃ plot for Groups 2a and 2b, with a Levantine I composition. Note they are distinguished for different MnO contents, higher in Group 2a (full circles) with respect Group 2b (empty circle).

Brill, who also observed two groups of similar samples in Jalame glasses (Brill, 1988), stated that levels of MnO <0.4 % are natural impurities; those samples with higher concentrations indicate deliberate addition, presumably to affect the colour.

For what concerns the low calcium-low alumina glass belonging to Group AQ/3, Figure 4.2.4, a, b shows it is consistent with glasses of the small *Série* 3.2 of Foy et al. (2003). This series, dating 5th-6th century AD, is included in the Group 3 of Foy et al (2003), with the *Série* 3.1 and 3.3 (corresponding to Levantine I and Levantine II groups of

4. Raw materials in glass production: the textural, chemical and mineralogical study

Freestone), but it is distinguished for levels particularly low of calcium and alumina. Foy et al. (2003) do not exclude that this type of glass was also produced in the Syro-Palestine region, but with sands out to the coast between Jalame and Apollonia, where sands are characterized by higher levels of alumina. As the glasses of the *Série 3.2*, the AQ/3 glass has MnO contents about 1% (MnO= 0.98 ± 0.25 wt%, Table 4.2.1), indicating it is an intentional addition.

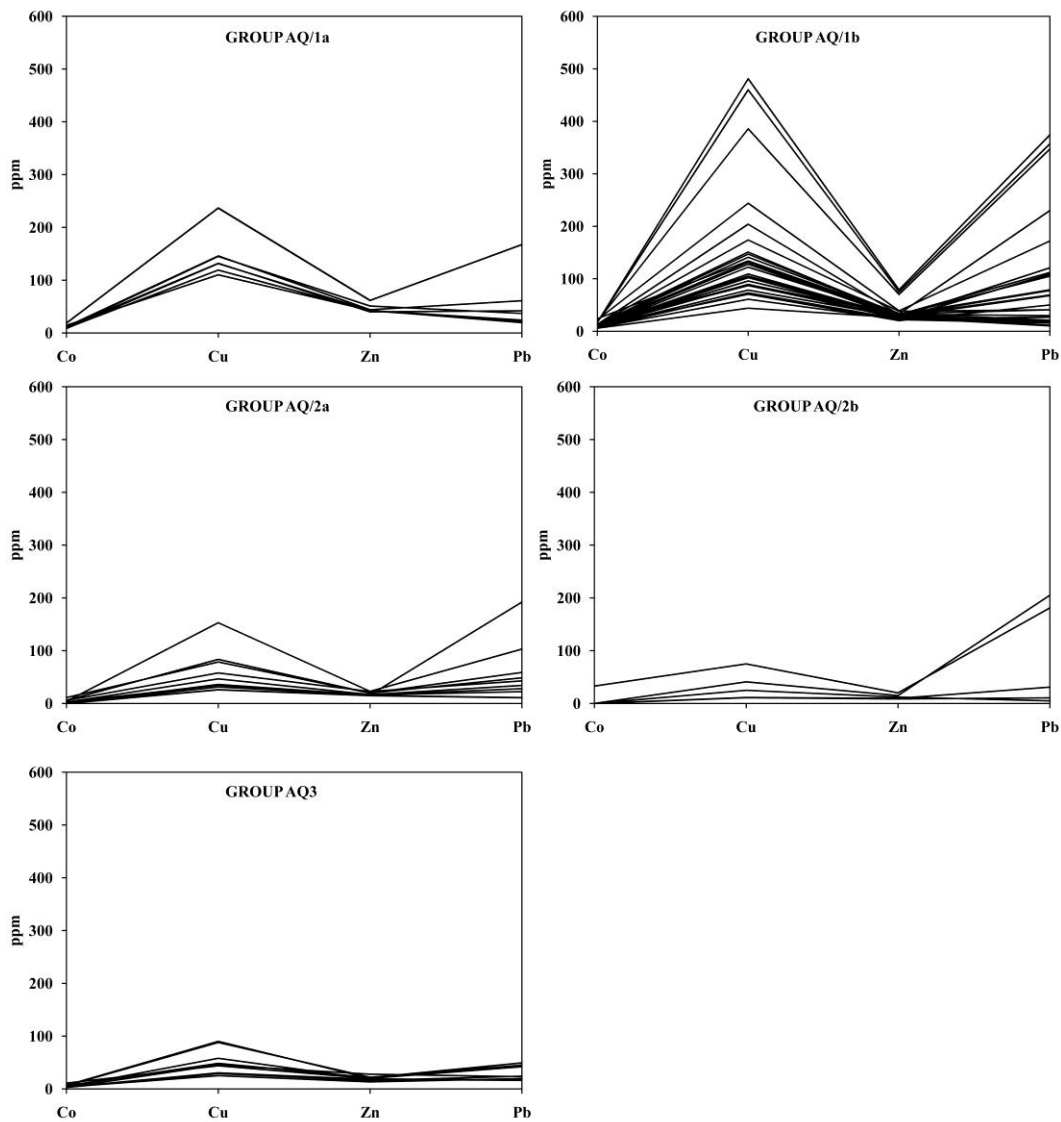


Figure 4.2.6: The concentration of recycling indicators, expressed as ppm, in all the glasses of Aquileia groups. Note the higher values of these elements in Groups AQ1a and AQ1b with respect the others.

4. Raw materials in glass production: the textural, chemical and mineralogical study

The trace elements that usually give information about the extent of recycling, such as Co, Zn, Sn, Cu, Pb (Freestone et al., 2002), are differently distributed in the Aquileia groups. Generally it is assumed that low levels of these elements (in the 1-100 ppm range) originated from constituents (heavy minerals) of the glass sand (Wedepohl and Baumann, 2000), while the presence of these elements in the 100-1000 ppm range may be explained by recycling of earlier glass and blue glass frit or cullet added during melting (Freestone, 1992; Jackson, 1996).

As shown in Figure 4.2.6 and Table D.4, 28 on 37 samples with HIMT composition (Group AQ/1a and AQ/2b) present clear evidence of recycling, with copper and lead contents particularly high in Group 1b with respect to Group 1a, suggestive of a stronger recycling. On the other hand only 3 on 15 glasses with Levantine I composition (Group AQ/2a and AQ/2b) present recycling indicators, while there is no evidence for recycling amongst any of the samples of Group AQ/3 (Fig. 4.2.6, Table D.4), indicating that the vast majority of these glasses were from newly manufactured material.

In the histogram in Figure 4.2.7, a, the distribution of the glass types analyzed in the present work (Ising forms 106, 116, 117, 104, 111, 87 or 120 and 132) are reported in function of the compositional groups. All the glass types are well represented in groups with HIMT composition (AQ/1a and AQ/1b), whereas forms Isings 104 and 132 (bottles) completely lack in groups of Levantine I and Série 3.2 composition (AQ/2a, AQ/2b, AQ/3). Moreover, in group AQ/3 only three of the seven analyzed types are present: Isings 116 (cups), 111 and 106 (beakers). Therefore, these evidences tend to exclude relationships between types and compositional groups, at least for what concerns cups and beakers. On the other hand it seems that a low quality glass, as HIMT type, was preferred for the production of bottles, but further studies on a major number of samples are required to confirm this hypothesis. Conversely, a dependence clearly appears when considering compositional groups in relation to the chronology. Figure 4.2.7, b shows that in the period late 3rd-5th century AD the assemblage of Aquileia samples is dominated by glasses with HIMT composition (Groups AQ/1a and AQ/1b), but in the later centuries (5th-8th) the three compositional groups (HIMT, Levantine I and Série 3.2) become more or less equivalent. The same predominance of HIMT over Levantine I glass was observed in 4th century samples from Britain (Foster and Jackson, 2009), but the reason of this are still unclear and can be only speculated on

4. Raw materials in glass production: the textural, chemical and mineralogical study

at the present. Freestone et al. (2002) hypothesizes that HIMT glass was a cheaper or more aesthetically pleasing option than Levantine I glass, while Foster and Jackson (2009) explain the dominance of HIMT glass since it was easier to remelt and form into artefacts at region where glass forming was less well understood and where the technology was less developed.

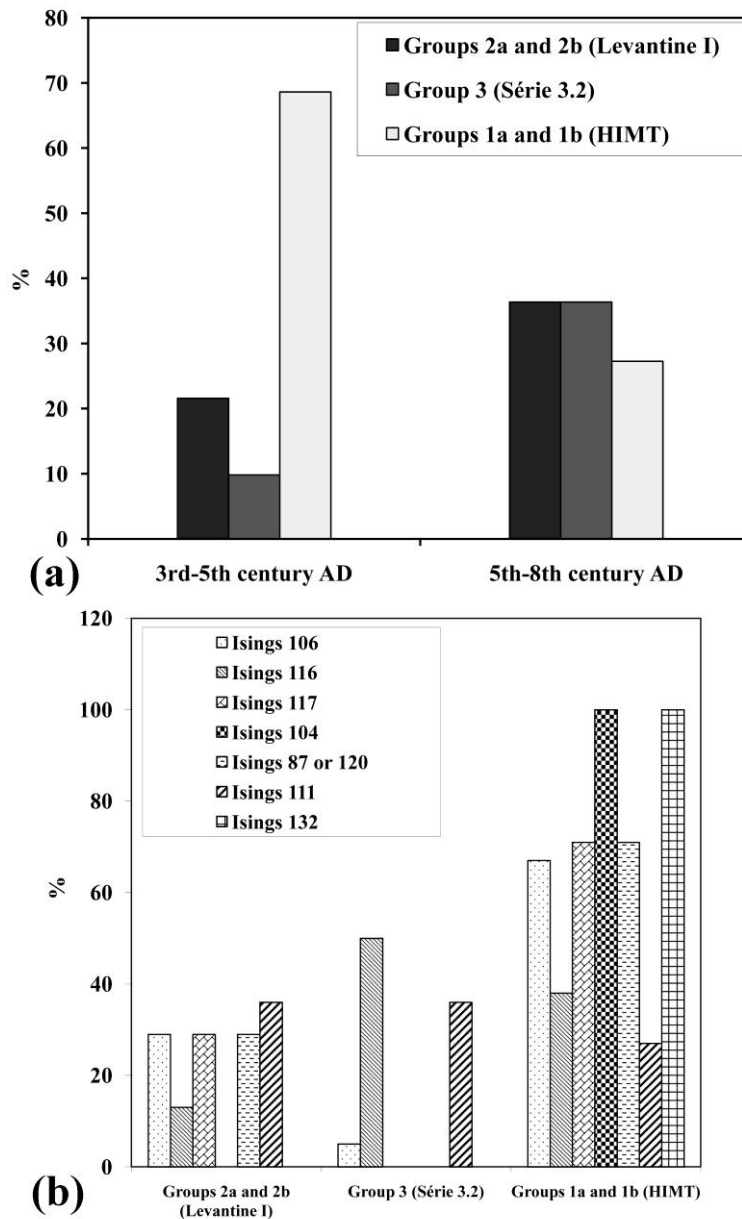


Figure 4.2.7: (a) istogram representing the relationship between compositional groups and types for Aquileia glasses; (b) istogram which represents the abundances of the main Aquileia compositional groups with respect two chronological periods: late 3rd-5th century AD and 5th-8th century AD.

4.3 Late Roman/early Medieval glass from Tuscany: a comparison with Aquileia glasses.

The chemical data of 15 glasses from the Tuscan sites of Pieve di Pava, Pieve di Coneo and S. Genesio are reported in the following section. These samples, Late Roman/early Middle Age in date, are mainly composed of beakers type Isings 111 and were analyzed for comparison with the Aquileia assemblage.

4.3.1 Bulk chemistry

The chemical results, given by XRF and EPMA, are listed in Tables D.6 and D.7, Appendix D. For the samples analyzed by XRF, Cl, S, Sb and Sn were checked by EPMA. The composition of major and minor elements is expressed as weight per cent of oxides; traces are expressed as part per million (ppm). As for Aquileia glasses, these samples are all soda-lime-silica glass in composition, with SiO₂, Na₂O and CaO in the ranges 61.45-67.83 wt%, 16.80-20.29 wt% and 5.40-8.73, respectively. They were produced using natron as flux, since their values of potassium and magnesium are lower than 1.5 wt% (K₂O= 0.42-0.87 wt%, MgO= 0.58-1.36 wt%) (Table D.6). Notwithstanding the low number of samples, their chemical composition clearly indicates the presence of two compositional groups, called TUS1 and TUS2; two samples, SG106-1 and SG111-3 (Table D.6 and D.7) are considered as outliers.

The average composition, together with the corresponding standard deviation, of compositional groups and outliers is reported in Table 4.3.1.

<i>wt%</i>	TUS2 (N= 10)	TUS3 (N= 3)	SG106-1 (N= 1)	SG111-3 (N= 1)
SiO₂	65.95±1.46	66.43±0.90	61.45	63.68
Na₂O	17.66±0.60	18.94±1.85	17.80	16.80
CaO	7.32±0.67	6.07±1.08	5.81	8.06
Al₂O₃	2.38±0.08	2.01±0.08	2.84	2.68
K₂O	0.74±0.10	0.48±0.09	0.46	0.71
MgO	0.99±0.12	0.65±0.07	1.07	1.36
Fe₂O₃	1.08±0.18	0.61±0.09	4.08	1.42
TiO₂	0.13±0.02	0.11±0.02	0.59	0.26
MnO	1.18±0.22	1.22±0.11	1.64	1.93

4. Raw materials in glass production: the textural, chemical and mineralogical study

P_2O_5	0.14±0.05	0.05±0.03	0.18	0.14
Sb_2O_3	<0.04	<0.04	<0.04	<0.04
SO_3	0.70±0.025	0.37±0.07	0.26	0.26
Cl	1.26±0.08	1.26±0.06	1.37	1.14

Table 4.3.1: Mean chemical compositions and standard deviations for the identified groups and outliers. Major and minor elements are expressed as weight per cent (N= number of samples).

Groups TUS1 and TUS2, including ten and three samples respectively, have in common a similar colour, varying from pale green/blue to colourless (Table A.3), but they differ essentially for calcium and aluminium contents, lower in group TUS2 with respect to TUS1 ($CaO = 6.07 \pm 1.08$ wt% vs 7.32 ± 0.67 wt%; $Al_2O_3 = 2.01 \pm 0.08$ wt% vs 2.38 ± 0.08 wt%) (Fig. 4.3.1, b, c, Table 4.3.1). As shown in Figure 4.3.1, Group TUS2 is quite comparable with the group AQ/3, from Aquileia with a chemical composition similar to that of Série 3.2 of Foy et al. (2003) (Fig. 4.3.1).

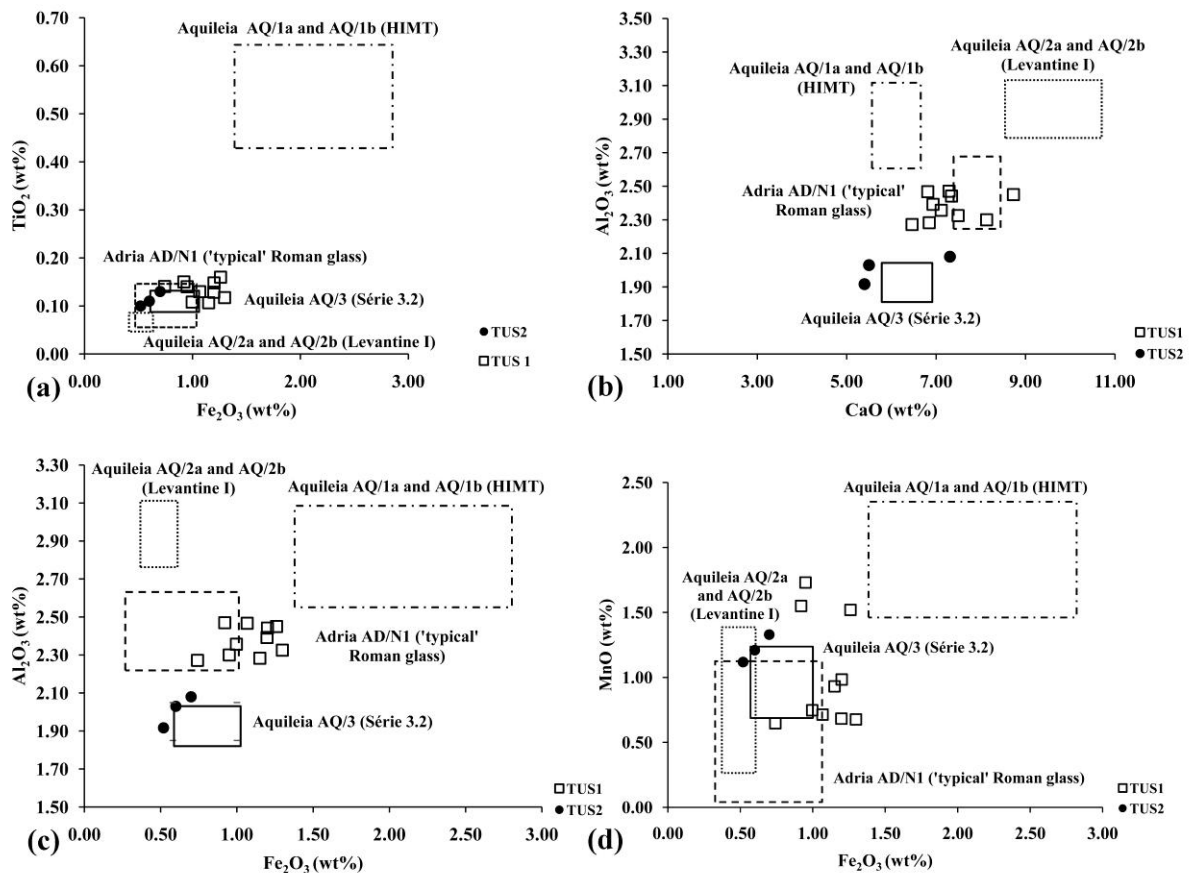


Figure 4.3.1: Plot of the samples of the two *S. Genesis* groups (TUS1, and TUS2). (a) TiO_2 vs Fe_2O_3 ; (b) Al_2O_3 vs CaO ; (c) Al_2O_3 vs Fe_2O_3 ; (d) MnO vs Fe_2O_3 . Plotted areas refer to Late Antiquity/Early Middle

4. Raw materials in glass production: the textural, chemical and mineralogical study

Age groups recognized at Aquileia (Groups AQ/1a, AQ/1b, AQ/2a, AQ/2b and AQ/3, see section 4.2) and to the Roman Group AD/N1 observed at Adria (see section 4.1).

On the other hand, Group TUS1 does not show any comparison with the ‘classical’ Late Antiquity compositional groups identified at Aquileia. Its chemical composition well corresponds to that of the earlier glass (Fig. 4.3.1), dating 1st-3rd century AD (e.g. Adria Group AD/N1, with a ‘typical’ Roman composition), excepting for three samples (SG111-5, PP111-4, PP111-5) with higher MnO contents (Fig. 4.3.1 d). These samples show also the presence of recycling indicators, such as copper and lead, in the range 100-1000 ppm (Cu= 96-105 ppm; Pb= 42-133 ppm, Table D.7), suggesting that manganese contents particularly high could be also a consequence of recycling. Anyway, manganese is an intentional addition in all glasses of the two compositional groups, since it was always detected at levels >0.5 % (Table D.6, Fig. 4.3.1 d).

Samples SG106-1 and SG111-3, yellow-green in colour, both show the typical characteristics of the HIMT glass. In fact, they have higher iron, titanium and manganese (Fe_2O_3 = 4.08 and 1.42 wt%, TiO_2 = 0.59 and 0.26 wt%, MnO= 1.64 and 1.93 wt%) than Groups TUS2 and TUS3 (Fe_2O_3 = 1.08 ± 0.18 and 0.61 ± 0.09 wt%, TiO_2 = 0.13 ± 0.02 and 0.11 ± 0.02 wt%, MnO= 1.18 ± 0.22 and 1.22 ± 0.11 wt%) (Table 4.3.1).

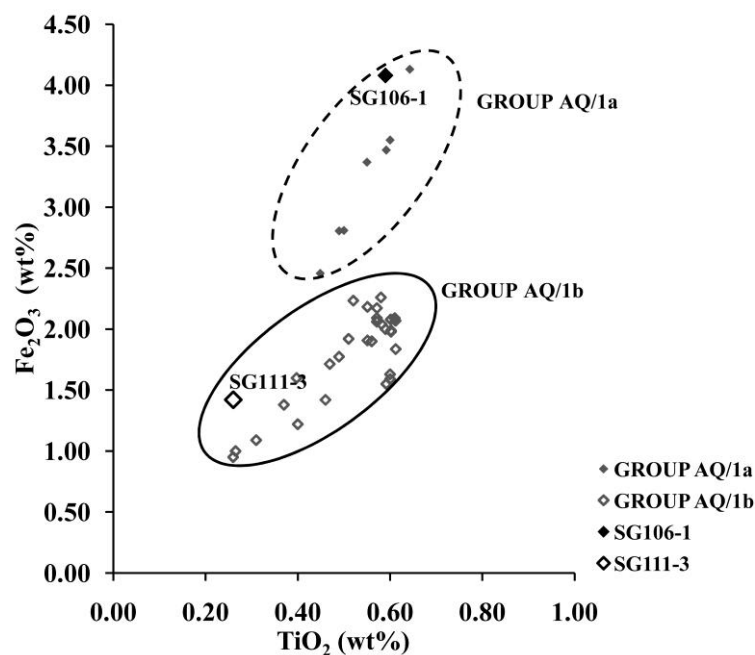


Figure 4.3.2: Fe_2O_3 vs TiO_2 plot showing the perfect agreement between the Tuscan samples SG106-1 and SG111-3 (black symbols) and Groups AQ/1a and AQ/1b (grey symbols) from Aquileia.

4. Raw materials in glass production: the textural, chemical and mineralogical study

Also the high atomic number elements, such as zirconium and chromium, present higher contents in these two samples ($Zr= 284$ and 128 ppm vs 75 ± 5 ppm and 63 ± 5 ppm; $Cr= 76$ and 188 ppm vs 15 ± 3 ppm and 13 ± 2 ppm) (Table D.7), suggesting the use of an impure sand source. This hypothesis is well confirmed by the perfect correspondence between samples SG106-1 and SG111-3 and Aquileia Groups AQ/1a ('strong' HIMT) and AQ/1b ('weak' HIMT), respectively (Fig. 4.3.2). As regards trace elements, in the vast majority of the samples of group TUS1, except PP111-3, PP11-4 AND PP111-5, copper, lead, tin and antimony were revealed at very high levels ($Cu= 2812-9408$ ppm, $Pb= 4174-25832$ ppm, $Sn= 768-3087$ ppm, $Sb= 3700-16279$ ppm, Fig. 4.3.3, b, c, Table D.7). This evidence suggests a stronger recycling of coloured and/or colourless glass, since all these elements were extensively used as colouring, decoloring and/or opacifying agents in glass-making.

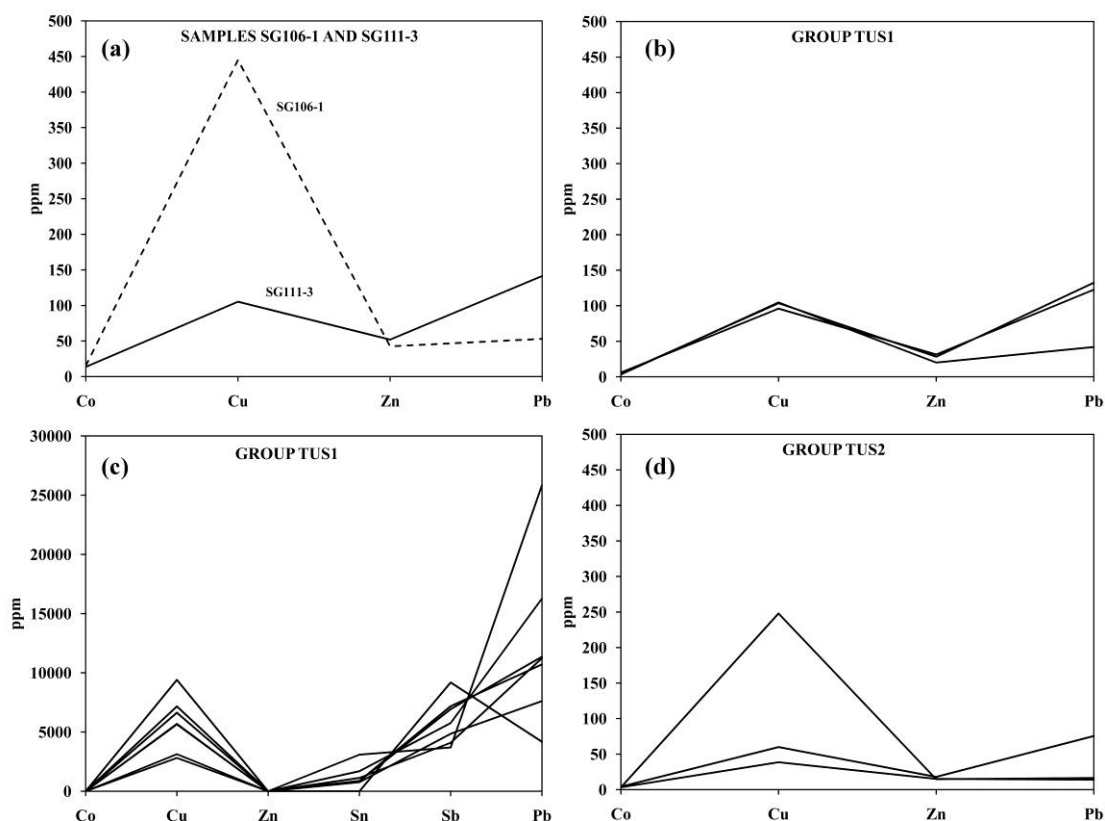


Figure 4.3.3: The concentration of recycling indicators, expressed as ppm, in all the glasses of Tuscan groups. (a) Samples SG106-1 and SG111-3; (b) Group TUS1 with recycling indicators in the range 100-1000 ppm; (c) Group TUS1 with recycling indicators >1000 ppm; (d) Group TUS2.

4. Raw materials in glass production: the textural, chemical and mineralogical study

In particular, it is worth noting that antimony was one of the main decolouring agents used in Roman times, also used for producing calcium antimonate opacifiers, but, from the end of the 3rd century AD, it was gradually replaced by manganese (Jackson, 1996; Silvestri et al., 2008) and by tin-based opacifiers (Mass et al., 1998; Henderson, 2000; Greiff and Schuster, 2008). Therefore, taking into account the chronological pattern of the samples of group TUS1 (4th-8th centuries AD), the presence of Sb_2O_3 is mostly suggestive of recycling of Roman colourless/opaque glass, and not of its intentional addition as a decolouriser.

The presence of recycling indicators was detected in samples SG106-1 and SG111-3, with HIMT composition, and also in Group TUS2, but at generally lower levels with respect the samples of group TUS1 (Table D.7, Fig. 4.3.3, a, d). It is interesting to note that the glass of Group AQ/3 from Aquileia, similar in composition to Group TUS2 and comparable to the Série 3.2 of Foy et al. (2003), does not show any recycling indicators (see section 4.2).

In synthesis, notwithstanding Aquileia and Tuscan samples are similar for dating and typology, some differences between the glasses from the two sites are evident. Glass coming from Aquileia, particularly that with Levantine and Série 3.2 composition, was generally from newly manufactured material. On the contrary, the vast majority of the glass coming from the Tuscan sites appears to have been manufactured by recycling earlier glass (1st-3rd century glass). This very interesting evidence is difficult to be interpreted. At this stage of the study it is reasonable to hypothesize that, during Late Antiquity/Early Middle Age, the different geographical location affected the distribution of 'fresh' glass, facilitating the commercial exchanges between Aquileia and the primary workshops likely located in the Eastern Mediterranean. However it will be necessary to extend our knowledge about the Late Antiquity/Early Middle Age glass from both the Adriatic and Tyrrhenian side of Italy to better support this hypothesis.

4.4 Early and High/Late Medieval glass from Rocca di Asolo

The investigation about raw materials used in glassmaking from the 6th century BC until Late Middle Age is here concluded with the chemical characterization of thirty-

4. Raw materials in glass production: the textural, chemical and mineralogical study

three samples coming from Rocca di Asolo and dating from the early Middle Age to High/Late Middle Age.

The Asolo sample set is both composed of window panes (7th-10th century AD and 15th century AD) and objects (beakers and bottles), all 12th-15th century AD in age.

4.4.1 Bulk chemistry

The chemical data are listed in Table D.8 (Appendix D): major and minor elements are expressed as weight per cent of oxides and traces in parts per million (ppm). For the beakers decorated with blue rims, sample labels include the letters ‘t’ to indicate the colourless body and ‘b’ for the blue glass. All samples are soda-lime-silica glass with SiO₂, Na₂O and CaO in the ranges of 61.8-70.9 wt%, 9.6-19.1 wt% and 3.7-12.8 wt%, respectively. Early Medieval samples have lower potassium and magnesium contents (K₂O=0.56-0.89 wt%, MgO=0.64-1.44 wt%) than the others (K₂O=2.09-2.88 wt%, MgO=1.79-4.49 wt%) (Table D.8). This suggests that the High and Late Medieval samples, including four window panes and 21 objects (beakers and bottles) were produced with soda-rich plant ash as a network modifier, whereas the Early Medieval ones, comprising eight window panes, were produced with natron as flux.

Natron glass

Some interesting observations may be made about the Asolo natron glass, in spite of their low number. As shown in the plots in Figure 4.4.1, they fall into two groups with differing chemical characteristics, called for convenience groups N/1 and N/2. Group N/1 contains only two pale blue panes; group N/2 contains six panes, yellowish-green in colour. With respect to group N/2, group N/1 has higher SiO₂ contents (69.46±0.77 wt% vs 65.59±1.16 wt%, Table 4.4.1) and lower MgO and MnO (MgO= 0.79±0.21 wt% vs 1.31±0.08 wt%, MnO= 0.90±0.45 wt% vs 1.87±0.21 wt%, Table 4.4.1; Fig. 4.4.1, a, b, d). Both groups are consistent with some of the major compositional groups of natron glasses identified in the first millennium AD in the Western Mediterranean (Table 4.4.1). Group N/1 of Asolo glasses is both similar to “Group 3” of Foy et al. (2003) and “Group A2/1” of Silvestri et al. (2005) (Table 4.4.1; Fig. 4.4.1), including Roman and Early Medieval glasses found in the West. This group is thought to be the ‘typical’ Roman glass, produced with coastal sands of the Syro-Palestinian region, probably near the mouth of the river Belus (Foy et al., 2003). However, unlike reference

4. Raw materials in glass production: the textural, chemical and mineralogical study

Groups 3 and A2/1, group N/1 has higher Sb_2O_3 (0.21 ± 0.8 wt%), which is under the EPMA detection limit in group N/2 (Table 4.4.1; Fig. 4.4.1, c).

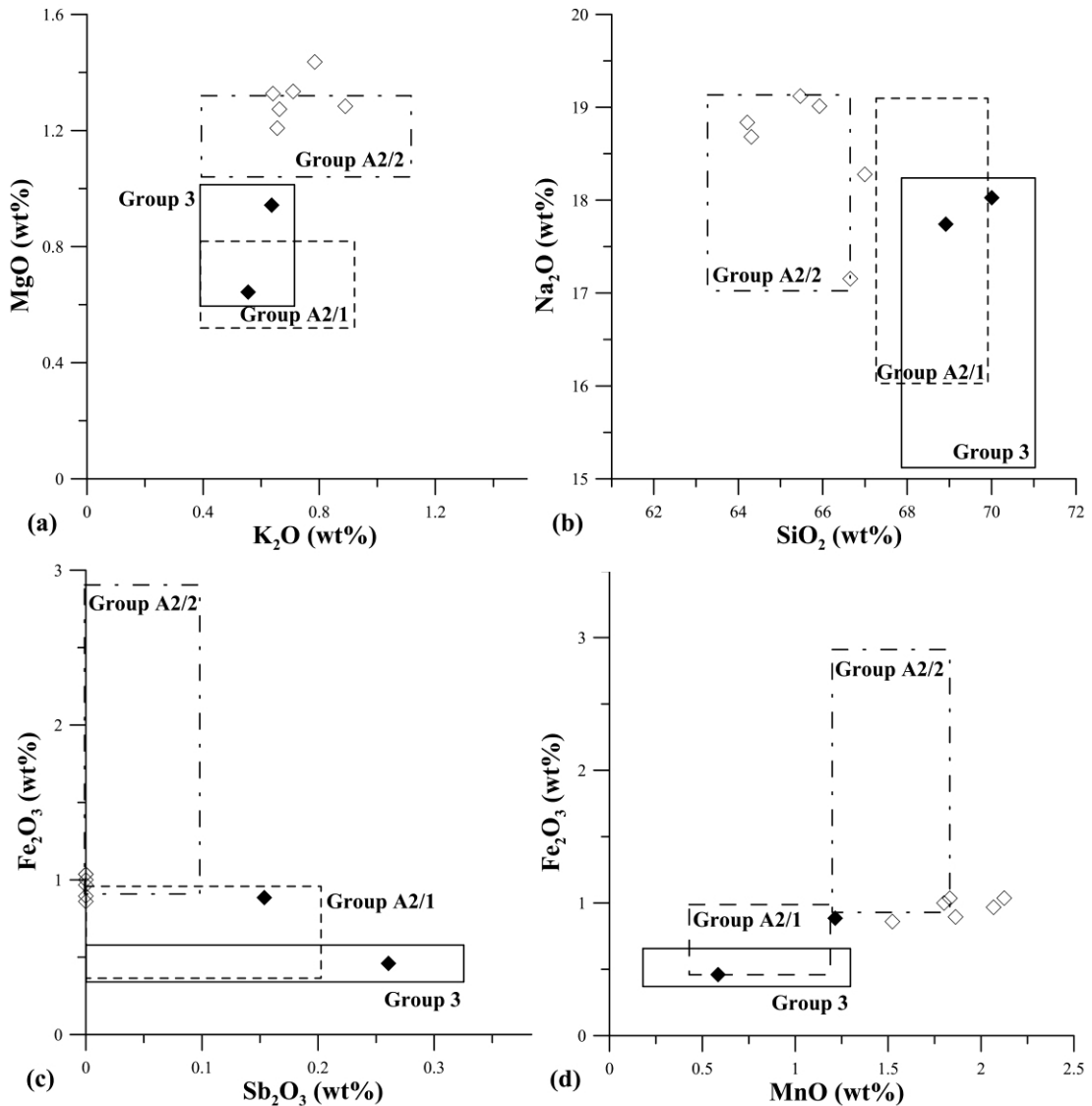


Figure 4.4.1: Plots of samples of groups N/1 (♦) and N/2 (◇): (a) MgO vs K₂O; (b) Na₂O vs SiO₂; (c) Fe₂O₃ vs Sb₂O₃; (d) Fe₂O₃ vs MnO. Plotted areas refer to Group 3 (continuous line), according to Foy *et al.* (2003) and to Groups A2/1 and A2/2 (dotted line), according to Silvestri *et al.* (2005).

The presence of antimony in Early Middle Ages coloured glass is suggestive of recycling of earlier glass, since the use of antimony stopped at the end of the 3rd century AD (Jackson, 1996; Silvestri *et al.*, 2008). The practice of recycling of earlier glass has already been observed for Early Middle Ages glass from other Italian sites

4. Raw materials in glass production: the textural, chemical and mineralogical study

(Mirti et al., 2000; Verità et al., 2002). Following Silvestri (2008), a recycling index (RI) was calculated, with a value of about 24%, indicating that the group N/1 samples were probably produced by recycling about 24% of colourless antimony glass in the batch.

On the other hand, Group N/2, shows a good match with “Group A2/2” of Silvestri et al. (2005) (Fig. 4.4.1, a, b, c, d; Table 4.4.1), composed of HIMT glass from North-East Italy and dated to the 5th-8th centuries AD. In fact this group presents all the typical characteristics of HIMT glass, that are high contents of Fe₂O₃ (0.97±0.07 wt%), MnO (1.87±0.21 wt%) and MgO (1.31±0.08 wt%), together with positive correlations between Fe₂O₃ and Al₂O₃ ($R^2 = 0.89$).

Generally speaking the composition of Asolo natron glasses shows many analogies with the Late Antiquity Tuscan samples. The predominant compositional groups are represented by HIMT and by 1st-3rd century recycled glass – no other groups of those attested at Aquileia and in the Mediterranean until the end of the 1st millennium AD, such as Levantine I and Série 3.2, were recognized in Asolo.

	Group N/1 (N=2)	Group 3	Group A2/1	Group N/2 (N=6)	Group A2/2	Group A/1 (N=15)	Venetian glass 'low Al'	Group B/1	Group A/2 (N=4)	Group A/3 (N=6)	Venetian glass 'high Al'
SiO ₂	69.46±0.77	69.36±1.64	68.53±1.38	65.59±1.16	65.03±1.59	67.36±1.48	67.26±1.58	68.25±1.15	67.24±1.05	68.04±2.17	66.68±1.54
Na ₂ O	17.88±0.20	16.77±1.55	17.42±1.49	18.51±0.73	18.17±0.97	12.49±1.03	12.75±1.4	12.00±0.91	9.97±0.48	12.95±1.37	11.39±2.43
CaO	7.01±0.00	7.81±0.94	7.21±0.77	8.07±0.48	7.73±1.10	10.10±0.98	8.97±1.53	9.51±0.91	12.24±0.46	7.30±2.43	10.25±2.8
Al ₂ O ₃	2.38±0.09	2.53±0.35	2.53±0.31	2.52±0.14	2.78±0.17	1.59±0.44	1.47±0.58	1.66±0.20	2.78±0.19	3.37±0.51	3.17±0.68
K ₂ O	0.60±0.06	0.55±0.14	0.67±0.26	0.72±0.10	0.79±0.39	2.41±0.22	2.32±0.5	2.26±0.16	2.40±0.21	2.40±0.22	2.37±0.28
MgO	0.79±0.21	0.62±0.14	0.62±0.14	1.31±0.08	1.18±0.14	3.76±0.44	3.28±0.57	3.32±0.25	2.88±0.06	1.98±0.20	2.71±0.5
Fe ₂ O ₃	0.67±0.30	0.51±0.15	0.67±0.23	0.97±0.07	1.92±0.99	0.60±0.22	0.51±0.21	0.65±0.24	0.45±0.02	1.26±0.25	0.74±0.45
TiO ₂	0.14±0.07	0.07±0.02	0.11±0.04	0.16±0.01	0.28±0.09	0.08±0.02	0.11±0.06	0.10±0.02	0.08±0.01	0.23±0.09	0.13±0.08
MnO	0.90±0.45	0.73±0.58	0.81±0.37	1.87±0.21	1.51±0.3	1.24±0.72	0.97±0.52	1.33±1.05	1.22±0.27	2.19±0.32	1.31±0.44
P ₂ O ₅	0.10±0.00	0.13±0.10	0.11±0.07	0.12±0.02	0.13±0.09	0.27±0.04	0.34±0.09	0.21±0.08	0.22±0.05	0.39±0.06	0.35±0.13
Sb ₂ O ₃	0.21±0.08	0.09±0.24	0.06±0.13	<0.06	0.03±0.07	<0.06	nr	0.00±0.01	<0.06	<0.06	nr

Table 4.4.1: Mean chemical compositions in weight per cent (element oxides) and standard deviations for identified groups of Asolo. Also reported: comparisons between chemical composition of identified groups (**bold**) and those of natron and plant ash glass identified in Western Mediterranean from mid-first millennium AD to mid-second millennium AD (*Italic*) (Group 3 from Foy et al., 2003; Groups A2/1 and A2/2 from Silvestri et al., 2005; Venetian glass “low-Al” and “high-Al” from Verità and Zecchin, 2009) (N=number; nr= not reported).

4. Raw materials in glass production: the textural, chemical and mineralogical study

Soda ash glass

Ash glass from Asolo was obtained with ash from coastal plants, which introduces high levels of Na₂O (9.58-14.29 wt %, Table D.8) and low levels of K₂O (2.09-2.88 wt%, Table D.8) when compared with wood ash (Na₂O= 0.89±0.99 wt%, K₂O= 13±5 wt %) (Wedepohl et al., 2011). The high level of CaO (3.70-12.83 wt%, Table D.8) is also due to plant ash and not to the carbonatic fraction of sand, as confirmed by analyses of Levantine plant ash, which typically have high CaO (Brill, 1970; Ashtor and Cevidalli, 1983; Verità, 1985). During the Middle Ages, coastal plant ash was reported to have been imported into Italy from the Eastern Mediterranean (Levantine ash) (Verità and Zecchin, 2009) or from near Alicante in Spain (Frank, 1982). Because of the different nature of the soil and of the plants used, these two types of ash produce different glass compositions: Spanish ash yields glass with a Na₂O/K₂O ratio of about 2, and Levantine ash glass in which the Na₂O/K₂O ratio is about 5 (Cagno et al., 2008, 2010). In the Asolo ash glass samples, the Na₂O/K₂O ratio varies from 4.2 to 6.7, suggesting that Levantine ash was used in their production. These data may support the hypothesis of Venetian provenance: from the end of the 14th century Asolo was under the influence of Venice, the most important Italian glass manufacturer and the main importer of Levantine ash in this period. In Venice, the use of Levantine ash had become mandatory by the early 14th century, because the government was determined to ensure the high quality of Venetian glassware (Jacobi, 1993).

On the basis of their chemical characteristics, the Asolo soda ash glass is subdivided into three groups: group A/1, composed of 15 samples, A/2 (4 samples) and A/3 (6 samples). A first distinction can be made between group A/1 and groups A/2 and A/3 in view of their Al₂O₃ contents: group A/1 has lower Al₂O₃ (1.59±0.44 wt%) with respect to groups A/2 and A/3 (2.91±0.33 and 3.35±0.57 wt%, respectively) (Table 4.4.1). As already observed by other authors (Cagno et al., 2008, 2010; Verità and Zecchin, 2009), this evidence suggests the use of different silica sources to produce Asolo soda ash glass: a purer silica source, such as siliceous pebbles, for the samples of group A/1, and sands richer in feldspars for those of groups A/2 and A/3. The separation into three groups is well illustrated in Fig. 4.4.2: groups A/2 and A/3, as already mentioned, have higher Al₂O₃ contents with respect to group A/1, whereas the distinction between groups A/2 and A/3 is given by the Fe₂O₃ contents, higher in group A/3 (1.26±0.25 vs

4. Raw materials in glass production: the textural, chemical and mineralogical study

0.45±0.02 wt% in group A/2, Table 4.4.1). In addition, group A/3 has lower MgO and higher TiO₂ (Fig. 4.4.2) and MnO (Table 4.4.1) than the other groups. These data, particularly the higher contents of Fe₂O₃ and TiO₂, may indicate the presence of greater amounts of heavy minerals in the sand used to produce the samples of group A/3.

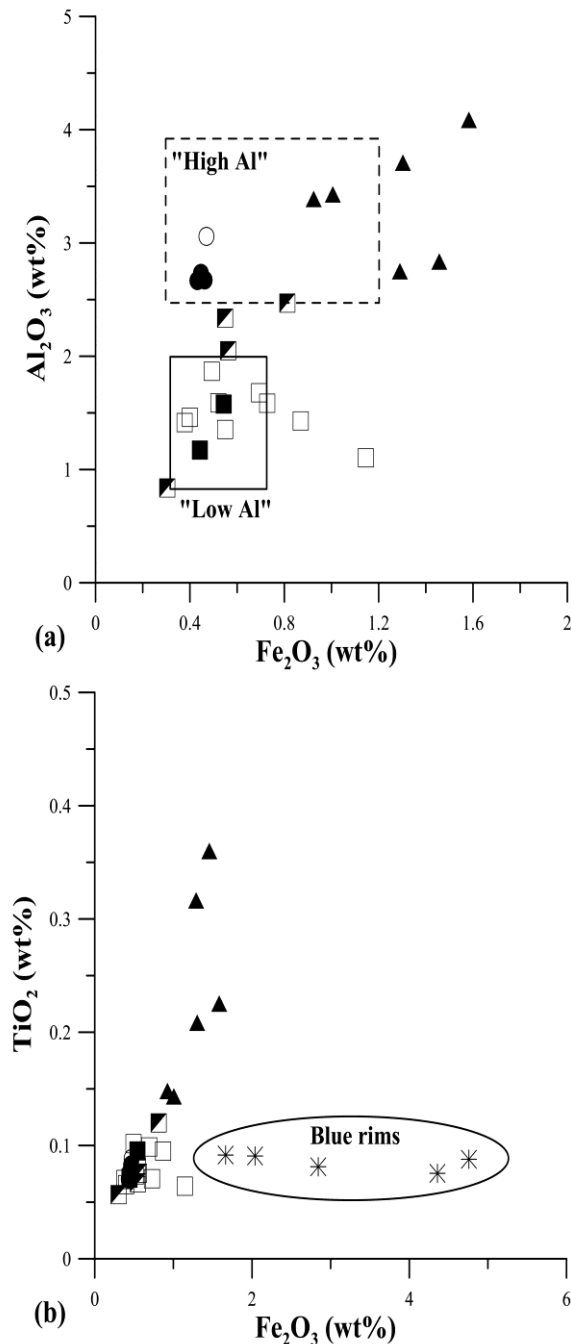


Figure 4.4.2: Plots of samples of A/1 (squares), A/2 (circles) and A/3 (triangles) groups: (a) Al₂O₃ vs Fe₂O₃, plotted areas refer to "High-Al" and "Low-Al" groups according to Verità and Zecchin (2009); (b) TiO₂ vs Fe₂O₃. Each symbol has characteristic indicating type of sample: full symbol, bottle; empty symbol, beakers; halved symbol, window panes; star, blue rims.

4. Raw materials in glass production: the textural, chemical and mineralogical study

As shown in Figure 4.4.2, group A/1 is mainly composed of window panes and beakers (both *nuppenbecher* and flat base glasses) and groups A/2 and A/3 comprise the vast majority of the bottles. This evidence is suggestive of a relationship between raw materials and type: a purer sand source, probably originally siliceous pebbles, was employed to produce the more precious products, such as window panes and beakers, and a lower-quality sand was used to produce bottles. The same subdivision into “low-Al” and “high-Al” glasses, recognised in the Asolo soda ash samples, has been observed in some Venetian glass, dating to the 11th-14th centuries (Verità and Zecchin, 2009) (Fig. 4.4.2, a), suggesting the possible provenance of Asolo findings from Venice. In particular, groups A/2 and A/3 show a good match with the chemical composition of “high-Al” Venetian glass, and group A/1 has composition similar to the “low-Al” group (Table 4.4.1). Group A/1 is also similar to group B/1 of Silvestri et al. (2005), including Medieval glass from Grado (province of Gorizia, NE Italy) and Vicenza (Table 4.4.1), with composition comparable to the “Islamic” glass found in Israel and Syria and dated to the 9th-10th centuries AD (Henderson, 2002). It is worth noting that the history of Venetian glass-making is closely related to the Levantine (Byzantine and Islamic) tradition, for the importation of both raw glass and raw materials, such as soda ash (Verità and Zecchin, 2009). In this context, the compositional homogeneity between 9th-10th century Islamic glass and 11th-14th Venetian glass is suggestive not only of a relation between Islamic and Venetian glass-making, but also of a technological continuity from the Early to High/Late Middle Ages.

4.4.2 Colouring and decolouring agents

The colour of the vast majority of glass findings varies from green to yellow and pale blue; five beakers have deep blue decorative rims, and were analysed separately (ASO-17b, ASO-18b, ASO-19b, ASO-20b, ASO-21b). Iron was probably the main colouring element and was introduced into the glass as an impurity. The TiO_2 versus Fe_2O_3 plot (Fig. 4.4.2, b) does show that the contents of these two elements are closely related in most of the samples, indicating that iron was added unintentionally, together with titanium, as mineral impurities in the sand. Manganese was the decolouring agent used deliberately, its contents varying from 0.58 to 2.68 wt% (Table D.8). It was added to all

4. Raw materials in glass production: the textural, chemical and mineralogical study

samples, since contents above 0.5 wt% are considered intentional additions (Jackson, 2005). Group A/3 has the highest Mn percentage (2.29 ± 0.23 wt%, Table 4.4.1), to better contrast the colouring effect caused by high Fe (1.31 ± 0.28 wt%, Table 4.4.1). In two samples, ASL-01 and ASL-08, Sb_2O_3 is also present (0.15-0.26 wt% respectively, Table 4.4.2) - the main decolouring agent, together with manganese, used in Roman times. However, its contents are too low to be considered as an intentional addition so, as already mentioned, the presence of Sb_2O_3 in some Asolo natron samples indicates recycling of Roman glass.

The five high-Fe and low-Ti samples in the dotted area of Figure 4.4.2, b are the deep blue decorative rims: in this case, the higher iron content is due to the raw materials added to colour the glass. Except for colouring agents which, according to Mirti et al. (1993), may have been added to the glass batch intentionally but are not related to the basic raw materials, blue rims have a chemical composition similar to that of the corresponding colourless body (Table D.8). This indicates that the same base glass was used to produce both colourless and coloured (blue) glass, and that it was modified by adding colouring and/or decolouring agents. Among trace elements, higher percentages of lead (0.11-0.18%, Table D.8) were found in three colourless beakers (ASO-18t, ASO-19t, ASO-21t) and are probably due to the recycling of coloured glass scraps or cullets.

As already mentioned, analyses show that the blue glass was obtained by adding a Co-based colourant to the same glass employed for the colourless body (Table D.8). In this context, the elements related to the colourant were quantified by subtracting the composition of the colourless glass from the coloured and possible correlations between them were investigated. In all five blue rims, cobalt correlates with copper and iron (Fig. 4.4.3, a, b), suggesting that these elements were associated in the ores exploited to produce the colourant.

4. Raw materials in glass production: the textural, chemical and mineralogical study

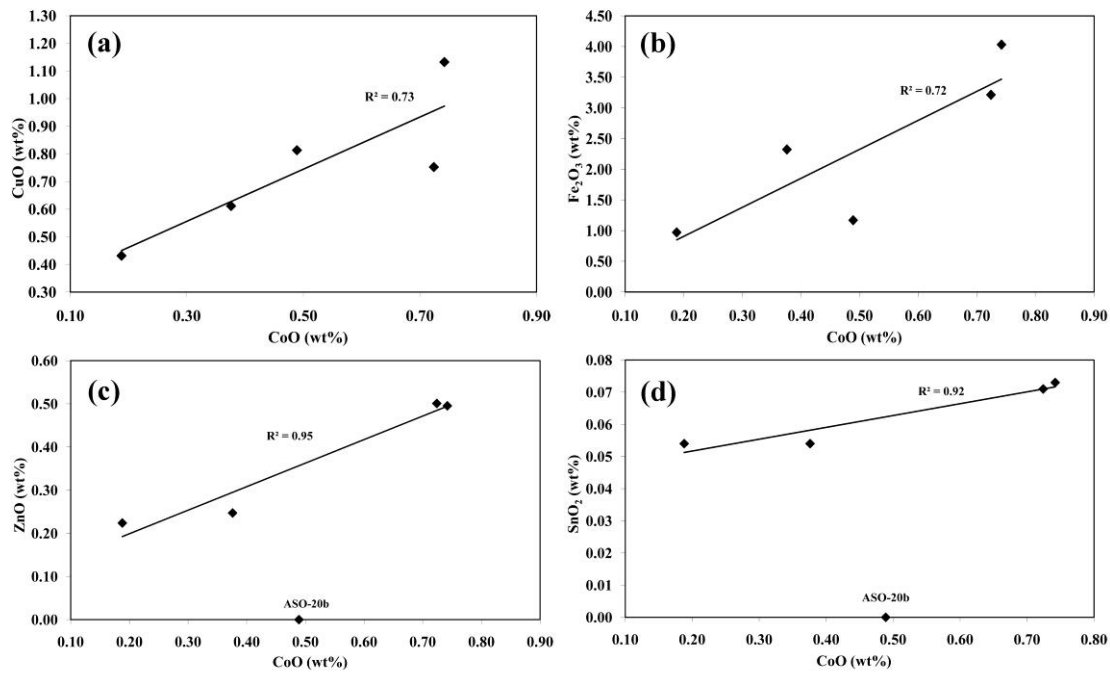


Figure 4.4.3: Plots (a) CuO-CoO; (b) Fe₂O₃-CoO; (c) ZnO-CoO; (d) SnO₂-CoO (wt%) for blue rims, obtained subtracting chemical composition of colourless glass from coloured (see text for details). R² value also reported in each plot.

In four blue rims (ASO-17b, ASO-18b, ASO-19b, ASO-21b), the high cobalt content (0.19-0.78 wt% as CoO) is associated with high Cu (0.78-0.19 wt% as CuO), Fe (0.97-4.03 wt% as Fe₂O₃), Zn (0.22-0.5 wt% as ZnO) and Sn (0.05-0.7 wt% as SnO₂), with a strong correlation between these elements (Fig. 4.4.3)

a, b, c, d). Significant amounts of Pb (0.15-0.23 wt%, as PbO) were also revealed, due to the addition of colourant. These data suggest a Co source linked to lead-zinc ores; as reported by Gratuze et al. (1992), the blue glass coloured with this type of raw material forms a homogeneous group dating to the 13th-15th centuries AD. Sample ASO-20b is different from the other blue glass samples: Zn and Sn are not present (Fig. 4.4.3 c, d) and Co (0.49 wt%, as CoO) is associated with Cu (0.81 wt% as CuO), Fe (1.17 wt% as Fe₂O₃), and Ni (0.15 wt%, as NiO) (Table D.8), suggesting a different source. Three inclusions with irregular shape and rounded edges were observed in this sample (Fig. 4.4.4).

4. Raw materials in glass production: the textural, chemical and mineralogical study



Figure 4.4.4: SEM-BSE image of normal section of sample ASO-20b. Dark grey area is blue glass of decorative rim. Two inclusions (paler grey) are embedded in glass matrix; black line: chemical profile shown in Figure 4.4.5.

Their quantitative chemical profiles (Fig. 4.4.5), along the black line in Figure 4.4.4, indicate that they are basically composed of an association of iron, cobalt and nickel, and are considered to be residues of raw materials added to colour the glass. The chemical composition of the colourless body of sample ASO-20t also differs from other colourless beakers, due to its higher Na_2O , MgO , Fe_2O_3 and lower K_2O and MnO (Table D.8), suggesting a different production technology.

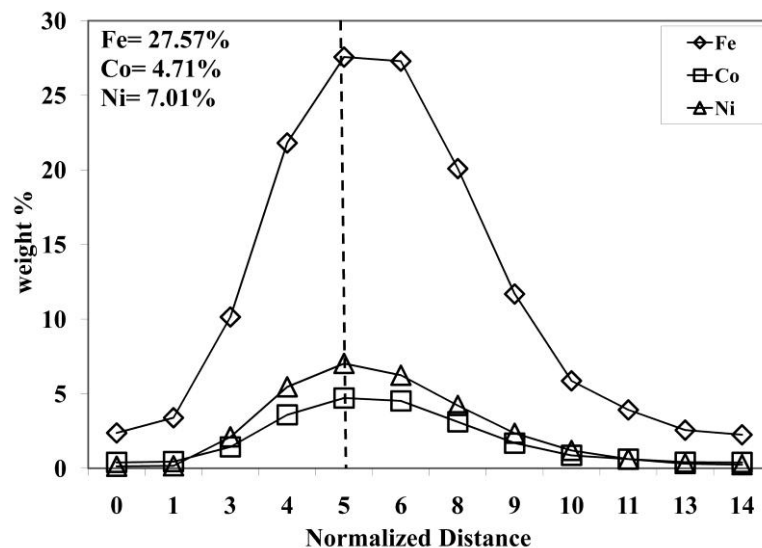


Figure 4.4.5: Chemical profile (EPMA analysis) of one inclusion in sample ASO-20b. Data expressed in weight per cent of elements. Dotted line: Fe, Co and Ni contents of central point of inclusion also reported.

4.5 Conclusions

The analytical approach involving textural, mineralogical and chemical characterization on a total of 178 glass samples spanning from the 6th century AD to the 15th century AD, allowed to well characterize the type of raw materials and production technologies employed in glassmaking during this period.

Results indicate that samples can be grouped by age, indicating routine glass production processes. Chemical data evidence that the vast majority of the transparent samples are soda-silica-lime glass, with natron as flux for Pre-Roman, Roman, Late Roman and Early Medieval glass and plant ash for High and Late Medieval ones. An exception is constituted by a little group of intensely coloured Roman glasses (emerald green, one blue and one black), which appears to have been produced using a plant ash as network modifier, suggesting they were imported from geographical areas where glass was also produced with sodic ashes.

By means of major, minor and trace elements composition, different groups have been identified and usefully compared with the major compositional groups present in the literature. As concern natron glass, no relationships have been found between its chemical composition and types and/or production techniques. The extraordinary consistency of this type of glass and the principal compositional groups widespread in Mediterranean sites leads to suppose that huge quantities of raw glass were produced in few primary workshops and then traded in secondary workshop (localized production), although chemical analyses did not give any direct indication about the provenance of raw materials.

Notwithstanding their different chronological pattern, Pre-Roman (6th-2nd centuries AD) and Roman (1st-3rd centuries AD) glasses from Adria show a homogeneous chemical composition, which implies continuity in the use of raw materials and production technologies in a large period, excluding relationships between these Iron Ages glasses and the earlier, Final Bronze Age, northern Italian productions. This continuity is also supported by the use of the same opacifiers: calcium antimonate for white, opaque blue, light blue and wisteria glass, lead antimonate for yellows. The only variation observed between Pre-Roman and Roman samples concerns the production technologies of blue glasses. Indeed, although the chromophore is the same (cobalt) in

4. Raw materials in glass production: the textural, chemical and mineralogical study

both the periods, the chemical and textural evidences indicate that the Co-bearing raw materials were likely less refined in Pre-Roman productions.

The majority of Pre-Roman and Roman glasses (Group AD/N1) has a chemical composition similar to that of the ‘typical’ Roman glass, suggesting that the same raw materials were used in their manufacture. However, the presence of two other small compositional groups (AD/N2a and AD/N2b) indicates that different source of raw materials could have been exploited during Roman period. In particular, Group AD/N2b is related to the well attested production of the Sb-colourless glass, involving the use of high purity sands, while Group AD/N2a does not show any comparison with literature group.

For some reasons not yet clarified, from the end of the 3rd-early 4th century AD a change in the aesthetic properties of the glass occurred and coincided also with a change in glass composition, leading the hypothesis that new sources of raw materials were exploited in this period. The Late Roman/Early Medieval glass from the site of Aquileia (Groups AQ/1a, AQ/1b, AQ/2a, AQ/2b and AQ/3) shows a perfect correspondence with some of the most important compositional groups recognized in Mediterranean from the 4th century onwards (HIMT, Levantine I and Série 3.2) and generally appears to have been made from newly manufactured material. However, the geochemical differences observed in HIMT Aquileia assemblage allowed to define two subgroups of HIMT glasses (Groups AQ/1a and AQ/1b), which indicate that different ores were likely exploited for the production of this type of glass. In particular one of these subgroups (Group AQ/1a) was never reported in literature and then can be considered as a new compositional group within the HIMT assemblage.

Contemporary glasses from northeastern inland site (Asolo) and from western sites (Tuscany) show marked differences when compared with Aquileia glasses, since most of them are made by recycled glass of the earlier Roman period (e.g. Group AD/N1). Glass type HIMT and Série 3.2 constitutes a minor percentage of Asolo and Tuscan sample set and, in any case, appears to have been subjected to a strong recycling. These evidences imply the influence of the geographical position on the distribution of ‘fresh’ glass: the strategic location of Aquileia allowed an easier supply of newly manufactured material, whereas in other areas it was likely more convenient to recycle old glass.

4. Raw materials in glass production: the textural, chemical and mineralogical study

As concerns High/Late Medieval glasses (Rocca di Asolo samples) three compositional groups have been identified (A/1, A/2 and A/3), indicating that at least three different silica sources were employed in their production. A purer silica source, probably siliceous pebbles, was used for window panes and the vast majority of the beakers, whereas two types of sand were mostly employed to produce bottles. This evidence suggests a correlation between chemical composition and type, although a larger number of data, based on both chemical and typological analysis, is necessary to support this hypothesis. A probable Venetian origin of Rocca di Asolo findings is supported by the similarity with Venetian glasses of the same period. In addition, the good match between Rocca di Asolo ash samples and ancient glass from Grado and Vicenza, of “Islamic” composition (9th-10th centuries AD), may be another indication of Venetian provenance, due to the well-attested relationship between Venetian and Islamic glass-making, and testifies to technological continuity from the early to High/Late Middle Ages. This chemical evidence also matches the political situation of the Rocca which, from the end of the 14th century until its decay, was under the influence of the Venetian Republic, one of the most important centres of glass manufacture and trade in western Europe.

For what concerns the colour of all the glasses here investigated, iron is likely the main colouring agent in unintentionally coloured glasses and it was introduced in the batch as an impurity. In colourless glasses its effect is neutralized by adding manganese and/or antimony oxides, the principal decolouring agents used in ancient times. On the other hand, the intensely colours observed in many Pre-Roman (blue) and Roman (blue, emerald green, purple, amber, black) glasses are due to the effect of different chromophores: manganese for purples, cobalt for blues, copper for emerald greens, iron for black. Discernable colouring agents have not been revealed in amber glasses: in this case the colour is likely due to a (Fe⁺³S⁻²) complex, which formed in reducing conditions, but further analysis on the oxidation states of these elements are necessary to prove this hypothesis.

CHAPTER 5

THE PROVENANCE OF RAW MATERIALS IN GLASS: THE ISOTOPIC APPROACH

Provenance determination of archaeological and historical artefacts relies on the assumption that there is a scientifically measurable property that will link an artifact to a particular source or production site (Degryse et al., 2010a; Degryse et al., 2009a). In this respect, mineralogical, petrographical or elemental chemical analyses are the techniques most often used to try to identify where inorganic artefacts were produced. In ancient glass provenancing, chemical composition may provide a characterization of the glass type, which may then suggest a specific source. However, although attempts to provide a provenance for glass by elemental analysis continue, a direct relationship between mineral raw materials and the artefacts made from them can be transformed at high temperatures (Degryse et al., 2009a). In many recent studies, new questions about glass production have been addressed using radiogenic and stable isotopes (Degryse et al., 2009a and references therein), since transformations as melting have a little effects on the isotopic ratio.

5.1 Features and principles of the technique

Different isotopes of an element have the same atomic number but different atomic masses, since they have differing numbers of neutrons. Radioactive decay is the spontaneous disintegration on an unstable radioactive parent isotope to a radiogenic daughter and a nuclear particle. Some isotopes, e.g. those of light elements such as hydrogen, oxygen or nitrogen, have negligible radioactivity and are called stable. However, a fair number of elements with relatively large atomic masses are radioactive (Degryse et al., 2009a). Such parent and resulting radiogenic daughter isotopes are often used for dating the time of formation of minerals or rocks, but are also very useful in tracing the sources of detrital matter (Banner, 2004). Moreover, variations in many stable isotope ratios reflect different geological origins, due to different formation processes. The isotopic composition of a raw material is thus largely dependent on the

geological age and origin of that material. Conversely, especially the heavy isotopes of e.g. lead, strontium and neodymium are, due to their relatively high masses at low internal mass differences (Faure, 1986), not fractionated during technical processes. The isotopic composition of the artefact will hence be identical, within analytical errors, to the raw materials of which it was derived, while the signatures of different raw materials used, and hence the resulting artefacts, may differ (Brill and Wampler, 1965; Gale and Stos-Gale, 1982).

5.1.1 Strontium and Neodymium

There are four naturally occurring isotopes of strontium with the following approximate abundances $^{84}\text{Sr}= 0.55\%$, $^{86}\text{Sr}= 9.75\%$, $^{87}\text{Sr}= 6.96\%$, $^{88}\text{Sr}= 82.74\%$.

The isotopic abundances of ^{84}Sr , ^{86}Sr and ^{88}Sr are constant in nature. These species are neither radioactive nor the decay products of any naturally radioactive isotope. Geological processes do not produce any fractionation of strontium isotopes. There are small natural variations in the abundances of ^{87}Sr , however, due to variable increments of ^{87}Sr produced by the radioactive beta decay of ^{87}Rb which constitutes about 28% of natural rubidium. The variations of ^{87}Sr are small because rubidium occurs in low abundance in most natural materials and the half-life of ^{87}Rb is long (50×10^9 years). The ^{87}Rb - ^{87}Sr chronometer has been extremely useful in determining geological and cosmological ages and also the isotopic composition of strontium has been useful as tracer of various geological processes (Wedepohl, 1971). However, as demonstrated by recent studies (Degryse et al., 2006b; Degryse and Schneider, 2008; Degryse et al., 2009b), of particular interest in provenancing raw materials of ancient glass is the variation in the isotopic composition of marine carbonates (e.g., shell and limestone).

Calcium carbonate permits Sr^{2+} to replace Ca^{2+} but excludes Rb^+ . As a result, calcite has a very low Rb/Sr ratio, and its $^{87}\text{Sr}/^{86}\text{Sr}$ ratio is not significantly altered by radioactive decay of ^{87}Rb to ^{87}Sr after deposition (Banner, 2004). Instead, the isotope composition of Sr in calcite deposited in the oceans results from mixing of different isotopic varieties of Sr that enter the oceans. The principal sources of marine Sr having distinctive $^{87}\text{Sr}/^{86}\text{Sr}$ ratios are: (1) old granitic basements rocks of the continental crust (high Rb/Sr, high $^{87}\text{Sr}/^{86}\text{Sr}$); (2) young volcanic rocks along midocean ridges, in oceanic islands, and along continental margins (low Rb/Sr, low $^{87}\text{Sr}/^{86}\text{Sr}$); (3) marine carbonates

rocks on the continents (low Rb/Sr, intermediate $^{87}\text{Sr}/^{86}\text{Sr}$) (Banner, 2004). The isotopes of Sr are not fractionated during precipitation of calcite or aragonite from aqueous solutions because the mass difference between ^{87}Sr and ^{86}Sr is only 1.2%. Because the absence of isotope fractionation effects and the negligibly small production of radiogenic ^{87}Sr by decay of ^{87}Rb in carbonate rocks, marine and non-marine carbonate rocks record the isotope composition of Sr in the fluid phase at the time of deposition. Isotope analyses of Sr in a large number of marine limestones of Precambrian and Phanerozoic age have revealed that the $^{87}\text{Sr}/^{86}\text{Sr}$ ratio of seawater has varied systematically with time (Fig.5.1.1, Burke et al., 1982). These variations must have been caused by changes in the isotopic composition of Sr that entered in the oceans from various sources and by changes in the relative proportions of these inputs. It should be noted that the residence time of strontium in the oceans is long, relative to the rate of ocean mixing, so that geographical variations in the strontium isotope composition of seawater are negligible (Banner, 2004; Freestone et al., 2003). For example, the mean and standard deviation of 15 Holocene shells collected worldwide are given by DePaolo and Ingram (1985) as 0.709234 ± 0.000009 . A particularly noteworthy feature of Figure 5.1 is the rapid increase in $^{87}\text{Sr}/^{86}\text{Sr}$ over the past 40 million years or so. This is attributed to the uplift and erosion of the Himalayas, which contain rocks with high $^{87}\text{Sr}/^{86}\text{Sr}$, which is transferred to the oceans via groundwater and surface run-off (e.g., Basu et al. 2001). Modern marine shell has a $^{87}\text{Sr}/^{86}\text{Sr}$ value equivalent to that of modern seawater, from which it is precipitated, and this is significantly higher than, for example, the value for Cretaceous limestone (Fig.5.1.1).

5. The provenance of raw materials in glass: the isotopic approach



Figure 5.1.1: Variation in the strontium isotope composition of seawater versus time, based on Burke *et al.* (1982)(from Freestone *et al.*, 2003).

The application of strontium isotopes to the interpretation of ancient glasses depends primarily upon the assumption that the bulk of the strontium of many glasses is incorporated with the lime-bearing constituents in the glass (Wedepohl and Baumann, 2000). These lime-bearing components are likely to be, on the one hand, shell or limestone, comprising a mineral polymorph of calcium carbonate (i.e., aragonite and/or calcite) or, on the other, plant ash, which is usually lime-rich (e.g., Brill 1970; Verità 1985). It has been assumed that the contribution of natron to the strontium balance of glass is negligible (Freestone *et al.*, 2003), and minor contributions may be attributed to feldspars or heavy minerals in the silica raw material (Freestone *et al.*, 2003; Degryse *et al.*, 2006a). Where CaCO_3 was derived from Holocene beach shell, the $^{87}\text{Sr}/^{86}\text{Sr}$ ratio should reflect that of modern seawater and be close to 0.7092 (Fig. 5.1.1). If, on the other hand, the strontium was incorporated in the glass in the form of limestone, then it will have an isotopic signature that reflects that of the seawater at the time the limestone was deposited, modified by any diagenetic alteration that might have occurred to the limestone over geological time. For a glass made using plant ash, the $^{87}\text{Sr}/^{86}\text{Sr}$ value will reflect the bioavailable strontium from the soils on which the plants grew (Freestone *et al.*, 2003). Both the strontium isotopic ratio and strontium concentrations are useful indicators of the source of lime. Aragonite in shell may contain a few thousand ppm Sr. However, conversion of aragonite to calcite during diagenesis or

chemical precipitation of calcite or limestone will incorporate only a few hundred ppm of Sr (Freestone et al., 2003). Plant ash glasses can have high strontium contents, sometimes of the same order of magnitude as or higher than glasses made from natron and sand with shell (Freestone et al., 2003).

Neodymium is a rare earth element (REE), which has five stable isotopes (^{142}Nd , ^{143}Nd , ^{145}Nd , ^{146}Nd and ^{148}Nd) and two radioisotopes (^{144}Nd and ^{150}Nd). ^{147}Sm decays by alpha emission to stable ^{143}Nd , with a half-life of 1.53×10^{11} years. Variations in Nd isotopic compositions ($^{143}\text{Nd}/^{144}\text{Nd}$) are the result of elemental fractionations occurring between ^{143}Nd and its parent ^{147}Sm during radioactive decay. This has made Nd useful for age dating terrestrial and extraterrestrial materials as well as many other geologic applications (DePaolo, 1988). The isotopic variations are expressed relative to the stable, non-radiogenic isotope ^{144}Nd ($^{143}\text{Nd}/^{144}\text{Nd}$ ratio) and a sample's deviation from the value for the bulk earth at a given time is expressed using the epsilon notation ϵNd :

$$\epsilon\text{Nd} = \left(\frac{(^{143}\text{Nd}/^{144}\text{Nd})_{\text{sample}}}{(^{143}\text{Nd}/^{144}\text{Nd})_{\text{CHUR}}} - 1 \right) \times 10^4$$

where CHUR is a chondritic uniform reservoir, which represents a bulk earth Nd isotope composition deduced from measurements in chondrites (De Paolo and Wasserburg, 1976). Since different rock types can have different Nd isotopic compositions and because clastic sediments are in fact just mechanical disintegration products of igneous, metamorphic and older sedimentary rocks which are exposed in the source area, the Nd isotopic values of the sediments can help to identify the sediment source (Brems et al., in press). In particular, although actually the number of analyses is small, there seems to be significant differences in Nd isotopic signatures between the easternmost part of the Mediterranean Sea and the rest of the basin.

The introduction of neodymium isotopes in glass studies is very recent. Nd in glass is likely to have originated partly from the clay mineral content and partly, but principally, from the heavy mineral content of the silica raw material (Degryse et al., 2006b; Degryse and Schneider, 2008). The effect of recycling on the Nd isotopic composition of a glass batch is not significant, and neither is the effect of colourants and opacifiers (Freestone et al., 2005). This offers a great potential in tracing the origins of primary

glass production. The first example of this approach was shown in the provenance determination of early Byzantine 4th to 8th century glass from Syro-Palestine and Egypt (Degryse et al., 2006b; Freestone et al., in press). The consistency of the Nd isotope composition of the glass with Nile dominated sediments (Weldeab et al., 2002; Stanley et al., 2003) suggested an origin of these glass types situated in between the Nile delta and what is now Lebanon-Israel (Degryse and Shortland, 2009). In a second study (Degryse and Schneider, 2008), a Roman 1st to 3rd century glass showed exotic Sr-Nd isotopic compositions, which does not correspond to the signatures from the known production centres in Egypt and Syro-Palestine. These signatures were moreover not consistent with any possible glass raw material in the eastern Mediterranean, but do correspond well to sediments from the western Mediterranean, suggesting that primary production likely lies in the Western Roman Empire (Degryse and Shortland, 2009).

5.1.2 Oxygen isotopes

Oxygen has three stable isotopes: ^{16}O , ^{17}O and ^{18}O ; ^{16}O is the most abundant isotope of this element (99.762%). The stable isotopes are fractionated during changes in their states of aggregation and by chemical reactions between compounds in which the elements occur. The extent of fractionation of two isotopes of the same element is controlled primarily by the difference in their masses and by the temperature of the environment (Faure and Mensing, 2005). The resulting variations of the isotopic compositions convey information about the physical and geochemical processes that acted on the element and on the compounds in which it occurs.

Oxygen was, together with lead, the first isotope that was used to investigate the provenance of ancient glass. Its potential was pioneered by Brill and co-workers (Brill, 1970, 1988; Brill et al., 1999), which showed that isotopes of oxygen have characteristic ranges for certain glass groups. For a typical soda–lime–silica glass, the bulk of the oxygen is about 45% and approximately 70% of it enters the glass as a component of the silica. Even in strongly coloured glasses, the bulk of the oxygen is derived from the major components of the base glass (Leslie et al., 2006). For this reason the oxygen isotopic composition of ancient glass mainly depends on the silica source, with minor influences of flux and stabilizer (Brill, 1970; Brill et al., 1999). In addition, it was experimentally demonstrated that variations in melting time and temperature had no

measurable effects on the final oxygen signature of the glass (Brill et al., 1999). Therefore the isotopes of oxygen may be expected to be useful discriminants of raw material sources. The standard notation for oxygen isotope composition of a substance is $\delta^{18}\text{O}$, which expresses the deviation of the isotopic ratio of the material from Vienna Standard Mean Ocean Water (VSMOW):

$$\delta^{18}\text{O} = (R_{\text{SAMPLE}}/R_{\text{VSMOW}} - 1) \times 1000$$

where R is the ratio $^{18}\text{O}/^{16}\text{O}$. Silicate minerals are enriched in ^{18}O relative to SMOW and have positive ^{18}O values that range from +20‰ in quartz to values between +5 and +6‰ in ferromagnesian minerals such as olivine and pyroxene (Faure and Mensing, 2005); on the other hand, Egyptian natron, which is believed to have been extensively used in early glass-making, has a value around +40‰ (Brill et al., 1999).

In spite of its apparent promise and the important pioneering work of Brill and co-workers, oxygen isotope analysis has not been widely applied in the investigation of glass. Only recently Henderson et al. (2005), Leslie et al. (2006) and Silvestri et al. (2010) have contributed to amplify the database of oxygen isotope data for various archaeological glass samples and possible raw materials.

5.2 Materials

In the present work 38 samples were selected for the analysis of Sr and Nd isotopes and 40 for O isotope. They belong to Adria and Aquileia sample sets and are both Roman (1st-3rd century AD) and Late Roman/Early Medieval in date (4th-8th century AD). The selection was carefully conducted, in order to represent the various archeological types, colours and the different compositional groups identified and detailed in chapter 4.

5.3 Results and discussion

5.3.1 Strontium and neodymium isotopes

Strontium and neodymium composition and elemental concentrations of the glass samples are given in Table E.1, Appendix E.

5. The provenance of raw materials in glass: the isotopic approach

The $^{87}\text{Sr}/^{86}\text{Sr}$ ratios of the vast majority of the glass samples range between 0.70884 and 0.70916 (Tab.E.1, Fig. 5.3.1 a, b), independently from age, site, colour and compositional group, and are close to the ratio for the present-day seawater (0.7092). Along with their high Sr values (Sr= 322-534 ppm, Tab.E.1), this suggests that the source of strontium was marine shell and consequently that most likely beach sands were used. The $^{87}\text{Sr}/^{86}\text{Sr}$ ratio of the soda ash glass (sample AD-VE-2) is also similar to the present day water composition (0.70894, Tab.E.1). In recent work (Degryse et al., 2010a) it was demonstrated that the strontium intake of plants may be dominated by the total (rain)water ingested, and only moderately influenced by the bedrock geology, possibly resulting in a marine signature of the plant.

However, some samples show clearly different Sr isotopic signatures. The sample AD-B-4, defined as outlier since its unusual chemical composition (see section 4.1.2), differs from the other glass with a particularly high $^{87}\text{Sr}/^{86}\text{Sr}$ ratio ($^{87}\text{Sr}/^{86}\text{Sr}$ = 0.71089, Tab. E.1, Fig.5.3.1 a). This suggests that it was manufactured with a sand rich in minerals with more radiogenic strontium, probably feldspars, as suggested also by the higher aluminum contents observed in its bulk composition (see Table D.1, Appendix D). Both the two purple glasses analyzed show a different Sr signature, lower in sample AD-V-4 ($^{87}\text{Sr}/^{86}\text{Sr}$ = 0.70854) and higher in sample AD-V-2 ($^{87}\text{Sr}/^{86}\text{Sr}$ = 0.70955) (Tab. E.1, Fig. 5.3.1 b). This variation could be explained by the fact that sand is not the only source of strontium in purple glass, but also Mn-bearing raw material, added as colourant, introduces strontium in the batch (see section 4.1.2), and consequently modifies the $^{87}\text{Sr}/^{86}\text{Sr}$ ratio. The higher Sr contents (Sr= 592-657 ppm) in these two glasses with respect to the other samples (Sr= 322-534 ppm, Tab. E.1, Fig. 5.3.1 b) supports this hypothesis. Moreover, the ‘inhomogeneous’ Sr signature in the two purple samples is probably attributable to the use of different kind of Mn-bearing raw material, as already supposed in section 4.1.2. Finally, one blue glass of Group 2a (AD-B-7) and all the samples with HIMT composition (Group AQ/1a and AQ/1b) form a distinct group, which differs from other glasses for lower $^{87}\text{Sr}/^{86}\text{Sr}$ ratios ($^{87}\text{Sr}/^{86}\text{Sr}$ = 0.70832-0.70881, Tab. E.1, Fig. 5.3.1 b), suggesting the influence of a less radiogenic source of strontium. For HIMT glass, this characteristic has been already observed in glasses coming from Carthage, North Sinai, Billingsgate and Sagalassos (Freestone et al., 2005; Freestone et al., in press; Freestone et al., 2009; Degryse et al., 2009b).

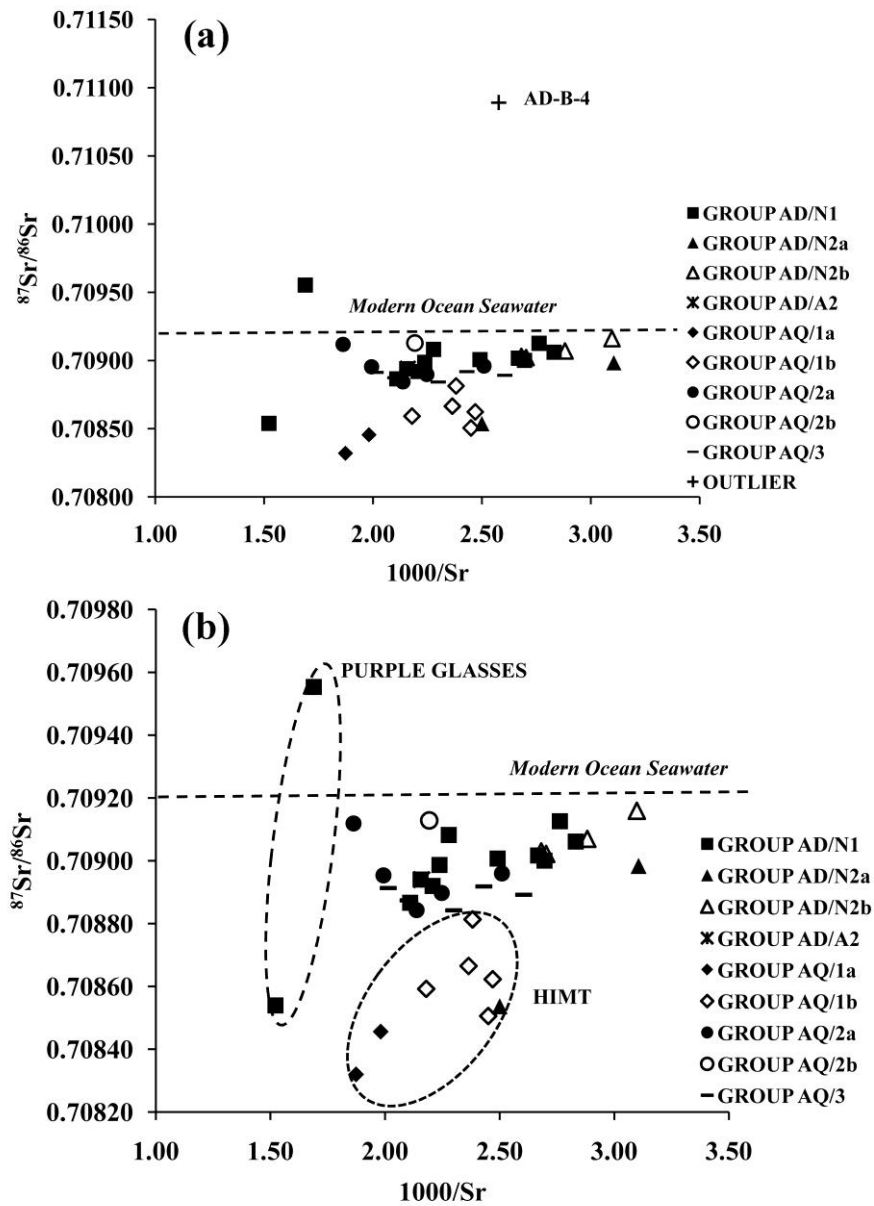


Figure 5.3.1: strontium ratios ($^{87}\text{Sr}/^{86}\text{Sr}$) vs strontium contents ($1000/\text{Sr}$). (a) All Roman and Late Roman/Early Medieval analyzed glasses; (b) All glasses without outlier AD-B-4. The isotopic signature of the Modern Ocean seawater is indicated by the dotted line.

Furthermore, $^{87}\text{Sr}/^{86}\text{Sr}$ ratios in HIMT glasses are negatively correlated with oxides such as Fe_2O_3 , MgO and TiO_2 and positively correlated with CaO (Fig. 5.3.2 a, b, c, d). The glass with a Levantine I composition (Group AQ/1a and AQ/2b) lies at the low iron, titanium, magnesium and high calcium end of the same trend (Fig. 5.3.2 a, b, c, d), suggesting that the HIMT glasses with low Fe_2O_3 are similar in general terms to the

5. The provenance of raw materials in glass: the isotopic approach

glasses with a Levantine I composition and were made using a sand rich in beach shell. As observed by Freestone et al. (2005, in press) these strong correlations indicate that HIMT glass is a mixture of two components: (1) a component rich in Fe_2O_3 , MgO and TiO_2 with lower CaO and lower $^{87}\text{Sr}/^{86}\text{Sr}$, and (2) a component with higher CaO and $^{87}\text{Sr}/^{86}\text{Sr}$, but lower Fe_2O_3 , MgO and TiO_2 .

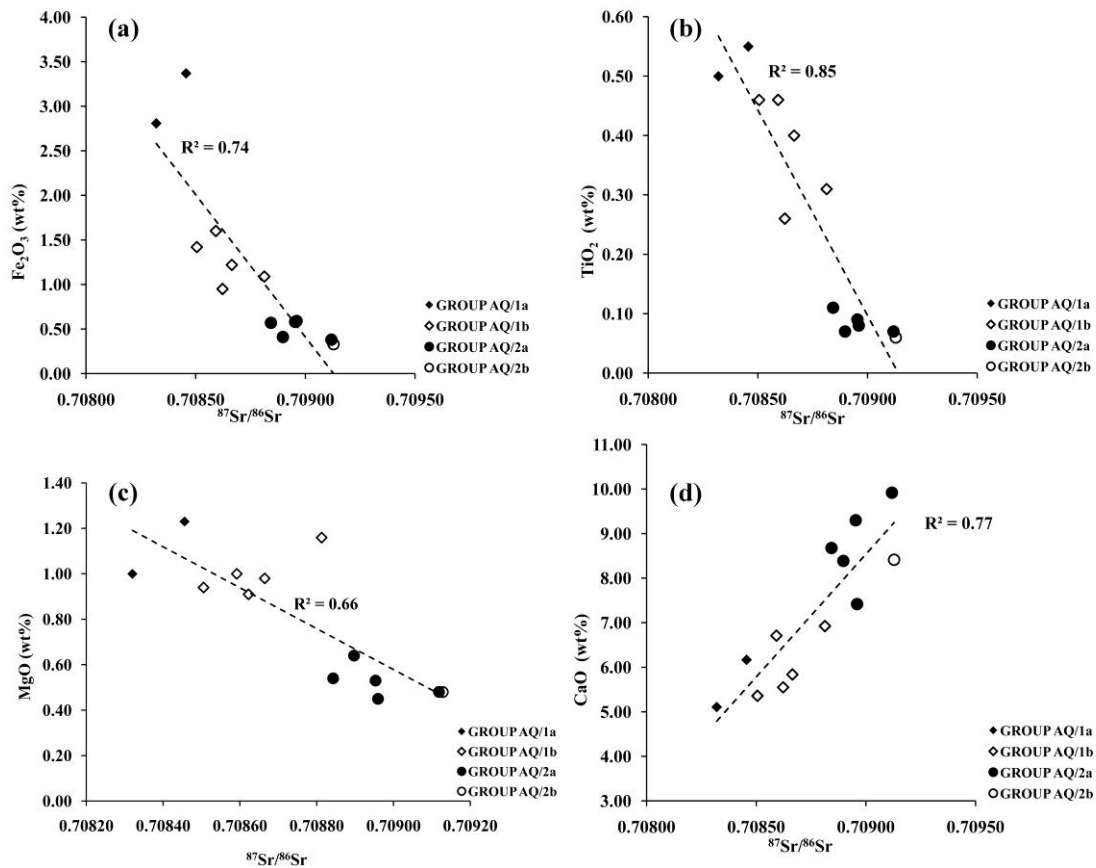


Figure 5.3.2: correlations between Sr ratios and (a) Fe_2O_3 ; (b) TiO_2 ; (c) MgO and (d) CaO for Groups AQ/1a, AQ/1b (HIMT composition) and AQ/2a, AQ/2b (Levantine I composition) from Aquileia.

The strontium isotopes of component (1) indicate that beach shell was a less significant source of strontium in HIMT glasses with higher iron, magnesium and titanium, as these have lower $^{87}\text{Sr}/^{86}\text{Sr}$ ratios. The sand therefore contained a significant proportion of its strontium in some other mineral or minerals, such as mafic minerals (e.g. pyroxene or amphibole), since $^{87}\text{Sr}/^{86}\text{Sr}$ ratios decrease with increasing Fe and Mg. The presence of strontium derived from ancient limestone can be excluded, since the Sr contents are too high to derive from calcite (Freestone et al., 2003). Neodymium and

strontium measurements on HIMT glasses from North Sinai, Carthage and Billingsgate (London) were reported by Freestone et al. (in press). They noted that the lower $^{87}\text{Sr}/^{86}\text{Sr}$ ratios of the HIMT range favoured an area of origin on the Egyptian coast, between Alexandria and Gaza, where the Nile strontium isotope signature dominates the sediments (Weldeab et al., 2002). Indeed $^{87}\text{Sr}/^{86}\text{Sr}$ values in silicates around the Mediterranean are higher than seawater except where the content of material derived from the Nile is exceptionally high, close to the delta in the Southeast (Krom et al., 1999; Weldeab et al., 2002). This model is also consistent with the higher levels of Mg, Fe, Ti etc observed in HIMT glasses, since the sands close the mouth of the Nile are richer of heavy minerals, mainly pyroxene and amphibole (Emery and Neev, 1960), which gradually decrease progressing up the eastern Mediterranean coast (Pomerancblum, 1966, Mange and Wright, 2007).

The analyzed glass shows a wide range of Nd isotopic signatures (Tab. E.1). The earlier glass, dating 1st-3rd century AD, is more heterogeneous, with $^{143}\text{Nd}/^{144}\text{Nd}$ between 0.51212 and 0.51251, corresponding to values between -2.59 and -10.04 for ϵNd (Tab. E.1). On the other hand, the Late Roman/Early Medieval glass, dating late 3rd-8th century AD, shows a much smaller range, with $^{143}\text{Nd}/^{144}\text{Nd}$ between 0.51236 and 0.51245, corresponding to values between -3.67 and -5.35 for ϵNd (Tab. E.1). A closer examination of the existing literature data was necessary in order to interpret these values.

Studies from Goldstein et al. (1984), Grousset et al. (1988) and Weldeab et al. (2002) have demonstrated that Nd isotopic signatures of the beach sands show a decrease in ϵNd from east to west (Brems et al., in press). Detrital deep-sea surface sediments in the North-Atlantic and the Mediterranean were measured by Frost et al. (1986) and Grousset et al. (1988). These studies showed that the sediments in the east-west axis ranged from -10.1 at Gibraltar to -3.3 at the mouth of the river Nile. The sediment load of the Nile, which dominates the sands in the south-eastern Mediterranean, has an exceptional high Nd isotopic composition, as it is dominated by East African volcanic rocks from the Ethiopian Plateau (Mange and Wright, 2007). Western Mediterranean sediments around the Spanish and southern French coasts have a homogeneous composition between -9.7 and -10.1. Sediment around the Italian coasts show a range between $\epsilon\text{Nd} = -12.4$ and -7.6 in Tyrrhenian Sea, and an ϵNd value of -10.8 in the

5. The provenance of raw materials in glass: the isotopic approach

Adriatic Sea. The variable values around the Italian peninsula are explained by the influence of African aerosols and Saharan dust (Grousset et al., 1988). In a study performed by Degryse and Schneider (2008), the Sr-Nd isotopic signature of possible silica raw materials for primary glassmaking was determined. Sands from the river Belus (Israel), from the river Volturno (Italy) and from near lake Fazda (Egypt) were analyzed. All these locations are mentioned in Pliny the Elder's *Naturalis Historia* (XXXVI, 194) as locations for primary glass production using local raw materials. In addition, also Tertiary deposits in Belgium were geochemically characterized, since they represent possible sand sources from the Gallic provinces, as described by Pliny. The results show that both the sands from river Belus and Volturno, considered suitable for glassmaking, present a Sr signature close to that of the modern seawater but are distinguished from the Nd isotopic signature ($\epsilon\text{Nd} = -4.8$ in Levantine sands and -6.9 and -9.9 in Volturno sands). On the other hand, sands from Egypt ($\epsilon\text{Nd} = -6.8$ and -8.6) and from Belgium ($\epsilon\text{Nd} = -11.4$ and -12.7) are clearly distinguished for their lower $^{87}\text{Sr}/^{86}\text{Sr}$ ratios, indicating that they are not influenced by shell material, which is absent in the sand (Degryse and Schneider, 2008). Moreover, in a recent work, Brems et al. (submitted *b*) analyzed the Sr and Nd isotopic composition of 76 beach sands from Spain, France and Italy. Results show that Spanish and French sands have relatively low ϵNd values from -12.4 to -8.0 , in close agreement with the data from the deep sea sediments. On the other hand, Italian sands show a wide range of ϵNd values between -12.8 and -3.0 (Brems et al., submitted *b*). Three sands from Italy were identified as being suitable for Roman glass production (Brems et al., submitted *a*). One comes from Tuscany and has a rather low ϵNd value of -9.42 . The other two come from Basilicata and Apulia region, in southeastern Italy, and have relatively high ϵNd values (-6.1 and -4.2 , respectively, Brems et al., submitted *b*) and coincide with the range of Nd isotopic signatures previously thought to be characteristic for an eastern Mediterranean origin (Degryse and Schneider, 2008; Freestone et al., in press). However, only the Apulia sand has a Sr-Nd isotopic composition comparable with the majority of the glasses analyzed in the present study ($^{87}\text{Sr}/^{86}\text{Sr} = 0.70867$, $\epsilon\text{Nd} = -4.2$, Brems et al., submitted *b*), since the other shows a too high $^{87}\text{Sr}/^{86}\text{Sr}$ ratio ($^{87}\text{Sr}/^{86}\text{Sr} = 0.71079$, Brems et al., submitted *b*).

In Figures 5.3.3, a, b $^{87}\text{Sr}/^{86}\text{Sr}$ ratios versus ϵNd data are plotted for the earlier samples (1st-3rd century AD) analyzed in the present study. Only two glasses dating 1st century AD, one purple with a typical Roman composition and one blue belonging to Group AD/N2a (with lower CaO, Tab. D.1), show relatively low ϵNd values ($\epsilon\text{Nd} = -10.04$ and -7.41 in AD-V-2 and AD-B-6, respectively).

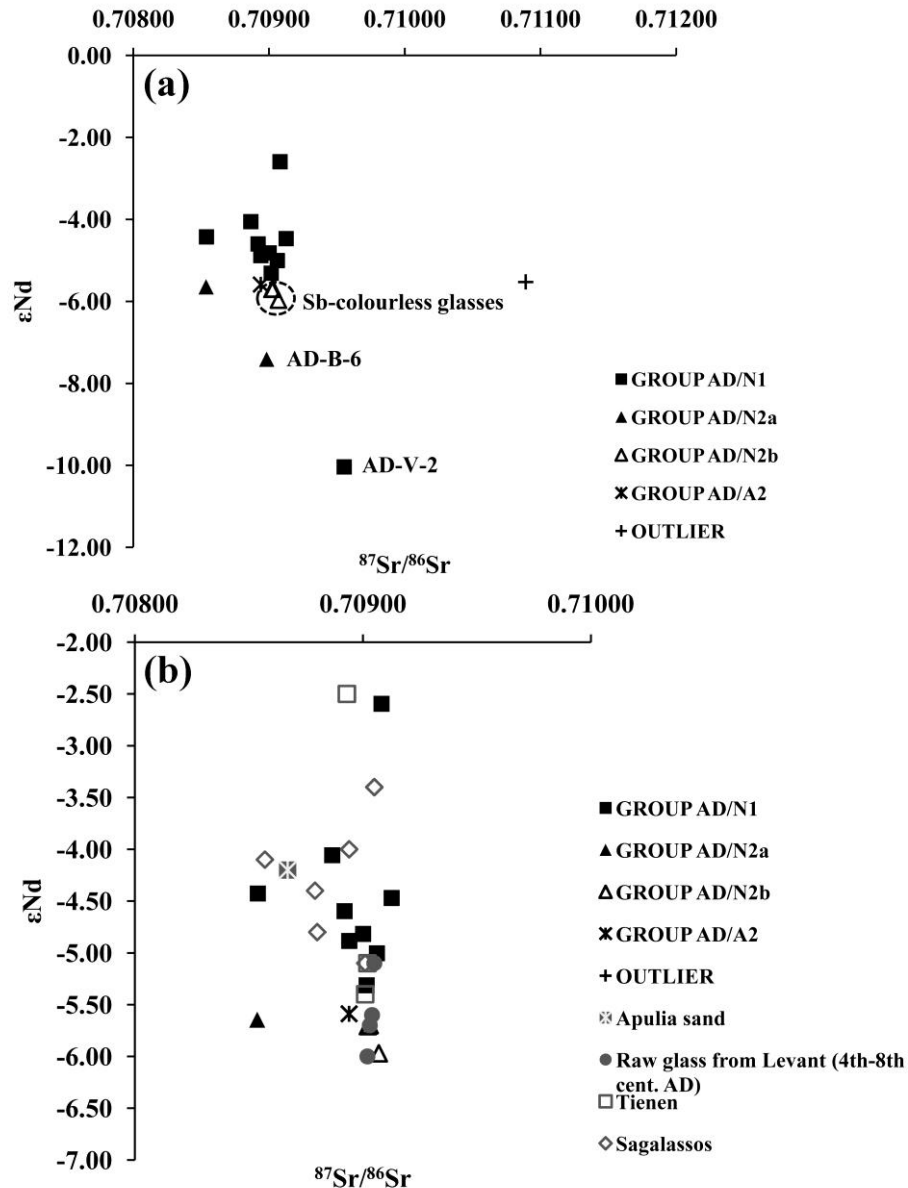


Figure 5.3.3: (a) $^{87}\text{Sr}/^{86}\text{Sr}$ vs ϵNd plot of Roman (1st-3rd century AD) samples from Adria; (b) $^{87}\text{Sr}/^{86}\text{Sr}$ vs ϵNd plot of Roman samples from Adria (excluding outlier and the two samples with lower ϵNd) compared with contemporary glass from Tienen and Sagalagassos (data from Degryse et al., 2009b; Degryse and Schneider, 2008), with 4th-8th century AD raw glass from Levantine localities (data from Freestone et al., in press) and with an Apulia sand suitable for glassmaking (Brems et al., submitted b).

5. The provenance of raw materials in glass: the isotopic approach

As previously explained, these signatures are inconsistent with any sediment in the eastern Mediterranean but correspond well to the range in isotopic values of beach and deep-sea sediments from the western Mediterranean, from the Italian peninsula to the French and Spanish coasts. The raw materials of this glass therefore likely lies in Western Roman Empire, as already suggested for some 1st-3rd century glass from Maastricht, Bocholtz, Tienen and Kelemantia (Degryse and Schneider, 2008; Degryse et al., 2009b), but actually this remains only a speculation due to the low number of analyzed sample. Conversely, the main part of Adria glass shows values between -4.06 and -5.97; one sample (AD-AM-2) has an ϵNd particularly high (-2.59) (Tab. E.1, Figg. 5.3.3, a, b). The large spread in the isotopic composition may indicate the use of multiple sand sources or, alternatively, an intense recycling of glass with different primary origins and thus different signatures. Generally speaking, relationships between isotopic composition and compositional group, colour, type and flux were not observed. An exception is constituted by the small Group AD/N2b, including three Sb-colourless glasses, which show a very homogeneous Nd composition ($\epsilon\text{Nd} = -5.70$ to -5.97 , Tab. E.1, Fig. 5.3.3, a). This evidence was already observed by Ganio et al. (in press) for Sb-colourless glass coming from the Embiez shipwreck (2nd-3rd century AD) and characterized by an average ϵNd value of -5.23 ± 0.10 . The general homogeneity of Nd composition in Sb-colourless glasses indicates that they represent a well distinct production and were subjected to a limited or selective recycling. The Sr-Nd isotopic composition of early Roman Adria glasses is identical or very similar to the signature of contemporary glass from Sagalassos and Tienen (Degryse et al., 2009b) and also to the known 4th-8th century AD primary production centres in the Levant ($\epsilon\text{Nd} = -5.0$ to -6.0 , Freestone et al., in press) (Fig. 5.3.3, b), suggesting an analogous provenance, although not necessarily in the same geographical area of aforementioned Late Byzantine glass units, especially for samples with a Nd isotopic signature between -4.88 and -2.59. This hypothesis is also reinforced by archaeological evidences, as the discovery of early Roman glass furnaces in Beirut, Lebanon (Kouwatli et al., 2008). However, in the light of the results of Brems et al. (submitted *b*), a southern Italian provenance cannot be excluded with total certainty, even if at the present it is not supported by any archaeological data. For this reason, further research is necessary to determine whether

suitable sand from Italy and Syro-Palestine can be distinguished by trace element patterns.

For what concerns Late Roman/Early Medieval glasses (late 3rd-8th century AD), Figure 5.3.4 shows that they are characterized by more homogeneous ϵNd values than early Roman glass. The separation in three main groups (Group AQ/1, Group AQ/2 and Group AQ/3), recognized on the basis of the chemical composition, is well confirmed by the ϵNd isotopic data, supporting the hypothesis of a limited recycling (see section 4.2.1).

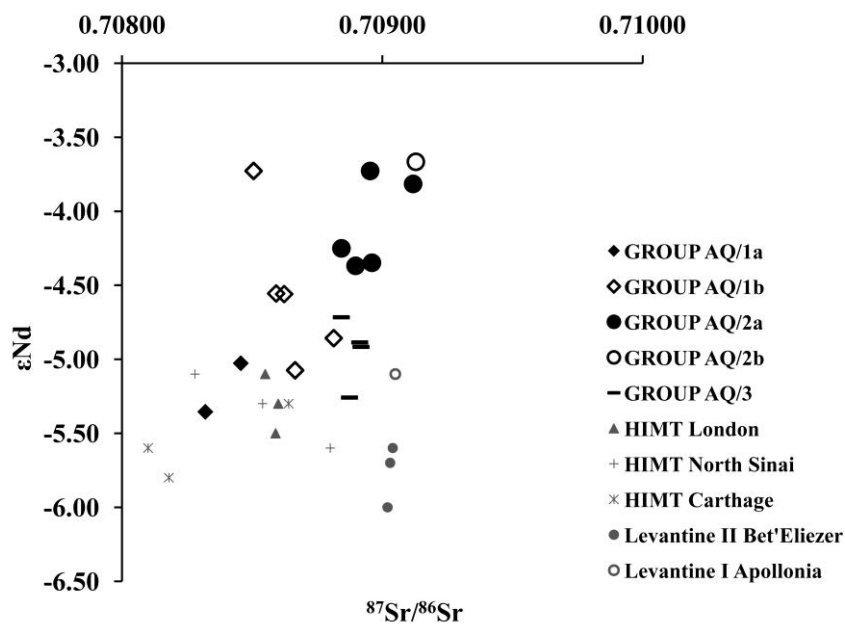


Figure 5.3.4: $^{87}\text{Sr}/^{86}\text{Sr}$ vs ϵNd plot of Late Roman/Early Medieval (late 3rd-8th century AD) samples from Aquileia. Reference data for HIMT and Levantine glasses are also reported (in grey, from Freestone et al., in press).

Group AQ/2 (subgroups AQ/2a and AQ/2b) and Group AQ/3, corresponding to group Levantine I and Série 3.2, respectively (Freestone et al., 2000, 2002, 2003; Foy et al., 2003), have a Nd composition between -3.67 and -4.37, and -4.72 and -5.26 ϵNd , respectively (Tab. E.1). These values are consistent with Nile dominated sediments and, together with the chemical similarity with glasses produced in the Syro-Palestinian region (Freestone et al., 2000), tend to support the hypothesis of an eastern Mediterranean origin rather than a production with southern Italian sands. However, as shown in Figure 5.3.4, the glasses of Groups AQ/2 and AQ/3 present different Nd

signatures with respect the Levantine raw glass coming from the primary workshops of Bet Eli'ezer and Apollonia (Israel) ($\epsilon\text{Nd} = -5.10$ and -6.00 , Freestone et al., in press), indicating their silica raw materials would not originate from exactly the same locations and suggesting that likely different materials were exploited.

The Nd signature of Groups 1a and 1b (HIMT glasses) ranges between -3.73 and -5.35 ϵNd (Tab. E.1). Notwithstanding only some samples show a Nd composition similar to that of other HIMT glasses reported in literature (Fig. 5.3.4, Freestone et al., in press), the ϵNd values consistent with Nile-dominated sediments, the differences in elemental composition (higher levels of Mg, Fe, Mn and Ti) and the lower $^{87}\text{Sr}/^{86}\text{Sr}$ ratios observed in these glasses concur to support, for the reasons already discussed, the hypothesis of an Egyptian origin.

5.3.2 Oxygen isotopes

The results of the oxygen isotopic analysis are reported in Table E.2. The samples are the same as analyzed for Sr and Nd isotopes with the addition of two plant ash glasses (AD-VE-3 and AD-VE-4).

For what concerns the Roman natron glasses, it can be observed that the vast majority of them show fairly homogeneous $\delta^{18}\text{O}$ values, ranging between 15.1‰ to 16.2‰ (VSMOW), with a mean value of $15.6\text{‰} \pm 0.2$ (Table E.2, Fig. 5.3.5, a). The compositional group, the type and the colour do not affect the $\delta^{18}\text{O}$ of these glasses: light blue/green, blue, amber and purple samples show, within the range of reproducibility, the same isotopic composition. Similarly, the $\delta^{18}\text{O}$ values measured on one sample decolourised with Mn and on three samples decolourised with Sb are identical to that of coloured glass (15.6‰ - 15.7‰ , Table E.2). Only one Sb-colourless glass (AD-I-2) shows a $\delta^{18}\text{O}$ value significantly higher with respect the other Roman natron glasses (17.5‰ , Table E.2, Fig. 5.3.5, a). In recent work, Silvestri et al., 2010 observed a similar behavior in some contemporary Sb-colourless glasses, which show $\delta^{18}\text{O}$ values systematically higher than those of coloured or Mn-colourless glasses (Fig. 5.3.5, a). The authors excluded that the enrichment in $\delta^{18}\text{O}$ depends on the addition of decolourizers and assessed it is likely due to the greater addition of flux in this glass type, which determines a higher percentage of Na_2O content. However this cannot be the explanation of the $\delta^{18}\text{O}$ enrichment in AD-I-2 sample, since it has the lowest Na_2O

value than the other Sb-colourless glasses (17.13 wt% vs 18.56-19.10 wt%, Table D.1, Appendix D). Therefore, the most likely explanation is the use of different raw materials (although neodymium data for this sample are lacking).

Figure 5.3.5, a shows a close similarity between the isotopic composition of coloured and Mn-colourless Adria samples (Group AD/N1) and that of the same types of glass coming from the Iulia Felix shipwreck (2nd-3rd century AD), suggesting the use of similar raw materials.

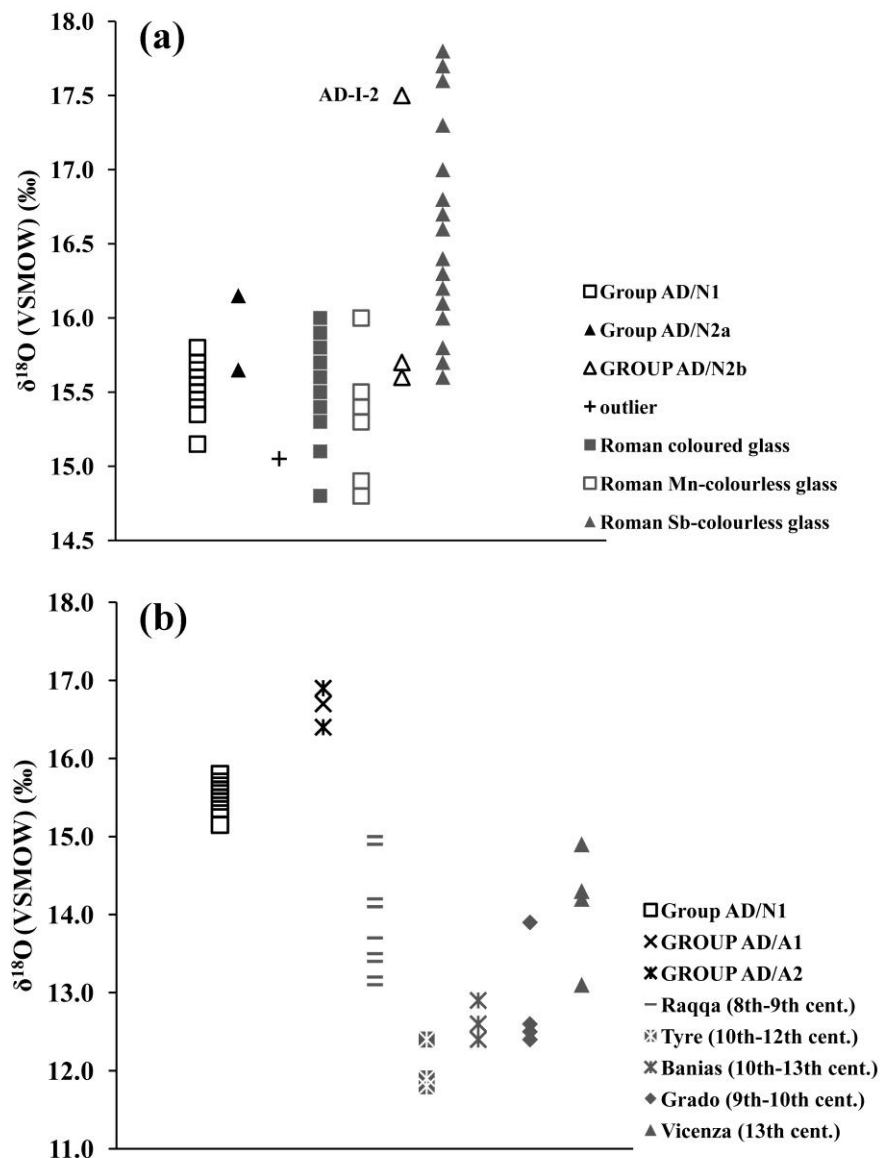


Figure 5.3.5: (a) comparison among $\delta^{18}\text{O}$ (VSMOW) values of natron Roman glass samples analyzed in this study and those already present in literature (grey symbols, data from Silvestri et al., 2010); (b)

5. The provenance of raw materials in glass: the isotopic approach

comparison among $\delta^{18}\text{O}$ (VSMOW) values of soda ash Roman glass samples analyzed in this study, those already present in literature and the natron glass from Adria (AD/N1) (grey symbols, data from Silvestri et al., 2010; Leslie et al., 2006; Henderson et al., 2005).

However, it is interesting to note that the two samples with ‘exotic’ neodymium signature (AD-V-2, AD-B-6, Tab. E.1, see previous section), indicative of a western Mediterranean provenance of raw materials, are perfectly indistinguishable on the basis of oxygen isotopes data (Tab. E.2, Fig. 5.3.5, a). A possible explanation of this evidence may come from the similarity in oxygen isotopic composition of probable raw materials (siliceous-calcareous sand), which, in addition to the same flux (natron) in similar ratios, make the glass samples isotopically indistinguishable.

On the other hand, soda ash Roman glasses form a homogeneous group, distinct from the natron glass for higher ^{18}O values ($16.7\text{‰}\pm 0.3$ vs $15.6\text{‰}\pm 0.2$ in natron glass, Table E.2, Fig. 5.3.5, b), suggesting the use of different raw materials. Literature data about similar glass are not reported, since the use of plant ash as a flux in the Roman period is rather rare. For this reason, Adria samples were compared to some plant ash glasses, dating from the 8th to the 14th century AD, from the eastern Mediterranean (Tyre, Baniyas and Raqqa; Leslie et al., 2006; Henderson et al., 2005), and from northeastern Italian sites (Grado and Vicenza; Silvestri et al. 2010). The results show that Adria samples do not show any similarity with these glasses (Fig. 5.3.5, b), suggesting they were manufactured from different raw materials and therefore that primary workshops of soda ash glass likely changed location from the Roman to the medieval period.

As shown in Figure 5.3.6, the oxygen isotopic data of Late Roman/Early Medieval glasses from Aquileia (late 3rd-8th centuries AD) are very close to those obtained for the earlier glass (Group AD/N1), the mean $\delta^{18}\text{O}$ values being almost identical ($15.6\text{‰}\pm 0.2$ for Group AD/N1 and $15.5\text{‰}\pm 0.4$ for Late Roman/Early Medieval glasses, Table E.2). The separation in the different compositional groups, recognized by means of elemental chemical analysis and confirmed by Sr-Nd data, is not possible using isotopes of oxygen, since all the results are completely overlapping.

In particular, the correspondence between Groups AQ/2a, AQ/2b (Levantine I composition) and Group AQ/3 (Série 3.2 composition) was well expected since, on the basis of Sr-Nd results, it was supposed they were both made with a Levantine sand. On the other hand, the close similarity of $\delta^{18}\text{O}$ values for Groups AQ/1a and AQ/1b (HIMT

composition) to Groups AQ/2a, AQ/2b and AQ/3 is more surprising, as they are thought to have been made from Egyptian sands (see previous section). However, the sands of the Levantine coast are primarily derived from Egypt, being transported to the Mediterranean by the Nile and moved up the eastern Mediterranean coast by marine currents and longshore drift (Emery and Neev, 1960; Pomerancblum, 1966; Stanley et al., 1997). Thus, the silicate components of the sands used for all the natron glasses may have ultimately originated in the same region, and therefore may carry a similar oxygen isotopic signature (Leslie et al., 2006).

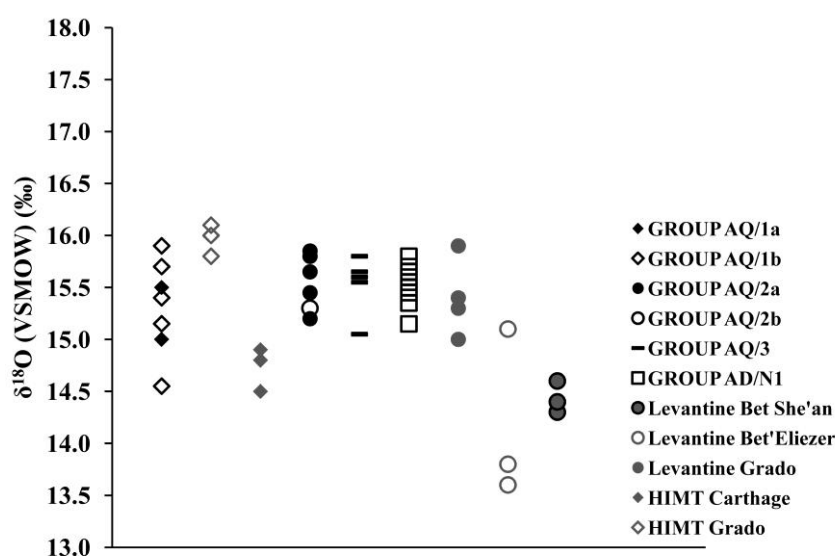


Figure 5.3.6: comparison among $\delta^{18}\text{O}$ (VSMOW) values of natron Late Roman/early Medieval glass samples analyzed in this study and those already present in literature (data from Leslie et al., 2006; Silvestri et al., 2010).

Comparisons among samples analyzed here and other data already present in the literature show interesting analogies and differences. The $\delta^{18}\text{O}$ of Late Roman/Early Medieval glasses (HIMT and Levantine I) from Grado, located in the northernmost coast of the Adriatic Sea, show a very good overlap with the present data (Fig. 5.3.6), suggesting that the same glass type was used in both the cities. Furthermore, this evidence tends to support the hypothesis of a centralized production, organized in few primary workshops which supplied both Aquileia and Grado.

Conversely, the Levantine and HIMT glasses measured by Leslie et al. (2006) appear mostly lower than the data in the present study (Fig. 5.3.6), despite their chemical

similarity. As already suggested by Leslie et al. (2006) and Silvestri et al. (2010), a possible explanation for the differences in oxygen composition could be the exploitation of different raw materials on the coast of the eastern Mediterranean, as also already suggested by Nd data. Supporting this possibility are the isotopic composition of two Belus samples, which have different ^{18}O values, due to different ratios between most abundant minerals (quartz and calcite), even though they were sampled from two different sites 200 m from each other (Silvestri et al., 2010). Moreover, another possibility may be the use of different sources of natron, with distinct isotopic signature which influenced the final glass in a different way (Silvestri et al., 2010).

In summary, the homogeneity in oxygen isotopic signature between Roman and Late Roman/early Medieval glasses from Adria and Aquileia indicates a common origin of their raw materials, notwithstanding the slight differences in chemical composition suggest that they do not come from exactly the same geographical area and that different materials were exploited. Moreover, the chemical and isotopic similarity between Late Roman/early Medieval glass from Grado and Aquileia, together with the chemical correspondence among Groups AQ/2a and AQ/2b and Levantine glass (see section 4.2.1), suggest they come from the same raw material source which tends to support the hypothesis that glass was imported in Adriatic zone from primary workshops likely located in the Near East.

5.4 Conclusions

The combined analyses of strontium, neodymium and oxygen isotopes proved to be a valid supplement to the chemical characterization for tracing the provenance of raw materials in ancient glass.

Nd is characteristic of the mineral fraction other than quartz in the silica raw material, while Sr is in most cases characteristic of the lime component. Except the glasses with HIMT composition (Groups AQ/1a and AQ/1b), the greater part of natron glass here analyzed, independently from the age, shows values of strontium close to the modern ocean seawater (0.7092), indicating that the source of lime was marine shell and then that coastal sands were likely employed in its production. However, chemical and isotopic data on purple glasses show that Mn-bearing colourants can introduce strontium in the batch and then modify both the total content and the isotopic signature.

All Late Roman/early Medieval (late 3rd-8th century AD) glasses from Aquileia show a Nile-dominated Mediterranean Nd signature (higher than $-6 \text{ } \epsilon\text{Nd}$), in some cases similar to that of 4th-8th century AD primary workshops in the Levant. In addition, Groups AQ/2a, AQ/2b and AQ/3 (Levantine I and Série 3.2) have a chemical composition close to contemporary glass produced in some Levantine workshops. Therefore, the chemical and isotopic data of these glasses concur to support the hypothesis of an eastern Mediterranean origin, likely in the Syro-Palestinian region, although not necessary in the same workshops reported in literature. On the other hand, HIMT glasses (Groups AQ/1a and AQ/1b), which show similar Nd signatures, are distinguished from Levantine glasses by lower $^{87}\text{Sr}/^{86}\text{Sr}$ values, also correlated to higher contents of Fe_2O_3 , TiO_2 , MgO and lower CaO . These evidences indicate that they were produced from geochemically distinctive, but geographically proximal sands. So far, the chemical and isotopic data seem to favour an area of origin on the Egyptian coast, between Alexandria and Gaza (Freestone et al., in press).

Assigning the primary origin to 1st-3rd century AD glasses is more difficult. The large spread in their isotopic composition suggests the use of multiple sand sources or, alternatively, an intense recycling of glass with different primary origins. Sb-colourless glasses represent an exception, since their homogeneous isotopic composition indicates that they are a well distinct production and were subjected to a limited or selective recycling. As the Late Roman/early Medieval glass from Aquileia, the majority of Roman glass coming from Adria show a relatively high Nd signature ($> -6 \text{ } \epsilon\text{Nd}$), similar to that of aforementioned 4th-8th century AD primary production centres located in the Syro-Palestinian coast, pointing to an analogous provenance. However, the slight but clear differences in major element chemistry among Roman Adria glasses and the Byzantine glass produced in the Levantine workshop raise the problem of a possible different origin. Indeed, notwithstanding it is probable that these variations could be due to exploitation of different ores along the Syro-Palestinian coast, the use of other primary sources cannot be completely excluded. In particular, the recent discovery in southern Italy of sand, suitable for glassmaking, and with a Nd signature coincident with the range of Nd values previously thought to be characteristic for an eastern Mediterranean origin (Brems et al., submitted *b*), represents a critical point in the application of Nd isotopes for provenancing ancient glass. Further geochemical studies

5. The provenance of raw materials in glass: the isotopic approach

on trace elements are essential to determine if Italian and Levantine sands can be distinguished, but it is also necessary to expand the current number of analyses of raw materials, as well as of more glass from primary furnace.

Only two Roman glasses with a different Nd signature (lower than $-7 \text{ } \epsilon\text{Nd}$) have been identified in Adria sample set. This data is inconsistent with any sediment in the eastern Mediterranean and tends to locate primary production in western Mediterranean or north-western Europe, as already suggested by other authors (Degryse and Schneider, 2008). It is interesting to note that these samples are chemically indistinguishable from the others, indicating that the main element and isotopic data not always concur. Conversely, both techniques are complementary, indicating that the preferred approach in investigation of ancient glasses is likely the use of the two methods in tandem.

For what concerns oxygen isotopes, it was observed that the contribution of both flux and sand to the isotopic composition of the glass makes it somewhat less powerful than neodymium in provenancing raw materials. Overall, oxygen isotopes appear to be quite effective as discriminants of glass raw material sources, in particular they proved to be a diagnostic method to discriminate natron and plant ash glass.

The substantial homogeneity in oxygen isotopes between natron Roman and Late Roman/early Medieval glasses from Adria and Aquileia implies the use of similar raw materials and suggests a common origin, although it is probable that different ores were exploited in the same area. Moreover, by combining the data of O, Sr-Nd and chemical analyses, the hypothesis that glass was produced in few primary workshops, likely located in Syro-Palestine and Egypt, and then imported in northern Adriatic area seems to be strongly supported.

CONCLUDING REMARKS

The evolution of glass production (type and provenance of raw materials, production technologies) in a large chronological period (6th century BC-15th century AD) and in a specific geographical area, the northeastern Adriatic Italy, was here mainly investigated. The sample set, including a total of 178 glasses, comes from some of the most important sites in the period and in the area considered, such as Aquileia, Adria and Rocca di Asolo. Few samples coming from Tuscan sites (San Genesio, Pieve di Pava and Pieve di Coneo), similar in age and types to Aquileia glasses, were also analyzed, in order to have a comparison among eastern and western Italy.

The analytical approach involved textural, mineralogical, chemical and isotopic (Sr, Nd, O) analyses and the results proved the complementarity of these techniques, suggesting that the preferred approach in investigation of ancient glasses should be the combined use of these methods.

A substantial continuity in the use of the type of raw materials (siliceous-calcareous sand in addition to natron) from Pre-Roman period until early Middle Ages was testified. The continuity between Pre-Roman and Roman production is also supported by the use of the same opacifiers: calcium antimonate in white and light blue, lead antimonate in yellow glasses. Conversely, a complete change in the use of flux is evident in High/Late Medieval glasses, in which natron was replaced by soda ashes. A little group of intensely coloured (emerald green, one blue and one black) soda ash glasses from Adria, dating 1st-3rd century AD, constitutes a peculiarity and suggest they were imported from geographical areas where the use of plant ashes was never interrupted.

Chemical analyses show that samples can be grouped by age, indicating routine glass production processes; on the other hand, no particularly relationships were observed between types and chemical composition. Different groups have been identified and usefully compared with the major compositional groups present in the literature. The extraordinary consistency of natron glass and the principal compositional groups widespread in Mediterranean sites tends to support the model of the localized

production, organized in a small number of primary workshops which supplied raw glass to a great number of secondary workshops, where the glass was re-melted and shaped into objects. Moreover, data collected in this study show that, at least in Late Roman/early Medieval period, the geographical position was an important factor influencing the distribution of newly manufactured glass. Indeed, it appears that the supply of 'fresh' glass was easier for the Aquileia, located in a strategic position on the northeastern Italian side and well connected by sea to the eastern Mediterranean area, than for other sites located in the opposite part of the Italian peninsula (Tuscan sites) or far away from the sea (Rocca di Asolo).

The transition from the use of natron to that of plant ash likely determined a change also in the organization of glass production and in the location of primary workshops. For what concerns northeastern Italy, although the transition of the glass industry from Roman to Medieval periods has not been completely understood, it is known that, at least from the 12th century ash glass was produced in Venice (Verità et al., 2002; Verità and Zecchin, 2009). The analytical and historical evidence on High/Late Medieval glasses from Rocca di Asolo strongly suggests that they come from Venice, giving a further indication of the fundamental role that this city played in glass manufacture and trade during Middle Ages.

For what concerns the provenance of raw materials, an essential contribution was provided from isotopic analysis, in particular those of Sr and Nd. At this stage the study mainly focused on a selection of Roman and Late Roman/early Medieval glasses, coming from Adria and Aquileia, respectively. The combination of isotopic and chemical data, together with archaeological evidence and literature data on both raw materials and glass from primary furnaces, suggests that the vast majority of Roman and Late Roman/early Medieval glasses analyzed in this study were likely produced in workshops located on the Syro-Palestinian and Egyptian coasts, although not necessarily in same *ateliers* so far identified. However, the recent discovery in southern Italy of sand with Nd signature coincident with the range of Nd values previously thought to be characteristic for an eastern Mediterranean origin (Brems et al., submitted *b*), implies that the use of primary sources located in western Mediterranean cannot be definitely excluded and necessitate further analyses on trace elements in order to determine if Italian and Levantine sands can be distinguished.

On the other hand, oxygen isotopes have been demonstrated to be a less powerful tool than neodymium for provenancing raw materials, since the contribution of the same flux and of the quartz contained in the sand, uniforms the isotopic signature of natron glass, making it indistinguishable. Conversely, they appear to be a diagnostic method to discriminate natron and plant ash glass.

In synthesis, the results collected in the present work tend to indicate that the origin of the majority of Roman and Late Roman/early Medieval glasses, coming from Adria and Aquileia, has to be localized in the eastern Mediterranean. However, this evidence does not exclude the possibility that secondary workshops could have been active in these cities and, in this respect, future studies on production indicators (drops, filaments, raw glass), never analyzed from an archaeometric point of view, are desirable.

On the other hand, during High Middle Ages the transition from natron to soda ash determined the affirmation of Venice as ‘point of reference’ for glass production in northern Adriatic area. However, the import in this city of Levantine ashes and the similarity among some Venetian and Islamic glasses suggest that exchanges of know-how and raw materials between the northern Adriatic Italy and the eastern Mediterranean still continued throughout the Middle Ages.

REFERENCES

- Aerts , B. Velde , K. Janssens , W. Dijkman , 2003, Change in silica sources in Roman and post-Roman glass, *Spectrochimica Acta part B* 58, 659-667.
- F. Aldsworth, G. Haggarty, S. Jennings, D. Whitehouse, 2002, Medieval glassmaking at Tyre, Lebanon, *Journal of Glass Studies* 44, 49-66.
- D. Allen, 1998, *Roman Glass in Britain*, ed. J. Dyer., Princes Risborough, Buckinghamshire: Shire Publications.
- Angelini, G. Artioli, P. Bellintani, A. Cardarelli, V. Diella, A. Polla, Residori, 2002, Project: “Glass materials in the protohistory North Italy”: a first summary, in C. D’Amico (Ed.), *Atti II Congresso Nazionale di Archeometria*, Patron Editore, Bologna, 581-595.
- Angelini, G. Artioli, P. Bellintani, V. Diella, M. Gemmi, A. Polla, A. Rossi, 2004, Chemical analyses of Bronze Age glasses from Frattesina di Rovigo, northern Italy, *Journal of Archaeological Science* 31, 1175-1184.
- I. Angelini, C. Nicola, G. Artioli, 2006, Studio analitico dei materiali vetrosi, in M. Venturino Gambari (Ed.), *Navigando lungo l’Eridano. La necropoli protogolasecchiana di Morano sul Po*, Museo Civico, Città di Casale Monferrato, 77-82, 111–117.
- R. Arletti, M.C. Dalconi, S. Quartieri, M. Triscari, G. Vezzalini, 2006, Roman coloured and opaque glass: a chemical and spectroscopic study. *Applied Physics A* 83, 239–245.
- R. Arletti, G. Vezzalini, S. Benati, 2010 a, Roman window glass: a comparison of findings from three different Italian sites, *Archaeometry* 52(2), 252–271.
- R. Arletti, C. Maiorano, D. Ferrari, G. Vezzalini, S. Quartieri, 2010b, The first archaeometric data on polychrome Iron Age glass from sites located in northern Italy, *Journal of Archaeological Science* 37, 703–712.
- R. Arletti, L. Rivi, D. Ferrari, G. Vezzalini, 2011, The Mediterranean Group II: analyses of vessels from Etruscan contexts in northern Italy, *Journal of Archaeological Science* 38, 2094-2100.

- E. Ashtor, G. Cevidalli, 1983, Levantine alkali ashes and European industries, *European Journal of Economic History* 12, 475–522.
- J. L. Banner, 2004, Radiogenic isotopes: systematic and applications to earth surface processes and chemical stratigraphy, *Earth Science Reviews* 65, 141-194.
- R. Basu, S. B. Jacobsen, R. J. Poreda, C. B. Dowling, P. K. Aggrawal, 2001, Large groundwater strontium flux to the oceans from the Narmada Basin and the marine strontium isotope record, *Science*, 293, 1470–3.
- M. J. Baxter, H. E. M. Cool, C. M. Jackson, 2005, Further studies in the compositional variability of colourless Romano-British vessel glass, *Archaeometry* 47, 45–68.
- L. Bertacchi, 2003, Nuova pianta archeologica di Aquileia, Edizioni del Confine, Udine.
- M. Bimson, I.C. Freestone, 1983, An analytical study of the relationship between the Portland vase and other Roman cameo glasses, *Journal of Glass Studies* 25, 55-64.
- J. Bonetto, 1993, L'area del Monte Ricco: evoluzione delle strutture insediative e di difesa dal VI/VII al XV/XVI secolo, in F. Bocchi, G. Rosada (Eds.), *Atlante Storico delle Città Italiane-Asolo*, Grafis Edizioni, Casalecchio di Reno (Bologna).
- J. Bonetto, M. Salvadori, in press, Aquileia. Edilizia domestica. I progetti di ricerca presso la cd. Domus delle Bestie ferite e presso l'area dei fondi ex Cossar, in *Primo Forum sulla ricerca archeologica in Friuli Venezia Giulia*, in L. Fozzati and G. Petrucci (Eds.), *Quaderni della Soprintendenza per i Beni Archeologici del Friuli Venezia Giulia*.
- S. Bonomi, 1996, Vetri Antichi del Museo Archeologico Nazionale di Adria, *Corpus delle Collezioni Archeologiche del Veneto*, Comitato Nazionale Italiano AIHV.
- D. Brems, M. Ganio, M. Walton, P. Degryse, In press, Mediterranean sand deposits as a raw material for glass production in Antiquity. *Annales du 18e Congrès de l'Association Internationale pour l'Histoire du Verre*, Thessaloniki.

- D. Brems, P. Degryse, F. Hasendoncks, D. Gimeno, A. Silvestri, E. Vassilieva, S. Luybaers, J. Honings, submitted *a*, Western Mediterranean sand deposits as a raw material for Roman glass production, *Journal of Archaeological Science*.
- D. Brems, submitted *b*, M. Ganio, K. Latruwe, L. Balcaen, D. Gimeno, A. Silvestri, F. Vanhaecke, P. Muchez, P. Degryse, Isotopes on the beach-Sr and Nd isotopic analysis for provenancing Roman glassmaking, *Journal of Analytical Atomic Spectrometry*.
- R. H. Brill, J. M. Wampler, 1965, Isotope studies of ancient lead, *American Journal of Archaeology* 71, 63-77.
- R. H. Brill, 1970, The chemical interpretation of the texts, in A. L. Oppenheim, R. H. Brill, D. Barag and A. von Saldern (Eds.) *Glass and glassmaking in ancient Mesopotamia*, Corning Museum of Glass, New York, pp. 105–128.
- R. Brill, 1988, Scientific Investigations of the Jalame glass and related finds, in G.D Weinberg (Ed.) *Excavations at Jalame: site of a glass factory in Late Roman Palestine*, University of Missouri Press, Columbia.
- R. H. Brill, 1999, *Chemical analyses of early glasses*, vols 1 and 2, Corning Museum of Glass, New York.
- M. Buora, L. Mandruzzato, M. Verità, 2009, Vecchie e nuove evidenze di officine vetrarie romane ad Aquileia, *Quaderni di Archeologia Friulana* XIX, 51-58.
- W. A. Burke, R. E. Denison, E. A. Hetherington, R. B. Koepnik, H. F. Nelson, J. B. Otto, 1982, Variations of seawater $^{87}\text{Sr}/^{86}\text{Sr}$ throughout Phanerozoic time, *Geology* 10, 516–19.
- K. H. Butler, M. J. Bergin, V. M. B. Hannaford, 1950, Calcium antimonates, *Electrochemical Society Journal* 97, 117-122.
- Cagno, S., Janssens, K., Mendera, M., 2008, Compositional analysis of Tuscan glass samples: in search of raw material fingerprints, *Analytical and Bioanalytical Chemistry* 391(4), 1389–1395.
- Cagno, S., Mendera, M., Jeffries, T., Janssens, K., 2010, Raw materials for medieval to post-medieval Tuscan glassmaking: new insight from LA-ICP-MS analyses, *Journal of Archaeological Science* 37(12), 3030-3036.

- S. Cagno, L. Favaretto, M. Mendera, A. Izmer, F. Vanhaecke, K. Janssens, 2011, Evidence of early medieval soda ash glass in the archaeological site of San Genesio (Tuscany), *Journal of Archaeological Science*, doi: 10.1016/j.jas.2011.12.031.
- M. C. Calvi, 1968, *I Vetri Romani del Museo di Aquileia*, Associazione nazionale per Aquileia.
- S. Campana, C. Felici, R. Francovich, L. Marasco, C. Lubritto, I. Passariello, F. Marzioli, N. De Cesare, M. Rubino, G. Borriello, A. D’Onofrio, F. Terrasi, 2007, L’utilizzo delle datazioni al radiocarbonio nel sito archeologico di Pava, in C. D’amico (Ed.), *Atti IV Congresso AIAR*, Patron Editore, Bologna.
- F. Cantini, 2010, Vicus Wallari-borgo San Genesio. Il contributo dell’archeologia alla ricostruzione della storia di un central place della valle dell’Arno, in *Vico Wallari-San Genesio. Ricerca storica e indagini archeologiche su una comunità del Medio Valdarno*, Firenze University Press.
- M. Chiabà, 2009, Dalla fondazione all’età tetrarchica, in: F. Ghedini, M. Bueno, M. Novello (Eds.), *Moenibus et portu celeberrima, Aquileia: storia di una città*, Istituto poligrafico e Zecca dello Stato, Roma, 7-22.
- G. Ciampoltrini, 2008, Vie e pievi, pievi e castelli. Storie parallele di due plebes baptismales del territorio di Lucca, in *Chiese e insediamenti nei secoli di formazione dei paesaggi medievali della Toscana (V-X secolo)*, Quaderni del Dipartimento di Archeologia e Storia delle Arti. Sezione Archeologica 64.
- P. Costagliola, G. Baldi, C. Cipriani, E. Pecchioni, A. Buccianti, 2000, Mineralogical and chemical characterization of the Medicean glass mosaic tesserae and mortars of the Grotta del Buontalenti, Giardino di Boboli, Firenze, *Italy Journal of Cultural Heritage* 1, 287-299.
- R.L. Cullers, S. Chaudhuri, N. Kilbane, R. Koch, 1979, Rare earths in size fractions and sedimentary rocks of Pennsylvanian-Permian age from the mid-continent of the USA, *Geochimica Cosmochimica Acta* 43, 1285-1302.
- K. Cummings, 2002, *A History of Glassforming*. University of Pennsylvania Press.
- P. Degryse, J. Schneider, U. Haack, V. Lauwers, J. Poblome, M. Waelkens, Ph. Muechez, 2006a, Evidence for glass ‘recycling’ using Pb and Sr isotopic ratios

- and Sr-mixing lines: the case of early Byzantine Sagalassos. *Journal of Archaeological Science* 33, 494-501.
- P. Degryse, J. Schneider, V. Lauwers, D. De Muynck, F. Vanhaecke, M. Waelkens, Ph. Muchez, 2006b, Sr and Nd isotopic evidence in the primary provenance determination of Roman glass from Sagalassos (SW Turkey), in K. Janssens, P. Degryse, P. Cosyns, J. Caen, L. Van't Dack (Eds.), *Annales du 17e Congrès de l'Association Internationale pour l'Histoire du Verre*, Anvers, 564-570.
 - P. Degryse, J. Schneider, 2008, Pliny the Elder and Sr-Nd isotopes: tracing the provenance of raw materials for Roman glass production, *Journal of Archaeological Science* 35, 1993-2000.
 - P. Degryse, J. Henderson, G. Hodgins, 2009a, Isotopes in vitreous materials, a state-of-the-art and perspectives, in P. Degryse, J. Henderson, G. Hodgins (Eds.), *Isotopes in vitreous materials, Studies in Archaeological Sciences*, Leuven University Press, 15-30.
 - P. Degryse, J. Schneider, V. Lauwers, J. Henderson, B. Van Daele, M. Martens, H.D.J. Huisman, D. De Muynck, Ph. Muchez, 2009b, Neodymium and strontium isotopes in the provenance determination of primary natron glass production, in P. Degryse, J. Henderson, G. Hodgins (Eds.), *Isotopes in vitreous materials, Studies in Archaeological Sciences*, Leuven University Press, Leuven University Press, 53-72.
 - P. Degryse, A. Shortland, 2009, Trace elements in provenancing raw materials for Roman glass production, *Geologica Belgica* 12/3-4, 135-143.
 - P. Degryse, A. Shortland, D. De Muynck, L. Van Heghe, R. Scott, Bert Neyt, Frank Vanhaecke, 2010a, Considerations on the provenance determination of plant ash glasses using strontium isotopes, *Journal of Archaeological Science* 37, 3129-3135.
 - P. Degryse, I.C. Freestone, J. Schneider, S. Jennings, 2010b, Technology and provenance study of Levantine plant ash glass using Sr-Nd isotope analysis, In J. Drauschke, D. Keller, (Eds.), *Glas in Byzanz e Produktion, Verwendung, Analysen, RGZM Tagungen Band 8*.

- M. De Min, 1987, Adria, in: *Il veneto nell'età Romana. II. Note di urbanistica e di archeologia del territorio*, Verona, 255-268.
- D. De Muynck, G. Huelga-Suarez, L. Van Heghe, P. Degryse, F. Vanhaecke, 2009, Systematic evaluation of a strontium-specific extraction chromatographic resin for obtaining a purified Sr fraction with quantitative recovery from complex and Ca-rich matrices, *Journal of Analytical Atomic Spectrometry* 24 (11), 1498-1510.
- D. J. DePaolo, G. J. Wasserburg, 1976, 'Nd isotopic variations and petrogenic models', *Geophysical Research Letters* 3, 249-252.
- D. J. DePaolo, B. I. Ingram, 1985, High resolution stratigraphy with strontium isotopes, *Science*, 227, 938-41.
- G. De Tommaso, 1990, *Ampullae vitreae. Contenitori in vetro di unguenti e sostanze aromatiche dell'Italia romana (I sec.a.C.-III sec.d.C.)*, Roma.
- J. Dik, K. Janssens, G. Van der Snickt, L. van der Loeff, K. Rickers, M. Cotte, Visualization of a lost painting by Vincent van Gogh using synchrotron radiation based X-ray fluorescence elemental mapping, *Analytical Chemistry* 80 (16), 6436 -6442.
- E. Eichholz, 1962, *Pliny, Natural history, vol. X, books XXXVI and XXXVII*, Heinemann, London/Harvard University Press, Cambridge, MA.
- K.O. Emery, D. Neev, 1960, *Mediterranean Beaches of Israel*, Geological Survey Israel Bulletin 26, 1-23.
- G. Faure, 1986, *Principles of isotope geology*, 2nd ed, John Wiley and Sons.
- G. Faure, T. M. Mensing, 2005, *Isotopes: Principles and application*, 3rd edition, John Wiley & Sons.
- D. Ferrari, A. Larese, G. Meconcelli Notarianni, M. Verità, 1998, *Glossario del vetro antico*, Venezia. Trad. Inglese D.B. Whitehouse.
- C. Fiori, M. Vandini, 2004, Chemical composition of glass and its raw materials: chronological and geographical development in the first millennium AD, in M. Beretta (Ed.), *When glass matters: Studies in the History of Science and Art from Graeco-Roman Antiquity to Early-Modern Era*, Leo S. Olschki, Firenze.

- S. J. Fleming, 1999, *Roman Glass: reflections on cultural change*, Philadelphia, University of Pennsylvania Museum of Archaeology and Anthropology.
- G. Fogolari, B. M. Scarfi, 1970, *Adria Antica*, Alfieri, Edizioni d'Arte, Venezia.
- E. Foster, C. M. Jackson, 2009, The composition of 'naturally coloured' late Roman vessel glass from Britain and the implications for models of glass production and supply, *Journal of Archaeological Science* 36(2), 189–204.
- D. Foy, M. Jezegou, 1998, Commerce et technologie du verre antique. Le témoignage de l'épave 'Ouest Embiez 1', in *Actes du 121e Congrès national des sociétés historiques et scientifiques, Archéologie-Méditerranée, Nice, 1996: Méditerranée antique. Pêche, navigation, commerce*, 121–34.
- D. Foy, M. Vichy, M. Picon, 2000, Lingots de verre en Méditerranée occidentale, in *Annales du 14th congrès de l'Association pour l'Histoire du Verre AIHV, Amsterdam*, 51-57.
- D. Foy, M. Picon, M. Vichy, V. Thirion-Merle, 2003, Caractérisation des verres de la fin de l'Antiquité en Méditerranée occidentale: l'émergence de nouveaux courants commerciaux, in D. Foy and M.D. Nenna (Eds.) *Échanges et commerce du verre dans le monde antique, Actes du colloque de l'Association Française pour l'Archéologie du Verre, Aix-en-Provence et Marseille, 7–9 juin 2001*, Editions Monique Mergoïl, Montagnac, 41–85.
- Frank, S., 1982, *Glass and archaeology*, Academic Press, London.
- I. C. Freestone, 1992, Theophilus and the composition of medieval glass, in B. P. Vandiver, J.R. Druzik, G.S. Wheeler and I.C. Freestone (Eds.), *Materials Issues in Art and Archaeology III, Materials Research Society Symposium Proceedings, volume 267, (San Francisco, California, U.S.A., 27 April-1 May 1992)*, Materials Research Society Pittsburg, Pennsylvania, 739-745.
- I. C. Freestone, 1993, Compositions and origins of glasses from Romanesque champlevé enamels, in N. Stratford (Ed.), *Catalogue of medieval enamels in the British Museum, British Museum, London, vol II*, 37–45.
- Freestone, I. C., 1994, Chemical analysis of 'raw' glass fragments, in *Excavation at Carthage, volume II, the Circular Harbour, north side. The site and finds other than pottery*, H. R. Hurst (ed.), *British Academy Monographs in Archeology, N°4*, Oxford University Press, Oxford.

- I. C. Freestone, Y. Gorin-Rosen, 1999, The great glass slab at Beth She'arim: an early Islamic glass-making experiment'?, *Journal of Glass Studies* 41, 105-116.
- I.C. Freestone, Y. Gorin-Rosen, M.J. Hughes, 2000, Primary glass from Israel and the production of glass in Late Antiquity and the Early Islamic period, In M.D. Nenna (Ed.), *La route du verre. Ateliers primaires et secondaires du second millénaire avant J.C. au Moyen Age. Travaux de la Maison de l'Orient Méditerranéen*, 33. TMO, Lyon, 65-82.
- I.C. Freestone, M. Ponting, J. Hughes, 2002, The origins of Byzantine glass from Maroni Petrera, Cyprus, *Archaeometry* 44, 257-272.
- I.C. Freestone, K. A. Leslie, M. Thirlwell, Y. Gorin-Rosen, 2003, Strontium isotopes in the investigation of early glass production: Byzantine and early Islamic glass from the Near East, *Archaeometry* 45(1), 19–32.
- I.C., Freestone, S. Wolf, M. Thirlwall, 2005, The production of HIMT glass: elemental and isotopic evidence. *Annales du 16e Congress of the Association Internationale pour l'Histoire du Verre*, London, 153-157.
- I. C. Freestone, 2006, Glass production in Late Antiquity and the Early Islamic period: a geochemical perspective, in M. Maggetti, B. Messiga (Eds.), *Geomaterials in Cultural Heritage*, Geological Society of London, Special Publications 257, 201-216.
- I.C. Freestone, 2008, Pliny on Roman Glassmaking, in M. Matinón-Torres, T. Rehren, (Eds.), *Archaeology, History and Science. Integrating Approaches to Ancient Materials* (UCL Institute of Archaeology Publications), Oxford, 77-100.
- I. C. Freestone, S. Wolf, M. Thirlwall, 2009, Isotopic composition from the Levant and the south-eastern Mediterranean region, in P. Degryse, J. Henderson, G. Hodgins (Eds.), *Isotopes in vitreous materials*, Studies in Archaeological Sciences, Leuven University Press, 31-51.
- I. C. Freestone, P. Degryse, J. Shepherd, Y. Gorin-Rosen, J. Schneider, In press, Neodymium and strontium isotopes indicate a Near Eastern origin for late Roman glass in London, *Journal of Archaeological Science*.
- C.D. Frost, R.K. O'Nions, S.L. Goldstein, 1986, Mass balance for Nd in the Mediterranean Sea, *Chemical Geology* 55, 45-50.

- N. H. Gale, Z. Stos-Gale, 1982, Bronza Age Copper Sources in the Mediterranean: a New Approach, *Science* 216, 11-19.
- F. Gallo, A. Marcante, G. Molin, A. Silvestri, 2011, Glass from *Casa delle Bestie Ferite* (Aquileia, UD): an archaeological and archaeometric study (Oral presentation), National Day of Study on Excavations at Aquileia, Padova (Italy), 21-22 February.
- M. Ganio, S. Boyen, D. Brems, R. Scott, D. Foy, K. Latruwe, G. Molin, A. Silvestri, F. Vanhaecke, P. Degryse, In press, Trade Routes across the Mediterranean: a Sr/Nd isotopic investigation on Roman colourless glasses, *Journal of the Society of Glass Technology*.
- E. Gliozzo, A. Santagostino Barbone, F. D'Acapito, M. Turchiano, I. Turbanti Memmi, G. Volpe, 2010, The Sestilia Panels of Faragola (Ascoli Satriano, Southern Italy): A Multi-Analytical Study of the Green, Marbled (Green and Yellow), Blue and Blackish Glass Slabs, *Archeometry* 52(3), 389-415.
- S.L. Goldstein, R.K. O'Nions, P.J. Hamilton, 1984, A Sm-Nd isotopic study of atmospheric dusts and particulates from major river systems, *Earth and Planetary Science Letters* 70, 221-236.
- Y. Gorin-Rosen, 2000, The ancient glass industry in Israel: summary of finds and new discoveries, in M.D. Nenna (Ed.), *La route du verre. Ateliers primaires et secondaires du second millénaire avant J.C. au Moyen Age. Travaux de la Maison de l'Orient Méditerranéen* 33, Lyon, 49-64.
- K. Govindaraju, 1994, 1994 Compilation of working values and sample description for 383 geostandards, *Geostandards Newsletter*, XVIII, Special Issue, July, 1-158.
- B. Gratuze, I. Soulier, J. N. Barradon, D. Foy, 1992, De l'origine du cobalt dans les verres, *Revue d'Archéométrie* 16, 97-108.
- Gratuze, C. Moretti, 2001, Lingotti e rottami di vetro destinati alla rifusione rinvenuti nelle navi naufragate in Mediterraneo (III sec a.C. – III sec. d.C): analisi chimica dei reperti e recenti ipotesi sull'organizzazione produttiva in vetrerie primarie e secondarie, in C. Piccioli, F. Sogliano (Eds.), *Il vetro in Italia meridionale e insulare*, VII Giornate nazionali di studio Comitato Nazionale Italiano AIHV, Napoli, 5-7 dicembre 2001, 401-13.

- B. Gratuze, Y. Billaud, 2003, La circulation des perles en verre dans le Bassin Méditerranéen, de l'Age du Bronze moyen jusqu'au Hallstatt, in D. Foy, M.D. Nenna, (Eds.), Echanges et commerce du verre dans le monde antique. Actes du colloque AFAV, Aix-en-Provence et Marseille 2001, Mergoil Editor, Montagnac, 11-15.
- L.R. Green, F.A. Hart, 1987, Colour and chemical composition in ancient glass: an examination of some Roman and Wealden glass by means of ultraviolet-visible-infra-red spectrometry and Electron microprobe analysis, *Journal of Archeological Science* 14, 271-282.
- S. Greiff, J. Schuster, 2008, Technological study of enamelling on Roman glass: The nature of opacifying, decolourizing and fining agents used with the glass beakers from Lübsow (Lubieszewo, Poland), *Journal of Cultural Heritage* 9, 27-32.
- D. F. Grose, 1989, *Early Ancient Glass: core-formed, rod-formed and cast vessels and objects from the late Bronze Age to the early Roman Empire, 1600 BC to AD 50*, Hudson Hills Press, New York.
- D.F. Grose, 1991, Early Imperial Roman cast glass: The translucent coloured and colourless fine wares, in *Roman Glass: two centuries of art and invention*, M. Newby and K. Painter, Editors. 1991, Society of Antiquaries of London: London.
- F. E. Grousset, P.E. Biscaye, A. Zindler, J. Prospero, R. Chester, 1988, Neodymium isotopes as tracers in marine sediments and aerosols: North Atlantic, *Earth and Planetary Science Letters* 87, 367-378.
- J. Guilaine, B. Gratuze, J.-N. Barrandon, 1990, Les perles de verre du Calcolithique et de l'Age du Bronze, in *Proceedings 1er Colloque de Beynac, "Le Bronze Atlantique"*, 10-14 Septembre 1990, 255-266.
- D.B. Harden, 1981, *Catalogue of Greek and Roman Glass in the British Museum, I*, London.
- I. Hartmann, K. Kappel, B. Grote, B. Arndt, 1997, Chemistry and Technology of Prehistoric Glass from Lower Saxony and Hesse, *Journal of Archaeological Sciences* 24, 547-559.

- J.W. Hayes, 1975, Roman and Pre-Roman Glass in the Royal Ontario Museum. A Catalogue, Toronto.
- J. Henderson, 1985, The Raw Materials of Early Glass Production, *Oxford Journal of Archaeology* 4, 267-291.
- J. Henderson, 1988, Glass production and Bronze Age Europe, *Antiquity* 62, 435–451.
- J. Henderson, 1993, Chemical analysis of the glass and faience from Hauterive-Champréveveres, Switzerland, in: A. M. Rychner- Faraggi (Ed.), *Hauterive Champréveveres, 9: Métal et Parure au Bronze Final*, Musée Cantonal d'Archéologie, Neuchatel.
- J. Henderson, 1996, Scientific analysis of selected Fishbourne vessel glass and its archaeological interpretation, in B. W. Cunliffe, A. G. Down, D. J. Rudkin (Eds.), *Chichester excavations IX, excavations at Fishbourne 1969-1988*, 189-192.
- J. Henderson, 2000, *The science and archaeology of materials*, Routledge, London.
- J. Henderson, 2002, Tradition and experiment in first millennium A.D. glass production - the emergence of early Islamic glass technology in late Antiquity, *Accounts of Chemical Research* 35(8), 594–602.
- J. Henderson, J. A. Evans, H. J. Sloane, M. J. Leng, C. Doherty, 2005, The use of oxygen, strontium and lead isotopes to provenance ancient glasses in the Middle East, *Journal of Archaeological Science*, 52, 655–74.
- D. J. Huisman, T. De Grot, S. Pols, B. J. H. Van Os, P. Degryse, 2009, Compositional variation in Roman colourless glass objects from the Bocholtz burial (The Netherlands), *Archaeometry* 5 (3), 413–439.
- C. Isings, 1957, *Roman Glass from Dated Finds*, Groningen-Djakarta.
- C. M. Jackson, 1996, From Roman to early Medieval glasses. Many happy returns or a new birth? in *Annales du 13e Congrès de l'Association Internationale pour l'Histoire du Verre (AIHV)*, Lochem, The Netherlands, 289–301.

- M. Jackson, L. Joyner, C.A. Booth, P.M. Day, E.C. Wager, V. Kilikoglou, 2003, Roman glass-making at Coppergate York? Analytical evidence for the nature of production, *Archaeometry* 45, 435-456.
- C. M. Jackson, 2005, Making colourless glass in the Roman period, *Archaeometry*, 47(4), 763–80.
- C. Jackson, J. Price, C. Lemke, 2006, Glass production in the 1st century AD: insights into glass technology, in K. Janssens, P. Degryse, P. Cosyns, J. Caen, L. Van't Dack (Eds.), *Annales du 17e Congrès de l'Association Internationale pour l'Histoire du Verre*, Anvers, 150-155.
- Jacoby, D., 1993, Raw materials for the glass industry of Venice and the Terraferma about 1370–about 1460, *Journal of Glass Studies* 35, 65–90.
- Kouwatli, H. H. Curvers, B. Sturt, Y. Sablerolles, J. Henderson, P. Reynolds, 2008, A pottery and glass production site in Beirut (015), *BAAL*, 10.
- M. D. Krom, R: A. Cliff, L. M. Eijsink, B. Herut, R. Chester, 199, The characterization of Saharan dusts and Nile particulate matter in surface sediments from the Levantine basin using Sr isotopes, *Marine Geology* 155, 319-330.
- S. Lahlil, I. Biron, L. Galois, G. Morin, 2006, Technological Processes to produce antimonate opacified glass through history, in K. Janssens, P. Degryse, P. Cosyns, J. Caen, L. Van't Dack (Eds.), *Annales du 17e Congrès de l'Association Internationale pour l'Histoire du Verre*, Anvers, 571-579.
- S. Lahlil, I. Biron, L. Galois, G. Morin, 2008, Rediscovering ancient glass technologies through the examination of opacifier crystals, *Applied Physics A* 92, 109–116.
- S. Lahlil, I. Biron, M. Cotte, J. Susini, 2010a, New insight on the in situ crystallization of calcium antimonate opacified glass during the Roman period, *Applied Physics A* 100, 683–692.
- S. Lahlil, I. Biron, M. Cotte, J. Susini, N. Menguy, 2010b, Synthesis of calcium antimonate nano-crystals by the 18th dynasty Egyptian glassmakers, *Applied Physics A* 98, 1–8.
- C. Lemke, 1998, Reflections of the Roman empire: the first century glass industry as seen through tradition of manufacture, in P. McCray, W.D. Kingery

- (Eds.), *The Prehistory and History of Glass and Glassmaking Technology, Ceramics and Civilisation*, vol. VIII, The American Ceramic Society, Columbus, Ohio, 269-291.
- K.A. Leslie, I.C. Freestone, D. Lowry, M. Thirlwall, 2006, Provenance and technology of near Eastern glass: oxygen isotopes by laser fluorination as a compliment to Sr, *Archaeometry* 48, 253-270.
 - C.S. Lightfoot, 1987, A Group of early Roman Mould-Blown Flasks from the West. *Journal of Glass Studies* 29: 11–18.
 - L. Mandruzzato, A. Marcante, 2005, *Vetri Antichi del Museo Archeologico Nazionale di Aquileia, Il Vasellame da Mensa, Corpus delle collezioni del Vetro nel Friuli Venezia Giulia, Comitato Nazionale Italiano AIHV.*
 - L. Mandruzzato, A. Marcante, 2007, *Vetri Antichi del Museo Archeologico Nazionale di Aquileia, Balsamari, olle e pissidi, Corpus delle collezioni del Vetro nel Friuli Venezia Giulia, Comitato Nazionale Italiano AIHV.*
 - M. A. Mange, D. T. Wright, 2007, *Heavy Minerals in Use*, vol. 58, Elsevier Science.
 - Y. A. Marano, 2009, *La città Tardoantica*, in: F. Ghedini, M. Bueno, M. Novello (Eds.), *Moenibus et portu celeberrima, Aquileia: storia di una città*, Istituto poligrafico e Zecca dello Stato, Roma, 23-33.
 - B. Mason, 1979, *Cosmochemistry, part I, Meteorites, Chapter B*, in M. Fleischer (Ed.), *Data of geochemistry, 6th edition*, US Geological Survey Prof. Paper 440-B-1.
 - J. L. Mass, R. E. Stone, M. T. Wypyski, 1998, The mineralogical and metallurgical origins of Roman opaque colored glasses, in P. McCray, W. D. Kingery (Eds.), *The prehistory and history of glassmaking technology*, The American Ceramics Society, Columbus, Ohio, 251–268.
 - J.L. Mass, M.T. Wypyski, R.E. Stone, 2002, Malkata and Lisht glassmaking technologies: towards a specific link between second millennium BC metallurgists and glassmakers, *Archaeometry* 44 (1), 67–82.
 - S.M. McLennan , 1989, REE in sedimentary rocks: influence of provenance and sedimentary processes, in B.R. Lipin, G.A. McKay (Eds.), *Geochemistry and*

Mineralogy of Rare Earth Elements, Reviews in Mineralogy 21. Mineralogical Society of America, 169-200.

- B. Messiga, M. P. Riccardi, 2001, A petrological approach to the study of ancient glass, *Periodico di Mineralogia* 70 (1), 50-70.
- Mirti, P., Casoli, A., and Appolonia, L., 1993, Scientific analysis of Roman glass from *Augusta Praetoria*, *Archaeometry* 35(2), 225–40.
- Mirti, P., Lepora, A., and Sagui, L., 2000, Scientific analysis of seventh-century glass fragments from the Cripta Balbi in Rome, *Archaeometry*, 42(2), 359-374.
- P. Mirti, P. Davit, M. Gulmini, 2002, Colourants and opacifiers in seventh and eighth century glass investigated by spectroscopic techniques, *Analytical and Bioanalytical Chemistry* 372, 221–229.
- P. Mirti, M. Pace, M. Negro Ponzi, M. Aceto, 2008, ICP–MS analysis of glass fragments of Parthian and Sasanian epoch from Seleucia and Veh Ardašīr (Central Iraq), *Archaeometry* 50, 429-50.
- P. Mirti, M. Pace, M. Malandrino, M. Negro Ponzi, 2009, Sasanian glass from Veh Ardašīr: new evidences by ICP-MS analysis, *Journal of Archaeological Science* 36, 1061-1069.
- C. Moretti, 2002, *Glossario del vetro veneziano*, Venezia.
- M. D. Nenna, M. Vichy, M. Picon, 1997, L’Atelier de verrier de Lyon, du Ier siècle après J.-C., et l’origine des verres “Romains”, *Revue d’Archéométrie* 21, 81-87.
- M. D. Nenna, M. Picon, M. Vichy, 2000, Ateliers primaires et secondaires en Égypte à l’époque gréco-romaine, in M. D. Nenna (ed.), *La route du verre. Ateliers primaires et secondaires du second millénaire av. J.-C. au Moyen Âge*, Travaux de la Maison de l’Orient Méditerranéen no. 33, Lyon, 97–112.
- M. D. Nenna, M. Picon, V. Thirion-Merle, M. Vichy, 2005, Ateliers primaire du Wadi Natrun: nouvelles decouvertes, *Annales du 16e Congres de l’association Internationale pour l’Histoire du Verre*, 59-63.
- R.G. Newton, 1985, The durability of glass: a review, *Glass Technology* 26, 21-38.
- R. Newton, S. Davison, 1996, *Conservation of glass*, Butterworth-Heinemann, Oxford.

- A.L. Oppenheim, 1973, Towards a history of glass in the Ancient Near East, *Journal of the American Oriental Society* 93, 259-266.
- S. Paynter, 2006, Analyses of colourless Roman glass from Binchester, County Durham, *Journal of Archaeological Science* 33, 1037-1057.
- M. Picon, M. Vichy, 2003, D'Orient en Occident: l'origine du verre à l'époque romaine et durant le haut Moyen Âge, in D. Foy, M.D. Nenna (Eds.), *Échanges et commerce du verre dans le monde antique*, Actes du colloque de l'Association Française pour l'Archéologie du Verre, Aix-en-Provence et Marseille, 7-9 juin 2001, éditions Monique Mergoil, Montagnac, 17-31.
- C. Pin, D. Briot, C. Bassin, F. Poitrasson, 1994, Concomitant separation of strontium and samarium-neodymium for isotopic analysis in silicate samples, based on specific extraction chromatography, *Analytica Chimica Acta*, 209-217.
- C. Pin, J.F.S. Zalduegui, 1997, Sequential separation of light rare-earth elements, thorium and uranium by miniaturized extraction chromatography: application to isotopic analyses of silicate rocks, *Analytica Chimica Acta* 339 (1-2), 79-89.
- A.M. Pollard, C. Heron, 1995, *Archaeological Chemistry*, Royal Society of Chemistry, 149-195.
- M. Pomerancblum, 1966, The distribution of heavy minerals and their hydraulic equivalents of the Mediterranean continental shelf of Israel, *Journal of Sedimentary Petrology* 36, 162-174.
- J. Price, 1991, Decorated Mould-Blown Glass Tablewares in the First century AD. In M. Newby & K. Painter (eds.), *Roman Glass: Two Centuries of Art and Invention*. pp. 56–75. The Society of Antiquaries of London, London.
- T. Rehren, E.B. Pusch, 2005, Late Bronze Age Egyptian glass production at Qantir-Piramesses, *Science* 308, 1756-1760.
- N. Rigoni, 1986, I materiali, in G. Rosada (Ed.), *Progetto Rocca: lo scavo 1985*, *Quaderni di Archeologia del Veneto*, II, Giunta Regionale del Veneto, Venezia, 39-69.
- Rosada, 1989, Asolo. Progetto Rocca: lo scavo 1987-1988, in G. Rosada (Ed.) *Indagini archeologiche ad Asolo, scavi nella Rocca Medievale e nel Teatro romano*, CEDAM, Padova, 66-69.

- B. Rütli, 1991, Die römischen Gläser aus Augst und Kaiseraugst, Augst.
- D.C.W. Sanderson, J.R. Hunter, S.E. Warren, 1984, Energy dispersive X-ray fluorescence analysis of 1st millennium AD glass from Britain, *Journal of Archaeological Science* 11(1), 53-69.
- Santagostino Barbone, E. Gliozzo, F. D'Acapito, I. Memmi Turbanti, M. Turchiano, G. Volpe, 2008, The Sectilia panels of Faragola (Ascoli Satriano Southern Italy): a multi-analytical study of the red, orange and yellow glass slabs, *Archaeometry* 50, 451–473.
- P. Santropadre, M. Verità, 2000, Analyses of the Production of Italian Vitreous Materials of the Bronze Age, *Journal of Glass Studies* 42, 25-40.
- E.V. Sayre, R.V. Smith, 1961, Compositional categories of ancient glass, *Science* 133, 1824-1826.
- E. V. Sayre, 1963, The intentional use of antimony and manganese in ancient glasses, in F. R. Matson, G. Rindone (Eds.), *Advances in glass technology*, part 2, Plenum Press, New York, 263–82.
- J.W.H. Schreurs, R.H. Brill, 1984, Iron and sulfur related colors in ancient glasses, *Archaeometry* 26, 199-209.
- A.J. Shortland, 2002, The use and origin of antimonate colorants in early Egyptian glass, *Archaeometry* 44 (4), 517–530.
- A. J. Shortland, 2003, Comments on J.L. Mass, M.T. Wypyski and R.E. Stone 'Malkata and Lisht glassmaking technologies: towards a specific link between the second millennium BC metallurgists and glassmakers', *Archaeometry* 44 (1), 67–82. Reply (2002) *Archaeometry* 45(1), 190–191.
- J. Shortland, 2004, Evaporites of the Wadi Natrun: seasonal and annual variation and its implication for ancient exploitation, *Archaeometry* 46, 497-516.
- J. Shortland, T. Schachner, I. C. Freestone, M. Tite, 2006, Natron as a flux in the early vitreous materials industry-sources, beginnings and reasons for decline, *Journal of Archaeological Science* 33(4), 521-530.
- A. J. Shortland, N. Rogers, K., Eremin, 2007, Trace element discriminants between Egyptian and Mesopotamian late Bronze Age glasses, *Journal of Archaeological Science* 34, 781-789.

- A. Silvestri, G. Molin, G. Salviulo, 2005, Roman and Medieval glass from the Italian area: bulk characterization and relationships with production technologies, *Archaeometry* 47, 797-816.
- A. Silvestri, 2008, The coloured glass of Iulia Felix. *Journal of Archaeological Science* 35, 1489-1501.
- Silvestri, G. Molin, G. Salviulo, 2008, The colourless glass of Iulia Felix, *Journal of Archaeological Science* 35, 331-341.
- A. Silvestri, A. Longinelli, G. Molin, 2010, $\delta^{18}\text{O}$ measurements of archaeological glass (Roman to Modern age) and raw materials: possible interpretation, *Journal of Archaeological Science* 37, 549–560.
- A. Silvestri, A. Marcante, 2011, The glass of Nogara (Verona): a “window” on production technology of mid-Medieval times in Northern Italy, *Journal of Archaeological Science* 38 (10), 2509-2522.
- C. Sotinel, 2001, L’utilisation des ports dans l’arc Adriatique à l’Époque Tardive (IV^e-VI^e siècles), in *Strutture portuali e rotte marittime nell'adriatico di età romana*, École Française de Rome, Trieste-Roma.
- D. J. Stanley, Y. Mart, Y. Nir, 1997, Clay mineral distributions to interpret Nile cell provenance and dispersal: II. Coastal plain from Nile delta to northern Israel, *Journal of Coastal Research*, 13, 506–33.
- J. D. Stanley, M.D. Krom, R.A. Cliff, J.C. Woodward, 2003, Nile flow failure at the end of the Old Kingdom, Egypt: strontium isotopic evidence, *Geoarchaeology* 18, 395-402.
- E.M. Stern, B. Schlick-Nolte, 1994, *Early Glass of the Ancient World 1600 BC – AD 50 Ernesto Wolfe Collection*, Verlag Hatje, Ostfildern, Germany.
- M. Sternini, 1995, *La fenicie di sabbia. Storia e tecnologia del vetro antico*, Edipuglia, Bari.
- D. Stiaffini, 1991, Contributo ad una prima sistemazione tipologica dei materiali vitrei medievali, in M. Mendera (Ed.), *Archeologia e storia del vetro preindustriale*, Atti del Convegno Internazionale, Colle Val d’Elsa-Gambassi, April 2-4 1990, Firenze, 177-266.

- D. Stiaffini, 1999, L'evoluzione morfologica del vasellame vitreo da mensa durante il Rinascimento. L'esempio della Toscana, *Archeologia Postmedievale* 3, 151-186.
- O. Tal, R. E. Jackson-Tal, I. C. Freestone, 2004, New Evidence of the production of raw glass at Late Byzantine Apollonia-Arsuf (Israel), *Journal of glass studies* 46, 51-66.
- M.F. Thirlwall, 1991, Long-term reproducibility of multicollector Sr and Nd isotope ratio analysis, *Chemical Geology* 94, 85-104.
- M. S. Tite, A. Shortland, Y. Maniatis, D. Kavoussanaki, S. A. Harris, 2006, The composition of the soda-rich and mixed alkali plant ashes used in the production of glass, *Journal of Archaeological Science* 33(9), 1284-1292.
- M. S. Tite, T. Pradell, A. J. Shortland, 2008, Discovery, production and use of tin-based opacifiers in glasses, enamels and glazes from the Late Iron Age onwards: a reassessment, *Archaeometry* 50, 67-84.
- Toniolo, 2007, Il vetro nell'Alto Adriatico, in D. Ferrari, A.M. Visser Travagli (Eds.), *Atti delle IX Giornate Nazionali di Studio AIHV*, Ferrara, 57-70.
- S. Tonietto, 2010, Indagini archeometriche sul mosaico paleocristiano a tessere vitree del sacello di S. Prodocimo (Padova). Caratterizzazione chimico-fisica e cristallografia dei materiali mediante metodiche analitiche micro-e non distruttive, Università di Padova, unpublished PhD thesis.
- P. Triantafyllidis, 2003, Classical and Hellenistic workshop from Rhodes, in D. Foy, M.D. Nenna (Eds.), *Echanges et commerce du verre dans le monde antique. Actes du colloque AHIV, Aix-en-Provence et Marseille 2001*. Mergoil Editor, Montagnac, 131-138.
- W. E. S. Turner, 1956, Studies in ancient glasses and glass-making processes. Part V. Raw materials and melting processes, *Journal of the Society of Glass Technology* 40, 276-300.
- M. Uboldi, M. Verità, 2003, Scientific analyses of glasses from late antique and early medieval archaeological sites in Northern Italy, *Journal of Glass Studies* 45, 115-37.
- M. Vallotto, M. Verità, 2000, Glasses from Pompeii and Herculaneum and the sands of the rivers Belus and Volturno, in J Renn, G. Castagnetti (Eds.), *Homo*

faber: studies on nature, technology and science at the time of Pompeii, presented at a conference at the Deutsches Museum, Munich, 21–22 March 2000, 63–73, 'L'Erma' di Bretschneider.

- V. Van Der Linden, P. Cosyns, O. Schalm, S. Cagno, K. Nys, K. Janssens, A. Nowak, B. Wagner, E. Bulska, 2009, Deeply coloured and black glass in the northern provinces of the roman Empire: differences and similarities in chemical composition before and after AD 150, *Archaeometry* 51 (5), 822–844.
- Van der Werf, A. Mangone, L. Carla Giannossa, A. Traini, R. Laviano, A. Coralini, L. Sabbatini, 2009, Archaeometric investigation of Roman tesserae from Herculaneum (Italy) by the combined use of complementary micro-destructive analytical techniques, *Journal of Archaeological Science* 36, 2625–2634.
- M. Verità, 1985, L'invenzione del cristallo Muranese: una verifica analitica delle fonti storiche, *Rivista della Stazione Sperimentale del Vetro* 1, 117–36.
- M. Verità, 2000, Tecniche di fabbricazione dei materiali musivi vitrei, *Indagini chimiche e mineralogiche*, in E. Borsook, F. Giuffredi Superbi, G. Pagliarulo (Eds.), *Medieval mosaics, light, color, materials*, Silvana Editoriale, Cinisello Balsamo, 25.34.
- M. Verità, A. Renier, S. Zecchin, 2002, Chemical analyses of ancient glass findings excavated in the Venetian lagoon, *Journal of Cultural Heritage* 3, 261–71.
- M. Verità, S. Zecchin, 2009, Thousand years of Venetian glass: the evolution of chemical composition from the origins to the 18th century, in K. Janssens, P. Degryse, P. Cosyns, J. Caen, L. Van't Dack (Eds.), *Annales du 17e Congrès de l'Association Internationale pour l'Histoire du Verre*, Anvers, 602-613.
- E.P. Vicenzi, S. Eggins, A. Logan, R. Wysoczanski, 2002. Microbeam characterization of Corning archaeological reference glasses: new additions to the Smithsonian microbeam standard collection, *Journal of Research of the National Institute of Standards and Technology* 107, 719-727.
- K. H. Wedepohl, 1971, *Geochemistry*, New York: Holt Rinehart and Winston.
- K. H. Wedepohl, 1995, The composition of the continental crust, *Geochimica et Cosmochimica Acta* 59, 1217–1232.

- K. H. Wedepohl, A. Baumann, 2000, The use of marine molluscan shells for Roman glass and local raw glass production in the Eifel area (Western Germany), *Naturwissenschaften*, 87, 129–32.
- K. H. Wedepohl, W. Gaitzsch, A. B. Follmann-Schulz, 2003, Glassmaking and glassworking in six Roman factories in the Hambach Forest, Germany, *Annales du 15e Congres de l'Association Internationale de l'Histoire du Verre AIHV*, 53-55.
- K. H. Wedepohl, K. Simon, A. Kronz, 2011, Data on 61 chemical elements for the characterization of three major glass compositions in Late Antiquity and the Middle Ages, *Archaeometry* 53(1), 81–102.
- S. Weldeab, K.C. Emeis, C. Hemleben, W. Siebel, 2002, Provenance of lithogenic surface sediments and pathways of riverine suspended matter in the eastern Mediterranean Sea: evidence from $^{143}\text{Nd}/^{144}\text{Nd}$ and $^{87}\text{Sr}/^{86}\text{Sr}$ ratios, *Chemical Geology* 186, 139-149.
- D. Whitehouse, 1988, *Glass of the Roman Empire*. Corning Museum of Glass, Corning, NY.
- S. Wolf, C. M. Kessler, W. B. Stern, Y. Gerber, 2005, The composition and manufacture of early Medieval coloured window glass from Sion (Valais, Switzerland) – a Roman glass making tradition or innovative craftsmanship?, *Archaeometry* 47(2), 361-380.
- C. Zaccaria, S. Pesavento Mattioli, 2009, Uomini e merci, in: F. Ghedini, M. Bueno, M. Novello (Eds.), *Moenibus et portu celeberrima, Aquileia: storia di una città*, Istituto poligrafico e Zecca dello Stato, Roma, 275-287.
- L. Zecchin, 1956, *I vetri del Museo di Adria*, Venezia.

APPENDIX A

In this Appendix the features (colour, type, age, production technique, provenance) of all the samples analyzed in the present study are reported. In addition, some pictures of the most representative colours/types are also shown.

LABEL	PROVENANCE	OBJECT	TYPE	AGE	COLOUR	PRODUCTION TECHNIQUE
AD-NF-1	Adria	Aryballos	Harden 1981, group 1, form 2	5th cent. BC	Blue, yellow, light blue and brown	Core-formed
AD-NF-2	Adria	n.i	Harden 1981, group 3	2nd cent. BC	Blue, yellow and white	Core-formed
AD-NF-3	Adria	Amphoriskos	Harden 1981, group 1, 2	5th cent. BC	Blue and white	Core-formed
AD-NF-4	Adria	Aryballos	Harden 1981, group 2	6th-5th cent. BC	Blue and yellow	Core-formed
AD-NF-5	Adria	Aryballos	n.i.	6th-5th cent. BC	Blue, yellow, light blue and white	Core-formed
AD-NF-6	Adria	Oinochoe	Harden 1981, group 2, 3	Late 4th cent. BC	Blue, yellow and white	Core-formed
AD-NF-7	Adria	Oinochoe	Harden 1981, group 2, 3	3rd cent. BC	Blue, yellow	Core-formed
AD-A-1	Adria	Cup	Isings 1957, form 25	Late 1st cent. BC-early 1st cent. AD	Light blue	Casting
AD-A-2	Adria	Cup	Isings 1957, form 3	First half 1st cent. AD	Light blue	Ribbing
AD-A-3	Adria	Cup	Isings 1957, form 3	First half 1st cent. AD	Light blue	Ribbing
AD-A-4	Adria	Cup	Isings 1957, form 3	First half 1st cent. AD	Light blue	Ribbing
AD-A-5	Adria	Cup	Isings 1957, form 3	First half 1st cent. AD	Light blue	Ribbing
AD-A-6	Adria	Cup	Isings 1957, form 3	First half 1st cent. AD	Light blue	Ribbing
AD-A-7	Adria	Cup	Isings 1957, form 3	First half 1st cent. AD	Light blue	Ribbing
AD-A-8	Adria	Jar	Isings 1957, form 64	Second half 1st-early 2nd cent. AD	Light blue	Blowing
AD-A-9	Adria	Jar	probably Isings form 67a	Second half 1st-early 2nd cent. AD	Light blue	Blowing
AD-A-10	Adria	Jar	Isings 1957, form 66	Second half 1st-early 2nd cent. AD	Light blue	Blowing
AD-A-11	Adria	Cup	Isings 1957, form 12	1st cent. AD	Light blue	Blowing
AD-VC-1	Adria	Toilet bottle	Isings 1957, form 101/104	2nd-4th cent. AD	Light green	Blowing
AD-VC-2	Adria	Bottle	Isings 1957, form 50/51	1st-3rd cent. AD	Light green	Blowing
AD-I-1	Adria	Cup	Hayes 1975, 3.42	1st cent. AD	Colourless	Casting

AD-I-2	Adria	Cup	Rutti 1991, 61	2nd cent. AD	Colourless	Blowing
AD-I-3	Adria	Cup	Isings 1957, form 96a	3rd cent. AD	Colourless	Blowing
AD-I-4	Adria	Cup	Isings 1957, form 42/Limburg	2nd cent. AD	Colourless	Mold Blowing
AD-I-5	Adria	Cup	ni	2nd-3rd cent. AD	Colourless	Blowing
AD-I-6	Adria	Cup	Isings 1957, form 42/Limburg	2nd cent. AD	Colourless	Mold Blowing
AD-V-1	Adria	Toilet bottle	Probably Isings 1957, form 6	First half 1st cent. AD	Purple	Blowing
AD-V-2	Adria	Probably jar	ni	1st cent. AD	Purple	Blowing
AD-V-3	Adria	Toilet bottle	ni	1st cent. AD	Purple	Blowing
AD-V-4	Adria	Jar	Jar	Late 1st cent. AD	Purple	Blowing
AD-VE-1	Adria	Cup	Isings 1957, form 3	Early 1st cent. AD	Olive green	Ribbing
AD-VE-2	Adria	Probably plate	ni	First half 1st cent. AD	Green	Casting
AD-VE-3	Adria	Plate	Isings 1957, form 46a	Second half 1st-First half 2nd cent. AD	Emerald green	Blowing
AD-VE-4	Adria	Plate	Isings 1957, form 46a	Second half 1st-First half 2nd cent. AD	Emerald green	Blowing
AD-B-1	Adria	Beaker	Isings 1957, form 29/30	1st cent. AD	Blue	Blowing
AD-B-2	Adria	Cup	Isings 1957, form 2	First half 1st cent. AD	Blue	Casting
AD-B-3	Adria	Cup	Isings 1957, form 1/18,3	First half 1st cent. AD	Blue	Casting
AD-B-4	Adria	Plate	Isings 1957, form 46a	Second half 1st-Early 2nd cent. AD	Blue	Blowing
AD-B-5	Adria	Glass chunk	-	-	Blue	-
AD-B-6	Adria	Cup	Isings 1957, form 2	1st cent. AD	Blue	Casting
AD-B-7	Adria	Cup	Isings 1957, form 3	1st cent. AD	Blue	Ribbing
AD-B-8	Adria	Ewer	Isings 1957, form 13	Half 1st cent. AD	Blue	Blowing
AD-B-9	Adria	Cup	Isings 1957, form 12	1st cent. AD	Blue	Blowing

AD-B-10	Adria	Cup	Isings 1957, form 12	1st cent. AD	Blue	Blowing
AD-B-11	Adria	Cup	Isings 1957, form 12	1st cent. AD	Blue	Blowing
AD-AM-1	Adria	Cup	Isings 1957, form 3	1st cent. AD	Amber	Ribbing
AD-AM-2	Adria	Ewer	Isings 1957, form 13	1st cent. AD	Amber	Blowing
AD-N-1	Adria	Dish	ni	Early 1st cent. AD	Black	Casting
AD-BB-1	Adria	Cup	Isings 1957, form 3	First half 1st cent. AD	Blue, light blue and white decorations	Sagging glass with former molds
AD-BB-2	Adria	Cup	Isings 1957, form 3	First half 1st cent. AD	Blue and white	Sagging glass with former molds
AD-BB-3	Adria	Probably jar	ni	1st cent. AD	Blue and white	Blowing
AD-VB-1	Adria	Cup	Isings 1957, form 3	Early 1st cent. AD	Purple and white	Sagging glass with former molds
AD-AB-1	Adria	Ewer	Isings 1957, form 13	Half 1st cent. AD	Amber and white	Blowing
AD-AB-2	Adria	Toilet bottle	De Tommaso 1990, 1	Half 1st cent. AD	Amber and white	Blowing
AD-AB-3	Adria	Toilet bottle	De Tommaso 1990, 1	1st-2nd cent. AD	Amber and white	Blowing
AD-AB-4	Adria	Toilet bottle	Mandruzzato and Marcante 2007, n° cat. 127-128	1st cent. AD	Amber and white	Blowing
AD-AB-5	Adria	Probably jar	ni	1st-2nd cent. AD	Amber and white	Blowing
AD-AB-6	Adria	Probably jar	ni	1st-2nd cent. AD	Amber and white	Blowing
AD-P-1	Adria	Cup	Probably Isings 1957, form 42	1st cent. AD	Light blue with wisteria rim	Blowing
AD-ABP-1	Adria	Probably jar	ni	1st-2nd cent. AD	Amber and white	Blowing
AD-BO-1	Adria	Dish	Grose 1991, p. 9, Tav. IIIe	Early 1st cent. AD	Opaque white	Casting
AD-BO-2	Adria	Ewer	Isings 1957, form 13-14	1st cent. AD	Opaque white	Sagging glass with former molds
AD-BO-3	Adria	Cup	ni	1st cent. AD	Opaque white	Blowing
AD-BLO-1	Adria	Toilet bottle	Probably Isings 1957, form 13/14	1st cent. AD	Opaque blue	Blowing
AD-R-1	Adria	Cup	Isings 1957, form 1/18	1st cent. AD	Colourless with blue and white trails	Reticella Glass

AD-R-2	Adria	Cup	Isings 1957, form 1/18	1st cent. AD	Colourless with white trails	Reticella Glass
AD-BG-1	Adria	Cup	Isings 1957, form 1	First half 1st cent. AD	Emerald green and yellow	Sagging glass with former molds
AD-AG-1	Adria	Probably cup	n.i.	1st cent. AD	Light blue and yellow	Blowing

Table A.1: *list of the analyzed samples from Adria.*

SAMPLE	PROVENANCE	OBJECT	TYPE	AGE (cent. AD)	COLOUR	PRODUCTION TECHNIQUE
AQ106-1	Aquileia	Beaker	Isings 1957, form 106c	Late 3rd-early 5th century AD	Green	Mold-Blowing
AQ106-2	Aquileia	Beaker	Isings 1957, form 106c	Late 3rd-early 5th century AD	Green	Mold-Blowing
AQ106-3	Aquileia	Beaker	Isings 1957, form 106c	Late 3rd-early 5th century AD	Green	Mold-Blowing
AQ106-4	Aquileia	Beaker	Isings 1957, form 106c	Late 3rd-early 5th century AD	Light blue	Mold-Blowing
AQ106-5	Aquileia	Beaker	Isings 1957, form 106c	Late 3rd-early 5th century AD	Green	Mold-Blowing
AQ106-6	Aquileia	Beaker	Isings 1957, form 106c	Late 3rd-early 5th century AD	Yellow	Mold-Blowing
AQ106-7	Aquileia	Beaker	Isings 1957, form 106c	Late 3rd-early 5th century AD	Yellow	Mold-Blowing
AQ106-8	Aquileia	Beaker	Isings 1957, form 106c	Late 3rd-early 5th century AD	Green	Mold-Blowing
AQ106-9	Aquileia	Beaker	Isings 1957, form 106c	Late 3rd-early 5th century AD	Green	Mold-Blowing
AQ106-10	Aquileia	Beaker	Isings 1957, form 106c	Late 3rd-early 5th century AD	Green	Mold-Blowing
AQ106-11	Aquileia	Beaker	Isings 1957, form 106c	Late 3rd-early 5th century AD	Light blue	Mold-Blowing
AQ106-12	Aquileia	Beaker	Isings 1957, form 106c	Late 3rd-early 5th century AD	Light blue	Mold-Blowing
AQ106-13	Aquileia	Beaker	Isings 1957, form 106c	Late 3rd-early 5th century AD	Light blue	Mold-Blowing
AQ106-14	Aquileia	Beaker	Isings 1957, form 106c	Late 3rd-early 5th century AD	Light blue	Mold-Blowing
AQ106-15	Aquileia	Beaker	Isings 1957, form 106c	Late 3rd-early 5th century AD	Light blue	Mold-Blowing
AQ106-16	Aquileia	Beaker	Isings 1957, form 106c	Late 3rd-early 5th century AD	Light blue	Mold-Blowing
AQ106-17	Aquileia	Beaker	Isings 1957, form 106c	Late 3rd-early 5th century AD	Light blue	Mold-Blowing
AQ106-18	Aquileia	Beaker	Isings 1957, form 106c	Late 3rd-early 5th century AD	Green	Mold-Blowing
AQ106-19	Aquileia	Beaker	Isings 1957, form 106c	Late 3rd-early 5th century AD	Green	Mold-Blowing
AQ106-20	Aquileia	Beaker	Isings 1957, form 106c	Late 3rd-early 5th century AD	Green	Mold-Blowing
AQ106-21	Aquileia	Beaker	Isings 1957, form 106c	Late 3rd-early 5th century AD	Light blue	Mold-Blowing
AQ116-1	Aquileia	Cup	Isings 1957, form 116	3rd-4th century AD	Light blue	Mold-Blowing
AQ116-2	Aquileia	Cup	Isings 1957, form 116	3rd-4th century AD	Colourless/Yellow	Mold-Blowing
AQ116-3	Aquileia	Cup	Isings 1957, form 116	3rd-4th century AD	Colourless/Yellow	Mold-Blowing
AQ116-4	Aquileia	Cup	Isings 1957, form 116	3rd-4th century AD	Green	Mold-Blowing
AQ116-5	Aquileia	Cup	Isings 1957, form 116	3rd-4th century AD	Colourless/Green	Mold-Blowing
AQ116-6	Aquileia	Cup	Isings 1957, form 116	3rd-4th century AD	Green	Mold-Blowing
AQ116-7	Aquileia	Cup	Isings 1957, form 116	3rd-4th century AD	Colourless/Green	Mold-Blowing
AQ116-8	Aquileia	Cup	Isings 1957, form 116	3rd-4th century AD	Green	Mold-Blowing
AQ117-1	Aquileia	Cup	Isings 1957, form 117	3rd-4th century AD	Light blue	Mold-Blowing
AQ117-2	Aquileia	Cup	Isings 1957, form 117	3rd-4th century AD	Yellow	Mold-Blowing
AQ117-3	Aquileia	Cup	Isings 1957, form 117	3rd-4th century AD	Green	Mold-Blowing
AQ117-4	Aquileia	Cup	Isings 1957, form 117	3rd-4th century AD	Green	Mold-Blowing
AQ117-5	Aquileia	Cup	Isings 1957, form 117	3rd-4th century AD	Green	Mold-Blowing
AQ-61	Aquileia	Lamp			Green	Mold-Blowing
AQ117-7	Aquileia	Cup	Isings 1957, form 117	3rd-4th century AD	Green	Mold-Blowing
AQ132-1a	Aquileia	Cylindrical bottle	Isings 1957, form 132	3rd-4th century AD	Green	Blowing
AQ132-1b	Aquileia	Cylindrical bottle	Isings 1957, form 132	3rd-4th century AD	Yellow	Blowing
AQ104-2	Aquileia	Bottle	Isings 1957, form 104	3rd-4th century AD	Yellow	Blowing
AQ104-3	Aquileia	Bottle	Isings 1957, form 104	3rd-4th century AD	Yellow	Blowing
AQ104-4	Aquileia	Bottle	Isings 1957, form 104	3rd-4th century AD	Green	Blowing
AQ104-5	Aquileia	Bottle	Isings 1957, form 104	3rd-4th century AD	Green	Blowing

AQ104-6	Aquileia	Bottle	Isings 1957, form 104	3rd-4th century AD	Yellow/Green	Blowing
AQ104-7	Aquileia	Bottle	Isings 1957, form 104	3rd-4th century AD	Yellow/Green	Blowing
AO/cfm-1	Aquileia	Cup	Isings 1957, form 87 or form 120	3rd-4th century AD	Green	Blowing
AQ/cfm-2	Aquileia	Cup	Isings 1957, form 87 or form 120	3rd-4th century AD	Green	Blowing
AO/cfm-3	Aquileia	Cup	Isings 1957, form 87 or form 120	3rd-4th century AD	Green	Blowing
AQ/cfm-4v	Aquileia	Cup	Isings 1957, form 87 or form 120	3rd-4th century AD	Green	Blowing
AO/cfm-4b	Aquileia	Cup	Isings 1957, form 87 or form 120	3rd-4th century AD	Light blue	Blowing
AQ/cfm-5	Aquileia	Cup	Isings 1957, form 87 or form 120	3rd-4th century AD	Green	Blowing
AQ/cfm-6	Aquileia	Cup	Isings 1957, form 87 or form 120	3rd-4th century AD	Green	Blowing
AQ111-1	Aquileia	Beaker	Isings 1957, form 111	Second half 5th to 8th century AD	Green	Blowing
AQ111-2	Aquileia	Beaker	Isings 1957, form 111	Second half 5th to 8th century AD	Light blue	Blowing
AQ111-3	Aquileia	Beaker	Isings 1957, form 111	Second half 5th to 8th century AD	Light blue	Blowing
AQ111-4	Aquileia	Beaker	Isings 1957, form 111	Second half 5th to 8th century AD	Green	Blowing
AQ111-5	Aquileia	Beaker	Isings 1957, form 111	Second half 5th to 8th century AD	Light blue	Blowing
AQ111-6	Aquileia	Beaker	Isings 1957, form 111	Second half 5th to 8th century AD	Light blue	Blowing
AQ111-7	Aquileia	Beaker	Isings 1957, form 111	Second half 5th to 8th century AD	Light blue	Blowing
AQ111-8	Aquileia	Beaker	Isings 1957, form 111	Second half 5th to 8th century AD	Green	Blowing
AQ111-9	Aquileia	Beaker	Isings 1957, form 111	Second half 5th to 8th century AD	Green	Blowing
AQ111-10	Aquileia	Beaker	Isings 1957, form 111	Second half 5th to 8th century AD	Light blue	Blowing
AQ111-11	Aquileia	Beaker	Isings 1957, form 111	Second half 5th to 8th century AD	Light blue	Blowing

Table A.2: List of the analyzed samples from Aquileia.

SAMPLE	PROVENANCE	OBJECT	TYPE	AGE (century AD)	COLOUR	PRODUCTION TECHNIQUE
SG111-1	San Genesio	Beaker	Isings 1957, form 111	Late 5th-8th	Light blue	Blowing
SG111-2	San Genesio	Beaker	Isings 1957, form 111	Late 5th-8th	Light blue	Blowing
SG111-3	San Genesio	Beaker	Isings 1957, form 111	Late 5th-8th	Yellow	Blowing
SG111-4	San Genesio	Beaker	Isings 1957, form 111	Late 5th-8th	Colourless	Blowing
SG111-5	San Genesio	Beaker	Isings 1957, form 111	Late 5th-8th	Yellow	Blowing
SG111-6	San Genesio	Beaker	Isings 1957, form 111	Late 5th-8th	Light blue	Blowing
SG106-1	San Genesio	Beaker	Isings 1957, form 106c	4th-early 5th	Green	Mold Blowing
PP111-1	Pieve di Pava	Beaker	Isings 1957, form 111	Late 5th-8th	Light blue	Blowing
PP111-2	Pieve di Pava	Beaker	Isings 1957, form 111	Late 5th-8th	Green	Blowing
PP111-3	Pieve di Pava	Beaker	Isings 1957, form 111	Late 5th-8th	Green	Blowing
PP111-4	Pieve di Pava	Beaker	Isings 1957, form 111	Late 5th-8th	Green	Blowing
PP111-5	Pieve di Pava	Beaker	Isings 1957, form 111	Late 5th-8th	Colourless/Yellow	Blowing
PC111-1	Pieve di Conèo	Beaker	Isings 1957, form 111	Late 5th-8th	Light blue	Blowing
PC111-2	Pieve di Conèo	Beaker	Isings 1957, form 111	Late 5th-8th	Green	Blowing
PC111-3	Pieve di Conèo	Beaker	Isings 1957, form 111	Late 5th-8th	Light blue	Blowing

Table A.3: List of the analyzed samples from Tuscan sites (San Genesio, Pieve di Pava and Pieve di Conèo).

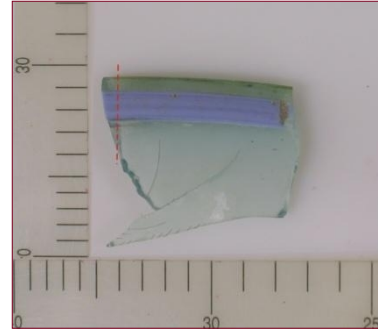
SAMPLE	PROVENANCE	OBJECT	TYPE	AGE (cent. AD)	COLOUR	PRODUCTION TECHNIQUE
ASL-01	Rocca di Asolo	Glass pane	-	7th-10th	Light blue	Cylinder process
ASL-02	Rocca di Asolo	Glass pane	-	7th-10th	Yellowish-brown	Cylinder process
ASL-03	Rocca di Asolo	Glass pane	-	7th-10th	Green	Cylinder process
ASL-04	Rocca di Asolo	Glass pane	-	7th-10th	Yellowish-brown	Cylinder process
ASL-05	Rocca di Asolo	Glass pane	-	7th-10th	Yellowish-brown	Cylinder process
ASL-06	Rocca di Asolo	Glass pane	-	7th-10th	Yellowish-brown	Cylinder process
ASL-07	Rocca di Asolo	Glass pane	-	7th-10th	Green	Cylinder process
ASL-08	Rocca di Asolo	Glass pane	-	7th-10th	Light blue	Cylinder process
ASL-09	Rocca di Asolo	Glass pane with circular shape	'Ruo'	15th	Yellowish-brown	Crown process
ASL-10	Rocca di Asolo	Glass pane with triangular shape	'Crossetta'	15th	Yellowish-brown	Crown process
ASL-11	Rocca di Asolo	Glass pane with triangular shape	'Crossetta'	15th	Yellowish-brown	Crown process
ASL-12	Rocca di Asolo	Glass pane with triangular shape	'Crossetta'	15th	Yellowish-brown	Crown process
ASO-01	Rocca di Asolo	Beaker	Nuppenbecher	13th-14th	Colourless	-
ASO-02	Rocca di Asolo	Beaker	Nuppenbecher	13th-14th	Light blue	-
ASO-03	Rocca di Asolo	Beaker	Nuppenbecher	13th-14th	Yellowish	-
ASO-04	Rocca di Asolo	Beaker	Nuppenbecher	13th-14th	Yellowish-green	-
ASO-05	Rocca di Asolo	Beaker	Nuppenbecher	13th-14th	Colourless	-
ASO-06	Rocca di Asolo	Bottle	Kropfflasche	13th-14th	Green	-
ASO-07	Rocca di Asolo	Bottle	Kropfflasche	13th-14th	Green	-
ASO-08	Rocca di Asolo	Bottle	Kropfflasche	12th	Light blue	-
ASO-09	Rocca di Asolo	Bottle	Kropfflasche	13th-15th	Green	-
ASO-10	Rocca di Asolo	Bottle	Kropfflasche	13th-15th	Green	-
ASO-11	Rocca di Asolo	Bottle	Kropfflasche	13th-15th	Green	-
ASO-12	Rocca di Asolo	Bottle	Anghistera	12th-15th	Light blue	-
ASO-13	Rocca di Asolo	Bottle	Anghistera	12th-15th	Yellowish-green	-
ASO-14	Rocca di Asolo	Bottle	Anghistera	15th-16th	Yellowish-green	-
ASO-15	Rocca di Asolo	Bottle	Anghistera	13th-15th	Yellowish-green	-
ASO-16	Rocca di Asolo	Bottle	Anghistera	13th-15th	Green	-
ASO-17	Rocca di Asolo	Beaker	-	14th-15th	Colourless, blue rim	-
ASO-18	Rocca di Asolo	Beaker	-	14th-15th	Colourless, blue rim	-
ASO-19	Rocca di Asolo	Beaker	-	14th-15th	Colourless, blue rim	-
ASO-20	Rocca di Asolo	Beaker	-	14th-15th	Colourless, blue rim	-
ASO-21	Rocca di Asolo	Beaker	-	14th-15th	Colourless, blue rim	-

Table A.4: *list of analyzed samples from Rocca di Asolo*

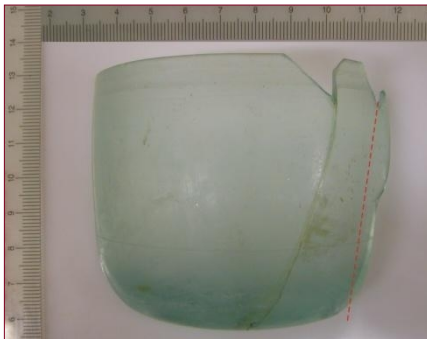
ADRIA



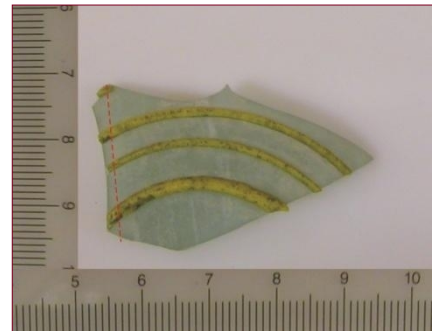
SAMPLE: AD-A-7
AGE: 1st cent. AD
COLOUR: Light blue
TYPE: Isings 3



SAMPLE: AD-P-1
AGE: 1st cent. AD
COLOUR: Light blue, wisteria
TYPE: Isings 42



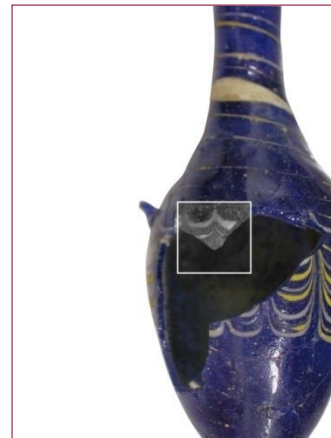
SAMPLE: AD-A-11
AGE: 1st cent. AD
COLOUR: Light blue
TYPE: Isings 12



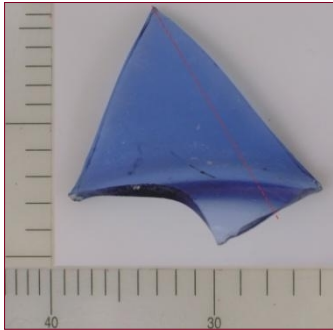
SAMPLE: AD-AG-1
AGE: 1st cent. AD
COLOUR: Light blue, yellow
TYPE: ni



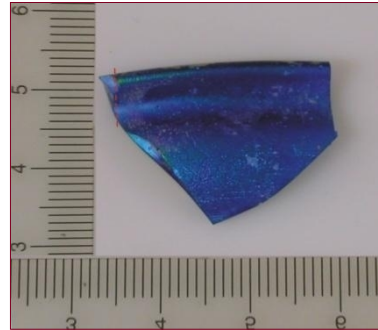
SAMPLE: AD-NF-5
AGE: 6th-5th cent. AD
COLOUR: Blue. White, yellow, light blue
TYPE: Aryballos



SAMPLE: AD-NF-2
AGE: 2th cent. AD
COLOUR: Blue. White, yellow
TYPE: Harden 1981, group 3



SAMPLE: AD-B-8
AGE: 1st cent. AD
COLOUR: Blue
TYPE: Isings 13



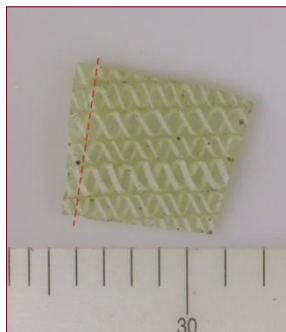
SAMPLE: AD-B-2
AGE: 1st cent. AD
COLOUR: Blue
TYPE: Isings 2



SAMPLE: AD-B-6
AGE: 1st cent. AD
COLOUR: Blue
TYPE: Isings 2



SAMPLE: AD-BB-2
AGE: 1st cent. AD
COLOUR: Light blue, wisteria
TYPE: Isings 3



SAMPLE: AD-R-2
AGE: 1st cent. AD
COLOUR: Colourless, white
TYPE: Isings 1/18



SAMPLE: AD-I-3
AGE: 1st cent. AD
COLOUR: Colourless
TYPE: Isings 96a



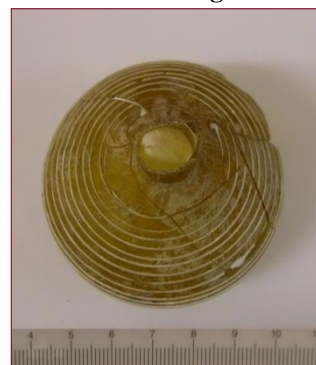
SAMPLE: AD-I-2
AGE: 1st cen. AD
COLOUR: Colourless
TYPE: Rutti 1991a, 61



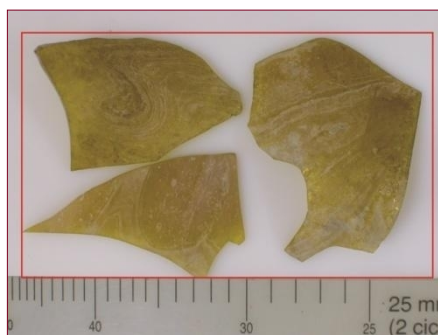
SAMPLE: AD-VB-1
AGE: 1st cen. AD
COLOUR: Purple, white
TYPE: Isings 3



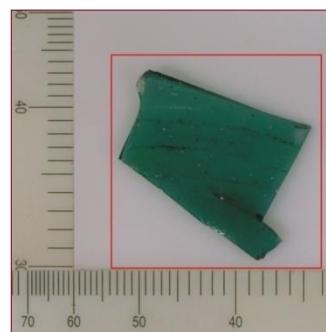
SAMPLE: AD-V-1
AGE: 1st cen. AD
COLOUR: Purple
TYPE: Isings 6



SAMPLE: AD-AB-4
AGE: 1st cen. AD
COLOUR: Amber, white
TYPE: Mandruzzato and Marcante 2007, n° cat. 127-128



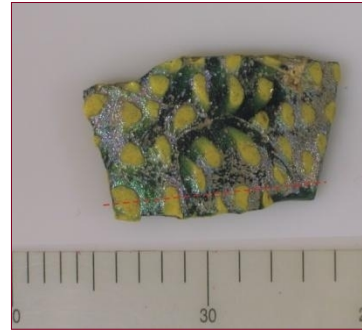
SAMPLE: AD-AB-2
AGE: 1st cen. AD
COLOUR: Amber
TYPE: De Tommaso 1



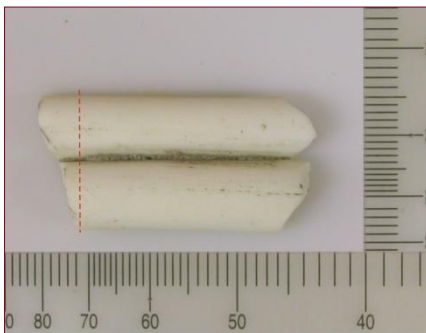
SAMPLE: AD-VE-3
AGE: 1st cen. AD
COLOUR: Emeralds green
TYPE: Isings 46a



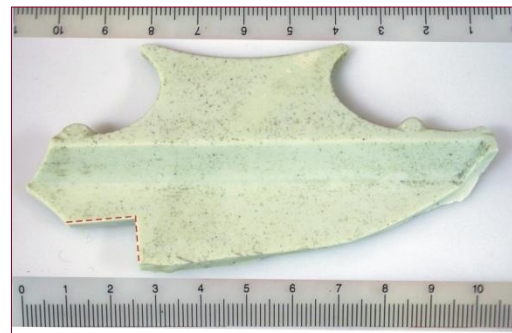
SAMPLE: AD-VE-4
AGE: 1st cent. AD
COLOUR: Emerald green
TYPE: Isings 46a



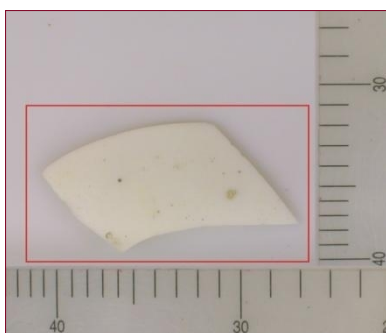
SAMPLE: AD-BG-1
AGE: 1st cent. AD
COLOUR: Emerald green, yellow
TYPE: Isings 1



SAMPLE: AD-BO-2
AGE: 1st cent. AD
COLOUR: Opaque white
TYPE: Isings 13-14



SAMPLE: AD-BO-1
AGE: 1st cent. AD
COLOUR: Opaque white
TYPE: Grose 1991, p. 9, Tav. IIIe



SAMPLE: AD-BO-3
AGE: 1st cent. AD
COLOUR: Opaque white
TYPE: ni



SAMPLE: AD-N-1
AGE: 1st cent. AD
COLOUR: blsck
TYPE: ni

AQUILEIA



SAMPLE: AQ106-11
AGE: late 3rd-5th cent. AD
COLOUR: Light blue
TYPE: Isings 106



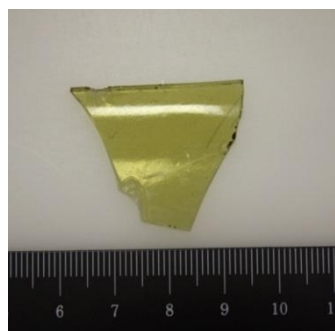
SAMPLE: AQ106-6
AGE: late 3rd-5th cent. AD
COLOUR: Yellow
TYPE: Isings 106



SAMPLE: AQ106-16
AGE: late 3rd-5th cent. AD
COLOUR: Green
TYPE: Isings 106



SAMPLE: AQ116-1
AGE: late 3rd-5th cent. AD
COLOUR: light blue
TYPE: Isings 116



SAMPLE: AQ116-4
AGE: late 3rd-5th cent. AD
COLOUR: Green
TYPE: Isings 116



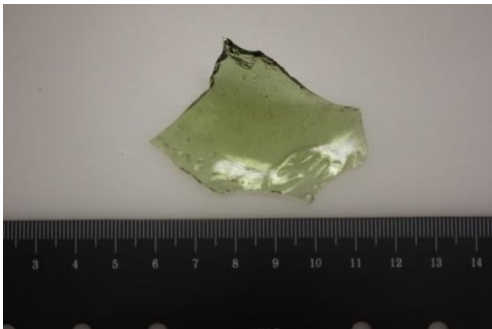
SAMPLE: AQ116-3
AGE: late 3rd-5th cent. AD
COLOUR: Colourless/yellow
TYPE: Isings 116



SAMPLE: AQ117-1
AGE: late 3rd-5th cent. AD
COLOUR: Light blue
TYPE: Isings 117



SAMPLE: AQ117-4
AGE: : late 3rd-5th cent. AD
COLOUR: Green
TYPE: Isings 117



SAMPLE: AQ104-5
AGE: late 3rd-5th cent. AD
COLOUR: green
TYPE: Isings 104



SAMPLE: AQ/cfm-4
AGE: late 3rd-5th cent. AD
COLOUR: Green/Blue
TYPE: Isings 87 or 120



SAMPLE: AQ/cfm-1
AGE: late 3rd-5th cent. AD
COLOUR: Yellow/Green
TYPE: Isings 87 or 120

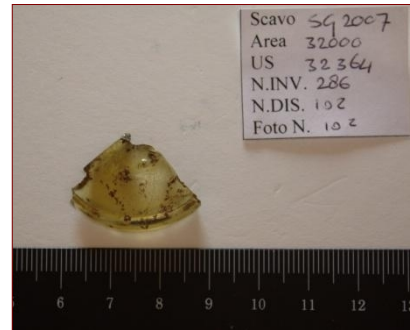


SAMPLE: AQ111-3
AGE: 5st – 8th cen. AD
COLOUR: Light blue
TYPE: Isings 111

TUSCANY



SAMPLE: SG111-1
AGE: 5th 8th cent. AD
COLOUR: Light blue
TYPE: Isings 111



SAMPLE: SG111-3
AGE: 5th 8th cent. AD
COLOUR: Yellow
TYPE: Isings 111



SAMPLE: SG111-4
AGE: 5th 8th cent. AD
COLOUR: Colourless
TYPE: Isings 111

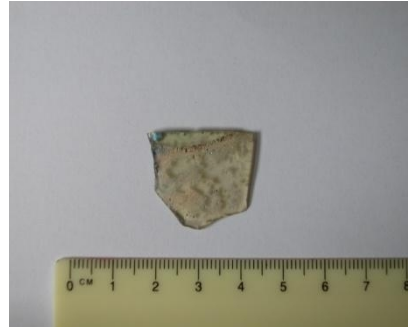


SAMPLE: SG111-6
AGE: 5th 8th cent. AD
COLOUR: Light blue
TYPE: Isings 111

ASOLO



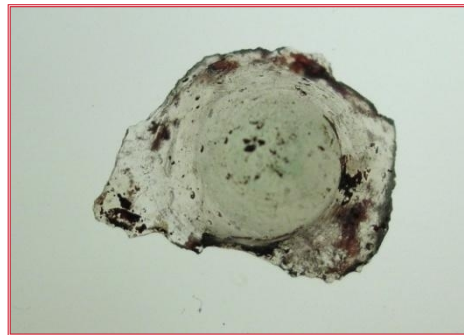
SAMPLE: ASL-01
AGE: 7th 10th cent. AD
COLOUR: Light blue
TYPE: Glass pane



SAMPLE: ASL-02
AGE: : 7th 10th cent. AD
COLOUR: Yellow
TYPE: Glass pane



SAMPLE: ASL-09
AGE: 15th cent. AD
COLOUR: yellow-brown
TYPE: Glass pane (ruo)



SAMPLE: ASO-01
AGE: 13th-14th cent. AD
COLOUR: Colourless
TYPE: Nuppenbecher



SAMPLE: ASO-06
AGE: 13th-14th cent. AD
TYPE: Kopfflascher



SAMPLE: ASO-17
AGE: 14th -15th cent. AD
TYPE: Beaker

APPENDIX B

In this Appendix all the analytical techniques employed to characterize each samples (XRPD, OM, SEM-EDS, XRF,LA-ICP-MS, MC-ICP-MS, EPMA, High Temperature Laser Fluorination) are listed.

SAMPLE	PROVENANCE	COLOUR	TEXTURAL AND SEMI-QUANTITATIVE ANALYSIS OF OPACIFIERS		MINERALOGICAL ANALYSIS		BULK ANALYSIS				ISOTOPIC ANALYSIS			
			OM	SEM-EDS	XRPD	XRF	EPMA	LA-ICP-MS	Sr	Nd	O			
AD-NF-1	Adria	transparent blue	X	X				X						
AD-NF-1Ib	Adria	opaque light blue	X	X				X						
AD-NF-1y	Adria	opaque yellow	X	X				X						
AD-NF-2	Adria	transparent blue	X	X				X						
AD-NF-2w	Adria	opaque white	X	X				X						
AD-NF-3	Adria	transparent blue	X	X				X						
AD-NF-3w	Adria	opaque white	X	X				X						
AD-NF-4	Adria	transparent blue	X	X				X						
AD-NF-5	Adria	transparent blue	X	X				X						
AD-NF-5Ib	Adria	opaque light blue	X	X				X						
AD-NF-5w	Adria	opaque yellow	X	X				X						
AD-NF-6	Adria	transparent blue	X	X				X						
AD-NF-6y	Adria	opaque yellow	X	X				X						
AD-NF-7	Adria	transparent blue	X	X				X						
AD-NF-7y	Adria	opaque yellow	X	X				X						
AD-B-1	Adria	transparent blue	X	X				X						
AD-B-2	Adria	transparent blue	X	X				X						X
AD-B-3	Adria	transparent blue	X	X				X						X
AD-B-4	Adria	transparent blue	X	X				X						X
AD-B-5	Adria	transparent blue	X	X				X						X
AD-B-6	Adria	transparent blue	X	X				X						X
AD-B-7	Adria	transparent blue	X	X				X						X
AD-B-8	Adria	transparent blue	X	X				X						X
AD-B-9	Adria	transparent blue	X	X				X						X
AD-B-10	Adria	transparent blue	X	X				X						X
AD-B-11	Adria	transparent blue	X	X				X						X
AD-BB-1	Adria	transparent blue	X	X				X						X
AD-BB-1w	Adria	transparent blue	X	X				X						X
AD-BB-1Ib	Adria	transparent light	X	X				X						X
AD-BB-2	Adria	transparent blue	X	X				X						X
AD-BB-3	Adria	transparent blue	X	X				X						X
AD-BB-3w	Adria	opaque white	X	X				X						X
AD-BLO-1	Adria	opaque blue	X	X				X						X
AD-R-1	Adria	colourless	X	X				X						X
AD-R-1b	Adria	transparent blue	X	X				X						X
AD-R-1w	Adria	opaque white	X	X				X						X
AD-R-2	Adria	colourless	X	X				X						X
AD-R-2w	Adria	opaque white	X	X				X						X
AD-A-1	Adria	transparent light	X	X				X						X
AD-A-2	Adria	transparent light	X	X				X						X

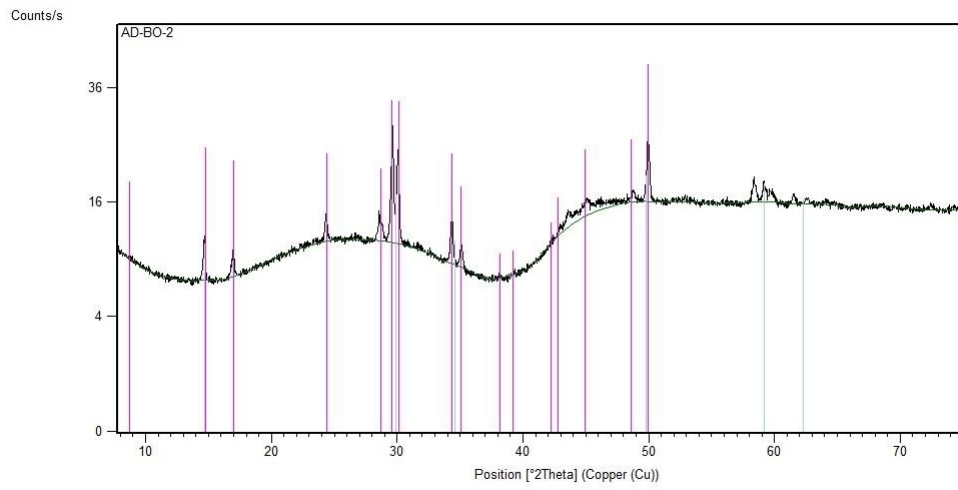
ASL-11	Rocca di Asolo	Yellowish-brown	X				X
ASL-12	Rocca di Asolo	Yellowish-brown	X				X
ASO-01	Rocca di Asolo	Colourless	X				X
ASO-02	Rocca di Asolo	Light blue	X				X
ASO-03	Rocca di Asolo	Yellowish	X				X
ASO-04	Rocca di Asolo	Yellowish-green	X				X
ASO-05	Rocca di Asolo	Colourless	X				X
ASO-06	Rocca di Asolo	Green	X				X
ASO-07	Rocca di Asolo	Green	X				X
ASO-08	Rocca di Asolo	Light blue	X				X
ASO-09	Rocca di Asolo	Green	X				X
ASO-10	Rocca di Asolo	Green	X				X
ASO-11	Rocca di Asolo	Green	X				X
ASO-12	Rocca di Asolo	Light blue	X				X
ASO-13	Rocca di Asolo	Yellowish-green	X				X
ASO-14	Rocca di Asolo	Yellowish-green	X				X
ASO-15	Rocca di Asolo	Yellowish-green	X				X
ASO-16	Rocca di Asolo	Green	X				X
ASO-17a	Rocca di Asolo	Colourless	X				X
ASO-17b	Rocca di Asolo	Transparent blue	X		X		X
ASO-18a	Rocca di Asolo	Colourless	X				X
ASO-18b	Rocca di Asolo	Transparent blue	X		X		X
ASO-19a	Rocca di Asolo	Colourless	X				X
ASO-19b	Rocca di Asolo	Transparent blue	X		X		X
ASO-20a	Rocca di Asolo	Colourless	X				X
ASO-20b	Rocca di Asolo	Transparent blue	X		X		X
ASO-21a	Rocca di Asolo	Yellowish	X				X
ASO-21b	Rocca di Asolo	Transparent blue	X		X		X

Table B.1: *List of the type of analysis performed on each sample.*

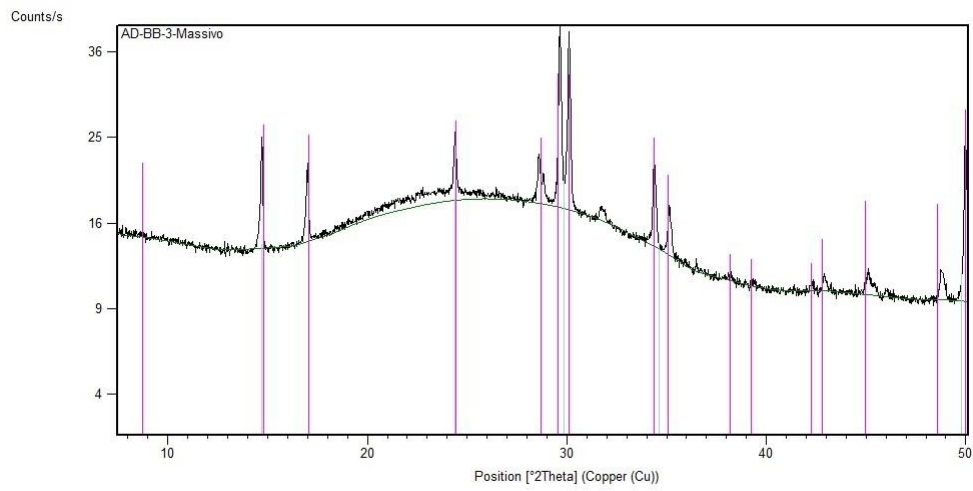
APPENDIX C

Diffraction patterns of the opacifying agents recognized in four Roman white glasses (AD-BO-2, AD-BB-3, AD-BO-1, AD-BO-3). The identification card of the crystalline phase is also reported (from the database of the PANalytical software X'Pert Highscore Plus).

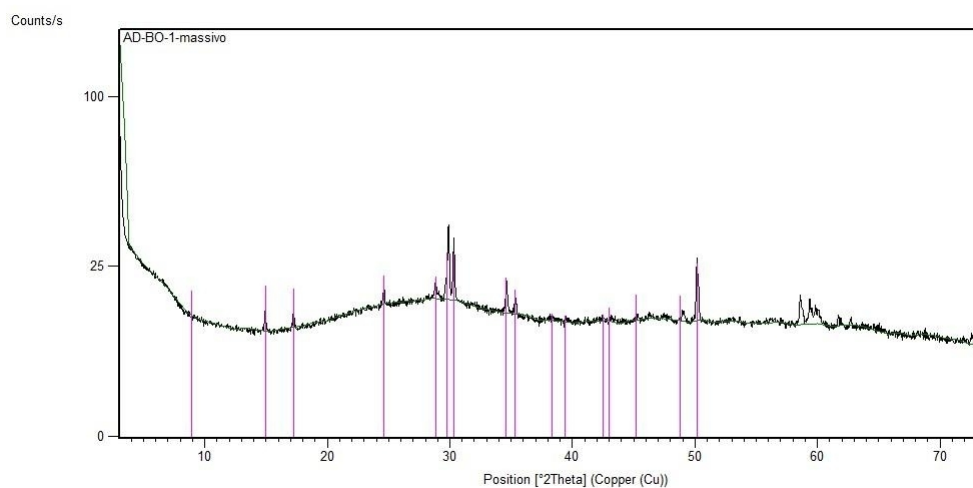
SAMPLE AD-BO-2



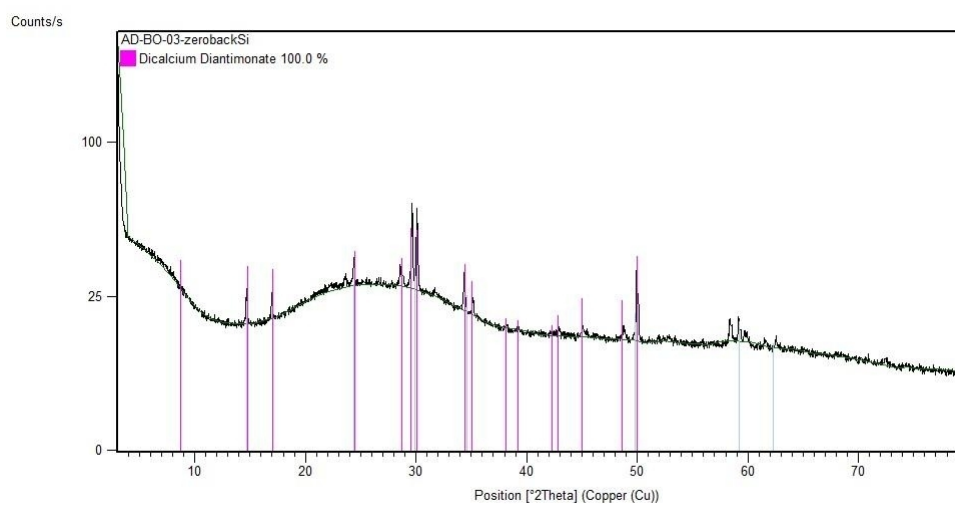
SAMPLE AD-BB-3



SAMPLE AD-BO-1



SAMPLE AD-BO-3



Name and formula

Reference code: 00-026-0293
 PDF index name: Calcium Antimony Oxide

Empirical formula: $\text{Ca}_2\text{O}_7\text{Sb}_2$
 Chemical formula: $\text{Ca}_2\text{Sb}_2\text{O}_7$

Crystallographic parameters

Crystal system: Orthorhombic

a (Å): 7.2900
 b (Å): 7.4500
 c (Å): 10.2000
 Alpha (°): 90.0000

Beta (°): 90.0000
Gamma (°): 90.0000
Volume of cell (10⁶ pm³): 553.97
Z: 4.00
RIR: -

Subfiles and Quality

Subfiles: Inorganic
Quality: Blank (B)

Comments

Color: Yellowish white
Additional pattern: To replace 2-1384.

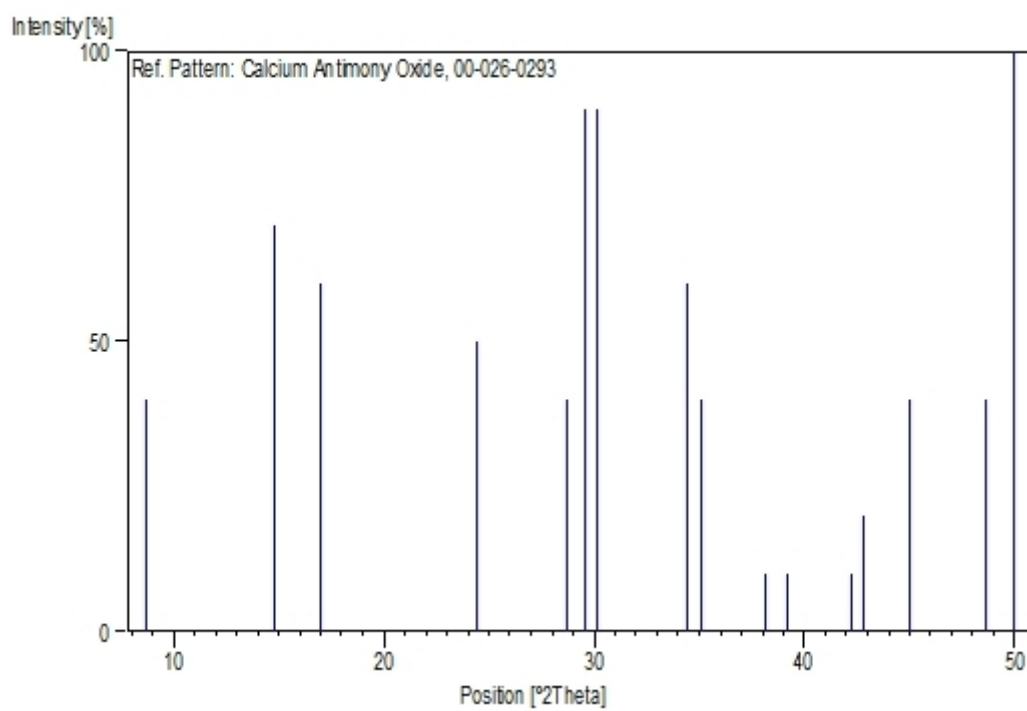
References

Primary reference: Butler et al., *J. Electrochem. Soc.*, **97**, 117, (1950)

Peak list

No.	h	k	l	d [Å]	2Theta[deg]	I [%]
1	0	0	1	10.10000	8.748	40.0
2	0	1	1	5.98000	14.802	70.0
3	1	1	0	5.20000	17.038	60.0
4	1	1	2	3.64000	24.435	50.0
5	2	1	1	3.11000	28.681	40.0
6	0	2	2	3.02000	29.555	90.0
7	2	0	2	2.96600	30.106	90.0
8	2	2	0	2.60600	34.385	60.0
9	0	0	4	2.55700	35.066	40.0
10	2	1	3	2.35600	38.168	10.0
11	1	3	1	2.29500	39.223	10.0
12	1	3	2	2.13700	42.257	10.0
13	3	1	2	2.11100	42.803	20.0
14	2	3	1	2.01400	44.974	40.0
15	0	4	0	1.87200	48.596	40.0
16	4	0	0	1.82400	49.961	100.0

Stick Pattern



APPENDIX D

Major, minor and trace elements composition of all transparent and opaque glasses analyzed. Results are expressed as wt% for major and minor elements, as ppm for traces, and are given by XRF, EPMA, and LA-ICP-MS.

SAMPLE	COLOUR	AGE	SiO ₂	Na ₂ O	CaO	Al ₂ O ₃	K ₂ O	MgO	Fe ₂ O ₃	TiO ₂	MnO	Sb ₂ O ₃	P ₂ O ₅	SO ₃	Cl	Tot	GROUP
AD-NF-1	Blue	5th BC	67.65	14.17	10.32	2.69	0.67	0.65	1.44	0.07	0.01	0.18	0.08	0.22	0.95	99.12	GROUP AD/NI
AD-NF-2	Blue	2nd BC	69.31	17.77	7.24	2.62	0.52	0.45	1.91	0.18	0.03	<0.04	<0.05	0.12	1.54	101.67	GROUP AD/NI
AD-NF-3	Blue	5th BC	69.41	16.86	8.53	2.44	0.33	0.57	1.03	0.06	0.01	0.22	<0.05	0.19	1.38	101.03	GROUP AD/NI
AD-NF-4	Blue	6th-5th BC	70.70	16.17	8.12	2.21	0.46	0.55	0.95	0.07	0.01	0.08	<0.05	0.19	1.15	100.65	GROUP AD/NI
AD-NF-5	Blue	6th-5th BC	71.02	15.14	8.44	2.27	0.65	0.46	1.15	0.05	0.01	0.26	<0.05	0.11	1.36	100.92	GROUP AD/NI
AD-NF-6	Blue	4th BC	66.96	15.31	10.28	1.87	0.65	1.03	1.97	0.17	0.03	<0.04	0.05	0.20	0.78	99.29	GROUP AD/NI
AD-NF-7	Blue	3rd BC	68.08	14.53	9.92	2.66	0.66	0.60	1.45	0.12	0.02	<0.04	0.05	0.18	0.85	99.11	GROUP AD/NI
AD-B-1	Blue	1st AD	67.71	18.01	7.78	2.46	0.73	0.59	0.86	0.06	0.50	0.05	0.17	0.20	1.34	100.46	GROUP AD/NI
AD-B-2	Blue	1st AD	65.02	16.83	7.62	1.89	1.97	1.94	1.28	0.10	1.40	<0.04	1.29	0.31	0.88	100.51	GROUP AD/AI
AD-B-3	Blue	1st AD	68.08	17.14	7.63	2.57	0.78	0.56	1.01	0.05	0.42	<0.04	0.10	0.15	1.53	100.03	GROUP AD/NI
AD-B-4	Blue	1st-2nd AD	68.21	16.32	4.63	4.29	0.93	0.43	1.77	0.08	1.31	<0.04	0.15	0.10	1.30	99.51	GROUP AD/NI
AD-B-5	Blue	-	68.81	18.30	7.57	1.79	0.32	0.43	0.92	0.06	0.01	<0.04	0.04	0.30	1.60	100.14	GROUP AD/NI
AD-B-6	Blue	1st AD	66.63	17.85	4.66	2.23	0.40	0.56	1.73	0.23	0.89	<0.04	0.03	0.25	1.19	96.67	GROUP AD/N2a
AD-B-7	Blue	1st AD	70.01	17.64	4.15	1.79	0.95	0.81	1.27	0.16	1.41	<0.04	0.29	0.19	1.40	100.07	GROUP AD/N2a
AD-B-8	Blue	1st AD	69.42	16.83	7.43	2.53	0.76	0.48	0.50	0.05	0.50	<0.04	0.12	0.16	1.34	100.12	GROUP AD/NI
AD-B-9	Blue	1st AD	67.33	17.09	7.86	2.53	0.82	0.55	1.14	0.05	0.79	<0.04	0.14	0.32	1.02	99.63	GROUP AD/NI
AD-B-10	Blue	1st AD	67.92	17.48	7.69	2.49	0.80	0.53	0.85	0.06	0.47	0.05	0.16	0.19	1.29	99.96	GROUP AD/NI
AD-B-11	Blue	1st AD	67.57	17.18	7.89	2.53	0.84	0.53	1.11	0.05	0.78	<0.04	0.15	0.32	1.03	99.97	GROUP AD/NI
AD-BB-1b	Blue	1st AD	66.22	17.77	9.22	2.34	0.55	0.58	0.73	0.05	0.39	<0.04	0.08	0.26	1.45	99.65	GROUP AD/NI
AD-BB-2	Blue	1st AD	68.16	17.48	7.83	2.50	0.89	0.61	0.87	0.05	0.64	<0.04	0.15	0.31	1.05	100.55	GROUP AD/NI
AD-BB-3	Blue	1st AD	69.52	17.01	7.94	2.49	0.54	0.53	0.82	0.05	0.17	<0.04	0.11	0.17	1.45	100.79	GROUP AD/NI
AD-R-1b	Blue	1st AD	66.75	19.21	7.40	2.76	0.89	0.60	0.97	0.05	0.58	<0.04	0.12	0.31	1.37	101.01	GROUP AD/NI
AD-A-1	Light blue	1st BC-1st AD	66.19	19.94	7.86	2.43	0.93	0.55	0.34	0.05	0.65	<0.04	0.17	0.44	0.86	100.42	GROUP AD/NI
AD-A-2	Light blue	1st AD	70.83	16.67	7.16	2.61	0.61	0.41	0.34	0.05	0.15	<0.04	0.12	0.20	1.61	100.76	GROUP AD/NI
AD-A-3	Light blue	1st AD	67.44	18.52	7.85	2.55	0.61	0.53	0.46	0.06	0.71	<0.04	0.12	0.20	1.59	100.64	GROUP AD/NI
AD-A-4	Light blue	1st AD	68.43	16.85	8.65	2.63	0.76	0.50	0.52	0.06	0.42	<0.04	0.14	0.22	1.28	100.45	GROUP AD/NI
AD-A-5	Light blue	1st AD	67.93	18.27	8.42	2.44	0.63	0.55	0.41	0.05	0.68	<0.04	0.13	0.22	1.33	101.07	GROUP AD/NI
AD-A-6	Light blue	1st AD	67.74	18.19	7.77	2.44	0.61	0.52	0.33	0.05	0.42	<0.04	0.12	0.22	1.44	99.86	GROUP AD/NI
AD-A-7	Light blue	1st AD	70.53	16.88	7.51	2.48	0.50	0.41	0.35	0.06	0.06	<0.04	0.11	0.14	1.44	100.46	GROUP AD/NI
AD-A-8	Light blue	1st-2nd AD	69.70	16.98	7.12	2.39	0.71	0.57	0.49	0.08	0.41	0.05	0.18	0.17	1.39	100.23	GROUP AD/NI
AD-A-9	Light blue	1st-2nd AD	70.60	15.85	7.82	2.46	0.48	0.47	0.30	0.05	0.71	<0.04	0.11	0.13	1.54	100.51	GROUP AD/NI
AD-A-10	Light blue	1st-2nd AD	69.60	16.69	7.10	2.57	0.84	0.59	0.53	0.09	0.45	0.07	0.22	0.18	1.18	100.11	GROUP AD/NI
AD-A-11	Light blue	1st AD	70.45	17.29	7.43	2.54	0.58	0.48	0.43	0.06	0.59	<0.04	0.12	0.20	1.53	101.70	GROUP AD/NI
AD-AG-1	Light blue	1st AD	68.91	18.24	7.35	2.61	0.48	0.54	0.32	0.05	0.60	<0.04	0.05	0.19	1.59	100.93	GROUP AD/NI

AD-P-1	Light blue	1st AD	68.86	17.78	8.25	2.53	0.63	0.57	0.40	0.05	0.62	<0.04	0.11	0.14	1.34	101.28	GROUP AD/N1
AD-BB-1lb	Light blue	1 AD	67.27	18.72	8.12	2.32	0.58	0.56	0.26	0.06	0.74	<0.04	<0.05	0.40	1.27	100.30	GROUP AD/N1
AD-VC-1	Light green	2nd-4th AD	65.07	18.91	8.41	2.28	0.56	0.97	0.80	0.13	0.74	0.09	0.07	0.38	1.33	99.73	GROUP AD/N1
AD-VC-2	Light green	1st-3rd AD	70.48	15.80	7.52	2.45	0.49	0.52	0.31	0.05	0.90	<0.04	0.10	0.19	1.26	100.08	GROUP AD/N1
AD-VE-1	Olive green	1st AD	68.49	17.65	8.16	2.35	0.65	0.69	0.39	0.06	0.09	<0.04	0.10	0.19	1.34	100.16	GROUP AD/N1
AD-VE-2	Emerald	1st AD	60.74	18.98	6.69	2.80	1.84	1.99	1.40	0.24	0.79	0.04	0.52	0.24	1.07	97.34	GROUP AD/A2
AD-VE-3	Emerald	1st-2nd AD	62.66	19.92	6.84	2.59	1.01	1.49	1.04	0.17	0.55	<0.04	0.36	0.19	1.56	98.38	GROUP AD/A2
AD-VE-4	Emerald	1st-2nd AD	67.63	15.83	5.10	1.78	1.37	1.44	0.99	0.16	0.40	<0.04	0.51	0.14	1.30	96.64	GROUP AD/A1
AD-BG-1	Emerald	1st AD	63.93	16.14	7.00	1.84	1.05	2.51	0.98	0.14	0.91	0.06	1.29	0.20	1.58	97.64	GROUP AD/A1
AD-I-1	Colourless	1st AD	66.35	18.78	9.36	2.21	0.60	0.72	0.35	0.05	0.85	<0.04	0.05	0.45	1.16	100.94	GROUP AD/N1
AD-I-2	Colourless	2nd AD	70.25	17.13	4.22	1.48	0.75	0.44	0.51	0.10	0.16	1.14	0.04	nd	nd	96.21	GROUP AD/N2b
AD-I-3	Colourless	3rd AD	68.28	18.49	6.38	2.16	0.55	0.53	0.46	0.08	0.54	0.41	0.09	nd	nd	97.97	GROUP AD/N1
AD-I-4	Colourless	2nd AD	68.69	19.10	5.40	2.02	0.50	0.54	0.45	0.09	0.09	0.51	0.05	0.34	1.52	99.29	GROUP AD/N2b
AD-I-5	Colourless	2nd-3rd AD	68.47	18.85	5.55	1.99	0.50	0.55	0.48	0.09	0.17	0.47	0.06	0.31	1.63	99.11	GROUP AD/N2b
AD-I-6	Colourless	2nd AD	70.44	18.56	5.38	1.60	0.37	0.43	0.26	0.05	0.01	0.60	0.02	0.27	1.57	99.56	GROUP AD/N2b
AD-R-1t	Colourless	1st AD	67.87	18.88	7.83	2.39	0.71	0.60	0.36	0.05	0.84	<0.04	0.11	0.46	0.92	101.03	GROUP AD/N1
AD-R-2	Colourless	1st AD	69.21	17.19	7.43	2.61	0.83	0.67	0.40	0.05	1.26	<0.04	0.08	0.15	1.55	101.43	GROUP AD/N1
AD-V-1	Purple	1st AD	68.73	17.32	7.47	2.41	0.55	0.61	0.45	0.06	1.99	<0.04	0.10	0.18	1.32	101.18	GROUP AD/N1
AD-V-2	Purple	1st AD	66.90	16.09	7.87	2.57	0.58	0.52	1.13	0.06	1.72	<0.04	0.11	0.16	1.26	98.97	GROUP AD/N1
AD-V-3	Purple	1st AD	67.77	16.86	7.79	2.29	0.51	0.55	0.37	0.05	1.55	<0.04	0.11	0.13	1.48	99.46	GROUP AD/N1
AD-V-4	Purple	1st AD	63.73	19.10	8.02	2.31	0.65	0.65	0.36	0.05	2.01	<0.04	0.12	0.37	1.15	98.51	GROUP AD/N1
AD-VB-1	Purple	1st AD	66.69	18.15	7.40	2.57	0.63	0.62	0.31	0.05	1.68	<0.04	0.08	0.24	1.22	99.64	GROUP AD/N1
AD-AM-1	Amber	1st AD	68.91	18.65	7.17	2.46	0.52	0.50	0.35	0.06	0.05	<0.04	0.12	nd	nd	98.78	GROUP AD/N1
AD-AM-2	Amber	1st AD	67.39	18.79	7.80	2.54	0.71	0.51	0.30	0.05	0.04	<0.04	0.11	0.22	1.50	99.95	GROUP AD/N1
AD-AB-1	Amber	1st AD	67.56	20.27	7.32	2.48	0.54	0.52	0.29	0.05	0.03	<0.04	0.09	0.26	1.89	101.31	GROUP AD/N1
AD-AB-2	Amber	1st AD	68.46	18.69	7.46	2.62	0.73	0.55	0.31	0.05	0.03	<0.04	0.16	0.17	1.74	100.97	GROUP AD/N1
AD-AB-3	Amber	1st-2nd AD	68.22	18.73	7.91	2.60	0.67	0.54	0.32	0.05	0.02	<0.04	0.14	0.14	1.57	100.91	GROUP AD/N1
AD-AB-4	Amber	1st AD	66.53	19.90	8.06	2.35	0.70	0.66	0.32	0.05	0.04	<0.04	0.08	0.32	1.70	100.71	GROUP AD/N1
AD-AB-5	Amber	1st-2nd AD	68.30	19.32	7.23	2.61	0.66	0.55	0.30	0.05	0.02	<0.04	0.12	0.18	1.73	101.06	GROUP AD/N1
AD-AB-6	Amber	1st-2nd AD	67.01	20.26	7.69	2.54	0.60	0.58	0.37	0.06	0.03	<0.04	0.08	0.37	1.53	101.11	GROUP AD/N1
AD-ABP1	Amber	1st-2nd AD	70.53	17.73	7.27	2.62	0.51	0.46	0.26	0.05	0.02	<0.04	<0.05	0.16	1.69	101.31	GROUP AD/N1
AD-N-1	Black	1st AD	60.66	19.93	7.12	2.67	1.49	2.40	1.88	0.26	0.32	<0.04	0.98	0.53	1.66	99.88	GROUP AD/A2

Table D.1: Chemical composition, expressed as wt% of element oxide, of transparent Adria glasses. Data are given by XRF or EPMA (see Table B.1, Appendix B, for details). For the samples analyzed by EPMA only means are reported. (nd: not determined). Colour, age and compositional group of each sample are also indicated.

SAMPLE	AD-NF-1	AD-NF-2	AD-NF-3	AD-NF-4	AD-NF-5	AD-NF-6	AD-NF-7	AD-B-1	AD-B-2	AD-B-3
COLOUR	Blue	Blue	Blue	Blue	Blue	Blue	Blue	Blue	Blue	Blue
Li	13	11	3.5	3.9	4.2	9.4	6.2	4.2	2.6	3.8
B	97	528	145	102	106	226	290	202	147	144
V	9.5	16	8.1	9.4	5.8	19	13	11	32	13
Cr	13	13	9.7	6.1	7.57	9.9	10	13	16	12
Co	357	720	1027	636	952	1861	1133	373	742	648
Ni	6.8	26	5.1	6.8	5.9	274	126	14	28	21
Zn	113	94	214	71	86	195	125	45	36	47
Rb	9.6	11	7.3	8.4	11	6.6	5.3	10	6.9	11
Sr	419	220	474	466	483	224	222	447	553	453
Y	7.3	8.3	6.8	6.9	7.0	4.5	3.8	5.7	4.7	6.3
Zr	39	87	31	33	30	71	57	31	50	29
Nb	1.5	3.4	1.2	1.2	1.1	2.5	1.8	1.2	1.6	1.0
Cs	0.11	0.20	0.065	0.054	0.11	0.15	0.13	0.074	0.090	0.089
Ba	179	176	180	185	185	75	64	250	315	235
La	7.0	10	6.5	6.4	6.2	7.5	7.0	6.0	5.4	6.5
Ce	12	19	11	11	11	14	12	11	10	11
Nd	7.4	9.2	6.0	6.0	6.2	7.7	5.4	6.0	5.4	5.9
Sm	1.4	1.8	1.4	1.3	1.4	1.1	1.2	1.4	0.94	1.2
Eu	0.38	0.42	0.38	0.41	0.39	0.36	0.33	0.36	0.32	0.51
Gd	1.4	1.5	1.4	0.98	1.0	0.91	0.85	1.2	0.97	1.2
Tb	0.22	0.25	0.18	0.16	0.22	0.17	0.11	0.18	0.15	0.20
Dy	1.3	1.6	0.77	1.2	1.2	0.91	0.74	0.93	0.95	1.2
Er	0.72	0.71	0.56	0.65	0.62	0.57	0.36	0.50	0.43	0.54
Yb	0.67	0.79	0.46	0.61	0.74	0.52	0.33	0.46	0.56	0.35
Lu	0.088	0.11	0.080	0.079	0.088	0.070	0.090	0.075	0.075	0.072
Hf	0.96	6.3	0.63	0.76	0.84	1.4	1.4	0.61	1.1	0.79
Ta	0.094	0.21	0.092	0.048	0.053	0.172	0.13	0.074	0.11	0.056
Pb	2506	320	333	125	322	1334	913	198	638	32
Th	0.96	2.3	0.75	0.65	0.67	1.4	1.3	0.69	0.93	0.65
U	2.9	1.6	1.5	2.2	0.64	1.5	1.7	0.99	0.98	0.69
Cu	1443	2238	791	841	1311	4173	1650	665	1178	600
As	5.0	5.0	5.6	6.7	4.1	26	14	2.5	5.2	2.7
Ag	0.88	0.35	0.21	0.047	0.047	0.40	0.34	0.14	1.4	0.066
Sn	4.4	7.3	0.48	0.62	1.2	28	13	48	65	11
W	<0.00	0.13	0.046	0.053	0.077	0.15	0.077	0.057	0.24	0.095
Tl	<0.008	<0.013	0.013	<0.017	0.013	<0.009	0.012	0.067	0.20	0.087
Bi	0.126	0.072	0.16	<0.013	0.017	0.12	0.081	0.017	0.081	0.026
In	0.28	1.3	0.31	0.23	0.21	8.0	4.6	0.50	0.88	0.42

SAMPLE	AD-B-4	AD-B-5	AD-B-6	AD-B-7	AD-B-8	AD-B-9	AD-B-10	AD-B-11	AD-BB-1b	AD-BB-2
COLOUR	Blue	Blue	Blue	Blue	Blue	Blue	Blue	Blue	Blue	Blue
Li	4.1	2.7	5.5	4.8	4.4	3.7	2.4	3.2	2.8	4.5
B	145	139	119	120	256	145	186	137	186	110
V	29	6.3	24	26	12	14	12	14	10	14
Cr	47	8.9	33	22	6.2	13	11	11	13	11
Co	1740	337	1106	616	209	543	386	528	300	387
Ni	64	4.9	31.1	27	12	28	14	26	13	17
Zn	32	82	27	53	23	60	47	63	31	41
Rb	18	6.3	7.3	5.0	9.9	10	10	11	8	12
Sr	388	371	322	400	425	474	436	474	474	465
Y	6.5	5.8	5.9	5.5	5.6	5.9	6.3	6.0	6.6	6.1
Zr	54	30	152	96	31	29	34	29	32	32
Nb	2.1	0.96	2.6	2.3	1.2	1.0	1.1	1.0	0.99	1.1
Cs	0.16	0.053	0.11	0.078	0.069	0.056	0.099	0.086	0.052	0.095
Ba	329	146	169	231	227	245	242	241	212	237
La	6.6	6.0	6.9	6.3	5.8	5.7	6.3	6.0	6.3	5.9
Ce	12	10	13	11	11	10	11	10	11	11
Nd	5.2	5.6	7.1	5.2	5.1	5.7	5.9	5.4	6.4	6.2
Sm	1.2	1.2	1.3	0.87	0.82	1.2	1.1	1.1	1.3	1.1
Eu	0.27	0.36	0.24	0.29	0.29	0.34	0.36	0.31	0.32	0.33
Gd	1.1	1.3	1.1	0.71	1.0	1.1	1.0	0.83	1.3	1.1
Tb	0.17	0.12	0.17	0.14	0.19	0.16	0.16	0.15	0.18	0.19
Dy	1.1	0.88	0.91	1.0	1.1	0.89	0.96	0.99	1.2	1.1
Er	0.69	0.54	0.58	0.50	0.49	0.60	0.49	0.55	0.51	0.49
Yb	0.72	0.55	0.72	0.50	0.64	0.55	0.57	0.52	0.59	0.53
Lu	0.10	0.048	0.087	0.12	0.057	0.079	0.11	0.055	0.12	0.078
Hf	1.4	0.60	3.9	2.3	0.76	0.61	0.78	0.69	0.87	0.70
Ta	0.15	0.043	0.18	0.15	0.050	0.070	0.074	0.072	0.052	0.078
Pb	22	14	48	204	23	49	155	50	92	69
Th	1.5	0.70	1.7	1.2	0.66	0.58	0.76	0.69	0.68	0.69
U	0.91	1.5	1.4	1.2	0.83	1.3	0.90	1.3	0.79	1.2
Cu	1726	928	1093	964	343	753	660	765	479	536
As	6.6	3.6	4.7	3.7	2.1	4.0	2.9	4.1	1.6	4.0
Ag	0.10	0.046	0.14	0.49	0.17	0.037	0.045	0.094	0.13	0.12
Sn	9.6	0.55	6.0	16	2.5	9.3	46	10	21	12
W	0.16	0.023	0.14	0.16	0.083	0.077	0.088	0.055	0.084	0.13
Tl	0.21	0.032	0.069	0.20	0.038	0.037	0.018	0.063	0.045	0.030
Bi	0.030	0.011	0.022	0.064	0.017	<0.009	0.038	0.014	0.039	<0.015
In	1.1	0.18	1.1	0.60	0.18	0.55	0.54	0.62	0.30	0.23

SAMPLE	AD-BB-3	AD-R-1b	AD-A-1	AD-A-2	AD-A-3	AD-A-4	AD-A-5	AD-A-6	AD-A-7	AD-A-8
COLOUR	Blue	Blue	Light blue	Light blue	Light blue	Light blue	Light blue	Light blue	Light blue	Light blue
Li	3.3	3.8	3.7	3.1	3.8	5.9	4.4	3.4	4.1	4.9
B	194	112	182	129	300	155	204	219	106	150
V	7.2	13	17	6.5	14	8.4	14	10	6.0	13
Cr	12	7.6	11	7.4	15	11	9.6	16	7.6	13
Co	366	857	21	1.2	6.0	5.9	20	14	2.1	20
Ni	12	25	9.5	3.4	11	7.4	9.4	9.4	4.8	8.7
Zn	39	36	15	11	16	16	17	16	9.9	23
Rb	7.8	9.9	13	8.2	9.0	11	8.5	8.1	7.1	8.5
Sr	407	430	462	362	486	482	479	438	375	400
Y	6.0	5.3	5.7	5.5	5.9	6.4	6.6	5.6	5.0	5.8
Zr	30	30	31	30	31	34	34	33	30	45
Nb	1.0	1.3	1.1	1.0	1.3	1.3	1.3	1.1	1.1	1.6
Cs	0.082	0.074	0.10	0.13	0.13	0.29	0.11	0.062	0.072	0.14
Ba	211	252	249	255	337	379	263	222	209	227
La	5.9	5.9	5.7	5.6	6.1	6.5	6.1	5.8	5.7	6.0
Ce	11	10	11	10	12	12	11	11	11	12
Nd	5.1	5.7	5.4	5.7	5.5	6.7	5.8	5.4	5.7	5.6
Sm	1.5	1.1	1.1	1.1	1.4	1.2	1.1	0.88	1.0	1.2
Eu	0.31	0.34	0.32	0.38	0.24	0.39	0.33	0.36	0.32	0.31
Gd	0.88	1.1	0.9	0.67	1.1	0.92	1.3	1.1	1.1	1.1
Tb	0.16	0.12	0.14	0.14	0.20	0.16	0.19	0.17	0.15	0.14
Dy	0.80	0.76	0.96	0.98	0.95	0.79	1.2	0.98	0.90	1.0
Er	0.61	0.51	0.48	0.53	0.52	0.65	0.53	0.49	0.57	0.51
Yb	0.47	0.42	0.53	0.41	0.41	0.45	0.50	0.65	0.65	0.73
Lu	0.086	0.074	0.083	0.070	0.068	0.060	0.065	0.071	0.063	0.11
Hf	1.1	0.65	0.77	0.7	0.88	0.98	0.82	0.87	0.71	1.2
Ta	0.064	0.074	0.068	0.053	0.080	0.082	0.053	0.062	0.077	0.086
Pb	30	159	8.8	7.8	20	75	124	157	11	178
Th	0.65	0.67	0.68	0.68	0.78	0.77	0.65	0.74	0.72	0.96
U	0.85	0.95	1.1	0.88	0.99	1.0	1.1	0.82	1.0	0.94
Cu	537	744	26	5.7	25	41	82	193	14	411
As	2.2	4.8	1.5	1.3	1.8	1.8	2.0	1.7	1.7	3.9
Ag	20	1.2	0.046	0.033	0.035	0.033	0.056	0.11	0.026	0.20
Sn	3.5	14	0.86	0.92	3.3	6.1	15	19	1.8	62
W	0.12	0.069	0.092	0.033	0.047	0.012	0.052	0.050	0.070	0.098
Tl	0.018	0.053	0.025	0.039	0.17	0.027	0.044	0.063	0.017	0.023
Bi	0.033	0.022	<0.010	<0.011	0.011	0.026	0.035	<0.012	0.032	0.040
In	0.41	0.59	0.024	0.008	0.031	0.018	0.086	0.087	0.018	0.29

SAMPLE	AD-A-9	AD-A-10	AD-AG-1	AD-P-1	AD-BB-11b	AD-VC-1	AD-VC-2	AD-VE-1	AD-VE-2	AD-VE-3
COLOUR	Light blue	Light blue	Light blue	Light blue	Light blue	Light green	Light green	Olive green	Emerlad green	Emerlad green
Li	3.5	5.9	2.9	4.1	nd	6.7	3.6	3.8	6.9	4.9
B	78	134	212	205	nd	168	121	112	257	155
V	15	15	11	13	nd	22	18	9.6	22	16
Cr	8.1	14	9.0	12	nd	15	7.3	14	33	28
Co	8.0	14	12	11	<200	11	3.8	1.7	15	6.3
Ni	14	9.3	9.0	10	<350	9.8	6.5	5.3	14	7.8
Zn	18	25	15	18	<300	26	9.4	11	79	52
Rb	7.6	11	6.8	11	nd	6.0	7.2	9.6	10	6.3
Sr	496	392	418	483	nd	825	464	447	463	423
Y	6.3	6.4	6.1	6.2	nd	6.0	6.0	6.1	6.9	6.3
Zr	29	49	31	31	nd	69	31	34	107	82
Nb	1.1	1.6	1.3	1.1	nd	2.5	1.1	1.2	3.4	2.7
Cs	0.046	0.12	0.068	0.061	nd	0.057	0.052	0.061	0.35	0.21
Ba	237	213	244	260	nd	231	293	197	481	416
La	6.0	6.7	6.0	6.1	nd	7.3	5.9	6.1	7.8	7.4
Ce	11	13	10	12	nd	13	10	12	15	13
Nd	6.1	6.4	5.5	6.0	nd	6.8	5.4	6.2	7.4	6.7
Sm	1.2	1.4	1.1	1.0	nd	1.1	1.2	1.2	1.5	1.3
Eu	0.32	0.32	0.38	0.39	nd	0.35	0.34	0.43	0.41	0.39
Gd	0.89	1.0	0.91	1.1	nd	1.3	1.2	1.2	1.4	1.1
Tb	0.17	0.16	0.16	0.17	nd	0.17	0.12	0.23	0.19	0.16
Dy	1.1	1.0	0.89	1.2	nd	1.1	1.1	0.93	1.1	1.1
Er	0.54	0.54	0.51	0.51	nd	0.60	0.53	0.53	0.68	0.72
Yb	0.51	0.58	0.52	0.44	nd	0.57	0.45	0.47	0.68	0.66
Lu	0.087	0.059	0.086	0.068	nd	0.096	0.085	0.063	0.12	0.11
Hf	0.69	1.3	0.80	0.85	nd	1.4	0.90	0.81	2.8	1.9
Ta	0.045	0.10	0.059	0.050	nd	0.13	0.059	0.076	0.21	0.18
Pb	6.4	196	15	40	<700	61	4.2	18	762	516
Th	0.71	1.1	0.74	0.68	nd	1.2	0.63	0.73	1.6	1.5
U	0.98	1.0	1.2	1.1	nd	0.98	0.95	0.88	1.0	0.98
Cu	9.7	417	16	53	<300	92	16	5.9	24029	17013
As	1.2	2.9	0.81	2.7	nd	12	2.8	1.8	9.7	7.7
Ag	0.027	0.40	<0.033	0.043	nd	0.17	<0.031	<0.036	13	7.1
Sn	0.53	72	1.2	7.5	<300	14	0.49	0.65	1981	1452
W	0.096	0.13	0.054	0.093	nd	0.14	0.10	0.071	0.14	0.036
Tl	0.13	0.034	0.064	0.092	nd	<0.007	0.013	0.020	0.057	0.053
Bi	<0.008	0.031	<0.013	<0.014	nd	0.075	0.013	<0.011	0.30	0.30
In	0.008	0.33	0.004	0.027	nd	0.088	0.003	0.006	8.2	6.1

SAMPLE	AD-VE-4	AD-BG-1	AD-I-1	AD-I-2	AD-I-3	AD-I-4	AD-I-5	AD-I-6	AD-R-1t	AD-R-2
COLOUR	Emerlad green	Emerald green	Colourless	Colourless	Colourless	Colourless	Colourless	Colourless	Colourless	Colourless
Li	3.9	4.8	2.6	nd	nd	5.5	4.6	2.6	4.1	5.1
B	101	194	76	nd	nd	224	247	135	175	162
V	18	26	17	13	16	9.6	9.9	5.3	21	26
Cr	19	14	13	26	14	9.7	12	7.6	11	9.7
Co	7.2	11	6.7	<3	3	1.8	2.3	0.81	9.6	12
Ni	10	23	13	5	4	3.8	4.6	2.3	11	24
Zn	30	785	14	24	22	16	14	11	17	28
Rb	6.1	3.8	8.5	13	17	6.1	5.4	4.2	11	13
Sr	328	721	592	323	375	347	370	373	498	587
Y	4.7	4.9	6.9	7	5	4.5	5.3	4.4	6.1	6.5
Zr	68	68	27	77	51	52	57	35	31	28
Nb	2.2	2.6	0.87	13	4	1.6	1.6	1.1	1.2	1.2
Cs	0.080	0.060	0.095	nd	nd	0.095	0.080	0.032	0.11	0.093
Ba	191	218	230	<10	195	143	150	110	273	293
La	5.7	6.2	6.7	<10	<10	5.3	5.6	4.6	5.8	6.4
Ce	10	11	12	51	22	9.83	10	8.26	11	11
Nd	5.3	5.6	6.0	<10	<10	4.5	5.3	4.6	5.3	6.1
Sm	1.1	1.0	1.0	nd	nd	1.2	1.4	0.79	0.96	1.3
Eu	0.28	0.31	0.34	nd	nd	0.23	0.25	0.24	0.37	0.30
Gd	0.86	1.1	1.1	nd	nd	0.69	0.99	0.89	0.78	1.2
Tb	0.16	0.16	0.14	nd	nd	0.11	0.15	0.13	0.18	0.17
Dy	0.80	1.1	1.2	nd	nd	0.80	0.90	0.77	1.00	1.1
Er	0.46	0.51	0.64	nd	nd	0.49	0.57	0.37	0.60	0.50
Yb	0.56	0.41	0.64	nd	nd	0.57	0.58	0.27	0.53	0.57
Lu	0.087	0.10	0.067	nd	nd	0.055	0.067	0.040	0.072	0.050
Hf	1.5	1.8	0.60	nd	nd	1.2	1.3	0.88	0.98	0.55
Ta	0.12	0.14	0.028	nd	nd	0.095	0.11	0.068	0.090	0.086
Pb	151	395	15	1192	116	53	47	225	9.9	10
Th	1.1	1.2	0.61	<3	<3	0.90	0.81	0.75	0.70	0.70
U	0.84	0.96	1.0	<3	<3	1.1	1.2	0.89	1.4	0.71
Cu	19551	16702	88	151	155	10	11	6.3	30	16
As	7.2	12	2.0	nd	nd	23	13	12	2.3	3.3
Ag	5.0	5.1	0.030	nd	nd	0.27	0.16	0.077	1.0	0.075
Sn	1656	999	0.75	nd	nd	2.1	2.3	4.6	0.78	0.85
W	0.077	0.13	0.063	nd	nd	0.072	<0.029	0.058	0.17	0.21
Tl	0.068	0.018	0.17	nd	nd	0.013	0.044	0.18	0.050	0.21
Bi	0.22	0.31	0.016	nd	nd	0.036	0.037	0.021	0.020	<0.009
In	6.7	3.9	0.007	nd	nd	0.011	0.009	0.023	<0.007	<0.009

SAMPLE	AD-V-1	AD-V-2	AD-V-3	AD-V-4	AD-VB-1	AD-AM-1	AD-AM-2	AD-AB-1	AD-AB-2	AD-AB-3
COLOUR	Purple	Purple	Purple	Purple	Purple	Amber	Amber	Amber	Amber	Amber
Li	3.8	6.0	3.6	4.5	4.7	nd	4.0	3.3	2.9	4.1
B	194	160	163	213	121	nd	168	333	251	243
V	39	13	18	38	34	10	6.7	4.8	6.1	6.5
Cr	10	7.8	13	18	13	13	8.3	9.1	9.8	11
Co	67	15	14	25	16	<3	3.6	2.0	3.5	2.7
Ni	28	9.9	21	27	20	3	3.5	3.4	4.2	4.4
Zn	38	19	30	25	23	15	8.1	8.8	10	8.9
Rb	8.1	8.2	6.8	8.2	10	15	11	9	8.9	10
Sr	626	592	581	657	595	353	439	381	379	384
Y	6.2	6.6	6.9	6.4	5.5	7	5.7	5.7	6.2	6.0
Zr	35	32	34	30	26	38	27	30	31	32
Nb	1.1	1.2	1.2	1.2	0.98	4	0.98	1.3	1.1	1.1
Cs	0.071	0.45	0.091	0.058	0.13	nd	0.077	0.054	0.072	0.072
Ba	383	1277	300	363	374	234	219	198	211	224
La	6.4	6.2	6.4	6.1	6.2	10	5.7	5.2	5.9	5.7
Ce	11	11	11	11	10	17	11	11	10	11
Nd	5.9	6.3	5.9	5.5	5.2	<10	6.1	5.1	5.5	5.6
Sm	1.1	1.0	1.3	0.93	1.1	nd	1.0	1.3	0.98	1.2
Eu	0.39	0.37	0.42	0.29	0.45	nd	0.36	0.36	0.38	0.33
Gd	1.0	1.2	1.0	0.97	1.1	nd	0.96	0.77	1.1	1.0
Tb	0.13	0.16	0.20	0.18	0.17	nd	0.16	0.16	0.16	0.16
Dy	1.2	1.1	1.2	1.1	1.0	nd	1.1	0.90	1.1	0.98
Er	0.63	0.54	0.59	0.62	0.56	nd	0.51	0.55	0.53	0.49
Yb	0.58	0.41	0.72	0.55	0.59	nd	0.52	0.49	0.54	0.49
Lu	0.091	0.086	0.094	0.067	0.056	nd	0.068	0.065	0.096	0.086
Hf	0.79	0.73	0.70	0.76	0.81	nd	0.80	0.79	0.76	0.99
Ta	0.082	0.063	0.10	0.050	0.072	nd	0.066	0.053	0.072	0.079
Pb	37	23	11	16	8.6	15	13	14	23	4.9
Th	0.74	0.78	0.78	0.64	0.58	<3	0.73	0.70	0.72	0.74
U	1.0	0.78	1.1	1.4	1.8	<3	1.9	1.1	0.69	0.75
Cu	138	26	15	24	12	48	10	8.0	12	13
As	3.4	2.9	2.2	2.5	2.1	nd	1.2	1.1	<0.57	1.1
Ag	0.040	0.030	<0.020	0.026	0.20	nd	<0.034	0.45	0.056	<0.035
Sn	5.8	2.1	1.8	1.8	0.67	nd	1.1	1.6	3.8	2.1
W	0.22	0.11	0.14	0.27	0.18	nd	0.058	0.034	0.10	<0.055
Tl	0.12	0.074	0.28	0.18	0.082	nd	0.020	0.024	<0.009	<0.012
Bi	0.017	0.014	0.022	0.008	0.058	nd	<0.009	<0.008	<0.012	<0.010
In	0.058	0.038	0.027	0.012	<0.009	nd	0.006	0.012	0.027	0.010

SAMPLE	AD-AB-4	AD-AB-5	AD-AB-6	AD-ABP1	AD-N-1
COLOUR	Amber	Amber	Amber	Amber	Black
Li	3.4	3.1	4.8	3.8	5.3
B	121	243	217	261	204
V	7.8	5.7	7.1	4.8	20
Cr	11	6.8	11	5.6	36
Co	2.3	2.4	1.6	0.86	12
Ni	3.6	4.4	3.7	2.1	8.6
Zn	8.1	8.3	9.1	5.1	33
Rb	10	9.5	9.3	8.6	6.5
Sr	440	370	416	380	449
Y	6.1	5.7	6.1	5.8	5.9
Zr	29	29	31	32	84
Nb	0.95	1.1	1.4	1.1	3.3
Cs	0.090	0.044	0.082	0.070	0.042
Ba	192	212	214	197	253
La	5.4	5.7	6.2	5.8	6.6
Ce	11	10	12	10	13
Nd	5.8	5.5	6.6	6.1	6.3
Sm	1.0	1.1	0.92	1.1	1.5
Eu	0.44	0.42	0.33	0.27	0.28
Gd	1.2	1.2	1.0	0.85	1.3
Tb	0.16	0.16	0.14	0.17	0.17
Dy	0.87	0.92	0.89	1.0	1.0
Er	0.46	0.50	0.55	0.61	0.59
Yb	0.51	0.56	0.42	0.50	0.55
Lu	0.052	0.078	0.050	0.074	0.078
Hf	0.82	0.58	0.73	0.71	1.9
Ta	0.081	0.060	0.086	0.043	0.18
Pb	11	7.2	7.8	4.7	17
Th	0.64	0.60	0.84	0.76	1.3
U	0.73	0.73	1.2	0.65	1.2
Cu	7.6	18	5.3	2.8	32
As	1.8	1.1	2.0	1.5	<0.172
Ag	0.055	<0.038	0.054	0.059	0.054
Sn	2.4	2.2	0.37	0.42	2.4
W	<0.040	0.036	<0.00	<0.035	0.11
Tl	0.016	<0.0095	0.027	<0.0153	0.009
Bi	<0.012	0.016	0.020	<0.012	<0.007
In	0.021	0.015	0.003	<0.013	0.026

Table D.2: Trace element composition, expressed as ppm, of transparent Adria glasses. Data are given by LA-ICP-MS, except for samples AD-BB-11b (EPMA data) and AD-I-2, AD-I-3, AD-AM-1 (XRF data). (nd: not determined).

SAMPLE	COLOUR	OPACIFIER	SiO ₂	Na ₂ O	CaO	Al ₂ O ₃	K ₂ O	MgO	Fe ₂ O ₃	TiO ₂	MnO	Sb ₂ O ₃	P ₂ O ₅	SO ₃	Cl	PHO	Total	Co	Ni	Cu	Zn	Sn
AD-BB-1w	white	Calcium antimonate	61.90	15.07	7.74	2.37	0.61	0.66	0.28	0.01	0.92	7.19	0.15	0.74	0.68	<0.08	98.30	<200	<350	<300	<300	<300
AD-BB-3w	white	Calcium antimonate	61.19	13.08	9.54	2.58	0.53	0.78	0.38	0.04	0.29	6.43	0.26	0.48	0.73	<0.08	96.30	<200	<350	<300	<300	<300
AD-R-1w	white	Calcium antimonate	63.88	12.96	5.66	2.37	0.84	1.37	0.49	0.10	0.95	4.80	0.36	0.40	0.58	5.34	100.10	<200	<350	491	<300	921
AD-R-2w	white	Calcium antimonate	64.41	13.16	7.97	2.62	0.74	0.84	0.38	0.03	1.02	7.15	0.14	0.51	0.52	<0.08	99.50	<200	<350	<300	<300	<300
AD-YB-1w	white	Calcium antimonate	62.14	14.63	9.08	2.40	0.61	0.89	0.30	0.02	0.85	6.60	0.14	0.61	0.63	<0.08	98.92	<200	<350	<300	<300	<300
AD-NF-5w	white	Calcium antimonate	68.44	12.92	7.30	2.32	0.69	0.49	0.25	0.02	<0.04	6.05	0.06	0.45	1.18	<0.08	100.20	<200	<350	<300	<300	<300
AD-NF-2w	white	Calcium antimonate	71.56	14.00	5.91	1.19	1.23	0.63	0.50	0.17	<0.04	2.93	0.11	0.34	0.88	<0.08	99.46	<200	<350	<300	<300	<300
AD-ABP-1w	white	Calcium antimonate	66.48	12.47	9.07	2.56	0.48	0.77	0.35	0.04	<0.04	5.84	0.18	0.47	0.75	<0.08	99.71	<200	<350	<300	<300	<300
AD-NF-3w	white	Calcium antimonate	67.34	14.42	9.09	2.41	0.50	0.66	0.43	0.05	<0.04	3.47	0.06	0.28	1.36	<0.08	100.08	<200	<350	<300	<300	<300
AD-AB-4w	white	Calcium antimonate	67.29	13.74	7.41	2.75	0.77	0.69	0.34	0.04	0.59	3.94	0.09	0.48	0.82	<0.08	98.95	<200	<350	<300	<300	<300
AD-BO-1	white	Calcium antimonate	59.83	8.67	4.84	1.93	0.63	0.87	0.47	0.06	0.78	7.29	0.21	0.27	0.46	13.06	99.37	<200	<350	494	<300	<300
AD-BO-2	white	Calcium antimonate	68.42	12.22	7.50	2.37	0.47	0.57	0.26	0.01	0.26	6.93	0.12	0.43	0.73	<0.08	100.28	<200	<350	<300	<300	<300
AD-BO-3	white	Calcium antimonate	66.51	12.28	7.28	2.38	0.43	0.59	0.25	0.01	0.25	7.48	0.10	0.47	0.80	<0.08	98.83	<200	<350	<300	<300	<300
AD-P-1wt	wisteria	Calcium antimonate	66.03	13.02	8.08	2.47	0.63	0.73	0.81	0.03	0.42	7.45	0.22	0.50	0.61	<0.08	101.00	896	<350	2192	<300	<300
AD-BLO-1	opaque blue	Calcium antimonate	70.09	13.70	8.04	2.66	0.57	0.67	0.54	0.06	0.41	1.90	0.18	0.32	1.05	<0.08	100.20	518	<350	784	<300	<300
AD-NF-1lb	light blue	Calcium antimonate	67.92	14.20	9.14	2.38	0.67	0.61	0.34	0.07	<0.04	1.27	<0.02	0.33	1.02	<0.08	97.98	<200	<350	1293	<300	<300
AD-NF-5lb	light blue	Calcium antimonate	67.38	13.46	7.86	2.01	0.52	0.50	0.27	0.05	<0.04	1.56	0.05	0.18	1.50	<0.08	95.36	<200	<350	2233	<300	<300
AD-NF-7y	yellow	Lead antimonate	57.35	11.73	5.67	1.92	0.46	0.47	1.01	0.06	<0.04	1.16	0.08	0.23	1.29	19.29	100.73	<200	<350	433	<300	<300
AD-BG-1y	yellow	Lead antimonate	65.96	13.65	3.38	1.94	0.52	0.72	1.21	0.17	0.76	0.65	0.12	0.21	1.46	9.91	100.65	<200	<350	<300	<300	1784
AD-AG-1y	yellow	Lead antimonate	63.85	13.65	7.01	2.67	0.58	0.70	0.70	0.06	0.56	0.76	0.08	0.28	1.02	8.76	100.67	<200	<350	<300	<300	<300
AD-NF-5y	yellow	Lead antimonate	62.51	11.70	7.04	1.89	0.56	0.42	0.75	0.05	<0.04	1.51	<0.02	0.07	0.88	15.96	103.40	<200	<350	2859	<300	<300
AD-NF-6y	yellow	Lead antimonate	58.50	10.94	4.77	0.92	0.22	0.53	1.15	0.10	<0.04	1.13	0.06	0.44	1.11	20.36	100.26	<200	<350	<300	<300	<300
AD-NF-1y	yellow	Lead antimonate	62.06	10.98	6.71	2.14	0.43	0.42	1.02	0.05	<0.04	1.20	0.06	0.32	0.74	15.61	101.76	<200	<350	992	<300	<300

Table D.3: Mean chemical composition (EPMA data) in weight per cent (element oxides) for Adria opaque glasses. Traces are expressed as ppm.

SAMPLE	COLOUR	AGE (cent. AD)	TYPE	SiO ₂	Na ₂ O	CaO	Al ₂ O ₃	K ₂ O	MgO	Fe ₂ O ₃	TiO ₂	MnO	Sb ₂ O ₃	P ₂ O ₅	SO ₃	Cl	Tot	GROUP	
AQ106-1	green	late 3rd-5th	Isings 106c	66.19	18.22	6.71	2.82	0.61	1.00	1.60	0.46	1.93	<0.04	0.07	0.25	1.08	100.94	GROUP AQ/1b	
AQ106-2	green	late 3rd-5th	Isings 106c	65.28	18.81	6.07	2.99	0.37	1.30	1.90	0.56	1.83	<0.04	0.04	0.13	1.51	100.79	GROUP AQ/1b	
AQ106-3	green	late 3rd-5th	Isings 106c	67.47	17.40	6.00	2.50	0.42	0.99	1.59	0.60	2.08	<0.04	0.06	0.26	1.22	100.59	GROUP AQ/1b	
AQ106-4	light blue	late 3rd-5th	Isings 106c	66.37	20.54	5.55	2.43	0.41	0.91	0.95	0.26	1.37	<0.04	0.04	0.23	1.82	100.88	GROUP AQ/1b	
AQ106-5	green	late 3rd-5th	Isings 106c	64.69	19.22	6.21	2.96	0.42	1.06	2.00	0.59	2.01	<0.04	0.04	0.28	1.34	100.82	GROUP AQ/1b	
AQ106-6	yellow	late 3rd-5th	Isings 106c	64.07	19.33	7.25	2.69	0.52	1.26	1.92	0.51	2.07	<0.04	0.08	0.32	1.27	101.29	GROUP AQ/1b	
AQ106-7	yellow	late 3rd-5th	Isings 106c	65.54	18.82	4.97	2.92	0.40	1.02	2.26	0.58	2.31	<0.04	0.04	0.25	1.19	100.30	GROUP AQ/1b	
AQ106-8	green	late 3rd-5th	Isings 106c	64.73	18.55	5.22	3.09	0.44	1.15	3.55	0.60	1.69	<0.04	0.12	0.27	1.20	100.62	GROUP AQ/1a	
AQ106-9	green	late 3rd-5th	Isings 106c	63.56	19.65	6.05	3.04	0.50	1.20	2.09	0.61	2.19	<0.04	0.08	0.21	1.43	100.61	GROUP AQ/1b	
AQ106-10	green	late 3rd-5th	Isings 106c	65.86	18.84	6.88	2.68	0.67	0.81	1.38	0.37	1.55	<0.04	0.06	0.29	1.19	100.57	GROUP AQ/1b	
AQ106-11	light blue	late 3rd-5th	Isings 106c	69.49	15.64	8.39	2.87	0.54	0.64	0.41	0.07	1.04	<0.04	0.10	0.24	1.17	100.59	GROUP AQ/2a	
AQ106-12	light blue	late 3rd-5th	Isings 106c	69.63	16.19	8.41	2.85	0.83	0.48	0.33	0.06	0.03	<0.04	0.09	0.10	1.53	100.53	GROUP AQ/2b	
AQ106-13	light blue	late 3rd-5th	Isings 106c	68.03	18.03	5.81	2.43	0.39	1.00	1.22	0.40	1.60	<0.04	0.05	0.22	1.47	100.64	GROUP AQ/1b	
AQ106-14	light blue	late 3rd-5th	Isings 106c	65.82	18.00	5.84	2.40	0.39	0.98	1.22	0.40	1.60	<0.04	0.05	0.26	1.15	98.11	GROUP AQ/1b	
AQ106-15	light blue	late 3rd-5th	Isings 106c	66.66	16.31	9.92	3.08	1.36	0.48	0.38	0.07	1.07	<0.04	0.13	0.19	0.71	100.36	GROUP AQ/2a	
AQ106-16	green	late 3rd-5th	Isings 106c	70.01	18.99	5.64	1.96	0.38	0.67	0.90	0.12	0.45	<0.04	0.17	0.05	0.29	1.49	100.11	GROUP AQ/3
AQ106-17	green	late 3rd-5th	Isings 106c	69.74	16.06	7.42	2.76	1.23	0.45	0.59	0.08	1.01	<0.04	0.20	0.18	0.81	100.53	GROUP AQ/2a	
AQ106-18	green	late 3rd-5th	Isings 106c	66.91	18.02	5.64	2.49	0.43	0.91	1.63	0.60	2.30	<0.04	0.04	0.26	1.14	100.37	GROUP AQ/1b	
AQ106-19	green	late 3rd-5th	Isings 106c	62.97	18.83	6.17	3.08	0.55	1.23	3.37	0.55	2.28	<0.04	0.15	0.30	1.24	100.72	GROUP AQ/1a	
AQ106-20	light blue	late 3rd-5th	Isings 106c	65.46	18.24	9.92	2.89	0.73	0.62	0.42	0.08	0.13	0.07	0.07	0.17	1.18	99.97	GROUP AQ/2b	
AQ106-21	light blue	late 3rd-5th	Isings 106c	65.69	18.51	9.85	2.92	0.72	0.62	0.49	0.08	0.14	<0.04	0.06	0.30	1.35	100.75	GROUP AQ/2b	
AQ116-1	light blue	late 3rd-5th	Isings 116	66.97	17.00	8.03	2.52	1.26	0.51	0.46	0.09	0.95	<0.04	0.13	0.15	0.97	99.05	GROUP AQ/2a	
AQ116-2	Colourless/yellow	late 3rd-5th	Isings 116	66.26	19.77	6.25	2.09	0.42	0.70	0.82	0.13	1.13	<0.04	0.05	0.26	1.72	99.60	GROUP AQ/3	
AQ116-3	Colourless/yellow	late 3rd-5th	Isings 116	67.57	20.16	5.93	1.85	0.36	0.69	0.74	0.12	1.36	<0.04	0.04	0.21	1.79	100.82	GROUP AQ/3	
AQ116-4	green	late 3rd-5th	Isings 116	64.87	19.35	6.10	2.58	0.46	0.96	2.23	0.52	1.69	<0.04	0.05	0.27	1.70	100.78	GROUP AQ/1b	
AQ116-5	Colourless/green	late 3rd-5th	Isings 116	67.20	19.87	6.29	2.11	0.43	0.70	0.82	0.13	1.13	<0.04	0.06	0.29	1.38	100.42	GROUP AQ/3	
AQ116-6	green	late 3rd-5th	Isings 116	69.85	18.55	5.76	1.84	0.35	0.44	0.44	0.08	1.06	<0.04	0.03	0.13	1.81	100.33	GROUP AQ/3	
AQ116-7	Colourless/green	late 3rd-5th	Isings 116	66.65	20.08	6.46	2.45	0.40	0.91	1.00	0.27	0.74	<0.04	0.04	0.34	1.34	100.68	GROUP AQ/1b	
AQ116-8	green	late 3rd-5th	Isings 116	65.26	18.67	6.03	3.00	0.37	1.28	1.91	0.55	1.89	<0.04	0.04	0.36	1.40	100.75	GROUP AQ/1b	
AQ117-1	light blue	late 3rd-5th	Isings 117	66.81	16.34	9.81	3.10	1.36	0.48	0.38	0.07	0.99	<0.04	0.12	0.15	0.54	100.14	GROUP AQ/2a	
AQ117-2	yellow	late 3rd-5th	Isings 117	62.73	21.42	5.23	2.40	0.32	0.77	1.55	0.59	2.19	<0.04	0.04	0.33	1.52	99.09	GROUP AQ/1b	
AQ117-3	green	late 3rd-5th	Isings 117	66.34	16.15	9.19	3.01	1.44	0.47	0.42	0.07	1.13	<0.04	0.21	0.20	0.73	99.37	GROUP AQ/2a	
AQ117-4	green	late 3rd-5th	Isings 117	65.54	17.49	6.23	3.04	0.66	1.07	2.80	0.49	1.69	<0.04	0.13	0.21	1.12	100.49	GROUP AQ/1a	
AQ117-5	green	late 3rd-5th	Isings 117	68.30	15.15	6.12	3.17	0.48	1.09	1.98	0.60	2.23	<0.04	0.05	0.15	1.16	100.48	GROUP AQ/1b	

AQ-6I	green	late 3rd-5th	—	63.78	18.76	6.01	2.97	0.51	1.15	2.17	0.57	2.40	<0.04	0.07	0.26	1.24	99.89	GROUP AQ/1b
AQ117-7	green	late 3rd-5th	Isings 117	64.95	18.25	6.19	2.82	0.55	1.02	1.71	0.47	1.95	<0.04	0.07	0.23	1.27	99.49	GROUP AQ/1b
AQ132-1a	green	late 3rd-5th	Isings 132	65.29	16.39	5.55	3.01	0.46	1.44	4.13	0.64	1.57	<0.04	0.15	0.16	1.32	100.11	GROUP AQ/1a
AQ132-1b	yellow	late 3rd-5th	Isings 132	67.84	14.93	6.29	3.14	0.45	1.10	2.04	0.58	2.44	<0.04	0.05	0.17	1.20	100.24	GROUP AQ/1b
AQ104-2	yellow	late 3rd-5th	Isings 104	63.80	19.78	6.03	3.05	0.50	1.18	2.07	0.61	2.14	<0.04	0.08	0.30	1.34	100.88	GROUP AQ/1b
AQ104-3	yellow	late 3rd-5th	Isings 104	64.32	18.33	5.15	3.07	0.43	1.13	3.47	0.59	1.63	<0.04	0.11	0.25	1.29	99.77	GROUP AQ/1a
AQ104-4	green	late 3rd-5th	Isings 104	66.30	17.65	6.45	2.95	0.66	1.03	2.46	0.45	1.58	<0.04	0.11	0.21	1.17	101.02	GROUP AQ/1a
AQ104-5	green	late 3rd-5th	Isings 104	65.61	18.80	5.99	3.16	0.56	1.19	1.84	0.61	1.91	<0.04	0.06	0.30	1.36	101.39	GROUP AQ/1b
AQ104-6	yellow/green	late 3rd-5th	Isings 104	62.57	19.58	5.95	3.02	0.49	1.16	2.08	0.60	2.15	<0.04	0.08	0.30	1.36	99.34	GROUP AQ/1b
AQ104-7	yellow/green	late 3rd-5th	Isings 104	63.81	20.45	5.56	2.75	0.43	0.99	2.09	0.57	2.00	<0.04	0.05	0.34	1.40	100.45	GROUP AQ/1b
AQ/cfm-1	green	late 3rd-5th	Isings 87 or 120	64.71	19.43	5.90	2.99	0.42	1.16	2.18	0.55	2.13	<0.04	0.05	0.23	1.42	101.17	GROUP AQ/1b
AQ/cfm-2	green	late 3rd-5th	Isings 87 or 120	66.39	18.30	6.41	2.76	0.49	0.93	1.77	0.49	1.98	<0.04	0.05	0.22	1.32	101.11	GROUP AQ/1b
AQ/cfm-3	green	late 3rd-5th	Isings 87 or 120	67.32	16.71	5.94	2.90	0.40	0.86	2.06	0.57	2.55	<0.04	0.06	0.20	1.34	100.90	GROUP AQ/1b
AQ/cfm-4b	light blue	late 3rd-5th	Isings 87 or 120	65.40	16.96	10.54	3.08	0.88	0.63	0.71	0.12	0.31	<0.04	0.08	0.19	1.41	100.32	GROUP AQ/2b
AQ/cfm-4v	green	late 3rd-5th	Isings 87 or 120	65.55	17.27	11.43	3.16	0.93	0.58	0.42	0.06	0.07	<0.04	0.07	0.18	1.43	101.16	GROUP AQ/2b
AQ/cfm-5	green	late 3rd-5th	Isings 87 or 120	64.34	18.77	5.81	3.05	0.42	0.99	1.99	0.60	1.62	<0.04	0.05	0.26	1.32	99.23	GROUP AQ/1b
AQ/cfm-6	green	late 3rd-5th	Isings 87 or 120	65.65	18.25	6.77	2.72	0.60	0.98	1.60	0.40	1.81	<0.04	0.08	0.23	1.20	100.29	GROUP AQ/1b
AQ111-1	green	5th-8th	Isings 111	65.33	20.43	7.14	1.95	0.43	0.72	1.10	0.15	0.96	<0.04	0.06	0.37	1.41	100.05	GROUP AQ/3
AQ111-2	light blue	5th-8th	Isings 111	68.75	20.00	6.90	1.95	0.45	0.70	1.04	0.15	1.03	<0.04	0.07	0.37	1.43	102.84	GROUP AQ/3
AQ111-3	light blue	5th-8th	Isings 111	66.55	17.07	8.68	2.88	1.45	0.54	0.57	0.11	1.58	<0.04	0.17	0.21	0.66	100.47	GROUP AQ/2a
AQ111-4	green	5th-8th	Isings 111	68.77	16.71	5.36	2.80	0.43	0.94	1.42	0.46	1.74	<0.04	0.04	0.19	1.31	100.17	GROUP AQ/1b
AQ111-5	light blue	5th-8th	Isings 111	69.17	19.16	5.79	1.88	0.39	0.61	0.64	0.10	0.84	<0.04	0.04	0.33	1.45	100.39	GROUP AQ/3
AQ111-6	light blue	5th-8th	Isings 111	64.77	17.23	10.35	3.06	1.50	0.51	0.38	0.06	1.22	<0.04	0.20	0.22	0.63	100.13	GROUP AQ/2a
AQ111-7	light blue	5th-8th	Isings 111	66.11	16.48	9.30	2.98	1.43	0.53	0.58	0.09	1.47	<0.04	0.18	0.18	0.72	100.04	GROUP AQ/2a
AQ111-8	green	5th-8th	Isings 111	65.60	17.96	5.11	2.79	0.55	1.00	2.81	0.50	2.04	nd	0.09	nd	nd	98.44	GROUP AQ/1a
AQ111-9	green	5th-8th	Isings 111	66.65	19.76	6.92	2.39	0.48	1.16	1.09	0.31	0.50	nd	0.11	nd	nd	99.37	GROUP AQ/1b
AQ111-10	light blue	5th-8th	Isings 111	65.08	17.51	9.82	2.99	1.36	0.54	0.52	0.09	1.32	nd	0.16	0.24	0.61	100.24	GROUP AQ/2a
AQ111-11	light blue	5th-8th	Isings 111	71.48	16.17	6.05	1.92	0.48	0.51	0.63	0.09	0.88	nd	0.04	nd	nd	98.24	GROUP AQ/3

Table D-4: chemical composition, expressed as wt% of element oxides, of Aquileia glasses. Data are given by XRF, except for Sb₂O₃, Cl and SO₃, given by EPMA. Colour, age and compositional group of each sample are also reported (nd: not determined).

SAMPLE	Co	Ni	Cu	Zn	Sn	Pb	Rb	Sr	Ba	Zr	Nd	La	Ce	Th	U	V	Ga	Y	Nb	Cr
AQ106-1	10	20	96	30	<300	78	15	459	964	221	<10	14	21	<3	<3	55	<5	11	6	54
AQ106-2	9	19	102	27	<300	20	12	423	867	260	<10	<10	10	<3	<3	60	<5	12	6	62
AQ106-3	12	18	88	26	<300	10	12	447	459	307	<10	<10	31	<3	3	46	4	12	6	70
AQ106-4	10	24	71	20	<300	50	13	405	369	130	<10	<10	<10	<3	<3	34	<5	7	4	32
AQ106-5	11	16	132	33	<300	30	14	446	668	282	<10	10	26	<3	<3	65	7	13	6	70
AQ106-6	7	22	122	32	<300	79	12	634	213	245	<10	<10	24	<3	<3	51	<5	13	5	57
AQ106-7	13	19	118	28	<300	10	12	371	974	276	<10	<10	29	<3	4	57	8	13	7	65
AQ106-8	8	41	131	43	<300	24	14	392	332	268	<10	16	26	<3	<3	90	<5	16	6	79
AQ106-9	19	18	386	70	<300	347	12	470	1137	283	<10	<10	13	<3	3	57	11	11	10	77
AQ106-10	7	16	73	23	<300	27	16	465	933	186	<10	18	17	<3	<3	42	<5	10	5	38
AQ106-11	<3	12	31	16	<300	28	15	445	317	40	<10	<10	14	<3	<3	13	11	8	3	22
AQ106-12	<3	6	11	10	<300	31	22	456	252	38	<10	<10	<10	<3	<3	7	8	7	4	13
AQ106-13	9	14	128	27	<300	121	13	413	376	185	<10	<10	21	<3	<3	37	9	10	6	42
AQ106-14	9	13	89	25	<300	109	10	423	369	183	<10	<10	19	<3	4	42	6	10	5	39
AQ106-15	<3	8	23	13	<300	22	26	537	429	38	<10	<10	<10	<3	<3	17	10	8	2	<6
AQ106-16	3	26	45	28	<300	23	14	384	176	61	12	<10	13	<3	<3	25	0	7	2	16
AQ106-17	3	11	47	17	<300	34	26	398	261	48	<10	<10	<10	<3	<3	18	<5	8	2	14
AQ106-18	8	15	78	28	<300	12	12	451	385	322	<10	<10	<10	<3	<3	53	5	12	6	70
AQ106-19	19	41	237	62	<300	167	13	505	590	260	<10	11	12	<3	<3	90	6	15	6	61
AQ106-20	<3	3	11	9	<300	11	21	522	289	42	<10	<10	<10	<3	<3	10	<5	8	4	9
AQ106-21	<3	23	25	12	<300	5	17	511	279	42	<10	11	12	<3	4	14	<5	8	<3	67
AQ116-1	4	6	153	23	<300	103	20	417	326	51	<10	15	<10	<3	3	21	7	8	<3	12
AQ116-2	6	13	88	22	<300	45	12	478	240	64	<10	11	<10	<3	<3	21	<5	7	<3	11
AQ116-3	4	10	58	19	<300	17	11	422	213	61	<10	<10	17	<3	<3	28	6	7	<3	14
AQ116-4	10	16	109	35	<300	25	11	462	1060	250	<10	10	<10	<3	<3	59	9	12	6	55
AQ116-5	7	12	90	20	<300	42	10	483	238	64	<10	<10	20	<3	7	24	<5	7	<3	14
AQ116-6	3	7	29	16	<300	24	11	419	252	50	<10	<10	<10	<3	4	20	<5	6	<3	7
AQ116-7	14	11	87	28	<300	68	12	515	245	137	<10	<10	21	<3	3	25	8	8	4	30
AQ116-8	9	15	109	28	<300	19	12	428	891	263	<10	<10	<10	<3	<3	60	<5	12	5	60
AQ117-1	<3	6	26	15	<300	11	24	545	397	37	<10	11	29	<3	4	17	9	8	<3	9
AQ117-2	6	18	44	26	<300	18	12	407	299	299	<10	23	15	<3	<3	52	<5	12	7	72
AQ117-3	<3	9	36	16	<300	192	25	446	335	41	<10	<10	15	<3	4	17	<5	8	3	7
AQ117-4	12	32	146	44	<300	61	15	444	454	228	<10	<10	<10	<3	3	76	5	15	6	58
AQ117-5	12	18	128	31	<300	11	13	435	748	259	<10	13	27	<3	3	68	9	13	7	66
AQ-61	22	17	244	39	<300	172	13	476	553	256	<10	<10	28	<3	3	52	<5	12	8	70

AQ117-7	13	15	151	31	<300	105	432	724	213	<10	<10	20	<3	<3	41	8	11	7	59
AQ132-1a	10	46	145	51	<300	37	443	256	287	<10	<10	30	<3	<3	102	<5	18	7	75
AQ132-1b	14	14	89	32	<300	16	450	939	252	<10	<10	14	<3	3	72	5	12	6	60
AQ104-2	17	17	481	79	<300	374	480	1007	292	<10	<10	14	<3	<3	60	11	13	10	80
AQ104-3	9	36	119	42	<300	22	396	317	266	14	11	22	<3	4	90	6	17	6	76
AQ104-4	11	29	132	40	<300	42	448	437	203	11	<10	18	<3	4	68	7	13	7	69
AQ104-5	11	15	105	30	<300	69	421	463	279	<10	<10	25	<3	<3	60	7	13	7	84
AQ104-6	17	17	460	75	<300	357	474	1027	288	<10	<10	13	<3	<3	54	<5	12	10	78
AQ104-7	12	14	123	29	<300	26	406	424	274	<10	<10	16	<3	<3	54	9	12	6	67
AQ/cfm-1	13	16	204	32	<300	112	434	555	258	<10	<10	13	<3	<3	50	10	10	7	61
AQ/cfm-2	24	23	134	33	<300	41	466	871	235	<10	<10	21	<3	<3	54	8	11	5	51
AQ/cfm-3	13	18	174	38	<300	41	440	894	271	<10	<10	18	<3	<3	66	8	13	7	60
AQ/cfm-4b	33	17	75	20	<300	181	625	970	64	<10	<10	14	<3	<3	18	<5	10	4	33
AQ/cfm-4v	<3	24	41	15	<300	205	672	296	38	13	<10	21	<3	<3	5	<5	9	4	52
AQ/cfm-5	11	31	141	34	<300	21	414	519	270	<10	<10	15	<3	<3	58	<5	11	6	105
AQ/cfm-6	12	28	147	33	<300	230	468	923	190	<10	<10	<10	<3	<3	47	<5	10	8	77
AQ111-1	11	14	44	20	<300	45	497	248	80	<10	<10	3	<3	5	36	2	10	2	21
AQ111-2	6	16	48	22	<300	49	476	256	79	10	8	2	<3	<3	36	6	9	3	22
AQ111-3	11	17	79	20	<300	59	468	497	57	<10	<10	15	<3	<3	40	<5	7	3	22
AQ111-4	7	35	61	22	<300	16	408	548	194	<10	<10	<10	<3	3	51	7	11	6	70
AQ111-5	4	11	25	13	<300	19	411	244	54	<10	<10	5	<3	<3	25	2	6	3	14
AQ111-6	3	8	35	16	<300	22	565	450	36	<10	<10	13	<3	<3	28	<5	10	2	<6
AQ111-7	6	13	58	23	<300	43	502	384	47	<10	<10	<10	<3	<3	29	6	9	2	13
AQ111-8	14	28	110	43	nd	20	420	976	233	<10	<10	<10	<3	<3	73	8	13	4	59
AQ111-9	6	9	38	19	nd	68	534	226	153	<10	<10	13	<3	<3	30	5	9	5	37
AQ111-10	6	8	83	20	<300	49	484	480	51	<10	<10	<10	<3	<3	25	<5	8	3	11
AQ111-11	3	11	30	18	nd	16	435	315	51	<10	<10	6	<3	<3	31	3	5	3	12

Table D.5: Trace elements composition, expressed as ppm, of Aquileia glasses. Data are given by XRF, except for Sn data, given by EPMA (nd: no determined).

SAMPLE	COLOUR	AGE (cent. AD)	SiO ₂	Na ₂ O	CaO	Al ₂ O ₃	K ₂ O	MgO	Fe ₂ O ₃	TiO ₂	MnO	Sb ₂ O ₃	P ₂ O ₅	SO ₃	Cl	TOT	GROUP
SG111-1	Light blue	Late 5th-8th	65.61	16.82	7.49	2.33	0.87	1.07	1.30	0.12	0.68	0.69	0.25	0.31	1.25	98.79	TUS2
SG111-2	Light blue	Late 5th-8th	67.69	17.86	7.11	2.36	0.83	0.91	1.00	0.11	0.75	0.58	0.07	0.28	1.10	100.63	TUS2
SG111-3	Yellow	Late 5th-8th	63.68	16.80	8.06	2.68	0.71	1.36	1.42	0.26	1.93	<0.04	0.14	0.26	1.14	98.44	OUTLIER
SG111-4	Colourless	Late 5th-8th	67.05	16.83	7.31	2.08	0.58	0.71	0.70	0.13	1.33	<0.04	0.09	0.30	1.22	98.33	TUS3
SG111-5	Yellow	Late 5th-8th	63.70	18.23	8.13	2.30	0.73	1.04	0.95	0.14	1.73	<0.04	0.13	0.29	1.27	98.64	TUS2
SG111-6	Light blue	Late 5th-8th	67.83	18.11	6.46	2.27	0.76	0.85	0.74	0.14	0.65	1.10	0.17	0.33	1.29	100.71	OUTLIER
SG106-1	Green	4th-early 5th	61.45	17.80	5.81	2.84	0.46	1.07	4.08	0.59	1.64	<0.04	0.18	0.26	1.37	97.55	TUS1
PP111-1	Light blue	Late 5th-8th	66.77	17.69	6.93	2.39	0.70	0.99	1.20	0.13	0.68	0.83	0.14	0.29	1.38	100.14	TUS3
PP111-2	Green	Late 5th-8th	65.40	20.29	5.40	1.92	0.43	0.58	0.52	0.10	1.12	<0.04	0.03	0.45	1.32	97.55	TUS3
PP111-3	Light blue	Late 5th-8th	66.85	19.70	5.50	2.03	0.42	0.67	0.60	0.11	1.21	<0.04	0.03	0.37	1.24	98.73	TUS2
PP111-4	Green	Late 5th-8th	64.29	16.87	8.73	2.45	0.67	1.28	1.26	0.16	1.52	<0.04	0.13	0.26	1.26	98.88	TUS2
PP111-5	Colourless/Yellow	Late 5th-8th	64.63	18.70	7.29	2.47	0.58	0.96	0.92	0.15	1.55	<0.04	0.06	0.34	1.28	98.94	TUS2
PC111-1	Light blue	Late 5th-8th	66.46	17.64	7.35	2.44	0.80	0.96	1.20	0.15	0.98	0.49	0.12	0.28	1.20	100.07	TUS2
PC111-2	Green	Late 5th-8th	65.27	17.58	6.85	2.28	0.61	0.91	1.15	0.11	0.93	0.37	0.12	0.28	1.37	97.84	TUS2
PC111-3	Green	Late 5th-8th	67.23	17.13	6.81	2.47	0.84	0.93	1.07	0.13	0.71	0.86	0.17	0.29	1.20	99.85	TUS2

Table D.6: Chemical composition, expressed as wt% of element oxides, of Tuscan glasses. Data are given by XRF or EPMA (for details see Table B.1, Appendix B). For the samples analyzed by EPMA only means are reported. Colour, age and compositional group of each sample are also reported.

SAMPLE	Co	Ni	Cu	Zn	Sn	Pb	Rb	Sr	Ba	Zr	Nd	La	Ce	Th	U	V	Ga	Y	Nb	Cr
SG111-1	<300	<350	9408	<500	1692	16279	nd	nd	nd	nd	nd	nd	nd	nd	nd	nd	nd	nd	nd	nd
SG111-2	<300	<350	2812	<500	768	7611	nd	nd	nd	nd	nd	nd	nd	nd	nd	nd	nd	nd	nd	nd
SG111-3	14	240	105	52	<400	141	14	755	433	128	<10	<10	13	<3	<3	51	5	9	6	188
SG111-4	4	6	60	18	<400	76	13	532	271	67	<10	<10	<10	<3	5	27	7	7	4	15
SG111-5	4	34	104	28	<400	133	14	704	397	69	<10	13	13	<3	<3	33	<5	8	4	18
SG111-6	<300	<350	3130	<500	<400	4174	nd	nd	nd	nd	nd	nd	nd	nd	nd	nd	nd	nd	nd	nd
SG106-1	15	39	445	43	<400	53	14	439	253	284	<10	14	23	<3	3	112	6	18	8	76
PP111-1	<300	<350	6639	<500	848	11362	nd	nd	nd	nd	nd	nd	nd	nd	nd	nd	nd	nd	nd	nd
PP111-2	3	10	248	15	<400	16	13	440	331	57	<10	10	<10	<3	<3	25	<5	6	<3	12
PP111-3	3	10	39	15	<400	14	12	426	349	64	<10	<10	<10	<3	<3	27	9	5	<3	12
PP111-4	6	21	96	31	<400	123	15	730	257	79	<10	<10	13	<3	3	38	<5	8	4	12
PP111-5	3	10	105	20	<400	42	14	592	339	75	<10	<10	12	<3	<3	31	<5	8	3	15
PC111-1	<300	<350	5645	<500	1130	11240	nd	nd	nd	nd	nd	nd	nd	nd	nd	nd	nd	nd	nd	nd
PC111-2	<300	<350	5696	<500	3087	25832	nd	nd	nd	nd	nd	nd	nd	nd	nd	nd	nd	nd	nd	nd
PC111-3	<300	<350	7165	<500	872	10710	nd	nd	nd	nd	nd	nd	nd	nd	nd	nd	nd	nd	nd	nd

Table D.7: Trace elements composition, expressed as ppm, of Tuscan glasses. Data are given by XRF or EPMA (see Table B.1, Appendix B for details) (nd: no determined).

SAMPLE	TYPE	SiO ₂	Na ₂ O	CaO	Al ₂ O ₃	K ₂ O	MgO	Fe ₂ O ₃	TiO ₂	MnO	Sb ₂ O ₃	P ₂ O ₅	SO ₃	Cl	CoO	CuO	NiO	ZnO	SnO ₂	PbO	GROUP
ASL-01	Glass window	68.92	17.74	7.01	2.44	0.64	0.94	0.89	0.19	1.22	0.15	0.10	0.29	1.26	<0.02	0.08	nd	<0.04	0.05	0.13	N/1
ASL-02	Glass window	65.47	19.12	8.34	2.35	0.64	1.33	0.89	0.17	1.86	<0.04	0.10	0.47	1.16	<0.02	<0.04	nd	<0.04	<0.04	<0.08	N/2
ASL-03	Glass window	64.31	18.68	8.63	2.59	0.71	1.33	0.97	0.16	2.07	<0.04	0.11	0.37	1.10	<0.02	<0.04	<0.05	<0.04	<0.04	<0.08	N/2
ASL-04	Glass window	66.65	17.15	7.27	2.67	0.89	1.28	1.04	0.18	1.83	<0.04	0.14	0.43	1.06	0.04	<0.04	<0.05	<0.04	0.07	<0.08	N/2
ASL-05	Glass window	65.92	19.01	7.82	2.56	0.66	1.21	1.00	0.14	1.80	<0.04	0.11	0.44	1.27	<0.02	<0.04	nd	<0.04	<0.04	<0.08	N/2
ASL-06	Glass window	64.21	18.84	8.25	2.59	0.78	1.44	1.04	0.17	2.12	<0.04	0.15	0.46	1.18	<0.02	<0.04	<0.05	<0.04	<0.04	0.11	N/2
ASL-07	Glass window	66.99	18.28	8.15	2.35	0.66	1.27	0.86	0.16	1.52	<0.04	0.09	0.37	1.25	<0.02	0.05	nd	<0.04	<0.04	<0.08	N/2
ASL-08	Glass window	70.00	18.03	7.01	2.32	0.56	0.64	0.46	0.09	0.58	0.26	0.10	0.29	1.50	<0.02	<0.04	nd	<0.04	<0.04	<0.08	N/1
ASL-09	Glass window	65.89	11.11	12.00	2.47	2.41	3.52	0.81	0.12	1.60	<0.04	0.28	0.22	0.79	<0.02	<0.04	nd	<0.04	<0.04	<0.08	A/1
ASL-10	Glass window	69.20	12.80	8.87	2.34	2.47	3.48	0.55	0.07	0.58	<0.04	0.21	0.30	1.00	<0.02	<0.04	nd	<0.04	<0.04	<0.08	A/1
ASL-11	Glass window	69.71	14.07	9.08	0.84	2.09	3.15	0.30	0.06	0.57	<0.04	0.24	0.30	1.08	<0.02	<0.04	nd	<0.04	<0.04	<0.08	A/1
ASL-12	Glass window	65.71	14.29	9.31	2.05	2.44	4.47	0.56	0.08	0.94	<0.04	0.28	0.28	1.12	<0.02	<0.04	<0.05	<0.04	<0.04	<0.08	A/1
ASO-01	Beaker (nuppenbecher)	68.78	12.51	9.10	1.87	2.74	3.22	0.49	0.10	0.75	<0.04	0.35	0.22	1.15	<0.02	<0.04	<0.05	<0.04	<0.04	<0.08	A/1
ASO-02	Beaker (nuppenbecher)	67.33	13.51	10.34	1.35	2.25	3.81	0.55	0.08	0.71	<0.04	0.28	0.23	1.17	<0.02	<0.04	<0.05	<0.04	<0.04	0.11	A/1
ASO-03	Beaker (nuppenbecher)	65.92	10.65	12.35	3.06	2.71	2.86	0.47	0.09	1.27	<0.04	0.30	0.22	0.94	<0.02	<0.04	<0.05	<0.04	<0.04	0.12	A/2
ASO-04	Beaker (nuppenbecher)	66.97	12.64	10.03	1.41	2.38	4.19	0.38	0.07	0.94	<0.04	0.23	0.29	0.98	<0.02	<0.04	<0.05	<0.04	<0.04	<0.08	A/1
ASO-05	Beaker (nuppenbecher)	67.29	13.11	10.31	1.46	2.45	3.60	0.40	0.07	0.75	<0.04	0.28	0.22	1.10	<0.02	<0.04	<0.05	<0.04	<0.04	<0.08	A/1
ASO-06	Bottle (kropfflasche)	67.51	10.51	10.05	3.39	2.52	1.79	0.92	0.15	2.49	<0.04	0.30	0.09	1.08	<0.02	<0.04	<0.05	<0.04	<0.04	<0.08	A/3
ASO-07	Bottle (kropfflasche)	65.87	13.12	8.54	4.09	2.29	1.83	1.58	0.23	2.52	<0.04	0.46	0.10	1.33	<0.02	<0.04	<0.05	<0.04	<0.04	<0.08	A/3
ASO-08	Bottle (kropfflasche)	69.22	12.53	8.64	1.58	2.88	3.33	0.54	0.10	1.47	<0.04	0.35	0.18	0.93	<0.02	0.05	<0.05	<0.04	<0.04	<0.08	A/1
ASO-09	Bottle (kropfflasche)	70.90	14.74	3.70	2.84	2.10	1.83	1.46	0.36	2.16	<0.04	0.42	0.08	1.36	<0.02	<0.04	nd	<0.04	0.08	0.17	A/3
ASO-10	Bottle (kropfflasche)	66.37	12.96	8.22	3.71	2.31	2.01	1.30	0.21	2.32	<0.04	0.43	0.10	1.21	0.03	<0.04	nd	<0.04	<0.04	<0.08	A/3
ASO-11	Bottle (kropfflasche)	70.57	13.26	4.95	2.75	2.47	2.15	1.29	0.32	1.97	<0.04	0.39	0.07	1.07	<0.02	<0.04	nd	<0.04	0.05	0.14	A/3

ASO-12	Bottle (<i>anghistera</i>)	68.45	9.70	11.97	2.73	2.29	2.82	0.45	0.08	1.34	<0.04	0.20	0.13	0.96	<0.02	<0.04	nd	<0.04	<0.04	<0.08	A/2
ASO-13	Bottle (<i>anghistera</i>)	67.55	9.96	11.79	2.67	2.30	2.86	0.46	0.08	1.44	<0.04	0.21	0.24	0.81	<0.02	<0.04	nd	<0.04	<0.04	<0.08	A/2
ASO-14	Bottle (<i>anghistera</i>)	68.19	12.00	10.98	1.17	2.24	3.99	0.44	0.07	0.75	<0.04	0.25	0.27	1.11	<0.02	0.05	nd	<0.04	<0.04	<0.08	A/1
ASO-15	Bottle (<i>anghistera</i>)	67.03	9.58	12.83	2.67	2.29	2.96	0.43	0.07	0.82	<0.04	0.18	0.29	0.91	<0.02	<0.04	nd	<0.04	<0.04	<0.08	A/2
ASO-16	Bottle (<i>anghistera</i>)	66.99	13.10	8.32	3.43	2.73	2.29	1.01	0.14	1.68	<0.04	0.35	0.11	1.07	<0.02	<0.04	nd	<0.04	<0.04	<0.08	A/3
ASO-17t	Beaker, colourless body	67.79	11.64	11.01	1.59	2.31	3.78	0.52	0.07	0.96	<0.04	0.28	0.25	0.97	<0.02	0.05	<0.05	<0.04	<0.04	<0.08	A/1
ASO-17b	Beaker, blue rim	65.19	11.11	10.55	1.72	2.34	3.66	2.84	0.08	0.92	<0.04	0.30	0.24	0.75	0.38	0.66	<0.05	0.25	0.05	0.15	–
ASO-18t	Beaker, colourless body	65.49	11.32	11.31	1.68	2.58	3.93	0.69	0.10	2.38	<0.04	0.32	0.22	0.85	<0.02	0.06	<0.05	<0.04	<0.04	0.11	A/1
ASO-18b	Beaker, blue rim	64.19	10.91	11.18	1.75	2.55	3.89	1.66	0.09	2.24	<0.04	0.32	0.20	0.71	0.19	0.49	<0.05	0.22	0.05	0.18	–
ASO-19t	Beaker, colourless body	65.53	11.80	10.46	1.59	2.58	4.16	0.73	0.07	2.49	<0.04	0.28	0.25	0.85	0.04	0.08	<0.05	<0.04	<0.04	0.13	A/1
ASO-19b	Beaker, blue rim	61.84	10.82	9.75	1.74	2.56	3.83	4.76	0.09	2.23	<0.04	0.29	0.21	0.59	0.78	1.22	<0.05	0.50	0.07	0.23	–
ASO-20t	Beaker, colourless body	65.56	13.16	10.21	1.43	2.12	4.49	0.87	0.10	1.04	<0.04	0.24	0.32	1.08	<0.02	<0.04	<0.05	<0.04	<0.04	<0.08	A/1
ASO-20b	Beaker, blue rim	63.74	12.66	9.72	1.53	2.12	4.27	2.04	0.09	1.03	<0.04	0.24	0.32	1.00	0.49	0.81	0.15	<0.04	<0.04	<0.08	–
ASO-21t	Beaker, colourless body	67.77	10.90	9.83	1.10	2.17	3.28	1.15	0.06	2.68	<0.04	0.24	0.25	0.93	<0.02	<0.04	<0.05	<0.04	<0.04	0.12	A/1
ASO-21b	Beaker, blue rim	64.02	10.11	9.32	1.34	2.15	3.11	4.36	0.08	2.66	<0.04	0.25	0.21	0.68	0.72	0.75	<0.05	0.50	0.07	0.20	–

Table D.8: Chemical composition of all glass samples, expressed as weight per cent (wt%). Only means are reported (nd: not detected). Type and compositional group also reported for each sample.

APPENDIX E

Results of the strontium, neodymium and oxygen isotopic analyses performed on a selection of Roman and Late Roman/early Medieval samples from Adria and Aquileia.

SAMPLE	PROVENANCE	COLOUR	AGE (cent. AD)	$^{143}\text{Nd}/^{144}\text{Nd}$	σ	Nd (ppm)	ϵNd	$^{87}\text{Sr}/^{86}\text{Sr}$	σ	Sr (ppm)	GROUP
AD-A-2	Adria	light blue	1st	0.512409	0.000042	5.7	-4.47	0.70913	0.00006	362	GROUP AD/N1
AD-A-11	Adria	light blue	1st	nd	nd	12.0	nd	0.70901	0.00007	401	GROUP AD/N2
AD-B-3	Adria	blue	1st	0.512402	0.000044	5.9	-4.60	0.70892	0.00005	453	GROUP AD/N3
AD-B-5	Adria	blue	—	0.512391	0.000046	5.6	-4.82	0.70900	0.00007	371	GROUP AD/N4
AD-B-9	Adria	blue	1st	0.512430	0.000039	5.7	-4.06	0.70887	0.00008	474	GROUP AD/N5
AD-AM-1	Adria	amber	1st	0.512381	0.000050	<10	-5.00	0.70906	0.00008	353	GROUP AD/N6
AD-AM-2	Adria	amber	1st	0.512505	0.000039	6.1	-2.59	0.70908	0.00009	439	GROUP AD/N7
AD-1-3	Adria	colourless	3rd	0.512366	0.000044	<10	-5.31	0.70902	0.00006	375	GROUP AD/N8
AD-VE-1	Adria	olive green	1st	nd	nd	6.2	nd	0.70899	0.00007	447	GROUP AD/N9
AD-VC-2	Adria	light green	1st-3rd	0.512388	0.000040	5.4	-4.88	0.70894	0.00006	464	GROUP AD/N10
AD-V-2	Adria	purple	1st	0.512123	0.000035	6.3	-10.04	0.70955	0.00009	592	GROUP AD/N11
AD-V-4	Adria	purple	1st	0.512411	0.000033	5.5	-4.43	0.70854	0.00006	657	GROUP AD/N12
AD-B-6	Adria	blue	1st	0.512258	0.000054	7.1	-7.41	0.70898	0.00004	322	GROUP AD/N2a
AD-B-7	Adria	blue	1st	0.512349	0.000040	5.2	-5.65	0.70854	0.00010	400	GROUP AD/N2a
AD-1-2	Adria	colourless	2nd	nd	nd	<10	nd	0.70916	0.00006	323	GROUP AD/N2b
AD-1-4	Adria	colourless	2nd	0.512332	0.000041	4.5	-5.97	0.70907	0.00006	347	GROUP AD/N2b
AD-1-5	Adria	colourless	2nd-3rd	0.512345	0.000046	5.3	-5.71	0.70902	0.00006	370	GROUP AD/N2b
AD-1-6	Adria	colourless	2nd	0.512346	0.000250	4.6	-5.70	0.70903	0.00008	373	GROUP AD/N2b
AD-VE-2	Adria	emerald green	1st	0.512351	0.000042	7.4	-5.59	0.70894	0.00007	463	GROUP AD/A2
AD-B-4	Adria	blue	1st-2nd	0.512355	0.000046	5.2	-5.53	0.71089	0.00007	388	OUTLIER
AQ106-1	Aquileia	green	late 3rd-5th	0.512404	0.000043	<10	-4.56	0.70859	0.00006	459	GROUP AQ/1b
AQ106-4	Aquileia	light blue	late 3rd-5th	0.512404	0.000033	<10	-4.56	0.70862	0.00009	405	GROUP AQ/1b
AQ106-14	Aquileia	light blue	late 3rd-5th	0.512378	0.000054	<10	-5.08	0.70866	0.00008	423	GROUP AQ/1b
AQ111-4	Aquileia	green	5th-8th	0.512447	0.000034	<10	-3.73	0.70851	0.00005	408	GROUP AQ/1b
AQ111-9	Aquileia	green	5th-8th	0.512389	0.000035	<10	-4.86	0.70881	0.00006	420	GROUP AQ/1b
AQ106-19	Aquileia	green	late 3rd-5th	0.512380	0.000045	<10	-5.03	0.70846	0.00008	505	GROUP AQ/1a
AQ111-8	Aquileia	green	5th-8th	0.512364	0.000036	<10	-5.35	0.70832	0.00008	534	GROUP AQ/1a
AQ106-11	Aquileia	light blue	late 3rd-5th	0.512414	0.000046	<10	-4.37	0.70890	0.00007	445	GROUP AQ/2a
AQ106-15	Aquileia	light blue	late 3rd-5th	0.512442	0.000041	<10	-3.82	0.70912	0.00006	537	GROUP AQ/2a
AQ106-17	Aquileia	green	late 3rd-5th	0.512415	0.000036	<10	-4.35	0.70896	0.00010	398	GROUP AQ/2a
AQ111-3	Aquileia	light blue	5th-8th	0.512420	0.000033	<10	-4.25	0.70884	0.00008	468	GROUP AQ/2a
AQ111-7	Aquileia	light blue	5th-8th	0.512447	0.000034	<10	-3.73	0.70895	0.00008	502	GROUP AQ/2a
AQ106-12	Aquileia	light blue	late 3rd-5th	0.512450	0.000042	<10	-3.67	0.70913	0.00008	456	GROUP AQ/2b
AQ106-16	Aquileia	green	late 3rd-5th	nd	nd	12.0	nd	0.70889	0.00009	384	GROUP AQ/3
AQ111-1	Aquileia	green	late 3rd-5th	0.512388	0.000038	<10	-4.89	0.70891	0.00010	497	GROUP AQ/3

AQIII-2	Aquileia	light blue	late 3rd-5th	0.512368	0.000049	10.0	-5.26	0.70887	0.00008	476	GROUP AQ/3
AQIII-5	Aquileia	light blue	late 3rd-5th	0.512386	0.000046	<10	-4.92	0.70892	0.00006	411	GROUP AQ/3
AQIII-11	Aquileia	light blue	late 3rd-5th	0.512396	0.000039	<10	-4.72	0.70884	0.00008	435	GROUP AQ/4

Table E.1: *Sr-Nd isotopic data and elemental compositions of the Roman and Late Roman/early Medieval samples from Adria and Aquileia. Reference groups are also reported for each sample. (nd: not detected).*

SAMPLE	PROVENANCE	COLOUR	AGE (cent. AD)	$\delta^{18}\text{O}$	Mean value $\delta^{18}\text{O}$ (‰)	σ	GROUP
AD-A-2	Adria	light blue	1st	15.4	15.5	0.07	GROUP AD/N1
AD-A-11	Adria	light blue	1st	15.6	15.8	0.14	GROUP AD/N1
AD-B-3	Adria	blue	1st	15.7	15.6	0.07	GROUP AD/N1
AD-B-5	Adria	blue	-	15.4	15.3	0.07	GROUP AD/N1
AD-B-9	Adria	blue	1st	15.7	15.5	0.14	GROUP AD/N1
AD-AM-1	Adria	amber	1st	15.6	15.5	0.07	GROUP AD/N1
AD-AM-2	Adria	amber	1st	15.6	15.8	0.14	GROUP AD/N1
AD-I-3	Adria	colourless	3rd	15.5	15.7	0.14	GROUP AD/N1
AD-VE-1	Adria	olive green	1st	15.8	15.6	0.14	GROUP AD/N1
AD-VC-2	Adria	light green	1st-3rd	15.1	15.2	0.07	GROUP AD/N1
AD-V-2	Adria	purple	1st	15.4	15.6	0.14	GROUP AD/N1
AD-V-4	Adria	purple	1st	15.8	15.8	0.00	GROUP AD/N1
AD-B-6	Adria	blue	1st	16.1	16.2	0.07	GROUP AD/N2a
AD-B-7	Adria	blue	1st	15.6	15.7	0.07	GROUP AD/N2a
AD-I-2	Adria	colourless	2nd	17.4	17.6	0.14	GROUP AD/N2b
AD-I-4	Adria	colourless	2nd	15.7	15.7	0.00	GROUP AD/N2b
AD-I-5	Adria	colourless	2nd-3rd	15.6	15.6	0.00	GROUP AD/N2b
AD-I-6	Adria	colourless	2nd	15.7	15.7	0.00	GROUP AD/N2b
AD-VE-2	Adria	emerald green	1st	16.8	17.0	0.14	GROUP AD/A2
AD-VE-3	Adria	emerald green	1st-2nd	16.3	16.5	0.14	GROUP AD/A2
AD-VE-4	Adria	emerald green	1st-2nd	16.8	16.6	0.14	GROUP AD/A1
AD-B-4	Adria	blue	1st-2nd	15.1	15.0	0.07	OUTLIER
AQ106-1	Aquileia	green	late 3rd-5th	15.5	15.3	0.14	GROUP AQ/1b
AQ106-4	Aquileia	light blue	late 3rd-5th	15.8	15.6	0.14	GROUP AQ/1b
AQ106-14	Aquileia	light blue	late 3rd-5th	15.2	15.1	0.07	GROUP AQ/1b
AQ111-4	Aquileia	green	5th-8th	14.4	14.7	0.21	GROUP AQ/1b
AQ111-9	Aquileia	green	5th-8th	15.8	16.0	0.14	GROUP AQ/1b
AQ106-19	Aquileia	green	late 3rd-5th	15.6	15.4	0.14	GROUP AQ/1a
AQ111-8	Aquileia	green	5th-8th	15.0	15.0	0.00	GROUP AQ/1a
AQ106-11	Aquileia	light blue	late 3rd-5th	15.4	15.5	0.07	GROUP AQ/2a
AQ106-15	Aquileia	light blue	late 3rd-5th	15.8	15.5	0.21	GROUP AQ/2a
AQ106-17	Aquileia	green	late 3rd-5th	15.3	15.1	0.14	GROUP AQ/2a
AQ111-3	Aquileia	light blue	5th-8th	15.9	15.8	0.07	GROUP AQ/2a
AQ111-7	Aquileia	light blue	5th-8th	15.8	15.8	0.00	GROUP AQ/2a
AQ106-12	Aquileia	light blue	late 3rd-5th	15.2	15.4	0.14	GROUP AQ/2b

AQ106-16	Aquileia	green	late 3rd-5th	15.5	15.6	15.6	0.07	GROUP AQ/3
AQ111-1	Aquileia	green	5th-8th	15.7	15.9	15.8	0.14	GROUP AQ/3
AQ111-2	Aquileia	light blue	5th-8th	15.8	15.5	15.7	0.21	GROUP AQ/3
AQ111-5	Aquileia	light blue	5th-8th	15.7	15.5	15.6	0.14	GROUP AQ/3
AQ111-11	Aquileia	light blue	5th-8th	15.1	15.0	15.1	0.07	GROUP AQ/3

Table E.2: $\delta^{18}O$ (VSMOW) of Roman and Late Roman/early Medieval glass samples from Adria and Aquileia. Compositional groups are also reported.